DURBAN UNIVERSITY OF TECHNOLOGY
INYUVESI YASETHEKWINI YEZOBUCHWEPHESHE

ANAEROBIC CO-DIGESTION OF AGRICULTURAL BIOMASS WITH INDUSTRIAL WASTEWATER FOR BIOGAS PRODUCTION

A thesis submitted in fulfilment of the academic requirements for the degree of Doctor of Engineering in Chemical Engineering in the Faculty of Engineering and The Built Environment at the Durban University of Technology, Durban, South Africa

Edward Kwaku Armah

Supervisors: Dr. Manimagalay Chetty

Prof. Nirmala Deenadayalu

2021

DECLARATION

I, **Edward Kwaku Armah** with student number 21752261, declare that:

i. the research reported in this thesis, except where otherwise indicated, is my original work.

ii. this thesis has not been submitted for any degree or examination at any other university.

iii. this thesis does not contain other persons' data, pictures, graphs, or other information, unless specifically acknowledged as being sourced from other persons.

iv. this thesis does not contain other persons' writing, unless specifically acknowledged as being sourced from other researchers. Where other written sources have been quoted, then:

a. their words have been re-written, but the general information attributed to them has been referenced;

b. where their exact words have been used, their writing has been placed inside quotation marks and referenced.

v. where I have reproduced a publication of which I am an author, co-author, or editor, I have indicated in detail which part of the publication was actually written by myself alone and have fully referenced such publications.

vi. this thesis does not contain text, graphics or tables copied and pasted from the Internet, unless specifically acknowledged, and the source being detailed in the thesis and in the references sections.

Signature:  Date: 26th March 2021

Edward Kwaku Armah (Student)

Signature:  Date: 26th March 2021

Dr. Maggie Chetty (Supervisor)

Signature:  Date: 26th March 2021

Prof. Nirmala Deenadayalu (Co-Supervisor)

ABSTRACT

With the increasing demand for clean and affordable energy which is environmentally friendly, the use of renewable energy sources is a way for future energy generation. South Africa, like most countries in the world are over-dependent on the use of fossil fuels, prompting most current researchers to seek an affordable and reliable source of energy which is also,a focal point of the United Nations Sustainable Development Goal 7.

In past decades, the process of anaerobic digestion (AD) also referred to as monodigestion, has proven to be efficient with positive environmental benefits for biogas production for the purpose of generating electricity, combined heat and power. However, due to regional shortages, process instability and lower biogas yield, the concept of anaerobic co-digestion (AcoD) emerged to account for these drawbacks. Given the considerable impact that industrial wastewater (WW) could provide nutrients in anaerobic biodigesters, the results of this study could apprise decision-makers and the government to further implement biogas installations as an alternative energy source.

The study aims at optimising the biogas production through AcoD of the agricultural biomasses: sugarcane bagasse (SCB) and corn silage (CS) with industrial WW sourced from Durban, KwaZulu-Natal, South Africa. The study commenced with the characterisation of the biomasses under this study with proximate and ultimate analysis using the Fourier transform infrared spectroscopy (FTIR), the thermo gravimetric analysis (TGA), the scanning electron microscopy (SEM) and the differential scanning calorimetry (DSC).

The untreated biomass was subjected to biochemical methane potential (BMP) tests to optimise and predict the biogas potential for the selected biomass. A preliminary run was carried out with the agricultural biomass to determine which of the WW streams would yield the most biogas.

Among the four WW streams sourced at this stage, two WW streams; sugar WW (SWW) and dairy WW (DWW) produced the highest volume of biogas in the increasing order; SWW > DWW > brewery WW > municipal WW. Therefore, both SWW and DWW were selected for further process optimisation with each biomass.

Using the response surface methodology (RSM), the factors considered were temperature (25-55 °C) and organic loading rate (0.5-1.5 gVS/100mL); and the response was the biogas yield (m^3/kgVS). Maximum biogas yield and methane (CH_4) content were found to be 5.0 m^3/kgVS and 79%, respectively, for the AcoD of CS with SWW. This established the association that existed among the set temperatures of the digestion process and the corresponding organic loading rate (OLR) of the AcoD process operating in batch mode.

Both CS and SCB have been classified as lignocellulosic and thus, ionic liquid (IL) pretreatment was adapted in this study to ascertain their potential on the biogas yield.

Results showed that the maximum biogas yield and CH_4 content were found to be 3.9 m^3/kgVS and 87%, respectively, after IL pretreatment using 1-ethyl-3-methylimidazolium acetate ([Emim][OAc]) for CS with DWW at 55°C and 1.0 gVS/100mL. The IL pretreatment yielded lower biogas but of higher purity of CH_4 than the untreated biomass.

Data obtained from the BMP tests for the untreated and pretreated biomasses were tested with the existing kinetic models; first order, dual pooled first order, Chen and Hashimoto and the modified Gompertz. The results showed that for both untreated and pretreated biomass, the modified

Gompertz had the best fit amongst the four models tested with coefficient of correlation, R^2 values of 0.997 and 0.979, respectively.

Comparatively, the modified Gompertz model could be the preferred model for the study of industrial WW when used as co-substrate during AcoD for biogas production.

The study showed that higher biogas production and CH_4 contents were observed when CS was employed as a reliable feedstock with maximum volume of the untreated and pretreated feedstock reported at 31 L and 20 L respectively.

DEDICATION

This book is dedicated to my wife and kids, unknown at the time of writing this thesis but to say that daddy loves you so much. Any time you read this piece, do not forget to put that beautiful smile on your face!!!!

Nana Kwasi (Ernest Armah Rockson), your death during the final year of my doctoral studies shall forever be remembered. May your humble soul rest well!

ACKNOWLEDGEMENTS

My outmost thanks go to the Almighty God for the gift of life, patience, wisdom, and knowledge all through these years. Also, I humbly express my profound gratitude to the following people who in diverse ways contributed in the writing of this thesis:

To my supervisor, Dr. Maggie Chetty and co-supervisor, Prof. Nirmala Deenadayalu throughout this work in terms of the directives, positive criticisms and immense contribution which made this work possible is very much appreciated.

Also, to my wonderful family; my dad (Mr. E. E. K. Armah), my mum (Mrs. Elizabeth Armah), big brothers (Mr. Rockson Armah and Mr. Thomas Armah) and my two beautiful sisters (Mrs. Faustina Armah and Mrs. Vera Armah). *The young ones brought forth;* Betty Armah Rockson, Michellin Armah Mintah, Brian Armah Mintah, Sarah Obeng and Sefarkor Ahiabley are also much appreciated. *It is my wish to see all of you excelling greater than me.* Truly, you are the inspiration for all my effort in excelling in all my work.

Most of the thanks go to Mr. Emmanuel Kweinor Tetteh and Mr. Claude Eda Tetteh for the recommendations. To Mr. Dennis Asante-Sackey, Mr. Jeremiah Adedeji, Dr. Mrs. Martha Chollom, Mr. Elorm Obotey Ezugbe, Mr. Boldwin Mutsvene, Ms. Devrani Naicker (Avy) for the HPLC analysis, Dr. Dennis Amoah and my able research team, to say, *you guys do rock.*

To the staff of Tongaat Hullet, Amanzimtoti Wastewater Treatment Plant (especially, Mgr. Stephen) and Clover (Pty) Limited during the sampling.

Finally, financial support was given by the National Research Foundation (NRF) and IWWT.

TABLE OF CONTENTS

LIST OF FIGURES

LIST OF TABLES

GLOSSARY

Acclimation: This refers to the adaptation of a bacterial center of populace for the decomposition of a substance.

Anaerobic digestion: The breakdown of organic substances in an oxygen free setting by bacteria.

Analysis of Variance (ANOVA): A term in which the deviation of observations are divided into different components.

Biogas: A gaseous fuel which largely consists of methane or carbon dioxide and formed during the breakdown of an organic substance in an anaerobic digestor.

Biodegradability: This term, generally depends on the molecular structure denoting its susceptibility to undergo a biologically mediated degradation.

Cellulose: An organic compound which is considered as a polysaccharide and consists of a linear chain of numerous amount of glucose units

Chemical Oxygen Demand (COD): This determines the complete amount of dissolved substances that are found in an effluent.

Co-digestion: The addition of secondary substrates in anaerobic digestion to advance the digestibility of organic substrates, thereby, improving the biogas potential.

Effluent or wastewater: This refers to waste streams which consists of organic and inorganic materials and flows from a manufacturing process.

Headspace: A space in an encircled container that is occupied by a gas phase.

Hemicellulose: These heterogeneous polymers play a supporting character in the fibre wall

Inoculum: A material from the effluent of a previous biogas plant, fermenting raw materials at anaerobic processing temperatures.

Mesophiles: These microbes grow extremely fine at moderate temperatures (30−40℃), and the temperature within this temperature is mesophilic temperature.

Regenerated cellulose: Cellulose that has been treated with chemicals and regenerated using co-solvents. It does contain lower molecular weight as compared to the native cellulose.

Sludge: This is the amassed solids separated from wastewater. Larger fractions comprise of microorganisms which are responsible for its degradation.

Thermophiles: These microbes grow very well at higher temperatures of 50−60℃, and such a temperature range is known as thermophilic temperature.

ABBREVIATIONS

2D	2-Dimensional
3D	3-Dimensional
AD	Anaerobic digestion
ADM1	Anaerobic digestion model number 1
ADM2	Anaerobic digestion model number 2
AFEX	Ammonia Fibre Explosion
ANOVA	Analysis of variance
APHA	American Public Health Association
Ar	Argon
[Amim][Cl]	1-allyl-3-methylimidazolium chloride
AcoD	Anaerobic co-digestion
$Al_2Si_2O_5(OH)_4$)	Kaolin clay
BBD	Box Behnken Design
BMP	Biochemical methane potential
BOD	Biological oxygen demand
$CaCO_3$	Calcium carbonate

CSTR	Continuously stirred tank reactor
$CH_4(g)$	Methane gas
Cu	Copper
Cr	Chromium
Ca	Calcium
CS	Corn silage
$Ca(OH)_2$	Calcium hydroxide
$CuSO_4$	Copper sulfate
$CO_2(g)$	Carbon (IV) Oxide
COD	Chemical oxygen demand
CV	Coefficient of variation
DENR	Department of Environmental and Natural Resources
DO	Dissolved oxygen
DSC	Differential Scanning Calorimetry
DMSO	Dimethyl Sulfoxide
DUT	Durban University of Technology
DWAF	Department of Water Affairs and Forestry
[EMIM][Cl]	1-ethyl-3-methylimidazoliumchloride

[EMIM][CH_3COO]	1-ethyl-3 -methylimidazolium acetate
FVW	Fruits and vegetable waste
FA	Fatty acid
FTIR	The Fourier Transform Infra-red
GDP	Gross domestic product
GC	Gas chromatograph(y)
HRT	Hydraulic retention time
H_2	Hydrogen gas
H_2SO_4	Tetraoxosulphate (IV) acid
He	Helium
HPLC	High Pressure Liquid Chromatograph(y)
$H_2S(g)$	Hydrogen sulphide
H_2O_2	Hydrogen peroxide
IWA	International Water Association
IL	Ionic liquid
ISR	Inoculum to substrate ratio
KOH	Potassium hydroxide
k	Kinetic rate constant

KZN	KwaZulu-Natal
K	Potassium
LCFA	Long chain fatty acids
LHW	Liquid hot water
MC	Mesophilic condition
MSW	Municipal solid waste
MWWTP	Municipal wastewater treatment plant
Mo	Molybdenum
Mg	Magnesium
MT	Mesophilic temperature
$NaSO_4$	Sodium sulfate
Ni	Nickel
N	Nitrogen
NH_4^+	Ammonium ion
NH_4Cl	Ammonium chloride
$N_2(g)$	Nitrogen gas
Na	Sodium
NH_3	Ammonia

NL	Normalized liters
NaOH	Sodium hydroxide
NGVs	Natural gas vehicles
NRF	National Research Foundation
OLR	Organic loading rate
pH	Potential hydrogen
Pb	Lead
SAO	Syntrophic acetate oxidation
SRT	Solid retention time
STP	Standard temperature and Pressure
SB	Sugarcane bagasse
sCOD	Soluble chemical oxygen demand
SMRI	Sugar milling research institute
SA	South Africa
S	Sulphur
SEM	Scanning Electron Microscope
STP	Sewage treatment plants
TiO_2	Titanium dioxide

TCL	Treatment cycle length
TGA	Thermogravimetric analysis
UASB	Upflow anaerobic sludge blanket
UV/Vis spec	Ultraviolet visible spectrophotometer
VFA	Volatile fatty acids
VS	Volatile solids
WB	Woody biomass
WWTP	Wastewater treatment plant
XRD	X-ray Diffractometer
Y_{biogas}	Biogas yield
Y_{CH4}	Methane yield
Zn	Zinc

RESEARCH OUTPUTS

LOCAL CONFERENCES/SEMINARS/COLLOQUIA

1. **Armah, E.K.,** Chetty, M., Deenadayalu, N. (2019). Biomethane potential of Agricultural Biomass with Industrial wastewater for biogas production. *Faculty of Applied Sciences Research Day,* 11th November 2019, Southern Sun-Elangeni Hotel, Durban, South Africa (Oral presentation).

2. **Armah, E.K.**, Chetty, M., Deenadayalu, N. (2019). Effects of particle size on biogas generation from sugarcane bagasse and corn silage. *4th Interdisciplinary Research and Innovation Congress,* Hilton Hotel, Walnut Road, Durban, South Africa (Oral presentation).

3. **Armah, E.K.,** Chetty, M., Deenadayalu, N. (2019). Anaerobic co-digestion of sugarcane bagasse and corn silage with industrial wastewater for biogas production. *SAIChE-IChemE Research day,* Mangosuthu University of Technology (MUT), Senate Chamber, KZN, South Africa (Presenter: 2nd runner up for the oral category)

4. **Armah, E.K.,** Chetty, M., Deenadayalu, N. (2019). Anaerobic co-digestion of agricultural biomass with industrial wastewater for biogas production. *National 3-minutes PhD competition-category for the Durban University of Technology (DUT),* Hotel Conference Hall, Durban, KZN, South Africa (Presenter: *Award for participation to represent DUT at the University of the Free State, Bloemfontein, SA)*

5. **Armah, E.K.,** Chetty, M., Deenadayalu, N. (2019). Anaerobic co-digestion of sugarcane bagasse and corn silage with industrial wastewater for biogas production. *SACI-KZN Postgraduate Research Colloquium*, Durban University of Technology (DUT), Ritson Campus, Durban, South Africa (*Award for the best PhD: oral presentation).*

6. **Armah, E.K.,** Chetty, M., Deenadayalu, N. (2018). Anaerobic co-digestion of sugarcane bagasse and corn silage with industrial wastewater for biogas production. *4th National Conference*

on Global Change under the theme, Sustainable futures through science and innovation, 3-6th December, 2018, University of Limpopo, Polokwane, South Africa (Poster presentation).

7. **Armah, E.K.,** Chetty, M., Deenadayalu, N. (2018). Anaerobic co-digestion of agricultural biomass with industrial wastewater for biogas production. *SAIChE-IChemE Research day*, University of KwaZulu-Natal (UKZN), Howard College, KZN, South Africa (Presenter: *Award for the best Poster Presentation).*

8. **Armah, E.K.,** Chetty, M., Deenadayalu, N. (2018). Anaerobic co-digestion of agricultural biomass with industrial wastewater for biogas production. *Research Focus Area Conference on Biomass Processing*, Garden Court Marine Parade, Durban, KZN, South Africa (Presenter).

9. **Armah, E.K.,** Chetty, M., Deenadayalu, N. (2018). Anaerobic co-digestion of agricultural biomass with industrial wastewater for biogas production. *National 3-minutes PhD competition-category for the Durban University of Technology (DUT),* Ritson Campus, Hotel Conference Hall, Durban, KZN, South Africa (Presenter).

INTERNATIONAL CONFERENCE

1. **Armah, E.K.,** Chetty, M., Deenadayalu, N. (2019). Biomethane Potential of Agricultural Biomass with Industrial Wastewater for Biogas Production. *PRES 19: 22nd International Conference on Process Integration, Modelling, Optimisation for Energy Saving and Pollution Reduction.* Agios Nikolaos, Crete, Greece, 20-23rd October 2019.

BOOK CHAPTER CONTRIBUTIONS

1. **Edward Kwaku Armah**, Maggie Chetty, Jeremiah Adebisi Adedeji, Donald Kukwa (2020). Valorization of lignocelluloses and microalgae for renewable energy production. *IntechOpen*. DOI: 10.5772/intechopen.93654.

2. **Edward Kwaku Armah,** Maggie Chetty, Babatunde Femi Bakare, Jeremiah Adebisi Adedeji, Donald Kukwa, Boldwin Mutsvene, Khaya Pearlman Shabangu (2020). Emerging trends in

wastewater treatment technologies: the current perspective (In-press), *IntechOpen.* DOI: 10.5772/intechopen.93898.

3. **Edward Kwaku Armah,** Maggie Chetty, Sudesh Rathilal, D. Asante-Sackey, and E. K. Tetteh (2020). Lignin: value addition is key to profitable biomass biorefinery. *Elsevier publications (under review).*

4. Tetteh, E.K., Rathilal, S., Chetty, M., **Armah, E.K.,** Asante-Sackey, D. (2019). Treatment of Water and Wastewater for Reuse and Energy Generation-Emerging Technologies. *IntechOpen*, DOI: 10.5772/intechopen.84474.

PEER REVIEWED JOURNAL ARTICLES

1. **Edward Kwaku Armah**, Maggie Chetty, Nirmala Deenadayalu (2020). Biogas production from sugarcane bagasse with South African industrial wastewater and novel kinetic study using response surface methodology. *Scientific African,* 10:1-9. DOI: 10.1016/j.sciaf.2020.e00556.

2. **Armah, E.K.**, Chetty, M., Deenadayalu, N. (2019). Biomethane Potential of Agricultural Biomass with Industrial Wastewater for Biogas Production. *Chemical Engineering Transactions,* 76, 1411-1416. DOI:10.3303/CET1976236.

3. **Armah E.K.,** Chetty M., Deenadayalu N., (2019). Effect of Particle Size on Biogas Generation from Sugarcane Bagasse and Corn Silage, *Chemical Engineering Transactions,* 76, 1471-1476. DOI:10.3303/CET1976246.

4. **Armah, E.K.,** Chetty, M., Deenadayalu, N. Biogas potential of sugarcane bagasse after ionic liquid pretreatment. *(In-preparation)*

5. **Armah, E.K.,** Chetty, M., Deenadayalu, N. Biogas potential of corn silage after ionic liquid pretreatment. *(In-preparation).*

6. **Armah, E.K.,** Chetty, M., Deenadayalu, N. Biogas generation from corn silage using response surface methodology. *(In-preparation).*

CHAPTER 1

INTRODUCTION

1.1. Background

Urbanisation has led to rapid production of “wastes” leading to poor management practices in developing nations (Tawoma 2015). This coupled with higher standards of living has increased the release of pollutants andgreenhouse gases (GHGs) into the environment (Teghammar 2013). This has led to a global crisis as the use of fossil fuel are still being consumed at a high rate (Fagerström *et al.* 2018). In most cases, these forms of energy originates from oil, coal, and natural gas, as many countries depend largely on a few countries for their fuel sources. However, this has driven the need for an alternative and suitable technology which is clean and cheap. The application of AD technology in biogas plants began decades ago to stabilise sewage located at wastewater treatment plants (WWTPs). Europe and Asia continue to be the first frontiers in the establishment of biogas plants but the surge for this alternative energy source is being adopted more recently in Africa (Scherer *et al.* 2009). The term renewable energy arises from various sources which includes wind, solar, tidal and biomass. Most of these renewable energies when upgraded could be employed for use as vehicle fuel, and for use in combined heat and power systems.

However, by means of supplementing the ratio of these renewables to meet the global demands, the European Union (EU) limits its requirements on trading of fossil fuels to encourage sources which are renewable and hence, sustainable.

The European Commission set goal for 2020 details that 20% of the energy consumption should possibly emanate from renewable energy with no exception to the transport sector (European Commission 2011).

According to Sager (2014), the unending dependence on coal does not encourage a climate-robust future in which the energy, water and food sectors are stable in supporting the needs of the growing population. The World Wild Fund for Nature (WWF) argues that South Africa could plan for a two-fold level of renewable energy dissemination by 2030 to supply about 20% share of electricity. From the same report, the capacity to generate expressive share of total electricity demand could cost about 2% of the gross domestic product (GDP) annually.

Biogas is considered a greener and sustainable energy source with less carbon dioxide (CO_2) emissions than fossil fuel usages. It contains about 50-60% CH_4 and 35% CO_2 and; the remaining representing components being ammonia (NH_3) and hydrogen sulfide (H_2S), etc. The digestate is rich in nutrients and could be useful in biofertilizer production after the biogas is collected (Abbasi, Tauseef and Abbasi 2012; Biarnes 2017). In South Africa, several industries produce millions of cubic meters of wastewater (WW) annually with large volumes released into water bodies, such as river's (Enitan 2015).

Anaerobic digestion (AD) has been adopted in the past decades for biogas production based on anaerobic monodigestion viz the use of single feedstock until some drawbacks encountered in anaerobic biodigesters paved the way for the adoption of anaerobic co-digestion. In AcoD, multiple feedstocks are used to enhance the biogas potential. For substrates such as sewage or municipal sludge, the quantification of the presence of microbes varies. However, the structure of the microbial community varies in relation to changes in substrate composition, intermediary

inhibition considerations, OLR, hydraulic retention time (HRT), reactor configuration and the temperature.

With respect to substrates considered insoluble, these process parameters are observed to be complex by the lack of dependable techniques for the quantification of microbial biomasses (Yu *et al.* 2013; Xie *et al.* 2016b). The key purpose of an AD process in WWT emphasizes the stabilisation of sewage sludge preceding land usage or land filling. The operation with sewage sludge under mono-digestion has been reported to occur at a lower OLR of 0.5gVS/mL and thus, the modelling requirements are often simplified for input variables such as OLR and HRT; and output variables such as the biogas production.

Kinetic modeling is useful for the design, prediction and the control of the AD processes as it assists engineers to develop new configurations of reactors and improve the efficacy of an existing operation (Batstone *et al.* 2002; Estes *et al.* 2013). These models are needed to comprehend and make predictions based on the several processes that do occur in AD reactors in both methane (CH_4) production and plant performance. With regards to the latter, different models have been established in describing and predicting an increased treatment efficiency and optimisation (Batstone *et al.* 2002; Parawira *et al.* 2005; Parsamehr 2012). Some of these kinetic models include the first order, Chen and Hashimoto, the dual pool first order, Contois, Monod, second order and the modified Gompertz model (Lebona *et al.* 2019). However, only a few studies have focused on the application of the anaerobic digestion model number 1 (ADM1) for the simulation of AcoD processes (Boubaker and Ridha 2008; Derbal *et al.* 2009) which is regarded as a complex system.

1.2. Motivation of the study

Globally, about 120-140 billion metric tonnes of biomass are produced from agricultural "waste" (UNEP, 2009). Also, according to the South Africa Department of Environmental and Natural Resources (DENR), agricultural "waste" is leading in the category of "wastes" produced in South Africa. However, over 40-42 million cubic meters of general "wastes" are produced annually across South Africa (Department of Energy 2015).

Consequently, a little over 5 million cubic meters of these "wastes" are generated yearly from the mineral sector, domestic, sugar factories, milling and the production sectors with the highest input being from the KwaZulu-Natal and Mpumalanga Provinces (Chamane 2008).

As a result, there are growing concerns to identify the worth of these "waste" by making them useful towards the production of renewable sources of energy. This could supplement the energy deficit and replace the over-reliance on the use of non-renewable forms of energy which is depleting. Also, the South Africa economy has received significant contribution from the sugarcane industry which is ascribed to its industrial and agricultural investments, providing higher employability and its linkages with major suppliers. (Primrose and Mugodo 2015).

The South African sugar milling plants currently stands at fourteen (14), of which there are six different companies (Primrose and Mugodo 2015). In view of this, there is a substantial potency for the South African sugar cane industry to further produce renewable energy from currently unexploited solid and liquid waste by-products which could have otherwise polluted the environment. South Africa is Africa's largest corn producer and was estimated that 14.9 and 11.3 million metric tonnes were produced in 2013 and 2014, respectively (Department of Agriculture

2017). South Africa expected experienced its largest maize crop in history in 2017 with surplus maize exported to South Korea and Taiwan.

1.3. Problem statement

The classifications that are used to produce bioenergy could significantly contribute to reducing GHGs emissions. This could be attained by adopting a non-polluting source of energy which would keep the environment safe and clean from these toxic emissions. It is known that the consumption of fossil fuel accounts for about 86% of the entire global energy consumption whilst renewable energy accounts for about 9% (Mustafa, Poulsen and Sheng 2016). They are also the predominant causes of global warming and its associated climate changes with adverse environmental effects. Large-quantities of "waste" are also generated from the industrial, agricultural, and domestic sector in South Africa. Nonetheless, landfill disposal is not a sustainable option as a result of urbanisation since large volumes of solid "wastes" are a challenge for landfill sites. Previous studies have also shown that little has been done using these biomass for the production of biogas with different substrates. Therefore, this present study does not only serve as a baseline data for literature but offers industrialists a feedstock base to make choices. However, the AD process to convert these biomasses or "waste" have several drawback which includes low CH_4 yield, process instability, biodigester failure, regional shortage, and feedstock availability (Nges et al., 2011). A remedy to these drawbacks could be the use of industrial wastewater (WW) as co-substrates to enhance the biogas potential.

Also, pretreatment strategies using green solvents such as ionic liquids have been reported to disrupt lignin, making the surface of the biomass accessible for microbial degradation.

The application of municipal solid waste (MSW) has gained increasing recognition in this regard. MSW consists of a variety of combined agricultural and food waste which is usually directed towards AD to produce biogas, a sustainable and alternative energy to partly replace fossil fuels for electricity generation. Table 1-1 demonstrates various substrates employed in literature for the production of biogas in a biochemical methane potential tes (BMP).

Table 1- 1. Some comparative studies of different substrates and biogas yield.

Substrates	**Temperature**	**Type of reactor**	**Biogas yield (m^3CH_4/gVS)**	**References**
MSW using sludge	Thermophilic	Batch	0.14	(Villamil *et al.* 2018)
MSW using sludge	Thermophilic	Continuous	0.18	(Villamil *et al.* 2018)
Food waste with sludge	Mesophilic	Batch	0.35	(Nagao *et al.* 2012)
Food waste and cattle manure	Mesophilic	Batch	0.39	(Nagao *et al.* 2012)
MSW with cow manure	-	Continuous	0.10	(Mao *et al.* 2015a)
MSW using sludge	Mesophilic	Batch	0.20	(Ratanatamskul, Wattanayommanaporn and Yamamoto 2015)
MSW: Vegetable oil	Mesophilic	Batch	0.69	(Campuzano and González-Martínez 2016)
MSW: Animal fat	Mesophilic	Batch	0.51	(Campuzano and González-Martínez 2016)

The novelty of this study focuses on the use of industrial WW in the AcoD process to replace synthetic nutrients (chemicals) as a supplement for the AD process. Furthermore, the study also

aims to ascertain if biomass pretreatment of sugarcane bagasse (SCB) and corn silage (CS) could enhance the biogas production using an ionic liquid solution.

1.4. Objectives of this study

The research aim focuses on the AcoD of agricultural biomass with industrial wastewater and sewage sludge for the production of biogas.

The specific objectives of the investigation undertaken were:

- To characterise the biomasses, sewage sludge and industrial wastewaters for adoption in anaerobic co-digestion
- To determine the biogas potentials when agricultural biomass was co-digested with industrial wastewater and sewage sludge under anaerobic conditions
- To investigate whether ionic liquid pretreatment renders biomass more bioavailable to microorganisms for the production of biogas.
- To compare AD kinetic models with the data obtained from the biochemical methane potential analysis

1.5. Research outline

The present study was accomplished as depicted in Figure 1-1.

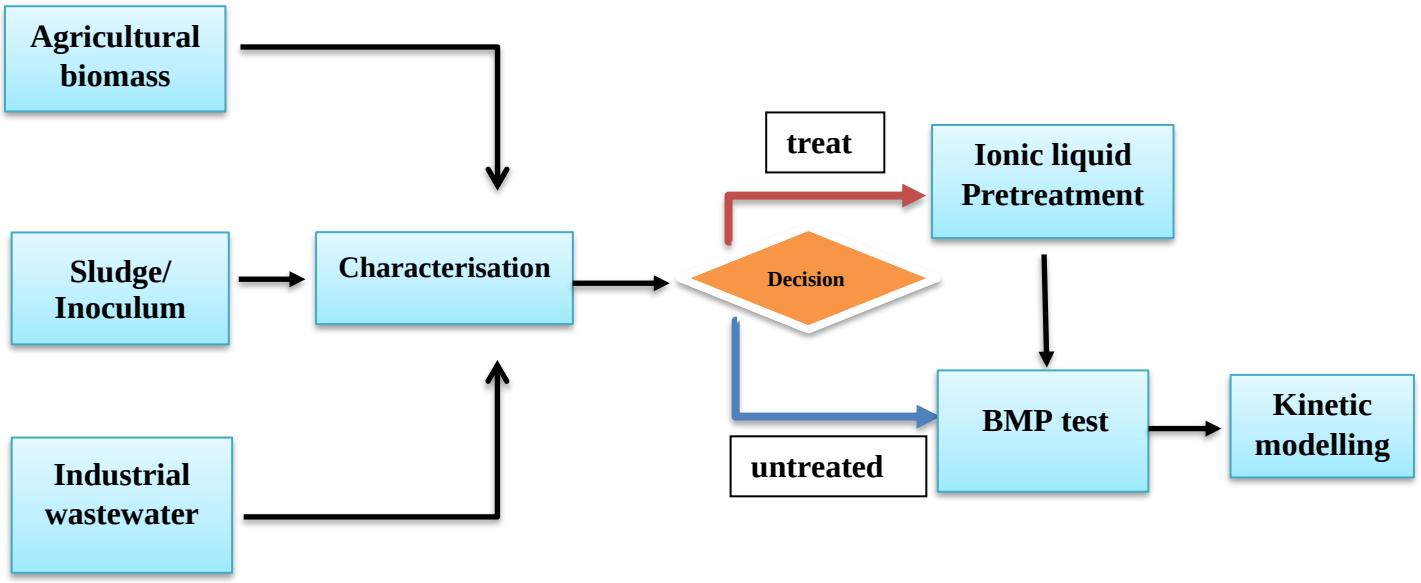

Figure 1- 1. Schematic block diagram employed in this present study.

1.6. Outline of thesis

This thesis consists of six (6) chapters which are outlined below.

CHAPTER 1: Presents a background of the study, the motivation behind the anaerobic digestion process of solid waste for the production of bioenergy with the objectives of the study, altogether with the research outline of the work.

CHAPTER 2: Presents a review of waste generation together with management strategies applied in South Africa. In addition, a detailed literature review of the AD process and AcoD with factors influencing the processes and biomass pretreatments were presented.

CHAPTER 3: This chapter addressed the experimental methodology employed in this study which comprises of the sampling, collection, storage, characterisation procedures and the biochemical methane potential analyses.

CHAPTER 4: This chapter details the protocols for the instruments employed in this study.

CHAPTER 5: The results obtained from each objective was discussed in this chapter.

CHAPTER 6: This chapter presents the general conclusions drawn from this study with various recommendations given for future research.

CHAPTER 2

LITERATURE REVIEW

2.1. Background

South Africa (SA) is faced with the shortage of water. Therefore, the Department of Water Affairs and Forestry (DWAF) has been authorized by the SA National Water Act (# 36 of 1998) in ensuring that water resources are utilized, sheltered, developed, accomplished and controlled in a realistic and sustainable approach (Chamane 2008). Stringent regulations have been imposed on the limitation caused by the wide diversity of both inorganic and organic contaminants in industrial wastewater releases. Also, there is an over-dependence on the usage of coal, a non-renewable source of energy because of the demand for electricity from Eskom which is a major provider of electricity. Larger volumes of waste are generated from municipal and industrial, sewage, the agricultural and domestic sectors due to urbanisation. Some of these wastes could be converted to produce bioenergy such as biogas (Tawoma 2015). According to the United Nation's Sustainability goals for 2030, food and agricultural waste can be used as renewable sources to contribute to about 20% of the overall energy consumption globally. To maximise these "wastes" as beneficial materials and energy feedstocks, the ability to conduct reliable material characterisation and the targeting of specific recalcitrance-related properties remain essential (Foston and Ragauskas 2012). South Africa is known to be one of the leading producers of sugarcane in Africa, with about 7 million tonnes of SCB being produced annually (Bodunrin et al., 2016). Wastewater generation is predominant in the province of KwaZulu-Natal and its existence cannot be underestimated. An alternative and sustainable way to use wastewater is to produce renewable energy sources which includes biogas and other fuels.

Industrial WW has shown much potential for biogas production and the co-digestion with agricultural biomass aims to increase the overall yield (Mateescu and Constantinescu 2011). It has the potential to be both a carbon source and a nutrient enrichment stream (Qian *et al.* 2016). AD has been found to be promising as a substitute for the production of bioenergy as anaerobic WWT results in biogas via the conversion of organic waste (Chamane 2008). Also, the AD process has been used in the past decades in most developed countries for the treatment of municipal, sewage and industrial WW (Priadi *et al.* 2014). Biogas contains large amounts of CH_4 and CO_2 which are further upgraded for use in combined heat and power (CHP) production facilities and for transport fuel (Maile, Muzenda and Mbohwa 2016c).

This chapter, however, introduces a general overview of the AD and AcoD processes, factors affecting AD, biomass used in the past decades for bioenergy production, pretreatments techniques employed, and the overview of relevant kinetic models as reported in literature with their applications.

2.2. Anaerobic digestion process

The AD of municipal WW sludge has received much attention since the 1900s and its is the most widely used sludge treatment method (Nazaroff and Alvarez-Cohen 2015). The secondary treatment of sludge through AD produces biogas since the main goal is to reduce the amount of sludge that needs to be disposed off in landfill sites. AD in a biogas plant is a well-proven process where organic matter is broken down gradually without the presence of oxygen to generate two streams which are the biogas and the digestate (Nayono 2010; Khalid *et al.* 2011; Liew, Shi and Li 2012). Prabhu and Mutnuri (2016) also defines the AD process as a naturally occurring and a

synergistic biotic process of microbial decomposition in the absence of oxygen (Gerardi 2003). It is believed that during this process, a large fraction of organic matter is broken down into smaller chemical components which includes CH_4, CO_2, hydrogen sulphide and manure (slurry). Earlier microorganisms for CH_4 production known to be isolated in the 1900s were the *Methanobacillus omelianskii*, *Methanosarcina barkeri*, *Methanobacterium formicicum*, and *Methanococcus vannielli* (Kougias and Angelidaki 2018). Four major steps are involved in an AD process which includes hydrolysis, acidogenesis, acetogenesis, and methanogenesis with a consortium of microorganisms responsible at each stage for a specific function (Bouallagui *et al.* 2004; Verstraete, Van de Caveye and Diamantis 2009; Khanal 2011). The AD stages, the type of conversion and bacteria involved are presented in Table 1-1. However, the AD process is not completed until the substrate has encountered all the four stages, with each having a unique microbial population that requires disparate ecological conditions (Eliyan 2007). Almost 65% of CH_4 is derived from acetic acids through acetate decarboxylation with the remaining 35% of CH_4 is formed from CO_2 reduction (Nayono 2010).

It is reported that acidogens and methanogens are considered to be the two-dominant species implicated in the last steps usually inhibited at acidic pH (low pH) while acidogens are fast growers and are slightly affected by environmental variations (Mateescu and Constantinescu 2011). AD was formerly designed for sewage sludge and animal manure (Prabhu and Mutnuri 2016). Studies have shown that manure and sewage sludge alone are not suitable materials known for higher potentials in most AD systems. To increase the efficiencies in the AD process, biodigesters are now operated via anaerobic co-digestion (AcoD) process where two or more feedstocks are fed into the same system (Vlachopoulou 2010a). A major advantage of industrial AD process is the higher volume of organic matter reduction (Kougias and Angelidaki 2018).

The AD of manure and sewage sludge have a lower potential for bioenergy production, however, these substrates can be improved by operating under AcoD (Vlachopoulou 2010b). The AD pathway for biogas production is outlined as in Figure 2-1.

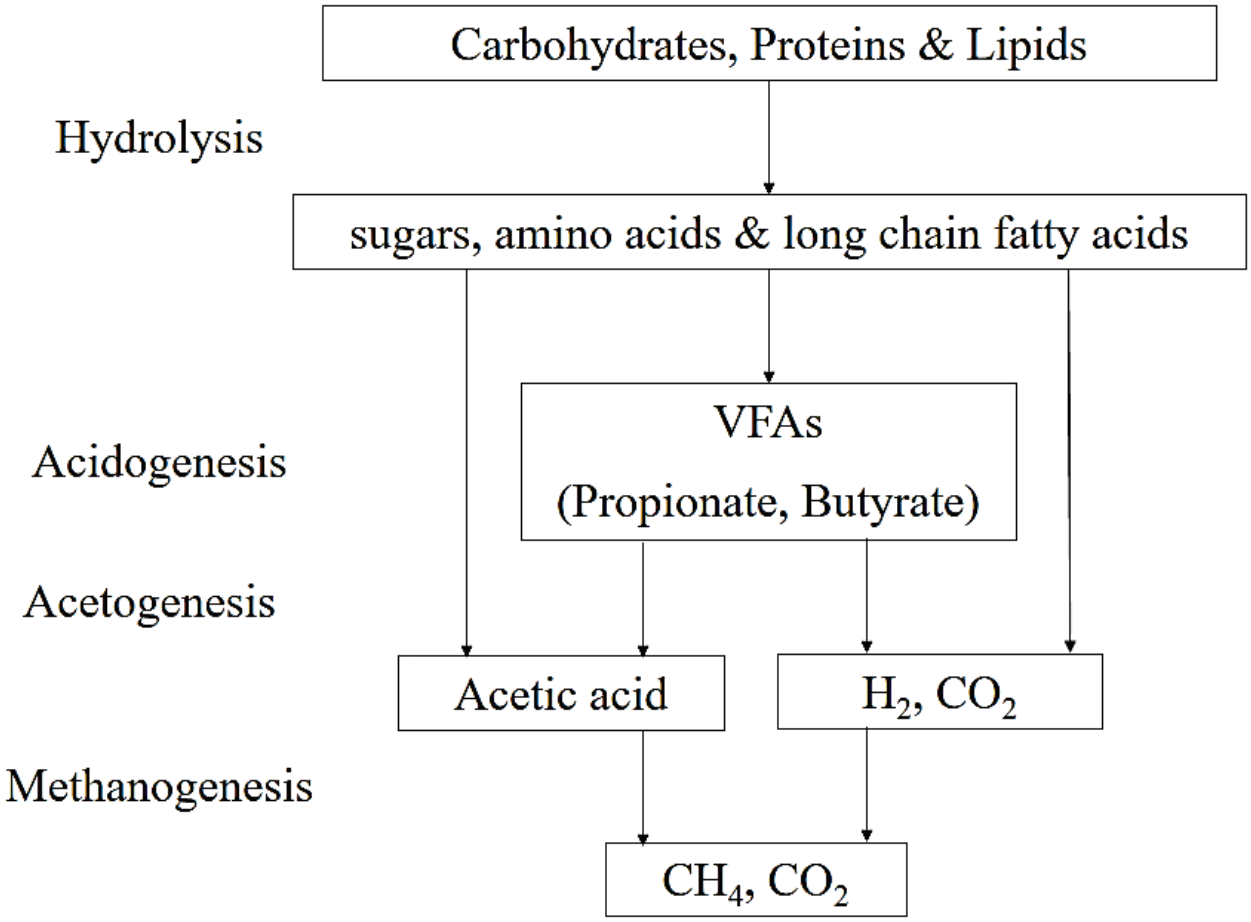

Figure 2- 1. Schematic pathway of the AD process adapted from Clifford (2017).

2.2.1 Stage 1- Hydrolysis

This stage is often referred as *the rate-limiting step* as materials considered rich in fibre are employed as feedstock (Vorgelegt 2017; Ravi 2018). Some of the bacteria involved during hydrolysis include the *Clostridium, Bacillus, Proteus vulgaris, Vibrio, Bacteroides* and

Staphylococcus (Deepanraj, Sivasubramanian and Jayaraj 2014a) as presented in Table 2-1. According to Saady and Massé (2015), the hydrolysis process defined earlier as the rate limiting step converts polymeric materials into fatty acids, amino acids and sugars. Carbohydrates are rapidly converted to simpler sugars which are fermented to VFAs by hydrolysis (Mata-Alvarez *et al.* 2014).

2.2.2 Stage 2 - Acidogenesis

In this stage, acids are formed and a class of anaerobes are responsible for the biodegradation process from the subsequent process (Esposito *et al.* 2012). Soluble organic compounds from the hydrolysis stage are then converted into organic acids (acetates, butyrates and propionic acids), alcohol, H_2 and CO_2 by acid forming bacteria known as acidogens (Eliyan 2007). Commonly found bacteria involved in the biodegradation processes are *Escherichia, Bacillus, Lactobacillus, Staphylococcus, Pseudomonas, Veollonella, Sarcina,* and *Desulfobacter* (Deepanraj, Sivasubramanian and Jayaraj 2014a) as presented in Table 2-1

2.2.3 Stage 3 - Acetogenesis

In this process, acetates are formed as a series of organic acids, viz butyrate, propionate and some alcohols derived from the acid forming stage (Monnet 2003a). However, the bridge that binds both acido- and aceto- processes indicates that acetogens become open to an environment with H_2. It is difficult to distinguish between the acidogenesis and the acetogenesis process as some molecules are degraded internally as reported in an earlier published work (Monnet 2003b). Most bacteria

involved in this stage includes; *Clostridium, Syntrophonas wolfeii* and *Syntrophomonas wolinii* (Deepanraj, Sivasubramanian and Jayaraj 2014a) as presented in Table 2-1. The principal acids (VFAs) produced in this stage are propionic (CH_3CH_2COOH), acetic (CH_3COOH), ethanol (C_2H_5OH) and butyric acids ($CH_3CH_2CH_2COOH$). Ethanol (C_2H_5OH) is also produced.

2.2.4 Stage 4 - Methanogenesis

Several micro-organisms have been employed for biodegradation in most AD bioreactors but among them, methanogens have been found to be the most sensitive, and difficult to study its culture-based methods (Prabhu and Mutnuri 2016). The methanogenic population at large, influences the fate of the AD process by using a polymerase chain reaction of a methyl coenzyme M reductase (*mcrA*) gene target as a molecular marker (Traversi *et al.* 2011; Nikolausz *et al.* 2013; Prabhudessai 2013). The bacteria could be either acetogens or hydrogenotrophs and includes the acetoclastic pathway and hydrogenotrophic pathway (Prabhu and Mutnuri 2016). Most bacteria involved in this stage include *Methanobacterium formicicum, Methanosaeta, Methanosarcina* and *Methanospirilum* (Deepanraj, Sivasubramanian and Jayaraj 2014a) as presented in Table 2-1. Other methanogens such as *Methanomicrobiales, Methanobacteriales,* and *Methanococcales* are also relevant for biogas production through the hydrogenotrophic pathway. Table 2-1 details the four main stages of the AD process, various chemical reactions and the microorganisms involved. The role played by methanogenic bacteria is largely reliant on hydrogen gas (H_2) balances in the system as this could lead to inhibition. A typical example is the marginally alkaline medium formed from by the ammonia through protein degradation. This counterbalances several VFAs produced as an acidic medium is generated which could result in digester failure.

Table 2- 1. The four (4) stages of the AD process, equations and microorganisms involved.

Breakdown process	**Type of conversion**	**Bacteria involved**
Hydrolysis $(C_6H_{10}O_5)n + nH_2O \rightarrow n(C_6H_{12}O_6)$	Proteins are converted to soluble peptides and amino acids, carbohydrates to soluble sugars and lipids to fatty acids or alcohols	*Clostridium* *Clostridium* *Micrococcus* *Lactobacillus*
Acidogenesis $C_6H_{12}O_6 + 2H_2O \longrightarrow 2CH_3COOH + 4H_2+CO_2$ $C_6H_{12}O_6 + 2H_2 \longrightarrow 2CH_3CH_2COOH + 2H_2O$ $C_6H_{12}O_6 \longrightarrow CH_3CH_2COOH + 2H_2+ 2CO_2$	Amino acids are converted to fatty acids, acetate and NH_3 and sugars to intermediary fermentation products	*Clostridium*
Acetogenesis $CH_3CH_2OH + H_2O \longrightarrow C_2H_3O_2^- + 2H_2$ $2CH_3CH_2OH + 2CO_2 \longrightarrow CH_4 + 2C_2H_3O_2^-$	Higher fatty acids or alcohols to hydrogen and acetate Volatile fatty acids and alcohols to acetate or hydrogen	*Clostridium* *Syntrophomonas wolfei*
Methanogenesis $CH_3COOH \longrightarrow CH_4 + CO_2$ $CO_2 + 4H_2 \rightarrow CH_4 + 2H_2O$	Acetates are finally converted to CH_4 and CO_2. H_2 and CO_2 are also converted to CH_4	*Methanosaeta, Methanosarcina* *Methanobacterium formicicum, Methanobrevibacterium*

The advancement and the optimisation of AD is needed to improve WWT sustainability such as its use in the treatment of different WW types. Municipal WW treatment, industrial wastewater treatment and agricultural farming are some of the applications found in the past decades. Some of the advantages of the AD process are stated as;

1. the biogas produced serves as a green source of energy for power generation

2. accommodation of higher chemical oxygen demand (COD) loading

3. it is employed for use in low strength wastewaters treatments with good configurations of reactors.

4. the removal of various toxicants in WW streams

2.3 Factors influencing the anaerobic digestion process

Studying and monitoring the discrepancies in anaerobic biodigesters is a vital step for decision making. Some of the process parameters include pH, temperature, organic loading rate (OLR) and the hydraulic retention time (HRT), and any sharp changes could affect the biogas rate. These parameters are detailed below;

2.3.1. Temperature

Different temperature ranges of anaerobic fermentation have been found to occur namely, psychrophilic (<25 °C), mesophilic (30 to 40 °C) and thermophilic (50 to 60 °C) (Bouallagui *et al.* 2009; Kwietniewska and Tys 2014). Mesophilic and thermophilic temperatures were adopted in this present study together with biodigester performances under room temperature of 25°C.

The temperatures reported during an AD process have stronger effects on the methanogenic consortia accessibility to the substrate (Young 2012). The overall digestion time could last for 3-7 days or 15-30 days for a typical digestion period under thermophilic and mesophilic temperatures respectively (Speece *et al.* 2006; Young 2012; Maile, Muzenda and Mbohwa 2016a). In a study by Tan *et al.* (2018), a thermophilically acclimated inoculum sludge was used for a mesophilic BMP test. It was found that the lag phase was prolonged during the fermentation process. Their recommendation was that in working with mesophilic BMP tests, mesophilically acclimated inoculum sludge should be used to evaluate the lag phase of the mesophilic CH_4 fermentation as adopted in this present study. A shorter lag phase encountered for thermophilic temperatures was attributed to higher metabolic rates during the AD process.

The thermophilic temperature has been found to be more advantageous to that of mesophilic temperature for several reasons. Some of the reasons include: thermophiles can survive at high OLR (Suhartini, Heaven and Banks 2014; Lina *et al.* 2018), shorter HRTs (approximately 5 days) (Maile, Muzenda and Mbohwa 2016a), achieving better long chain fatty acid degradation (Labatut, Angenent and Scott 2014) and produce low volumes of digestates which are dependent on substrate chemical composition (Kougias and Angelidaki 2018). In addition, this includes the advancement in the energy balance, lowers the capital cost with smaller biodigesters (Ghasimi *et al.* 2015) and the increase in the hydrolysis rate coupled with higher biogas production (Lina *et al.* 2018). A more stable reactor has been found to decrease the risk of having unexpected fouling and stress of the entire system, with an increase in OLR to the biodigester (Young 2012; Da Ros *et al.* 2017). Figure 2-2 shows the plot of the varying temperatures versus rate of AD.

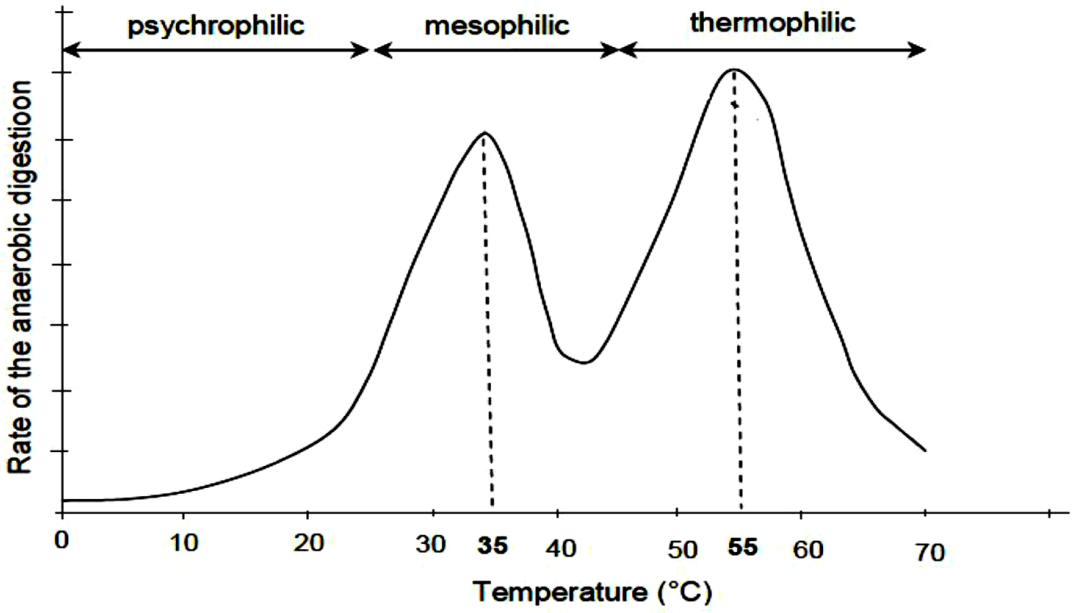

Figure 2- 2. Plot of the varying temperatures versus rate of AD reported in literature (Wu *et al.* 2019).

2.3.2. pH

The pH value during AD is an important parameter affecting the growth of microbes. It has been found that the pH of a biodigester is best kept within the desired ranges of 6.8 to 7.2 (Sreekrishnan, Kohli and Rana 2004), 6.0 to 8.5 (Kougias and Angelidaki 2018) or 6.8 to 7.5 (Hallenbeck 2011) by operating at an optimum OLR to achieve a higher biogas yield. Deressa *et al.* (2015) proposed that the AD process is sensitive to pH adjustment and that for a healthy system, the pH should be maintained at 6.7-7.4. pH surpassing or dropping sharply below the optimum ranges reported could cause a decline or a sudden decrease in CH_4 production (Kougias and Angelidaki 2018). This arises from organic acid accumulations in the biodigesters which could be corrected by CO_2 removal. The VFAs production rate is much higher than the CH_4 production rate, resulting in pH levels

below the optimum range which could inhibit methanogens because of the high level of sensitivity to acidic conditions (Khanal 2008; Nijaguna 2012).

2.3.3 Mixing or agitation

This process parameter ensures good contact between the combined substrates and the microorganisms present in the biodigester. Absence of stirring results in the reduction of specific gas production rate of reactors during the AD process (Gomez *et al.* 2006). Mixing is required in the digester to maintain homogeneity and stability by preventing solid deposition at the bottom of the biodigesters and producing a higher CH_4 yield (Kaparaju *et al.* 2008).

Mixing aids in combining freshly incoming materials during a continuous process with microorganisms, thereby, preventing the formation of scum in biodigesters which helps to maintain a uniform substrate concentration and other environmental factors (Deepanraj, Sivasubramanian and Jayaraj 2014b). Also, according to Madondo (2017), mixing during an AD process is useful as it aids in scum removal, and prevent the creation of layers at varied temperatures to ensure good interaction between the energetic biomass and the sludge. The AD process is able to perform with low mixing conditions (Gomez *et al.* 2006).

2.3.4 Organic loading rate (OLR)

This is the amount of organic matter, volatile solids (VS) or COD of the digester volume in a day (Vartak *et al.* 1997; Nayono 2010). Biogas production is much dependent on the loading rate as CH_4 yield has been found to increase with a reduction in the OLR (Vartak *et al.* 1997; Prabhu and Mutnuri 2016). Gomez *et al.* (2006) have also proposed in a study which contrasts with that of

Vartak *et al.* (1997) that AcoD estimated at varying OLR under low mixing conditions and a steady performance could be achieved when the system is overloaded. Overloading could easily lead to failure of biodigesters (Abbasi, Tauseef and Abbasi 2012; Haider *et al.* 2015). This could happen if there is inadequate mixing of the waste with slurry. Foaming has also been found to be problematic in most feedstocks used in the AD process resulting in digester failure (Moeller *et al.* 2012; Suhartini 2014). According to Trnovec and Britz (1998), the most favorable COD removal of the canning industry effluent was found to be between 89% and 93% at OLRs of 9.8 and 10.95 kg COD/m^3/d at an HRT of 10 hours and a substrate pH of 5.5. The effect of OLR on CH_4 production during AD of vegetables waste has also been investigated (Babaee and Shayegan 2011).

In this study, a complete-mix, pilot-scale digester with working volume of 70 liters operating at different organic feeding rates of 1.4, 2 and 2.75 kg VS/ (m^3/d) was employed. The composition of CH_4 between 49.7 and 64% and biogas production was 0.12 to 0.4 m^3 biogas/kgVS. It was observed that as the OLR increased, the VS degradation and biogas yield decreased. In determining the impact of OLR on psychrophilic AD of solid dairy manure, two laboratory-scale sequence batch bioreactors run in duplicate were also investigated (Saady and Massé 2015). This was operated at an OLR in the range of 6.0 to 8.0 g total COD (tCOD) kg^{-1} inoculum day^{-1} (d^{-1}) for approximately 210 days.

The OLR is thus calculated using the following equation according to Nayono (2010);

$$\mathrm{OLR} = \frac{\mathrm{OC_{fd}} \times \mathrm{Q_{fd}}}{\mathrm{V_r}} \quad \left[\frac{\mathrm{kg.m^{-3}} \times \mathrm{m^3.d^{-1}}}{\mathrm{m^3}}\right] \qquad (2.1)$$

Where

OC_{fd} is the substrate's concentration in terms of the COD or VS; V_r is the reactor volume; and Q_{fd} is the feeding rate of the substrate.

2.3.5 Hydraulic retention time (HRT)

The HRT is the average time a soluble compound remains in a bioreactor and is estimated by dividing the total capacity of the digestion tank by the rate at which matter is fed (Ibrahim, Quaik and Ismail 2016). This is also the average residence time a waste suspension in a bioreactor and it is calculated by comparing the volume of the liquid in the biodigester and the withdrawal rate of the effluent (Nayono 2010). The retention time for waste treated in a mesophilic digester ranges from 15 to 30 days and 12 to 14 days for thermophilic biodigesters (Monnet 2003a). Longer HRTs (more than 20 days) have been found to be suitable for AD as shorter HRTs below 20 days result in process instability due to VFAs accumulation (Dareioti and Kornaros 2014). Nonetheless, Nghiem *et al.* (2014) have also reported a stable CH_4 yield at an HRT of less than 20 days.

Zhang *et al.* (2006) also examined the effects of HRT on biohydrogen production. In their study, they observed an anaerobic microbial community grown with glucose in a continuous stirred tank reactor (CSTR) culture. The HRT is calculated using equation (2.2) according to Nayono (2010);

$$\mathrm{HRT} = \frac{V_r}{Q_w}\left(\frac{m^3}{m^3.d^{-1}}\right) \qquad (2.2)$$

where HRT = hydraulic retention time in days; Q_W = effluent withdrawal; and V_r = volume of the reactor.

2.3.6. Seeding/nutrient addition

Several enzymes make use of metal ions in anaerobic biodigesters (Jarvis *et al.* 1997; Zhang *et al.* 2003). Nutrient addition in the AD of water hyacinth (WH) has been found to be limiting (Xie, Qin and Yu 2004; O'Sullivan *et al.* 2010). A complex substrate source is preferable for a better nutritional balance within the process. Achieving an adequate growth rate of the microorganisms and enhancing the biogas production requires a suitable nutrient addition. Besides the electron acceptor required in anaerobic biodigesters, some energy sources such as proteins, fats, and carbohydrates are also required and are oxidized into useful products which aids in the stabilisation of the AD process (Schnürer and Jarvis 2009).

2.4 Effect of inoculation on AD process parameters

Since the four stages of the AD process for biomethane production are controlled by bacteria, the product formed varies with the type of bacterial population (Singh *et al.* 2012). During the AD process, the organic fraction of the substrate is mostly converted to CH_4 and CO_2 while other fractions are converted to sulphides by sulphate reducing bacteria which tend to compete with methanogens (Chynoweth, Owens and Legrand 2001). With regards to the OLR, the maximum CH_4 potential has been achieved at an inoculum to substrate ratio (ISR) of 2.0 at 332.9 mL/gVS. Also, higher ISR values have been reported to result in higher CH_4 yield (Rodriguez-Chiang and Dahl 2014). The lowest ISR of 0.5 also showed the occurrence of process inhibition due to VFA accumulation.

It has been found that higher amount of inoculum shows positive effect on the AcoD of food waste and rice husk (Haider *et al.* 2015). The use of inoculum has been found to ensure a stable

methanogenic community establishment in the shortest possible time of 5 to 10 days (O'Sullivan *et al.* 2010).

Upon the addition of higher amounts of inoculum to a biodigester, more anaerobic microorganisms are added leading to an increase in the biodegradation process. However, the biodegradation rate of the substrate and the lag phase as shown in figure 2-3 (a state where the microbes acclimatise to the medium and the physical conditions available by inducing the necessary enzymes for growth) are dependent on the concentration of microorganisms in a biodigester (Elbeshbishy, Nakhla and Hafez 2012; Rolfe *et al.* 2012). After the lag phase is the log phase where the microorganisms begin to stabilize until at the stationary phase where there is total acclimimatisation within the consortium. Over time, available feedstocks become used up and some microbes become denatured or over-saturated due to VFA production that takes place in the AD process. This affect the microbial activities and subsequently, lead to a decline (death phase) in the microbial population as depicted in figure 2-3. Figure 2-3 shows the lag phase pattern and the growth of the microbes with number of cells as a function of time.

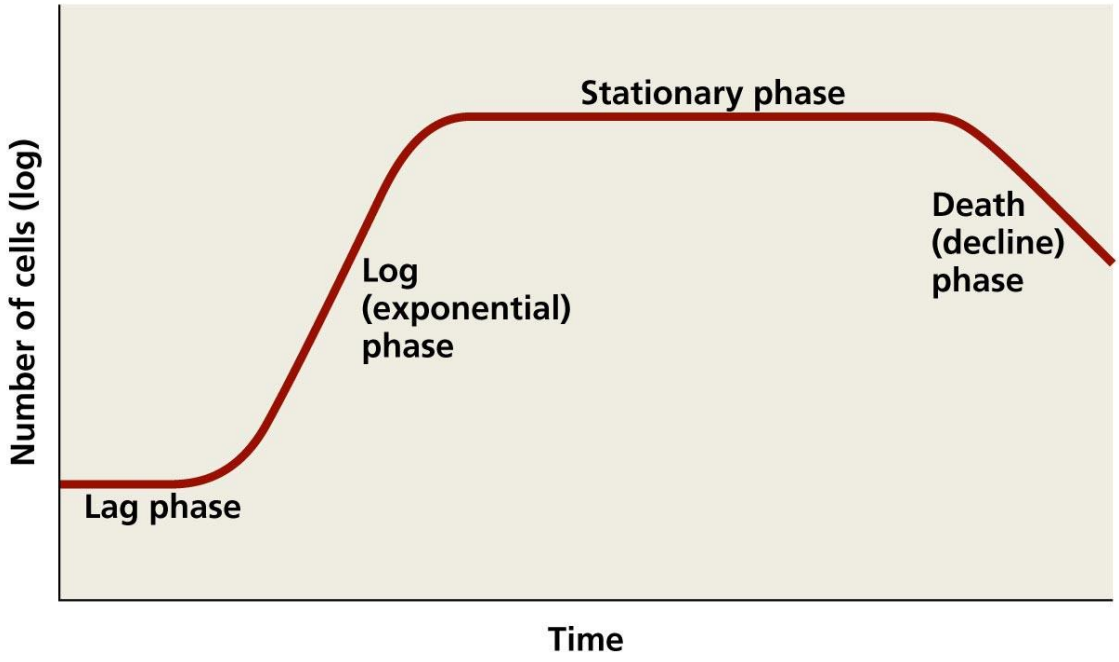

Figure 2- 3. Life cycle of inoculum for an AD process adapted from Rolfe *et al.* (2012).

A single stage digestion of vegetable waste has been found to be preferred over multi-stage digestion owing to its lower investment cost and simpler design. However, an exception to this is the high loading rate that affects the growth and methanogenic activity (Singh *et al.* 2012). It has been found that rapid acidification occurs as a result of the high biodegradable organic content of vegetable waste and the production of VFAs which inhibit the activities of methanogenic bacteria (Singh *et al.* 2012). Lignocellulose have high carbon and low nitrogen content which leads to a decrease in biogas production, therefore excess nitrogen is provided in the process to meet the optimum carbon-nitrogen ratio of 20 to 30 required by methanogens (Chandra, Takeuchi and Hasegawa 2012). Methanogenic bacteria are also sensitive to pH changes (Maile, Muzenda and Mbohwa 2016d). The methanogenic bacteria which strictly survive in the absence of molecular oxygen usually have a pH greater than 7. They can survive optimally in the pH range of 6.5 to 7.5,

and sometimes up to 8.5 (Anonymous, 1989; FAO/CMS, 1996). The amount of carbon and nitrogen in the waste also effects the growth of the anaerobes.

2.4.1 Sources of inocula

The assessment of a biogas plant can be measured by studying the variations in parameters such as temperature, OLR, HRT, nutrient addition, substrate to inoculum ratio (S/I), the addition of co-substrates and the pH (Karakashev, Batstone and Angelidaki 2005). More so, any sharp increase or decrease with regards to these parameters adversely, affect the biogas production process. For higher efficiencies, these parameters should be varied within a desirable range to operate biogas plants.

2.4.1.1 Nutrient addition

Trace nutrients such as cobalt (Co), nickel (Ni), iron (Fe), and molybdenum (Mo) together with macronutrients such as magnesium (Mg), sodium (Na), potassium (K), and calcium (Ca) are essential for cell growth. These nutrients found in the inoculum play vital roles in anaerobic reactor start-up and operation and may be supplemented to reaction mixture if necessary (Schattauer *et al.* 2011; Nges and Björnsson 2012). Nutrient addition is key as the anaerobic digestion of biomass has been found to be nutrient dependent (Xie, Qin and Yu 2004; O'Sullivan *et al.* 2010). It was found that high concentrations of trace elements such as nickel (Ni) (35.2 mg. kg^{-1}) and molybdenum (Mo) (15.4 mg. kg^{-1}) in the inoculum increases the CH_4 production resulting in volatile solids concentration of 140.7 mL/gVS (Parra-Orobio *et al.* 2018).

Methanogens require specific micronutrients for metabolism and bacteria growth (Gu *et al.* 2014). Higher concentrations of micronutrients in a particular inoculum contributes to better performances even though certain toxins have been found to inhibit the AD process (Chen, Cheng and Creamer 2008). The AD process may be improved by the presence of micronutrients and enzymatic activities such as the synergy between cellulase and xylanase in lignocellulosic degradation (Zhang, Lee and Jahng 2011).

Calcium carbonate ($CaCO_3$) has been established as a good buffer for the AD process and serves as a source of nutrients to microorganisms (Maile, Muzenda and Mbohwa 2016e). In the AD of food waste with cow manure at a ratio of 3:1, the biogas yield was 47 mL/gVS whilst that of fruit and vegetable waste was reported to be 37 mL/gVS(Njoku *et al.* 2015).

2.4.1.2 pH and temperature

The pH inside a biodigester has been found to enhance upon ammonium chloride (NH_4Cl) addition (Nges and Björnsson 2012). The inclusion of this buffering capacity to a particular feedstock was sustained at a pH within a favorable range for methanogenesis at 6.8-7.2 (Chen, Cheng and Creamer 2008). That is, methanogenic bacteria typically develop under inert conditions, with environmental pH of 6.8-7.2 as reported by Shah *et al.* (2014). The effect of low pH on methanogenic bacteria has been confirmed by various research reports and it has also been found that methanogenic bacteria are more sensitive to pH changes (Maile, Muzenda and Mbohwa 2016d). Acetate decomposers, *Methanosarcina* species and *Methanosarcina barkeri* were first isolated from the environment at an approximate pH of 5 while hydrogen-oxidizing methanogens and methylotrophic were found in a strongly alkaline environments (Mah and Sussman 1968). Psychrophilic, mesophilic and thermophilic microorganisms found within methanogens are

distinguishable. The temperature for a methanogenic consortium play a very important role in the AD process their enzymatic enzymatic structures are sensitive to changes (Gonzalez-Martinez *et al.* 2018).

It is evidenced that the temperature of BMP tests which is usually carried out at mesophilic (35ºC) or thermophilic (55°C) conditions should be the same as the operating temperature of the digester containing the inoculum. Increasing the diversity of the microbial community could also be achieved by mixing inoculum from different sources under a common temperature condition (Angelidaki *et al.* 2009).

2.4.1.3 Addition of co-substrates

Co-substrates could compensate for the shortage of nutrient in wastewater systems with mono-substrates. In a few studies, supplementation with commercial products present the various contributions in an inoculum (Tsapekos, Kougias and Angelidaki 2015). An appropriate range of nutrients is very important for an AD process. The demand for nutrients, macro and micro forms required for the AD process can be satisfied using inoculum only, without chemical addition (Gu *et al.* 2014). Inoculum does not only provide microorganisms for the biodegradation in AD but also serves as a source of nutrient supplement and adds to the alkalinity (Gu *et al.* 2014). Fresh cow dung has been extensively researched for use in biogas production. According to Jayaweera *et al.* (2007), WH was mixed with fresh cow dung as the inoculum to seed methanogens for the improvement of the C/N ratio. The biodegradability of the WH was improved during the AD process for biogas production (Jayaweera *et al.* 2007).

2.4.1.4 Organic loading rate

Higher values of the inoculum to feedstock (I/F) ratio shows an optimistic outcome for an AcoD process (Haider *et al.* 2015). However, the addition of large volumes of inoculum into a biodigester, improves the varieties of anaerobic microorganisms which subsequently, lead to an increase in the biodegradation process. The biodegradation rate of the substrate and the lag phase is dependent on the microorgnaisms concentration within a biodigester (Elbeshbishy, Nakhla and Hafez 2012). The AD in CSTRs have been found to operate at OLR below their optimum capacity in avoiding overloads and sludge retention times (SRT) in the order of 20 days or more.

2.4.2 Microorganism selection, culturing, and inhibition

Low volatile fatty acid (LVFA) concentration indicates adaptation and increased tolerance of the microbial community to high levels of free ammonia as well as high conductivity (Chen, Cheng and Creamer 2008; Schnürer and Nordberg 2008). Various inhibitory substances such as NH_3, sulfide, light metal ions, heavy metals and organics have been found to cause failures in anaerobic digesters as a result of their presence in substantial concentrations in wastes streams (Chen, Cheng and Creamer 2008). The presence of free NH_3 concentration (up to 7 g NH_4-N L^{-1}) in an inoculum inhibits methanogenic bacteria and hence, contributes to a slow rate of CH_4 production during a BMP test (Angelidaki and Ahring 1993; Chen, Cheng and Creamer 2008). An ammonium-based inoculum was observed to operate at a longer hydraulic retention time during the optimisation of biogas production in a CSTR reactor operated with grass manure (Liu *et al.* 2017a), The screening for the collection of microorganisms collected from the natural environments could help in the identification of strains that have higher inhibitor resistances. According to a study by Favaro *et al.* (2013), strains of *S. cerevisiae* were collected from grape marc in a winery revealed strains

which had comparatively higher resistance to furan aldehydes, aliphatic carboxylic acids and SCB hydrolysate. The advances in evolutionary engineering include yeast strains such as *Saccharomyces cerevisiae* which are known to exhibit an improved resistance to spruce wood hydrolysate (Koppram, Albers and Olsson 2012), corn stover hydrolysate (Koppram, Albers and Olsson 2012) and triticale straw (Smith, Van Rensburg and Görgens 2014). Also, Wimalasena *et al.* (2014) screened ninety (90) strains of the microbe, *Saccharomyces spp.*, with an evaluation of their resistance to acetic acid and furfural. It was deduced that a vital prediction of the microbes is dependent on the specific productivity of the microorganism present. This results from the fact that the resistance to inhibitors is not suitable to make microorganisms suitable for an industrial production process. Cellulosic enzyme inhibition can be side-stepped by the enzymatic hydrolysis of cellulose and microbial fermentation simultaneously (Jönsson and Martín 2016). In recent years, the adoption of process designs have been devised where fermentative microorganisms contribute to enzyme supplies (Olson *et al.* 2012). Some of these designs includes the consolidated bioprocess (CBP) and the fed batch mode (Hoyer, Galbe and Zacchi 2010; Olson *et al.* 2012). Table 2.2 presents a comparative study of the different feedstocks, inoculum used and the CH_4 contents reported in previous studies.

Table 2- 2. Comparative study of the different feedstocks, inocula used and methanse contents.

Feedstock	**Inoculum**	**Temperature**	**pH**	**HRT (days)**	CH_4 **content (%)**	**References**
Food waste	Cow manure	29ºC	6.0-7.2	55	47	(Deressa *et al.* 2015)
Fruit and vegetable waste	Cow manure	29ºC	6.0-7.2	55	37	(Deressa *et al.* 2015)
Municipal solid waste	Cow dung	37ºC	6.5-7.5	4	58	(Maile, Muzenda and Mbohwa 2016e)
Fruit and vegetable waste	Cow dung	37ºC	6.5-7.5	5	55	(Maile, Muzenda and Mbohwa 2016d)
Miscanthus Fuscus	Cow dung	37ºC	6.7-7.0	20	27	(Tetteh *et al.* 2017)
WH	Cow dung	30ºC	7.4-8.5	36	51	(Njoku *et al.* 2015)
SCB	Sewage sludge	37ºC	5.5-8.5	23	50	(Simo, Jong and Kapseu 2016)
Sugar beet	Slaughterhouse waste and pig manure	37ºC	6.5-7.5	40	58	(Nges and Björnsson 2012)

2.5 Types of anaerobic digestion biodigesters

There are several types of anaerobic biodigester that have been employed in the past decades. Some of these includes the upflow and down flow fixed-bed biodigesters, batch biodigesters, continuously stirred tank biodigesters and the upflow anaerobic sludge blanket (Young 2012).. The start-up of an anaerobic biodigester is considered a delicate step for a successful AD operation (Haider *et al.* 2015). However, it is for this reason that specific amount of inoculum is added to biodigesters together with substrates thereby providing the necessary microorganisms to start-up AD. It is found that the rate of substrate biodegradation and the lag phase is dependent on the concentration of the microorganisms (Elbeshbishy, Nakhla and Hafez 2012).

2.5.1 Upflow and down flow fixed-bed biodigesters

In the treatment of industrial wastewater using the upflow fixed-bed reactor, the wastewater is made to pass through a particle medium resulting in a large amount of the retained biomass not being attached to the packing column (Chamane 2008). The unattached material is returned in the interstices between the medium particles partially by settling and partly through the influence of physical contact. A drawback in the use of this system has been blockages due to excess biomass accumulation which in turn results in decreased retention capacity of the bed. In the case of the down flow fixed bed reactor, the suspended solids and biofilm solids is carried down with the liquid flow and out of the biodigester. Systems such as these are found to withstand severe hydraulic overloading conditions even with slight reduction in treatment efficiency (Wu *et al.* 1996; Al-Dahhan *et al.* 1997; Chamane 2008). Figure 2-4 shows the schematic diagram of the upflow and downflow fixed bed reactors.

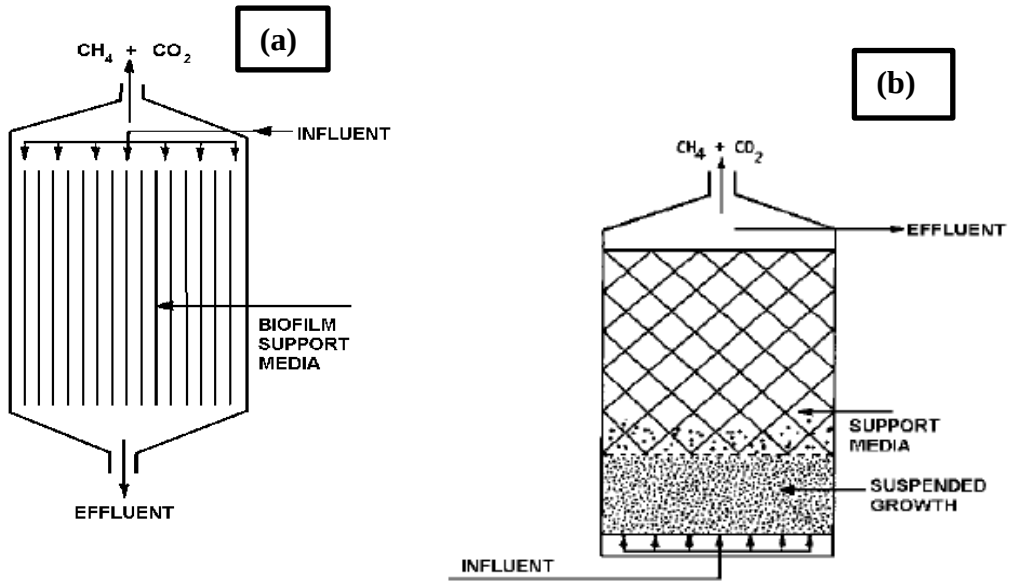

Figure 2- 4. Schematic diagrams of (a) downward flow fixed bed reactor (b) upflow fixed and fixed bed reactor (Chamane 2008; James 2015; Kong, Wang and Ren 2015).

2.5.2 Batch biodigesters

BMP tests have since been employed in the past decades for small scale laboratory study in batch biodigesters (Maile, Muzenda and Mbohwa 2016e). According to Adl, Sheng and Gharibi (2012), anaerobic batch tests are the standard method for the determination of CH_4 yield potential of substrates. The decision based on the time to terminate the experiment is observed to be vital in these tests. These biodigesters are operated by the combination of anaerobic inoculum and wastes in a sealed vessel. In practice, the feed (influent) is fed to the reactor followed by the homogenising of the substrates and finally, the completion of the reaction where the effluent is collected with respect to time, t, as illustrated in Figure 2.5 (a), (b) and (c), respectively. It has been found that reactions under batch systems usually involve purging biodigesters with non-reactive gases such

as nitrogen gas (N_2), argon (Ar) or hydrogen gas (H_2) to create the anaerobic digestion environment (Young 2012) as employed in this present study. The use of batch digesters is gaining increasing recognition because it is simple to operate as the sludge is pumped and received, until the desired volume is attained. The system is left to degrade at an HRT of 20-45 days as the remaining solids are pumped out of the system (Moody *et al.* 2009; Koupaie, Johnson and Eskicioglu 2017). When the system is supplemented with an alkaline solution to reduce the pH from inhibitory levels, fouling is not a major interest. Batch processes do not provide information regarding possible negative or positive synergistic effects on the CH_4 yield as they can be used to assess changes in degradation kinetics and CH_4 formation (Koch, Helmreich and Drewes 2015). Also, these kind of biodigesters have been found to absorb the disturbances of shock loadings under low mixing and present a major drawback in maintenance (Gomez *et al.* 2006). These drawbacks arises from the remaining solids that adhere to the walls of the biodigesters, and which are not fully flushed out within the system leading to the formation of dead spaces requiring full system cleaning (Young 2012; Mao *et al.* 2015b).

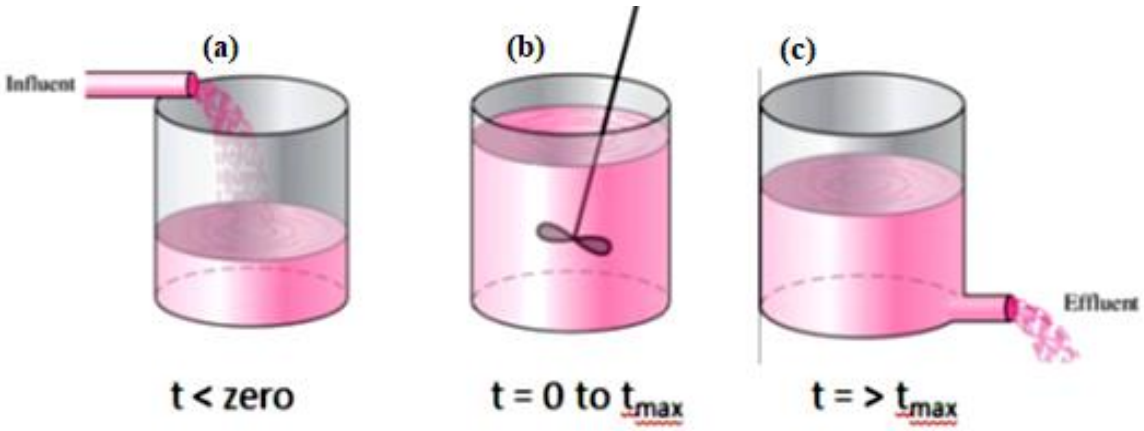

Figure 2- 5. Schematic of a batch anaerobic digester adapted from Chamane (2008).

2.5.3 Continuous stirred tank reactors (CSTR)

CSTRs are a mechanical agitation unit that consist of a vertical shaft along several baffles with impellers. The activity of agitation in the CSTR vessel is generally obtained by a paddle or screw systems positioned near the base of the assembly (Chamane 2008). Figure 2-6 depicts the schematic of a typical CSTR.

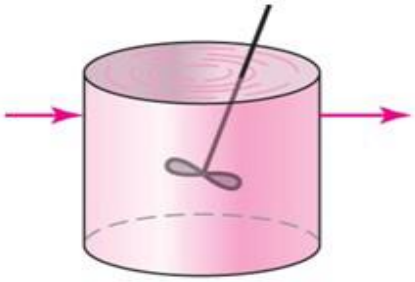

Figure 2- 6. Schematic of a typical CSTR with stirrer adapted from Chamane (2008).

It is vital to study the performances of CSTRs for bioenergy production from organic and other waste materials. CSTRs are largely designed for the treatment of slurries such as manure with a total suspended solid (TSS) within the range of 30 to 80g/L (Kougias and Angelidaki 2018). The use of a CSTR in chemical industries is to convert reactants into valuable products (Cahyari, Syamsiah and Prasetya 2016). It has been found to be used commonly for liquid substrate reactions and is seldomly used for gas phase reactions. The conversion or the fermentation of organic wastes into renewable fuel such as biohydrogen occur in three phases namely liquid, solid or gas phase (Arooj *et al.* 2008). The control at optimum conditions, for example, pH, reduction of substrates and inhibitory chemical concentration of the fermentation is a challenging task for a three phase CSTR. A change in the OLR has been found to cause significant drawback in the use of CSTR in terms of its stability and performance (Cahyari, Syamsiah and Prasetya 2016). At high OLRs, there exists the tendency for the accumulation of VFAs and other inhibitory compounds resulting

in lower volume of gas production and yield. The same way, a lower OLR has been found to reduce the instability of CSTRs because of adequate ratios among the source of substrates and certain microbial population. Also, the low OLR foils the accumulation of VFAs which controls and maintains the environmental conditions at optimum pH levels of 4 to 6 (Yang and Wang 2017).

Continuous digesters are operated and maintained in the same way as the semi-continuous digesters but the latter involves the constant feeding and drawing of substrates at the same rate. Setbacks in the use of continuous digesters include timing requirements at steady state and difficulty in usage, posing a problem during overloading (Young 2012).

In a study involving biohydrogen production in an anaerobically controlled CSTR using corn starch as substrate at an HRT of 158 days, the VFA profile supported the fact that the butyrate or acetate ratio was the most important parameter to justify hydrogen production at various HRTs (Arooj *et al.* 2008). Figure 2.7 depicts a simple CSTR system consisting of an input and an output stream with constant feedstock quantities prepared for the AD process. In the bioreactors below, feeding is carried out by reactants A and B which are converted through a series of biological steps to form the products, C and D (Achinas and Euverink 2016).

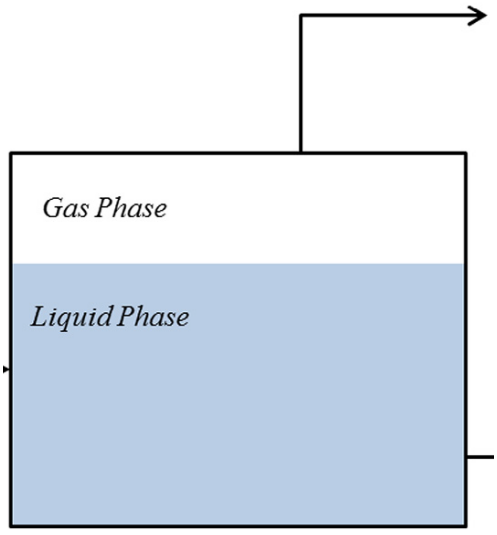

Figure 2- 7. Schematic of a typical CSTR adapted from Achinas and Euverink (2016).

2.5.4 Upflow anaerobic sludge blanket (UASB)

Studies on the high-rate anaerobic sewage treatment started in the early 1980s with the 64 m^3 UASB pilot plants located in California, Colombia, and Brazil (Dutta, Davies and Ikumi 2018). With this build-up, the process was altered to full-scale conditions and slowly introduced into the market (Van Lier *et al.* 2010; Van Lier *et al.* 2015). With a steady rise in the number of large scale municipal UASB sewage treatment plants (STPs) installed in most sub-tropical countries, it led to Brazil and India adopting this technology. The design of a UASB digester is to treat low and medium strength wastewaters at high volumetric loading rates and thus a shorter HRT (Chamane 2008). The phase separator of the UASB is positioned at the top of the reactor, dividing it into a lower digestion zone and an upper settling zone (Wu *et al.* 2018). Because the entire process is based on the immobilisation of the biomass in the form of sludge granules, no supporting system is required therein. WW is presented homogeneously through the bottom of the reactor which then passes the sludge bed and the settling zone through the orifice between the phase separators. On the top of the digestion zone is a settler which enables the system to maintain a large sludge mass

in the reactor as the effluent is discharged relatively free of suspended solids. The use of an UASB has been found to be very efficient for treating wastewater with increasing recognitions as organic materials are degraded to generate biogas and other biofuels (Zhen *et al.* 2017). Advantages in the use of UASB includes the low space requirements, low operating cost power, system compactness, negligible or no energy consumption, stabilised excess sludge production, potential for energy recovery and low-cost accessibility of sewage for agricultural reuse purposes (Van Lier *et al.* 2010; Xu *et al.* 2018). For the optimal performance of a UASB reactor, discharging sludge with a low volumetric sludge activity is very important which is the case for most municipal UASB (Van Lier *et al.* 2010). However, the separation of inert particulates in a UASB reactor of an inorganic sludge portion of the bottom sludge increases progressively. Further, in most CSTRs, discharging sludge from the upper levels from the lower level or drain, prevents the buildup of inert. Figure 2.8 shows the schematic of the UASB.

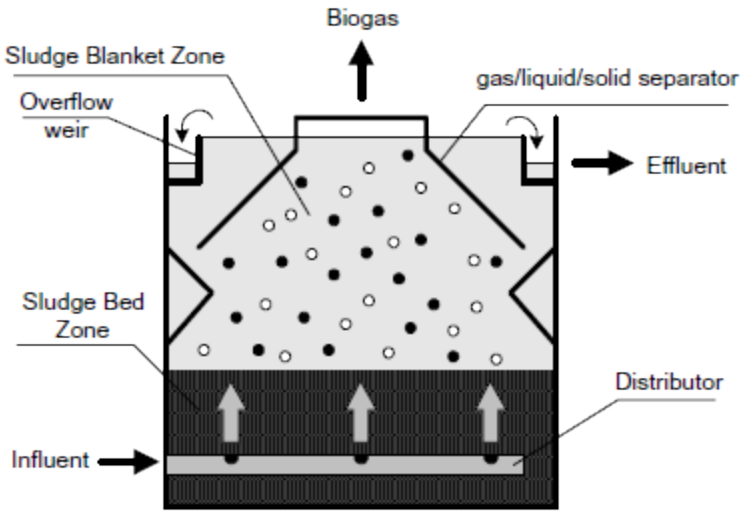

Figure 2- 8. Schematic of a upflow anaerobic sludge blanket (Van Lier et al. 2015).

2.5.5 Digester design

The design of a typical anaerobic digester depends predominantly on the composition of substrate in terms of the solids concentration and the flow rate; and system implementation viz operation and maintenance which are influenced by the economic constraints. Basic design parameters include:

1. flow type: batch, continuous or intermittent

2. stirring systems such as mechanical stirrers

3. temperature ranges from 20°C to 70°C

4. solid retention times (SRT) of 10 to 50 days which largely depends on process temperature and flow rate

5. the organic loading rate which depends on the SRT, flow rate and the number of units in operation

2.6 Anaerobic co-digestion (AcoD)

AcoD was defined as the simultaneous digestion of two or more substrates which is a viable choice in overcoming the drawbacks of mono-digestion and to improve plant's economic feasibility (Eliyan 2007; Mata-Alvarez *et al.* 2014). Patil *et al.* (2014) defined AcoD as the simultaneous digestion of more than one type of waste in the same unit with advantages such as better digestibility and cost sharing. However, several studies have been devised to find ways to improve the performance of biodigesters with this concept of AcoD (Esposito *et al.* 2012).

AcoD improves biogas yield and has been gaining more recognition in the past few decades for providing nutrients and regulation of pH which improves methanogen's efficacy (Haider *et al.*

2015). It has been found that substrates with higher C/N ratios such as paper from the pulp industry and most crop residues are deficient in nitrogen, a vital nutrient source for microbial cell growth (Martin-Ryals 2012). A reportedly high value for the C/N ratio is limited by its nitrogen availability. Also, for substrates with lower C/N ratios, such as some animal manures, toxic ammonia build-up is likely to become a major drawback. Co-digestion of waste biomass and crop biomass has been found to achieve a significant improvement in CH_4 yield compared to digestion of only the waste biomass (Nges 2012; Kougias and Angelidaki 2018). Inhibition in anerobic biodigesters by ammonia is as a result of high nitrogen concentrations which lead to biodigester failures. The co-digestion of cattle manure and chicken manure with fruit and vegetable wastes was observed to be a promising combination in the AD process to produce biogas. The daily CH_4 production and cumulative CH_4 yield were found to be highest for the co-digestion of these substrates in a ratio of 80:20 compared to single substrates (Tawoma 2015). Co-digestion of fruit and vegetable with cattle slurry have also been studied with the feed containing over 30% of these biomasses. This results in high concentrations of volatile fatty acids being produced (Callaghan *et al.* 2002a). Lignocellulosic biomass has a higher potential for bioenergy production through AD. Nonetheless, its high C/N ratio and the complexity of its structure which comprises of 20-25% lignin is inhibited during monodigestion (Paul and Dutta 2018). The monodigestion of energy crops still struggle to meet the decreasing targets faced by the drawbacks encountered in the AD process when compared to AcoD with slurry and energy crops (Fagerström *et al.* 2018).

AD of single substrates present drawbacks associated with substrate characteristics (Mata-Alvarez *et al.* 2014) as AcoD produces higher yield of biogas than AD (Kainthola, Kalamdhada and Goud 2019). Also, the need for co-substrates during AD in a biogas plant has been proposed to acquire both positive and negative effects on the operation which could include the use of bone and meat

meal addition due to its high nitrogen content (Hutňan 2016). Hence, a promising way to optimise the BPR is anaerobic co-digestion (Silvestre *et al.* 2014). To achieve the anaerobic degradation requirements and to compensate for the nitrogen deficiency of rice straw, Kainthola, Kalamdhada and Goud (2019) proposed that the co-digestion with another nitrogen-rich co-substrate could also enhance the biomethane production. Their study thus exhibited the need for AcoD to improve the physicochemical and biochemical state of the process as compared to monodigestion.

With an increase in the amount of cattle manure and organic loading, the CH_4 yield decreased with volatile solids. AcoD of protein rich wastes with carbohydrate rich materials results in a mixed substrate that has a good buffering capacity and a balanced C/N ratio favorable for anaerobic digestion. That is, the performance of the anaerobic digester is improved and biogas production is enhanced (Esposito *et al.* 2012). There is inhibition of single substrates in the AD process by certain types of wastes because of the unbalanced nutrients in feedstocks, rapid digester acidification (Callaghan *et al.* 2002b), high nitrogen and heavy metals concentration, low organic matter content, and the long chain fatty acids. This depends on the substrate to be used and could inhibit the activity of methanogens (Mata-Alvarez *et al.* 2014; Haider *et al.* 2015). The AD process of single and readily biodegradable organic feedstocks could result in the failures of reactors in the absence of buffering agent for pH adjustment (Demirel and Scherer 2008).

The remedy to this is the addition of another feedstock which serves as the co-substrate by adding nutrients and an alkali for the control of the pH in the reactor (Bouallagui *et al.* 2009). Although several advantages have been stated earlier, below are advantages of the AcoD process reported in the past decades;

1. provision of rich balance in the nutrient for C/N ratio boost (Liu *et al.* 2016; Tsapekos *et al.* 2017)

2. inhibitory compounds become easily diluted, thereby sidestepping the decline of the AD process (Tsapekos, Kougias and Angelidaki 2015)

3. it has also been found to enhance the yield of CH_4 production (Dennehy *et al.* 2017)

4. promotion of the synergistic effects leading to advanced biodegradation (Pagés-Díaz *et al.* 2014; Kougias *et al.* 2015).

5. the loading of readily biodegradable matter has been found to increase according to the chemical composition of the substrates (Borowski, Domański and Weatherley 2014)

6. the buffer capacity of the influent mixture has been found to be improved as it maintains the pH levels within the range for methanogenesis (Zhang *et al.* 2013; Wei *et al.* 2015)

2.7 Types of feedstock/biomass (lignocelluloses) for anaerobic digestion

Biomass provides a source of carbon in the AD process. A renewable form of energy such as biogas can be produced from a diverse range of feedstocks which contains biodegradable organic matter (Ravi 2018). It is projected that the yearly production worldwide of lignocellulosic biomass includes both agricultural residues and greenhouse biomass which is about 181.5 billion tonnes (Paul and Dutta 2018). Renewable energy usage has become progressively important globally to attain the variations needed in addressing the impacts of global warming. Hence, the type of biomass required is principally dependent on the energy conversion processes, coupled with the form in which the energy is required (McKendry 2002). CH_4 yield has been found to be dependent on the feedstock-type and the digester system with its corresponding HRT. Ravi (2018) reports that manure from livestock exists as the commonest feedstock suitable for the AD process although the energy content in manure is lower as compared to other substrates. Nutrients (micro and macronutrients) have altered the use of manure to co-digest with energy crops to enhance the yield

of biogas (Weiland 2010). Lignocellulosic materials are generally composed of polymers such as cellulose, hemicellulose and lignin which constitutes the main building blocks (Hamelinck, Van Hooijdonk and Faaij 2005; Hendriks and Zeeman 2009a) and are associated with each other in a hetero-matrix to different degrees. It has reported that factors such as crystallinity of cellulose, lignin content, and particle size do restrict the digestibility of the hemicellulose and cellulose, present in the particular biomass (Hendriks and Zeeman 2009a). The feedstocks could be in the form of decomposable waste materials such as wastepaper, grass clippings, animal wastes and leftover food.

2.7.1 SCB as biomass for biogas production

Harvested sugarcane is conveyed to the sugar mills where it is washed, fed into a system of knives where it is shredded. Water is then added to the chopped fibre and hard-pressed to recover the cane juice.Bagasse is obtained as the dry fibrous deposit which remains when sugarcane is shredded during the extraction for the juicThis is used as animal feed, in paper making or as fuel to generate energy. Additionally, the cane juice is preserved with lime and hot water, making it less acidic and prevent its conversion to glucose. Janke *et al.* (2015) proposed that as a result of the higher lignin content in SCB, its pretreatment process could enhance their degradability for use in bioenergy production. It has also been employed in the past decades to generate biofuels for the production of energy and heat. However, it becomes a readily obtainable biomass for the production of bioenergy via hydrolysis or enzymatic saccharification (Mkhize *et al.* 2016). Table 2-3 depicts the percentage compositions of cellulose, lignin and hemicellulose in bagasse.

Table 2- 3. Lignocellulosic composition of the raw SCB (%w/w, dry basis)

Cellulose	Hemicellulose	Lignin	References
47.0	27.0	23.0	(Kosinkova *et al.* 2015)
38.8	26.0	32.4	(Aditiya *et al.* 2016)
45.5	27.0	21.1	(Mood *et al.* 2013)
38.4	23.2	25.0	(Rabelo *et al.* 2011)
45.0	25.8	19.1	(Behera *et al.* 2014)
39.5	25.6	30.4	(Chandel *et al.* 2012)
43.8	28.6	23.5	(Yashas Gowda *et al.* 2018)

The sugar industry in South Africa makes a significant input through the employability of people in sugarcane production and for further processing.

About 16 to 20 million tonnes of sugarcane is harvested in South Africa per year from the sugarcane industry. With this amount generated, 120-130 kg of SCB is accumulated after the extraction of the sugar for bioenergy conversion. The consideration of SCB as a rich agro-industrial based by-product has been used in other applications such as the pulp and paper making industry, levulinic acid production and also in the ethanol biorefineries (Gnanambal and Swaminathan 2015).

Sugarcane is largely found in the provinces of KwaZulu-Natal, Eastern Cape, and Mpumalanga. The sugar industry is a diverse industry combining the agricultural activities for sugarcane cultivation with the industrial production of raw and refined sugar, syrup, and specialized sugars and a range of by-products. The South African sugar industry contributes an estimated average of about R2 billion to the country's foreign exchange earnings annually. In total, 50% of about 2.5 million tons of sugar produced in SA is exported to Swaziland, Lesotho, Botswana, and Namibia. The remainder is exported to various markets in Africa, the Middle East, the Far East (Korea and Japan), North America and Asia. Figure 2-9 depicts the sugar export seasons from 2009-2019 with

percentage ranges to Japan, Korea, Malaysia, and other African countries. Some of the sugar milling companies in SA are the Tongaat-Hulett sugar company, Illovo sugar limited, the Transvaal sugar Ltd, and the UCL Company Ltd.

Some of the challenges encountered in the sugar industry includes; the strengthening of the rand against the dollar, low global market process, and slower records of rainfall pattern in the SCB areas or belts.

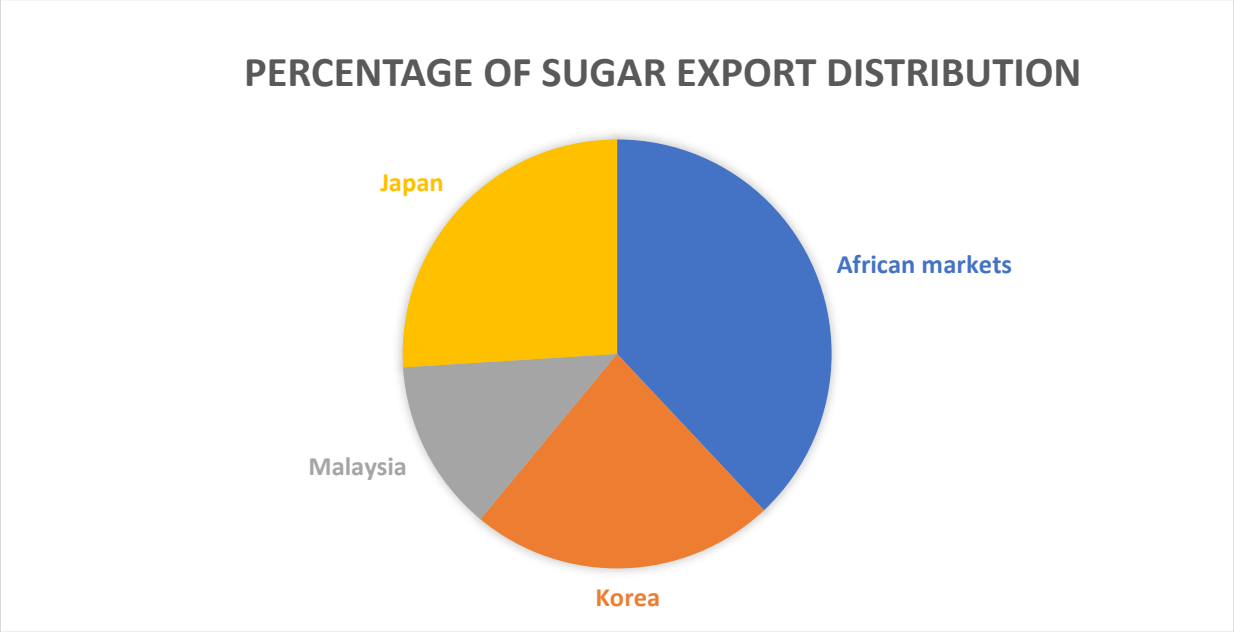

Figure 2- 9. Sugar export distribution rate in South Africa.

2.7.2 CS as biomass for biogas production

CS is considered a high-quality forage feedstock that is employed on dairy farms which has gained recognition for use as a high energy crop. According to Amon *et al.* (2007b), maize could be conserved as silage for use in anaerobic biodigesters as this was found to increase the overall CH_4 yield. Energy crops such as corn have been found to be co-digested with livestock manure to produce biogas in biodigesters (Amon *et al.* 2007a). Corn is reaped, chopped and generally ensiled

to preserve it for use in AD reactors for the biogas production (Ravi 2018). It has been found that reactors that use lignocellulosic material as substrate have shorter retention times with pretreatment methods applied before substrates are fed to the bioreactors to enhance the biogas yield (Gerardi 2003).CS rich in carbohydrate containing high lactic acid concentrations and low concentrations of higher VFAs have been reported to be disposed to aerobic deterioration (Zhang *et al.* 2018).

2.8 Composition of lignocellulose

Lignocellulose are macromolecules that comprises of holocellulose (cellulose and hemicellulose) which are bonded to lignin, a poly-phenylpropanoid macromolecule. Other components of a lignocellulosic biomass includes ash and extractives (not discussed in this work). It has been proposed that these polymer in a plant serve as the main storage for chemical energy (McKendry 2002). Cellulose, hemicellulose and lignin form structures called microfibrils, which are organized into macrofibrils that contribute to structural stability in the plant cell wall (Rubin 2008). In HPLC quantification, cellulose comprises of glucose, cellobiose and hydroxymethylfurfural. Hemicellulose is composed of xylose, arabinose, furfural, glucuronic and acetic acids.

2.8.1 Cellulose

Cellulose consists of a linear chain made up of β-D-glucose units linked by 1,4-β-glucosidic bonds (Updegraff 1969; Crawford 1981). Cellulose is an important structural constituent of the primary cell wall of green plants, algae and oomycetes. It is considered as the most abundant organic polymer on earth (Dieter *et al.* 2005). The application of biorefining to bagasse, a lignocellulose,

requires its fractionation into cellulose, hemicelluloses and lignin (Rocha *et al.* 2011). The early step involves biomass pretreatment where a substantial part of the hemicelluloses is solubilised, and the cellulosic portion is activated towards enzymatic hydrolysis and further processed for ethanol or biogas production. The schematic representation of the cellulose structure is shown in Figure 2-10.

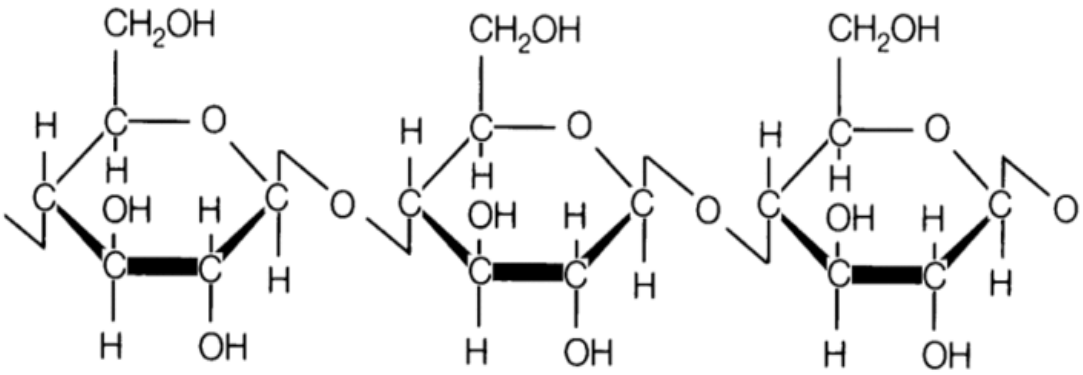

Figure 2- 10. Chemical structure of cellulose (Yoshiharu, Langan and Chanzy 2002).

2.8.2 Hemicellulose

Hemicellulose is a polymer which is also found in almost all plant cell walls (Scheller and Ulvskov 2010). Hemicellulose consists of a random, nebulous structure and is easily hydrolysed by dilute acid or alkali (Gibson 2013). It is the second most abundant component of lignocellulose, consisting of C5 and C6 sugars such as arabinose, galactose, glucose, mannose, and xylose. The schematic representation of the hemicellulose structure is shown in Figure 2-11.

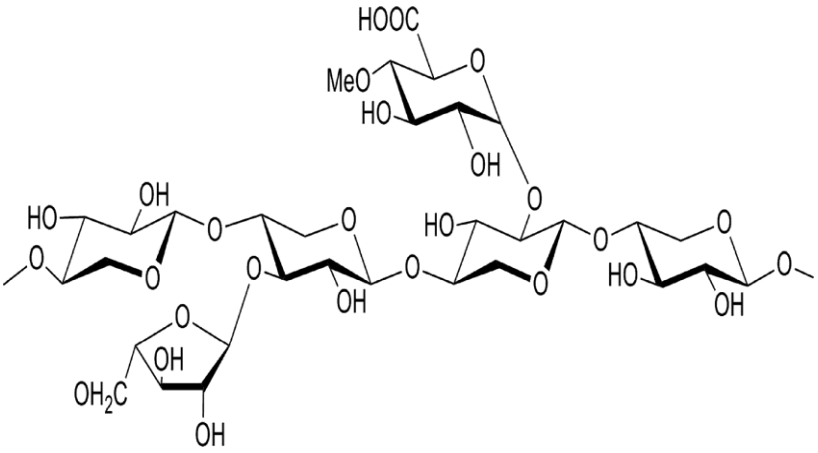

Figure 2- 11. Chemical structure of hemicellulose (Scheller and Ulvskov 2010).

2.8.3 Lignin

After its discovery somewhere in the 1800s by a Swiss botanist, lignin has long been considered to be a complex organic polymer which form the structural materials for supporting tissues of vascular plants and microorganisms (Martone *et al.* 2009). It is important in cell wall formation, especially in wood. Chemically, lignin is formed by cross-linked phenolic polymers (Stuart, Gargulak and McNally 2001). Its main compositions are the p-coumaryl alcohol (H), coniferyl alcohol (G) and sinapyl alcohol (S). It is synthesized by the polymerization of these compositions as the ratio within the polymers. The schematic representation of the lignin structure showing the p-coumaryl, coniferyl and sinapyl alcohols is depicted in Figure 2-12.

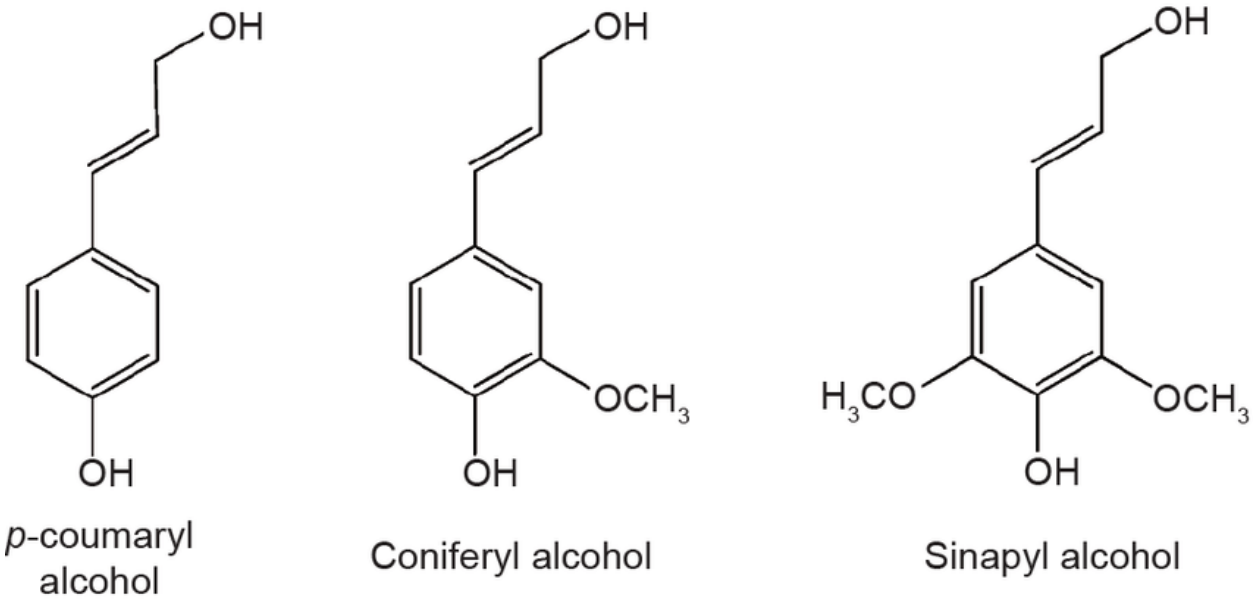

Figure 2- 12. Chemical structure of the three compositions of lignin (Martone et al. 2009).

2.9 Lignocellulosic biomass pretreatment techniques

Biomass pretreatment is critical as this process has been found to increase the CH_4 yield in an AD process. This is performed as a result of the nature of the intricate structure and the lignin content of the lignocellulosic biomass, which contributes to recalcitrance in the AD process (Hu and Ragauskas 2012; Paul and Dutta 2018). Pretreated biomass then becomes more porous for microbial digestibility and increases the surface area but certain inhibitory substances could adversely affect anaerobic microbes (Paul and Dutta 2018). Lignin in lignocellulosic biomass has been found to produce AD inhibitory phenolic compounds (Paul and Dutta 2018). The main aim of biomass pretreatment is therefore to enhance the breakdown of the lignocellulosic biomass (Hendriks and Zeeman 2009a). Cellulose and hemicellulose are broken down by enzymatic saccharification to simple sugars and further digested by microorganisms through the AD process to produce biogas (Sindhu *et al.* 2017). The use of organic solvents, alkalis and peroxide ozone as chemical pretreatments for lignocellulose increases cellulose enzymatic degradability by the

removal of lignin, while acid pretreatments hydrolyses hemicellulose into sugars. A study has shown that pretreatment of biomass prior to an AD process could lead to the solubilisation of particulate organic matter in sewage sludge (Nges 2012). Different types of pretreatments methods with various processes involved and varieties of feedstocks in literature is summarised in Table 2-4 and Table 2-5.

Table 2- 4. Pretreatment methods of lignocellulosic materials with various processes involved (Kumakura, Kojima and Kaetsu 1982; Sun and Cheng 2002; Alvira et al. 2010).

Types of pretreatments	**Pretreatment Process involved**
Chemical	Ozonolysis, alkaline hydrolysis, acidic hydrolysis, oxidative delignification, organosolv process
Physical	Irradiation, mechanical crushing, mechanical comminution, pyrolysis
Physico-chemical	Steam explosion, ammonia fibre explosion, CO_2 explosion
Biological	Use of microorganisms such as fungi to degrade lignin in the lignocellulosic material, for example, White rot fungi

Table 2- 5. Varieties of feedstocks in literature and pretreatments methods used in literature.

Pretreatment Methods	**Feedstocks**	**References**
Milling	Food waste	Zhang *et al.* (2007)
Grinding	Municipal solid waste	Maile, Muzenda and Mbohwa (2016b)
Hydrothermal	SCB	Simo, Jong and Kapseu (2016)
Ultrasonic	SCB	Liyakathali (2014)
Ionic liquids	WH	Gao *et al.* (2013)
Hydrothermal	SCB	(Ribeiro *et al.* 2017)
Alkali	Cattle dung	Dar and Tandon (1987)
Thermochemical	WH	Patel, Desai and Madamwar (1993)
Ultrasonic	Activated sludge	Wang *et al.* (1999)
Acidic	Newspaper	Xiao and Clarkson (1997)
Steam	Softwood	Söderström *et al.* (2002)
Carbon dioxide	SCB	Zheng, Lin and Tsao (1998)
Lime	Switchgrass and corn stover	Chang *et al.* (2001)
Biological	Olive mill wastewater	Dhouib *et al.* (2006)
Liquid hot water	(SCB)	Laser, Schulman and Allen (2002)

The principle of pretreatment is evidenced in Figure 2-13 as the lignocellulosic structure is broken down, exposing the cellulose, hemicellulose and lignin components

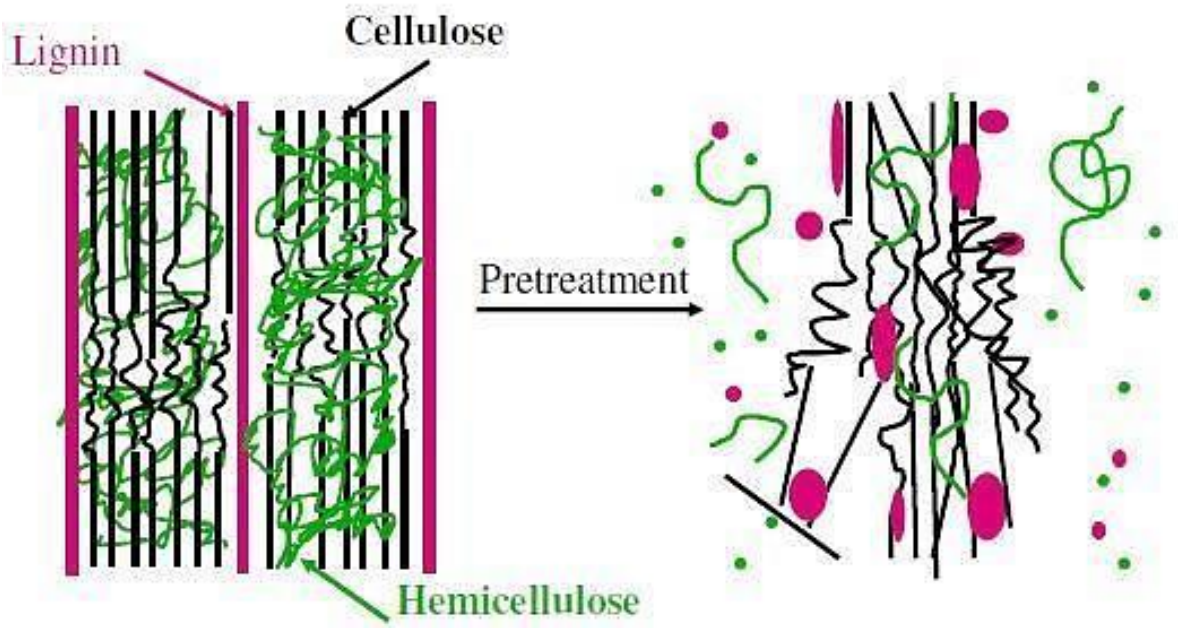

Figure 2- 13. Structural formation for cellulose, lignin, and hemicellulose disruption after lignocellulosic biomass pretreatment modified from (Brandt et al. 2013); Akhtar, Idris and Lai (2014).

2.9.1 Hydrothermolysis pretreatment

Fan *et al.* (2016) in a study proposed that lignocellulosic changes that occur during hydrothermal pretreatment for bioenergy production is an efficient method to disrupt lignin and hemicellulose and expose cellulose. They concluded that it is impossible for this pretreatment method to completely remove lignin present in a lignocellulosic feedstock. In the hydrothermolysis of sunflower oil cake for 1, 2, 4 and 6hr intervals at 25°C to 200°C, it was observed that the cellulose solubilisation rate was low (5%) whiles the hemicellulose content decreased from 13% to 6% at 200°C (Fernández-Cegrí *et al.* 2012). For wheat straw at 200°C, cellulose crystallinity reduced as the cellulose hydrolysis rate was increased (Ibbett *et al.* 2013). Lignin repolymerisation occurred at 140°C to 180°C for wood in 12 to 192 minutes after 75% removal of lignin (Trajano *et al.* 2013).

Improving the biogas production of SCB by hydrothermolysis was studied by Simo, Jong and Kapseu (2016). Their findings were that, the pretreatment method increased the biogas yield by approximately 15%.

2.9.2 Liquid hot water (LHW) pretreatment

In liquid hot water pretreatment, biomass is subjected to boil at high temperatures and high pressures, thereby, maintaining water at the liquid phase (Brandon *et al.* 2008). LHW is known to potentially enhance cellulose digestibility and pentose recovery with little or no inhibition (Van Walsum *et al.* 1996). Hendriks and Zeeman (2009b) stated that, LHW aids in solubilising hemicellulose, thereby making cellulose accessible. However, the pH is maintained between 4 and 7 to avoid inhibitors during pretreatment as this minimises monosaccharide formation. The temperature range commonly used is 170°C to 230°C with operating pressures greater than 5MPa (Talebnia, Karakashev and Angelidaki 2010). LHW produces higher yields of bioenergy production with low undesired products generation (Hamelinck, Van Hooijdonk and Faaij 2005). In a study by Yang and Wyman (2004), it was found that flow-through systems were capable of eliminating more lignin and hemicellulose from corn stover than a batch system. In the same study, acid addition resulted in an increase in lignin and hemicellulose removal which is in contrast to that of Hendriks and Zeeman (2009b). Larger amounts of cellulose and lignin removal using external acid with the flow-through method is in contrast with that reported in the past decades (Prutsch 1991).

2.9.3 Acid pretreatment

Lignocellulosic pretreatment with acids at ambient temperatures are carried out to enhance hemicellulose solubilisation, thereby making cellulose accessible for enzyme degradation with a dilute or a strong acid (Hendriks and Zeeman 2009b). In this process, solubilised hemicelluloses are exposed by hydrolytic reactions to produce furfural and specific monomers in acidic conditions (Ramos 2003). The use of dilute acids has been found to be effective when handling a lignocellulosic biomass with high lignin content. Solubilised lignin rapidly condenses and precipitates into acidic forms. Hemicellulose solubilisation and lignin precipitation are therefore noticeable during strong acid pretreatment. A drawback in the use of this method is the risk of the formation of inhibiting compounds (Hendriks and Zeeman 2009b). However, the use of dilute acid pretreatment has gained numerous research interest than the use of concentrated acids (Zheng, Pan and Zhang 2009). This is because concentrated acids are known to be corrosive, toxic, expensive and require reactors that need stronger construction materials to resist corrosion. Higher xylose yield is a distinguishing factor of dilute acid pretreatment over steam-explosion (Alvira *et al.* 2010). An acid-base ratio of 1% H_2SO_4 and 4% NaOH on SCB increased the cellulose content from 35.2% to 83.4%, reduced lignin from 22.2% to 9.3% and hemicellulose from 24.5 to 3.2% (Zheng, Pan and Zhang 2009). However, dilute sulphuric acid has gained larger usage in acid-base treatment because it is efficient and inexpensive, but not environmentally friendly and hence, not adopted in this present study.

2.9.4 Alkaline pretreatment

Pretreatment with alkaline medium is found to more effective on hardwoods as its efficiency depends largely on the pretreatment conditions and substrate (Yang and Wyman 2004). This

pretreatment method removes lignin from lignocellulosic feedstock including the acetyl groups in hemicellulose (Chen, Ye and Sheen 2012). Alkali pretreatment neutralises hydrolysate (Akhtar, Idris and Lai 2014). However, this method is very effective when lignin content is low in lignocellulosic biomass. A sharp increase in lignin content, reduces the efficiency of this method. Alkali extraction thus leads to the solubilisation and redistribution of lignin and at further modifications, into crystalline cellulose. Another unique feature of this mode of pretreatment is the cellulose structural changes leads to a thermodynamically stable form. The chemical pretreatment of SCB by Aguiar, Ferreira and Monteiro (2010) to yield exoglucanases and endoglucanases, reduced breakages of the fibres upon the addition of 2% H_2O_2 with 1.5% NaOH at 121°C for 15 minutes. Cellulose content increased by more than unity as hemicellulose content decreased by 8.5 times. Some alkali that have been used include, KOH, NaOH, $Ca(OH)_2$, anhydrous ammonia and hydrazine (Saritha and Arora 2012).

2.9.5 Ionic liquid pretreatment

Many studies have been carried out in the past decades relating to the applications of ionic liquids (ILs) into biomass fractionation and cellulose modifications and dissolutions. Cellulose dissolution has gained increasing recognition when compared to hemicellulose and lignin, since it serves as the site for energy storage (Kougias and Angelidaki 2018) and this could be converted into bioethanol. It has been found that the interactions of imidazolium ILs with cellulose is of great interest and thus, further investigations into the use of ILs for cellulose bioprocessing is required. The unique capabilities of some ILs to selectively dissolve biomass components or whole native biomass have been demonstrated (Reddy 2015). Hence, the application of ionic liquids to lignocellulosic materials in areas such as fractionation, cellulose composites preparation and its

derivatives, analysis, and removal of pollutants is a new avenue for the efficient utilisation of this solvents (Zhu 2008). Also, the selection of a better IL and its co-solvent is very crucial to obtain the optimal cellulose and lignin recoveries. It has been found that the addition of co-solvent aids in decreasing the viscosity of the IL mixture, facilitating the dissolution of the cellulose and subsequently leading to additional swelling and reduction of the recalcitrant nature of the cellulose crystalline structure and intermolecular interactions. In view of this, an IL/co-solvent solution was employed in this present study where water was used as the co-solvent. Some merits that arise from the use of aqueous IL pretreatment stems from low volumes which leads to greater chances of recycling and a reduction in viscosity (Fu and Mazza 2011) than for non-aqueous IL pretreatment, and thus, employed in this study.

Commonly found ILs includes 1-ethyl-3-methylimidazoliumchloride [Emim][Cl], 1-ethyl-3-methylimidazolium acetate [Emim][CH_3COO], 1-allyl-3-methylimidazolium chloride [Amim][Cl], 1-butyl-3-methylimidazolium chloride [Bmim][Cl], 1-butyl-3-methylimidazolium acetate [Bmim][CH_3COO], and 1-butyl-3-methylimidazolium methylsulfate [Bmim][$MeSO_4$] (da Costa Lopes *et al.* 2013; Reddy 2015). Table 2-6 shows different ionic liquids with lignocellulosic biomass and their recoveries.

Table 2- 6. Different ILs reported in literature and operating parameters with lignocellulose recovery contents.

#	Type of ionic liquid	Feedstock	Temp (°C)	Time (hr)	% Recovery	References	Comments
1	[Emim]OAc[]	SCB pellet	200	0.5	Lignin removal of 86.67 % (m/v)	(Gueh 2018)	N/A
2	[Bmim][HSO_4]	SCB pellet	200	0.5	Lignin removal of 142.23 % (m/v)	(Gueh 2018)	N/A
3	[Emim][OAc]	SCB	120	0.5	32% lignin removal	(Qiu, Aita and Walker 2012)	5% (w/w) [Emim][OAc] followed by hydrolysis
4	[Emim][OAc]	SCB	120	2	80% glucose yield	(da Silva *et al.* 2011)	
5	([Emim][OAc]) & [HNEt3][HSO4]	SCB	120	6, 12 & 24	68% glucose yield	(Mkhize *et al.* 2016)	[HNEt3][HSO4] was found to be inexpensive compared to ([Emim][OAc]). Pretreatment time is dependent on pretreatment temperature.
6	[Emim][OAc] & [Bmim][Cl]	Softwood (southern yellow pine) & hardwood (red oak)	110	16	35% reduction in lignin; 59 % holocellulose recovered	(Sun *et al.* 2009)	Red oak showed higher and faster dissolution than southern yellow pine. [Emim][OAc], a better solvent than 1-butyl-3-methylimidazolium chloride for wood dissolution
7	[Emim][OAc]	Bagasse	145	0.25	69.7% holocellulose recovered	(Yoon *et al.* 2012)	There was a good correlation between the experimental and the predicted yields
8	[Bmim][Cl]	Corn stover	130	2	96% cellulose recovered after 5 hours of alkali + IL	(Geng and Henderson 2012)	1% NaOH (90°C, 1 h) + IL. Solubilisation of 75% of lignin and 37% of hemicellulose.

N/A – not applicable

Figure 2-14 shows a typical lignocellulose biomass pretreatment using IL and the fractionation procedure for lignocellulosic biomass with IL is depicted in Figure 2-15.

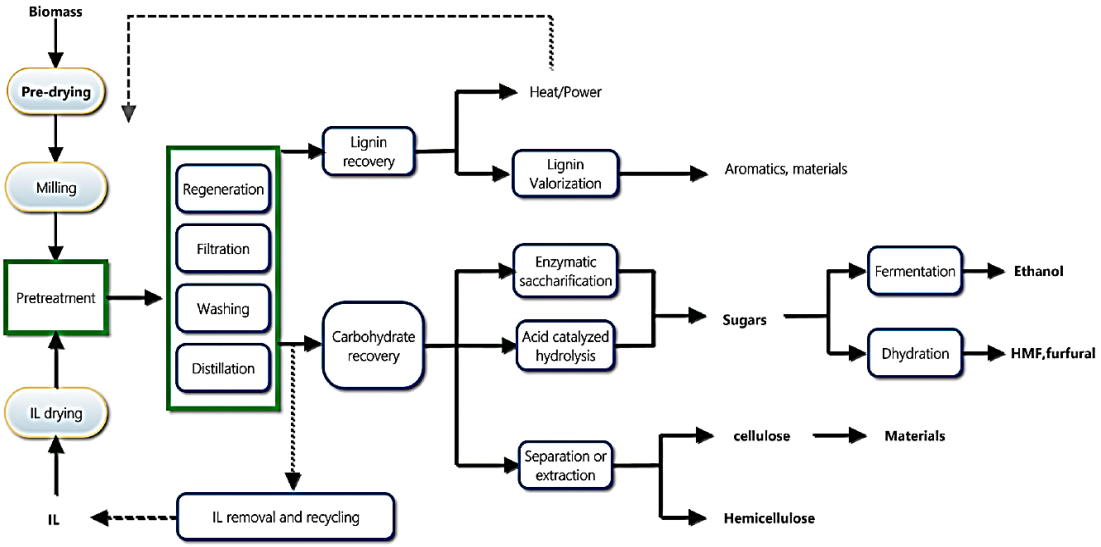

Figure 2- 14. Typical pretreatment routes routes for biomass using ILs (Hou et al. 2017) (procedure of extracting lignin from biomass) accoridng to Hou et al., 2017.

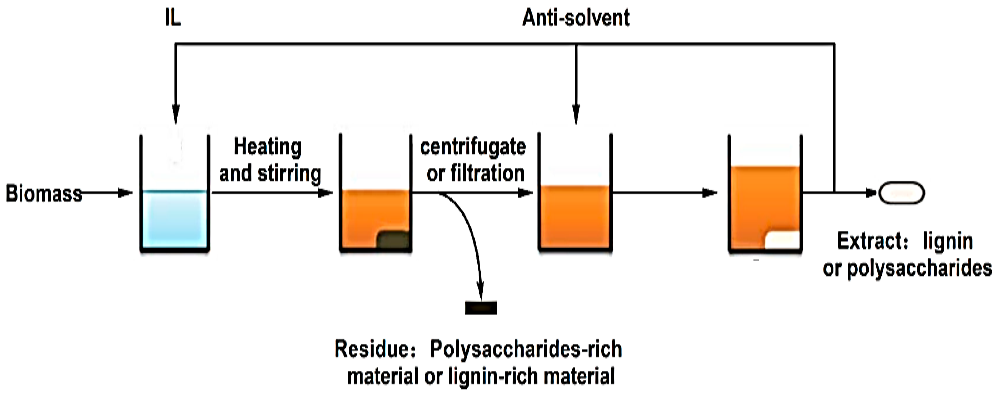

Figure 2- 15. Lignocellulosic fractionation with IL according to (Hou et al. 2017).

2.9.6 Biological pretreatment

Delignification of lignocellulosic feedstock also involves biological means using enzymes or microorganisms. Biological pretreatment makes use of lignocellulosic biomass which undergo degradation by microorganisms such as white, brown and the soft rot fungi, and bacteria. This leads to the release of enzymes to degrade hemicellulose, lignin, polyphenols and cellulose in trace quantities (Zheng, Pan and Zhang 2009; Akhtar, Idris and Lai 2014).

The white rot fungus, *Phanerochaete chrysosporium* has been reported to have the highest growth rate and efficiency for lignin degradation. In carrying out biological pretreatment, two major processes are performed (Ravi 2018). The first process is to extract enzymes released by dissimilar microbes and feeding them to the anaerobic system. Parawira (2012) carried out research using enzymes of cellulase and β-glycosidase prior to AD with mixed sludge to enhance the yield of CH_4 by 15%. In the second process, cellulolytic or lignin degrading microbes are utilised in the pretreatment of the substrates in biodigesters. With the biological pretreatment, the chemical composition and the lignocellulosic structure becomes available for enzyme breakdown. The brown and soft rots attack cellulose and thus impart lignin modifications to lignin whilst the lignin components are degraded by the white rot fungi (Zheng, Pan and Zhang 2009). It has been observed that the effect of fungal pretreatment depends largely on the lignocellulosic biomass characteristics under consideration (Liu *et al.* 2017b). Fungal pretreatment using *Ceriporiopsis subvermispora* in this study was found to increase the biomethane potentials of both forestry residues and agricultural lignocellulosic residues. Some microorganisms which have been used in the past decades include *Ceriporia lacerate, Sterum hirsutum, Polyporus brumalis,* and *Pharnerochaete chrysosporium*.

2.10 Industrial wastewater treatment

The treatment process of these organic fractions could be anaerobic or aerobic, thus, maximizing the waste recovery and recyclability (Mata-Alvarez, Mace and Llabres 2000). The design of a WWTP is a complex engineering task that requires knowledge on process engineering and the design of mathematical programming (Dragan, Zubov and Sin 2017). An approach that is gaining increasing recognition is the addition of a co-substrate such as food waste. Recovering the potential of food waste as a renewable energy source is one of the great challenges of waste management in the future (Browne and Murphy 2013). The effect of WWTPs across developed nations stems from the fact that most of these facilities do have only have the primary sedimentation treatments. Others, from the other part of the globe include more treatment facilities by way of reducing the volume of sludges (Gomez *et al.* 2006). In stabilising sewage sludge from municipal wastewater treatment for reuse and environmental disposal, the AD process has been found to be play a vital role in this regard (Yoshida, Christensen and Scheutz 2013).

Several WWTPs are noted for a high volume of solid material from the primary and secondary setlling units (activated sludge), collectively referred to as sewage sludge (Nghiem *et al.* 2014). A typical WWTP is shown in Figure 2-16. Sewage sludge discharges produce certain by-products whose treatment accounts for 50% of the entire operating costs of all WWTPs (Appels *et al.* 2008). The conventional WWT consist of a preliminary, primary and secondary treatment in the activated sludge unit. The aim is to cause a reduction in the solids content and improvement in the dewatering process.

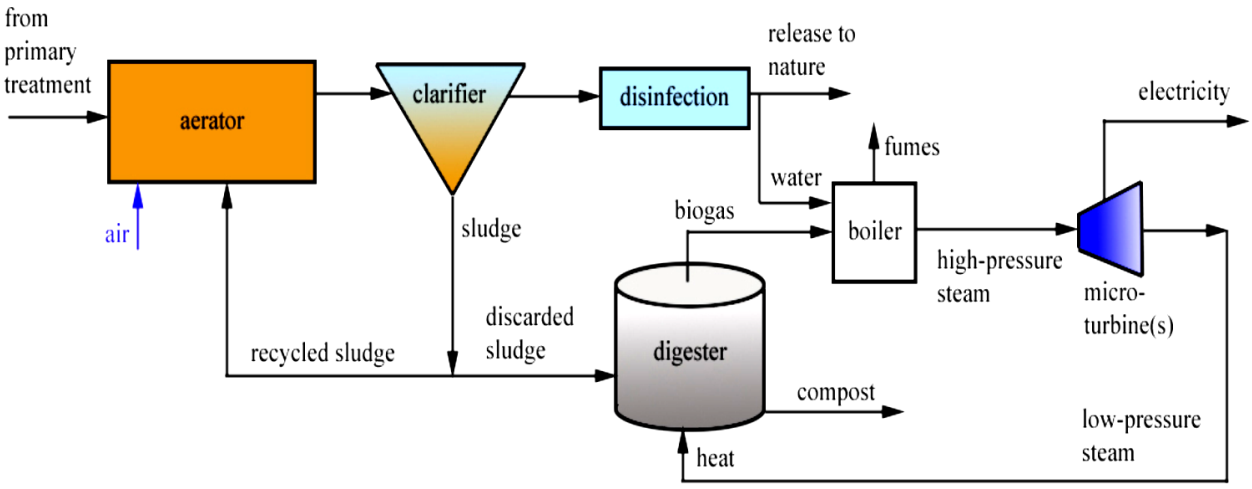

Figure 2- 16. A typical WWTP adapted from Nazaroff and Alvarez-Cohen (2015).

2.11 Parameters for biomass and substrate characterisation

2.11.1 Volatile solids (VS)

VS refers to the solids that remain after filtration which have been dried, weighed and kindled at 600°C (Deressa *et al.* 2015). Martin-Ryals (2012) also classified VS as the sample solids lost upon ignition by firing at a temperature of 550 ± 25°C, which represents the biomasses' organic matter fraction excluding the inorganic salts and ashes. It is important to also note that higher VS content improves the yield of biogas (Patil *et al.* 2014).

2.11.2 Chemical oxygen demand (COD)

COD refers to the quantity of oxygen consumed by microbes to degrade organic matter that are present in WWTPs (Flörke 2013). By so doing, the dissolved oxygen is increased, rendering an ideal habitation for aquatic organisms within an ecosystem where the primary treatment could reduce the BOD by 20 to 30%, and suspended solids by 60% (Flörke 2013). A strong oxidising agent such as potassium dichromate is usually used for COD analysis under acidic conditions. COD can be measured in real-time with a COD analyser to improve the WW control and

effeiciency. It is often used as a quality parameter to assess the extent of organic pollutants in municipal and industrial wastewaters.

2.11.3 Ash

Biodegradation of a particular biomass, namely chemical means often produces a solid residue (McKendry 2002). When burnt in the presence of air, the residue is referred to as “ash”. The term “ash” could also refer to inorganic residue left after dry oxidation at 575°C (Sluiter *et al.* 2008). Thus, the ash content measures the mineral content with other inorganic materials present in a biomass which is employed to determine the summation of the biomass composition.

2.11.4 Moisture

The moisture content (MC) of lignocellulosic biomass is considered to be an influential factor in the control of biofuel product quality and properties (Daassi-Gnaba *et al.* 2017). The caloric value of wood fuel has been found to be reliant on the weight of wood but the delivered sample is almost always, never dry. The moisture content of lignocellulosic biomass has therefore become an integral component in the determination of the energy content (H.Hartmann and T.Böhm 2016; Torgrip and Fernández–Cano 2017). The method is based on the loss in weight determination of the biomass after drying which usually lasts for 24 hours at 60°C to 105°C. Some methods have been used in the determination of MC. The direct method is based on the drying process (Daassi-Gnaba *et al.* 2017) which was adapted in this present study. A drawback in this method is that, it is time consuming and can only be applied to small sample volumes (Samuelsson, Burvall and Jirjis 2006; Xu *et al.* 2017). The second method, which is the indirect method has been found to

be rapid and to operate un-destructively. This method is therefore found to be more suitable for the wood-to-energy industry requirements (H.Hartmann and T.Böhm 2016). Alternatively, it based on radiometric, thermal, acoustic, electrical and, hygrometric or acoustic technologies (Delfino *et al.* 2018).

2.11.5 Total solids (TS)

The TS content of a biomass indicates the quantity of dry material for a given volume of reactor with regards to the AD process (Tawoma 2015). Also, the total solids (TS) denote organics as well as inorganic matter in a particular biomass (Deressa *et al.* 2015). Low solids are largely characterised by TS values below 10%, intermediate solids have a TS value of 15% and high solids implies a TS content ranging from 20 to 40%. The solid concentration influences the reactor design, configuration and process economics (Hamilton 2009). Higher solid content have been found to be attributed to reduced reactor volumes and reduced water requirements with low operating costs (Neshat *et al.* 2017).

2.12 Kinetic model study in AcoD

The term, process modelling is a suitable tool for predicting and describing the effectiveness of an AD process. Kinetic modelling has been found to be applied on different levels of complexity (El-Sayed Zaher 2005). The design for the optimisation of an AD process for biogas production could be improved through validated kineticmodels from mechanistic studies. This requires an indepth knowledge of the bacterial biochemical kinetics associated with the complex transport phenomena and stochiometric relationships associated with AD. Identifying the process mechanism and the

representative kinetics is necessary to better understand the designs of suitable biodigesters and the prediction of the overall biogas potentials. In this regard, kinetic studies are mostly conducted in establishing the most suitable reaction rate model that is basically derived from mechanistic reaction pathways to capture the reactant reaction rate and the rate of formation of the product with the best fit. Also, another significance of the study of kinetics is to provide evidence for the mechanisms of chemical processes as the reaction mechanisms is of practical applications in predicting what is the most effective way of causing a reaction to occur (Li *et al.* 2016).

From this background, Chen and Hashimoto (Zainol 2012) developed a kinetic model for substrate application and CH_4 production which suggested that the Contois kinetic models would be more suitable than the Monod kinetic models in predicting the digester performances. In view of all these, several kinetic models have been employed in the past decades for the AcoD process to present the overall biogas production. Some of these models include the; first order (Lebona *et al.* 2019), Chen and Hashimoto (Zainol 2012), dual pool first order, Contois (Hu, Thayanithy and Forster 2002), Monod (Tsapekos *et al.* 2018), second order and the modified Gompertz model (Lebona *et al.* 2019). However, the selection of the choice of different model to adopt in a particular study is very crucial as the relationships between these parameters and the process or biological parameters can be complicated by the interactions. For example, the modified Gompertz kinetic model equation is a modified form of the Gompertz equation which is commonly used to simulate the cumulative biogas production (Tsapekos *et al.* 2018). However, the former has gained much applications in AD processs than the latter due to its complexity and its large data requirements. Kinetic studies are very important for industrial anaerobic reactor designs (Kovalovszki *et al.* 2017). This is an important tool to better understand the anaerobic degradation, the design of reactors and its operation. It is a generally accepted approach used in defining the

specific parameters of system performance to control and predict the plant performances and to optimise the process for normal operation or to scale up pilot studies. It is important to understand that the results of the kinetic modelling could be used for the estimation of treatment efficiencies and system characteristics of full-scale reactors operating at similar conditions. Kinetic analysis is usually carried out to predict and demonstrate the performance of biological treatment systems. The kinetics defines the reaction rate with which a microbial population converts substrate into biogas using the organic material from the wastewater. To better develop and determine the ultimate CH_4 production as well as the hydrolysis kinetic constant, Li *et al.* (2016) studied the kinetics of CH_4 production and hydrolysis in batch mode for non-biodegradable organic fractions of green and air-dried corn stover.

2.13 Design of experiment (DOE)

Design of experiment (DOE) is a software used to develop a correlation between input facors affecting a process affaecting a process and its response as the output (Kweinor-Tetteh *et al.* 2018). It can also be used to obtain statistical data by classifying the optimal factors and levels for the process. However, the choice of model can have an influence on the precise valuation and the cost of running experiments for the responses or outputs. Responses are evaluated from the selected optimal points from the experimental design. Optimisation is carried out to obtain the operating conditions which can be applied to a process to maximise an output and produce the best response. Moreover, a large number of experimental runs are required for process optimisation. The software application aids in the generation of experimental matrix with a minimum number of runs, becoming the alternative option other than the one-factor-at-a-time (OFAT) approach. In the OFAT approach, one factor is kept constant while the other factors are varied to obtain the best yield. However, a multivariant approach to designing a set of experiment for optimisation is the

most suitable, hence, adopting the response surface methodology was preferred. The input factors and outputs variables or responses for a system performed under a set of design of experiments is depicted as Figure 2-17.

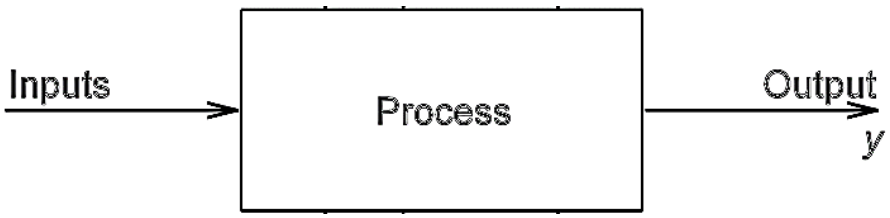

Figure 2- 17. Key elements of a design of experiment.

2.13.1 Response surface methodology (RSM)

Response Surface Methodology (RSM) is very important in experimental design and has been applied successfully in many fields to minimise the number of experimental runs for optimisation and developing new processes. Some of these include sugar and oil refinery wastewater (Kweinor-Tetteh *et al.* 2018) and biogas production. Therefore, RSM is an efficient tool to control and stimulate the complex influential factors of the AD process. In order to establish the interactive effect of variables, the RSM design technique is used mostly for the experimental designs, analysing, and modelling the experimental data to optimise the response. The Box Behnken and the central composite designs are typical of the RSM. However, in this present study, the Box–Behnken design (BBD) of the RSM was employed other than the composite central design (CCD) as reported in a previous study (Tetteh *et al.* 2020). The following are the reasons for the model choice:

1. With the same number of factors, it is found to generate fewer quantity of experimental runs which translates into lesser time and resource requirements without conceding accuracy.

2. It is found to be predominantly efficient in estimating the correlation coefficient (R^2) for a specified model, experimental errors and good data fitness in the design, modelling and optimisation of an process.

A remarkable feature of the RSM is that it simultaneously optimizes a process with several operating variables for the enhancement of process performances of complex interactions between variables and responses.

CHAPTER 3

MATERIALS AND EXPERIMENTAL METHODOLOGY

3.1 Introduction

This chapter was structured in the following sections: **section 3.1** details the sample collection and storage media used in this study, s**ection 3.2** gives an overview of the analytical procedures for the characterisation processes, s**ection 3.3** describes the procedure for the BMP test with the untreated biomass, s**ection 3.4** details the procedure adapted for the BMP test after ionic liquid pretreatment and in **section 3.5,** the kinetic model equations are outlined.

3.1.1 Sample collection and storage

The selection of the biomasses for use as feedstocks in this present study was the first step to determine their bioavailability. In this study, both SCB and CS were used as the feedstocks for the anaerobic co-digestion process. The selection of the SCB and CS was based on the feedstock bioavailability in the province of KwaZulu-Natal. There is approximately 8 million tons of corn produced annually with about 2.2 to 3.0 million tons of CS generated whilst an annual sugarcane milling capacity of approximately 22 million, corresponding to an average production of about 3.3 million tons of SCB (Enitan 2015). The rich content with regards to the presence of cellulose in these lignocellulosic biomasses makes them suitable for use as energy groups for biogas production.

The addition of the nutrient-rich wastewater streams sourced from Durban, South Africa was to replace the synthetic food source for the microbes during AD.In the study by Tetteh *et al.* (2017),

a synthetic feed in the form of a solution which was purchased from the Chemical Laboratories was prepared from copper (II) sulphate (CuSO4), Iron (III) sulphate, etc to serve as nutrient and enhancers during the AD of *Miscanthus Fuscus* and cow manure. This was found to increase the operational cost of the AD as compared to the use of industrial WW which is not purchased, but sourced freely from onsite About 1 kg of mill-run SCB was received from the Sugar Milling Research Institute (SMRI) in Durban, KwaZulu-Natal (KZN), SA. It was washed, dried and stored in airtight plastic containers at room temperature prior to use. The SCB was further sieved to 0.4 mm on dry weight basis. About 0.8 kg of CS was received from Cedera Agriculture Institute, KZN, SA and stored in airtight plastic containers at room temperature before use. To increase the surface area for the digestion process, CS was sieved to 0.4 mm on dry weight basis. This included a range of particles from 0 to 4 mm. The size distribution analysis was not considered in this work. The selection of the particle size of 0.4 mm is presented in sections 3.3.1 and 5.3.1. Figure 3-1 shows the photographs of the SCB and CS used in this study.

Figure 3- 1. Photographs of (a) SCB and (b) CS used in this study.

Twenty-five (25) litres of inoculum from the anaerobic digesters was sourced from Amanzimtoti Wastewater plant which treats domestic and industrial effluents. The sewage sludge was collected after the primary settling tank from the same wastewater plant into 10L containers with the pH and temperature recorded onsite. Twenty-five (25) liters each, of brewery wastewater (BWW), dairy wastewater (DWW), sugar wastewater (SWW) and municipal wastewater (KWW) were periodically sampled for each set of experiment and preserved in a cold room at 4 ºC prior to analysis. This storage method is similar to that reported by Gu *et al.* (2014). However, samples were taken periodically from sampling sites per scheduled times prior to analysis after storage.

3.2 Characterisation

3.2.1 Ultimate and proximate analysis

The ultimate analysis was carried out using the energy dispersive x-ray diffractometer (EDX) which is shown in the Appendix (Figure A-7). 1g of untreated and pretreated SCB or CS were collected in centrifuge tubes, kept in a refrigerator and stored overnight at 4°C. The proximate analysis was carried out to determine the total solids, moisture content, volatile solids, ash contents and the fixed solids based on the standard methods according to the American Public Health Association (APHA 1998). The procedures of the proximate analysis for the SCB or CS and the substrate mixture for the liquid fraction are divided into categories (A) and (B) respectively.

(A) Proximate analysis for the SCB or CS: solids

- **Total solids (TS)**

2g of feedstock (SCB or CS) was used for the TS measurement. Pre-dried aluminum weighing dishes were placed in a PF 200 convection oven at 105 ± 3°C (Thermo fischer scientific, Waltham, Massachusetts, USA) for 4 hours and cooled in a desiccator. The aluminum dishes were pre-dried to the nearest 0.1mg. The dish containing the oven dried sample was weighed to the nearest 0.1mg and the mass was recorded using an analytical balance (Ohaus, Pioneer series, New Jersey, USA). Sample with dish was put back into the convection oven operating at 105 ± 3 ºC and dried to constant weight. The TS was then calculated from equation (3.1).

$$\%TS = \left[1 - \left(\frac{K_1 - K_2}{K_1}\right)\right] \times 100\ \% \qquad (3.1)$$

Where %TS denotes the percentage of total solid, K_1 is the mass of the received sample and K_2 is the mass of the sample after drying.

- **Moisture content**

2g of the pre-weighed feedstock (SCB or CS) were dried in a convection oven operating at 105°C for 4 hours and the moisture content was calculated from equation (3.2).

$$\% \text{ MC} = \left(\frac{A_1 - A_2}{A_1}\right) \times 100\% \quad (3.2)$$

Where % MC denotes the moisture content (%), A_1 is the sample mass (g) and A_2 is the mass of dried sample (g).

- **Volatile solids (VS)**

After the analysis for the TS, the sample was placed into an L9/11/SKM muffle furnace (Nabertherm-Industrieofenbau, Germany) at 550 ^{o}C for one hour. The VS was calculated from equation (3.3).

$$\% VS = \left(\frac{X_2 - X_3}{X_2}\right) \times 100\ \% \quad (3.3)$$

Where % VS is the volatile solids, X_2 is the sample mass prior to being placed in the muffle furnace and X_3 is the sample mass after removal from the muffle furnace.

- **Fixed solids**

The fixed solids were calculated directly from the TS and VS using the equation:

$$\% \text{ Fs} = \% \text{ TS} - \% \text{ VS} \quad (3.4)$$

Where % Fs = percent fixed solids; %TS = percent total solids and % VS = percent volatile solids.

- **Ash content**

The feedstock (SCB or CS) was placed in an aluminum crucible and then weighed to constant mass. 2g of the feedstock was transferred into the furnace operating at 600ºC for 4hrs or until whitish-grey ash was obtained. The crucible was allowed to cool from 200 to 300ºC. It was then transferred into a desiccator for an hour to cool down to room temperature and weighed. The ash content was then calculated using equation (3.5):

$$\% \text{ Ash } = \frac{M_{ash}}{M_{sam}} \times 100\% \quad (3.5)$$

Where M_{ash} is the mass of the ashed sample and M_{sam} is the mass of the sample only.

(B) Proximate analysis for the substrate mixture: the liquid fraction

- **Total solids (TS)**

An aluminum dish was heated at 105 ˚C for an hour, stored and cooled inside a desiccator. It was then weighed directly before use. 5mL of well mixed sample was pipetted into a pre-weighed crucible. The crucible containing the sample was weighed and placed in a PF 200 convection oven (Thermo fischer scientific, Waltham, Massachusetts, USA) at 105°C overnight. The crucible was then removed from the convection oven and placed in a dessicator to cool after which it was weighed. The TS was then calculated using equation (3.6):

$$\text{Total solid } = \frac{[A - B] \times 1{,}000}{\text{volume of sample (mL)}} \quad (3.6)$$

Where the mass of sample is A and mass of crucible is B.

- **Volatile solids (VS)**

After the measurement of the TS, the sample remaining was cooled to room temperature (25°C) and placed in the muffle furnace at 550 ºC for 30 minutes. The VS was calculated using equation (3.7):

$$\% VS = \left(\frac{X_2 - X_3}{X_2}\right) \times 100\ \% \qquad (3.7)$$

Where % VS is the volatile solids, X_2 is the sample mass prior to being placed in the muffle furnace and X_3 is the sample mass after removal from the muffle furnace.

- **Chemical oxygen demand (COD)**

Calibration

The calibration of the Hach DRB 200 thermoreactor was carried out by heating for 10 minutes

it up for at least 10 minutes 150°C. Thereafter, the chamber light was switched on when the blank sample (prepared according to manufacturer) was ready and the cuvette filled halfway. The blank was then loaded onto the spectrophotometer chamber and the lid was closed to await stabilisation of the instrument. Zeroing was done to finalise the calibration procedure.

Procedure

The blank solution was prepared by adding 10 mL distilled water to the COD reagent. 1mL sample (substrate mixture for the pre and post AD process) was then pipetted into a digestion tube. A further 9mL of distilled water was added to each digestion tube. For samples with higher concentrations, a green colour was observed and further dilution was required. 2mL of the concentrated sample was added into the COD vial containing the reagent in each tube. Using the

Hach DRB 200 thermoreactor, the digestion was carried out for 2 hours (120 minutes) at 150 °C. Thereafter, each sample was analysed using the spectrophotometer (Hach DR 3900, Manchester, United Kingdom) at a wavelength of 430nm in relation to the high range which could take up to 1500 mg/L. The photographs of the Hach DR 3900 spectrophotometer and the Hach DRB 200 thermoreactor used for the COD analysis are presented in Figure 3.2. The COD content was calculated according to equation (3.8).

$$\text{COD} = [\text{COD reading}] \times [\text{dilution factor}] \quad (3.8)$$

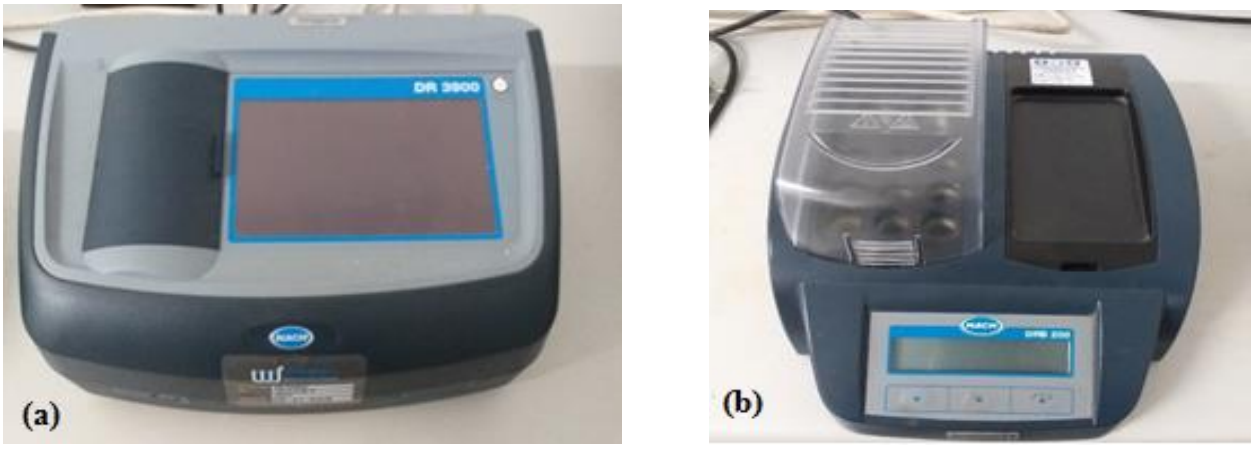

Figure 3- 2. Photograph of the (a) Hach DR 3900 spectrophotometer and (b) the Hach DRB 200 thermoreactor used for the COD analysis.

- **pH**

The pH was performed by immersing the pH probe into the standard buffers which have pH values of 4, 7 and 10. After the calibration was complete, the pH values for each of the substrate mixtures prior to the AD process and post AD were taken.

Figure 3- 3. Photograph of the digital pH meter (Ohaus Corporation, USA).

3.2.2 Scanning electron microscope (SEM)

The SEM was employed to give information about the surface morphology and composition of the SCB and CS. 1g of the untreated and pretreated biomass were collected in a centrifuge tube, placed in a refrigerator at 4°C and stored overnight for 12 hours. It was then transferred to a crucible and placed in a convection oven at 105°C for 2 hours prior to the SEM analysis (Tescan Mira3, Tescan, Czech Republic) and the EDX (Thermo Fisher Nova NanoSEM, FEI, USA). The SEM instrument is presented in the Appendix (Figure A-7). Images of the SCB or CS were taken at a magnification of 50µm and operating at 12keV for visualisation. Prior to the analysis, samples were sputter coated with gold before imaging to prevent charging effect on the surface of the specimen and to make the surfaces electrically conductive, thus avoiding degradation and build-up of charges on them.

3.2.3 Thermogravimetric analyser (TGA)/Differential scanning calorimeter (DSC)

The TGA was employed to measure the thermal stability of the SCB and CS. It also measures the changes in the mass of the SCB and CS at different temperatures. The DSC was employed to determine the rate of decomposition and oxidation of the SCB and CS in terms of the heat flow. It also gives evidences of the crystallinity of the feedstock under consideration. 1g each, of the untreated SCB or CS was heated at of 5°C/min under an unremitting flow of nitrogen (100 mL/min) at a temperature range from 10°C up to 800°C. The TGA and DSC instrument is presented in the Appendix (Figure A-9).

3.2.4 Fourier transform infrared spectrometer (FTIR)

The FTIR was used to detect the range of functional groups with respect to the changes in the molecular structures of the SCB and CS. For FTIR analysis, 1g of the SCB or CS was transported to an accredited center for analysis. The feedstock, SCB or CS was dissolved in chloroform and layered on a NaCl crystal and after evaporation of chloroform, the polymer film was subjected to FTIR. The spectra of the FTIR results were plotted using the Microsoft ORIGIN® tool. Figure 3-4 shows the photographs of the untreated and pretreated SCB and CS prior to the FTIR analysis. The photograph of the spectrum two FTIR instrument is presented in the Appendix (Figure A-8).

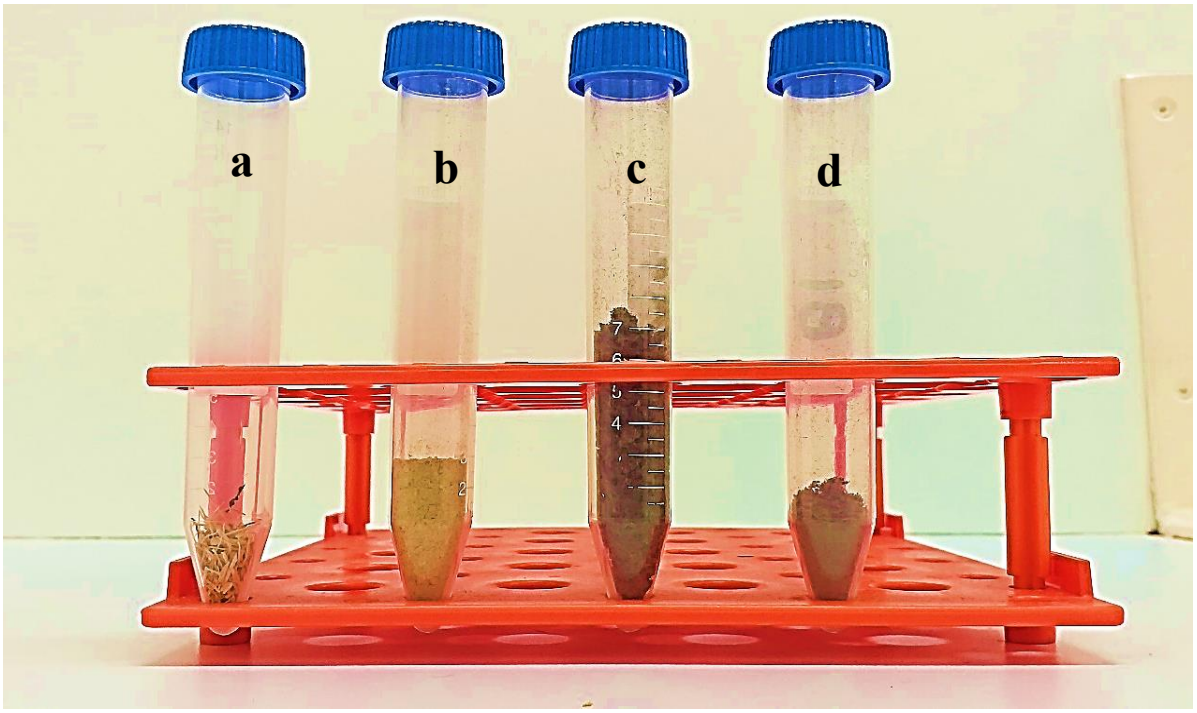

Figure 3- 4. Photographs of the (a) untreated SCB, (b) untreated CS, (c) treated SCB and (d) treated CS that was used for the FTIR analysis.

3.2.5 Compositional analysis of the SCB and CS

The hollocellulose and lignin content for the untreated biomass were determined according to the methods described by the Technical association of the pulp and paper industry (TAPPI) (TAPPI T203 om-83 (1983); TAPPI T222 om-83 (1983); TAPPI T223 hm-84 (1984); TAPPI T208 om-84 (1984); and TAPPI T211om-93 (1996). Deionised water was used for all parts of the experiment. In the determination of the cellulose, 2g of SCB or CS was added to 5g of sodium chlorite ($NaClO_2$) and 100mL of water. Thereafter, the mixture was then autoclaved for 30mins at 121 ± 3°C), filtered and weighed to constant weight. Figure 3-5 depicts the mixture prior to autoclaving.

Figure 3- 5. Prepared samples ready for autoclaving.

In the determination of the lignin, 1.0g of SCB or CS was weighed, placed in a 100mL beaker and 15mL of 72% sulphuric acid (73 to 74mL of acid in 100mL water) was added and stirred for one hour at room temperature. Furthermore, 360mL of water was added to a 1,000 mL flask, boiled at 100°C for about 4 hours, filtered and weighed. Figure 3-6 shows the preparation stages during the reaction time.

Figure 3- 6. Photograph taken during the lignin determination steps by (a) stirring of the reaction mixture with temperature control and (b) filtration process of the reaction mixture prior to oven drying.

In the determination of holocellulose, 5g of SCB or CS and water were added into a 500 mL flask which was refluxed by adding 1.5 g $NaClO_2$ and 0.5 mL of $C_2H_4O_2$. The unit was set for refluxing at 100 °C by continuously adding $NaClO_2$ and acetic acid until the SCB or CS turned white. The solids remaining were filtered and washed with water and dried at 100°C in a convection oven and weighed to a constant mass. Figure 3-7 shows the photograph of the setup for refluxing.

Figure 3- 7. Photo depicting the setup for refluxing during the holocellulose determination.

3.3 BMP tests for the untreated biomass

3.3.1 Effect of particle size on biogas production

The Retsch Muhle miller (Figure 3-8) was used to mill and reduce the SCB and CS to a required range of particle size. For homogenization, the feedstocks were milled into smaller sizes which renders them suitable for characterization. The photographs of the different particle sizes of the SCB and CS are presented in Figures 3-9 and 3-10. To determine the best particle size for both SCB and CS in this present study, a BMP test was performed to predict the biogas production rate in batch mode using a 1,000 mL biodigester (Schott bottles). BMP tests are usually employed to

determine the possible CH_4 obtainable from feedstocks from laboratory scale batch systems under controlled AD process parameters such as the digestion time, OLR and temperature (Maile, Muzenda and Mbohwa 2016e). In this present study, the variations were observed at 2 mm, 1 mm, 0.6 mm and 0.4 mm whilst the digestion time and the organic loading rate were 20 days and 0.5gVS/100mL, respectively. In all, eight (8) biodigesters were considered which corresponded to the letters "A" to "D" as shown in Figures 3-9 and 3-10. To each biodigester, 150mL each of sewage sludge and SWW together with 400mL of inoculum were added to make up to the 700mL mark with 200mL headspace and mass of biomass calculated per 100mL remaining to make up the 1,000 mL biodigester. For an OLR of 0.5gVS/100mL, 4.2g of CS and 5.1g of SCB were taken for each biodigester. This mass of SCB or CS was used all throughout the experiment regardless of the size of the biomass. Each biodigester was tightly fastened using screw caps with ports. These screw caps were fitted with silicone tubes to prevent leaks whilst the remaining ports were closed with small screw caps. Purging with non-reactive nitrogen gas was done to create the anaerobic environment inside each biodigester prior to the closure of the openings for 2 to 3 minutes each (Shin *et al.* 2019). Silicone tubes were used for the gas collection as they were connected to 2L measuring cylinders using the downward water displacement method. The biodigesters were mixed mechanically and periodically (to ensure uniformity and also, to prevent clogging), at least twice in a day prior to taking the measurements for the volume recorded daily. The experimental setup is similar to that presented as Figure 3-11.

Figure 3- 8. Photographs of the (A) Retsch Muhle miller for homogenising the agricultural biomasses (Retsch Technology, Haan, Germany) and a (B) a vibratronic machine (King Tester Corporation, Phoenixville, PA, USA).

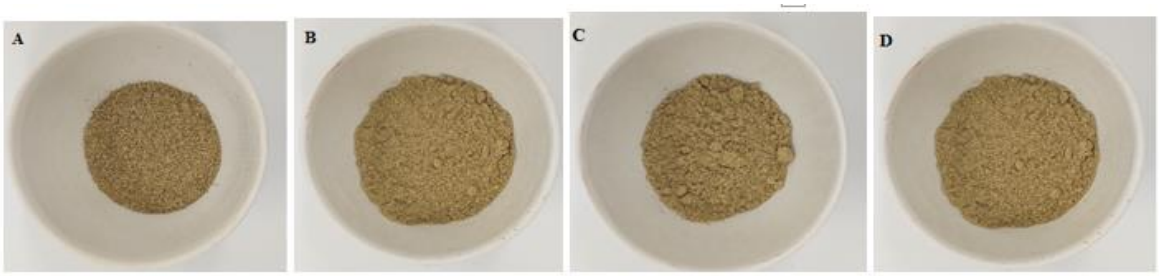

Figure 3- 9. Photographs of the milled CS for (A) 2.0 mm, (B) 1.0 mm, (C) 0.6 mm and (D) 0.4 mm.

Figure 3- 10. Photographs of the mill-run SCB for (A) 2.0 mm, (B) 1.0 mm, (C) 0.6 mm and (D) 0.4 mm.

3.3.2 Preliminary experiments of wastewater selection for process optimisation

In order to select the suitable WW stream with the selected biomass for optimisation, it was important to carry out a preliminary experiment using BMP tests with SCB or CS with the four (4) WW streams stated above in section 3.1.1. This was carried out at varying temperatures of 25°C, 35°C and 55°C at an OLR of 0.5 gVS/100mL for 25 days. The selection of a lower OLR of 0.5gVS/100mL was due to the fact that lower OLR has been established to enhance the biogas potential as overloading leads to biodigester failure (Prabhu and Mutnuri 2016). These operating temperatures were selected because biogas production has been been found viable within these ranges during optimization (Kwietniewska and Tys 2014).

Also, this is because most anaerobic biodigesters at WW treatment plants in South Africa, work within the range of 25°C to 60°C. The determination of the masses of SCB or CS that was fed into each biodigester in relation to the OLR is presented in Appendix B1. Hence, for an OLR of 0.5 gVS/100mL, 4.2g of CS and 5.1g of SCB were added. Table 3-1 presents the experimental design used for the substrate loading to each biodigester for the sewage sludge, inoculum and the WW stream. The BMP experiment was then carried out based on a similar method presented in section 3.3.1 using a 1,000 mL Schott bottles as the biodigesters. The daily biogas monitoring (volume),

biogas yield and the biogas compositions (CH_4 and CO_2 considered in this present study) were evaluated. Each set of experiments were carried out in duplicates with the averaged biodigesters designated in terms of A, B, C and D and interpreted below as:

A = Inoculum + sludge only

B = Inoculum + sludge + WW + CS

C = Inoculum + sludge + WW + SCB

D = Inoculum + sludge + WW

Table 3- 1. Experimental design for the substrate mixture.

Biodigester	Sludge (mL)	Inoculum (mL)	WW (mL)
A	400	400	--
B	150	400	150
C	150	400	150
D	200	400	200

3.3.3 Process optimisation

3.3.3.1 Response surface methodology

The design-Expert® software (Version 11.0.5.0, Stat-Ease Inc., Minneapolis, MA, USA) was used to design the experiment, optimise the process and develop the response model. The RSM of the Design-Expert aided in developing the mathematical relationship between the input variables (OLR and temperature) and the response (biogas yield) which was set at three different levels as presented in Table 3-2. The two input variables and their respective levels were denoted as A and B for temperature (25°C, 33°C, and 55°C) and the OLR (0.5 gVS/100mL, 1.0 gVS/100mL and 1.5gVS/100mL), respectively.

Table 3- 2. BBD design matrix for the input variables.

Input variables	**Symbols**	**Levels**		
		-1	0	1
Temperature (C)	A	25	35	55
OLR (gVS/100mL)	B	0.	1.0	1.5

However, the input variables's upper and lower limits were quantified together with the biogas yield as the response variable for the design of the experimental matrix. However, by the application of the BBD (chosen over the CCD of the RSM due to reasons stated in section 2.13.1), 13 experimental runs were designed with 5 centre points, 4 axial centre points and 4 factorial points. The data obtained were fitted into a quadratic polynomial model in analysing the correlation between the input variables and response. Table 3-3 depicts the set of runs which is represented as RX where the letter "R" stands for the term "Run" and the "X" represents the biodigester number. Also, included in the table are the masses of SCB or CS added to each biodigester per the OLR. The step-by-step calculations of the masses of SCB or CS are presented in Appendx B1.

Table 3- 3. Summary of the biodigester number, OLRs, temperatures and masses of untreated biomass added into each biodigester.

Biodigester ID	OLR (gVS/mL)	Temperature (°C)	SCB added (g)	CS added (g)
R1	1.5	55	15.4	12.5
R2	1.0	35	10.3	8.3
R3	1.5	35	15.4	12.5
R4	1.0	35	10.3	8.3
R5	1.5	25	15.4	12.5
R6	1.0	55	10.3	8.3
R7	1.0	35	10.3	8.3
R8	0.5	35	5.1	4.2
R9	1.0	25	10.3	8.3
R10	0.5	25	5.1	4.2
R11	1.0	35	10.3	8.3
R12	0.5	55	5.1	4.2
R13	1.0	35	10.3	8.3

3.3.3.2 Procedure for the BMP test

BMP tests have bee found to aid in the optimisation, establishment and the profitability of an AD plant regarding the yield and the gas quality (Raposo *et al.* 2011). Each biodigester (purchased from CC Imelmann Pty Ltd, Johannesburg) was set up as described in Table 3-4. The addition of 150mL each of the sludge and WW together with 400mL of inoculum was based on the substrate loading reported in a similar study (Prabhu and Mutnuri 2016).

Table 3- 4. Substrates loading in each biodigester prior to the AD process.

Biomass/feedstock	Volume added (mL)	Volatile solids content (%)	Biodigester working volume (mL)	Headspace (mL)
Sludge	150	-	800	200
Inoculum	400	-	800	200
Industrial wastewater	150	-	800	200
SCB	-	78	800	200
CS	-	96	800	200

The procedure for the BMP test have been presented above in section 3.3.1. The pH in each biodigester before the AD process was found in the range of 6.0 to 8.5, which is similar to what Kougias and Angelidaki (2018) reported without the need for any pH adjustment. Relatively, some authors have reported optimum pH values from 6.8 to 7.2 according to Sreekrishnan, Kohli and Rana (2004) and 6.8 to 7.5 by Hallenbeck (2011). Figure 3-11 depicts the experimental setup employed in this study consisting of the circulating water baths, 2L measuring cylinders, biodigesters with ports on the caps for purging and feeding.

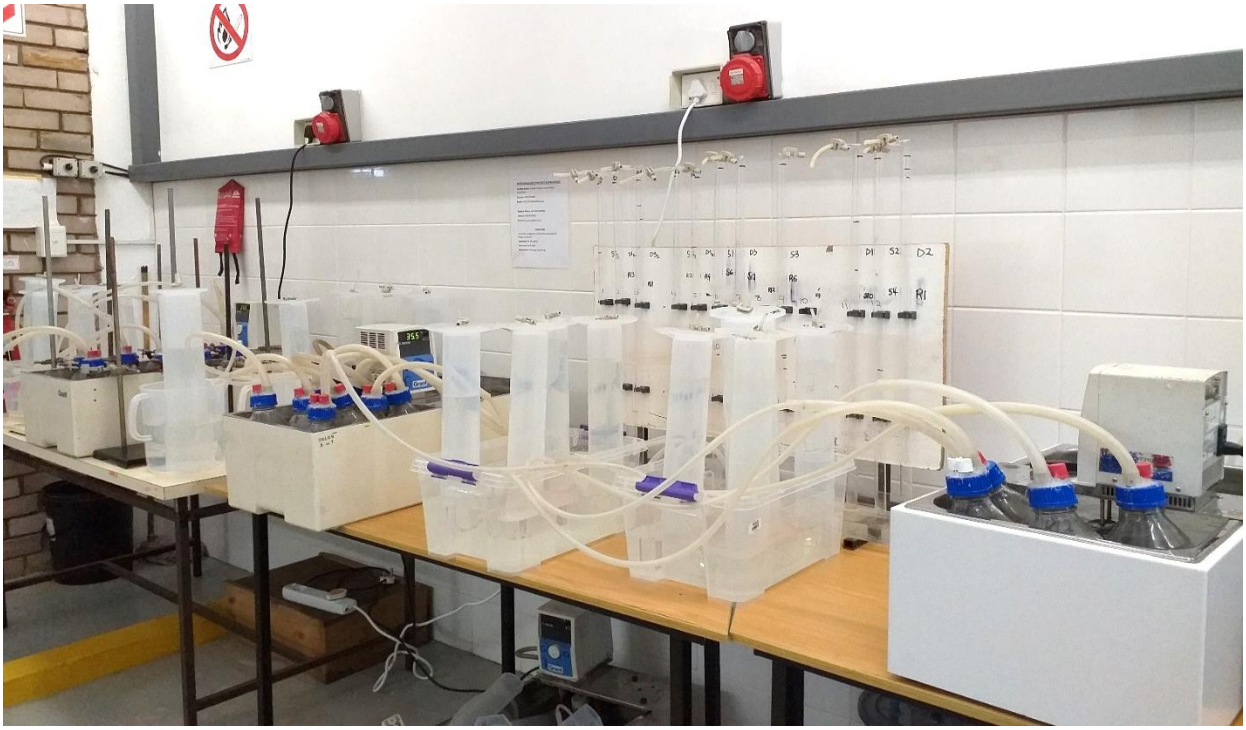

Figure 3- 11. Photograph of the BMP setup used in this study.

A gas chromatograph (Shimadzu GC 2014, USA) was calibrated using pure samples of CH_4 (99.9 $\%CH_4$) and CO_2 (99.9 $\%CO_2$) purchased from Afrox Gas and Gear, Durban, South Africa as depicted in the Appendix (Figure B-13). The retention times of the gas standards and specifications of the GC instrument employed in this study are presented in the Appendix (B10-1 and B10-2). Samples for GC analysis from each biodigester were taken at the end of the digestion time (30 days). This was to allow enough biogas accumulation in the headspaces of the biodigesters for analysis using a gas syringes of 100 µL volume. Exceptional cases were for biodigesters that were found to stop producing biogas for 5 to 10 days. In that case, the biogas was withdrawn from the silicone tube connected to the biodigesters with gas syringe and injected into the GC, made to stabilised and chromatograms recorded. This method was adapted from the standard procedure 2720C (APHA 1998).

3.4 BMP tests for the pretreated biomass

3.4.1 The thermophysical properties of 1-ethyl-3-methylimidazolium acetate [Emim][OAc]

The selection of the kind of IL plays a significant role in the fractionation of the lignocellulosic biomass. From Table 3-5, it could be deduced that when the IL, [Emim][OAc] is dissolved in water, higher glucose yield is achieved and hence, selected for ths study.

Table 3- 5. Comparative study of different ILs, process conditions and glucose yield.

Type of ionic liquid	**Biomass**	**Temperature (°C)**	**Time (hrs)**	**Glucose yield (%)**	**Reference**
[Emim][OAc]	SCB	120	2	80	Da silva et al., 2011
$[HNEt_3][HSO_4]$	SCB	120	6	68	Mkhize et al., 2016
[Emim][OAc]	Hardwood (red oak)	110	16	59	Sun et al., 2019
***[Emim][OAc] in H_2O**	**SCB**	**150**	**1.5**	**81**	**Fu & Mazza 2018**
[Mmim][DMP]	SCB	120	2	70	Bahrani et al., 2015
[Emim][OAc] (pure)	SCB	150	1.5	67	Fu & Mazza 2018

The [Emim][OAc] was purchased from Sigma Aldrich (Merck), South Africa with a purity > 95 wt %. Before the start of the process, the ILs were dried under vacuum for 12 hours at 50 °C. The thermophysical properties; refractive index and density of [Emim][OAc] were measured as a function of temperature at 25°C. The density was measured using the Anton Paar DMA 5000 density meter (Figure 3-12a) and the refractive index with an RF $M340^+$ refractometer (Figure 3-

12b). Ethanol and acetone were used for cleaning the instrument prior to each analysis. The densities and refractive index equipment temperature was monitored at 298.15 K.

Table 3- 6. Photograph of the (a) Anton Paar DMA 5000 density meter and (b) RF M340^{+} refractometer.

Also, the water content was determined to ascertain the water uptake by an IL during the experimental procedure using the Karl Fischer titration method. The 870 KF titrino plus Karl Fischer coulometer (Figure 3-13) was used for the determination of the water content of [Emim][OAc].

Figure 3- 12. Photograph of the 870 KF titrino plus Karl Fischer coulometer (Metrohm Herisan Switzerland).

3.4.2 Experimental procedure using the Parr reactor

The parr reactor was chosen for this study owing to its easier loading and catalyst removal, high sensitivity, simplicity, good temperature control and uniform catalyst distribution (Anderson *et al.* 2018). However, it aided in the fractionation of the SCB and the CS. In this study, 1.5g of SCB or CS was added to 48.5g of water to make-up 5% (w/w) [Emim][OAc] in a Parr reactor which is a PTFE liner vessel. The Parr reactor was controlled with a temperature and pressure using a circulating water bath operating at room temperature (25°C) to cool the reactor components. The following operating conditions were used: temperature of 150°C, reaction time of 90 minutes, stirrer speed of 80rpm (Bahrani, Raeissi and Sarshar 2015), pressure at 200 kPa (2 bars) and nitrogen gas according to a modified procedure by Fu and Mazza (2011). The step-by-step procedure during the use of the parr reactor for the biomass fractionation is presented below;

1. The stirrer was unscrewed at the topmost part of the stirrer component as the reactor vessel was placed on the bench. The connection strings were made to slide aside from the head.

2. The reactor vessel was made to rest on a benchtop as the six cap screws were loosen using a spanner in the split ring sections. The cone-pointed screws were loosened at the outer band and made to rest on a bench. The ring sections were then removed and the head with all the attached fittings made free to be easily lifted from the cylinder.

3. The sample (which contains a mixture of IL/H_2O solution and SCB or CS) was prepared and filled into the PTFE liner with a working volume of 50mL.

4. The PTFE liner was placed in the vessel, connected to the head of the vessel as the six caps were tightened to avoid leakages. The protection ring was inserted and connected to the stand which was made to close safely.

5. The heater band was placed in the vessel with all the valves closed, and the water bath was switched on to circulate water to the reactor. The nitrogen gas was then switched on.

6. The reactor controller was switched on (located at the back of the controller) and the working temperature was set by using the primary temperature controller.

7. The heater and the stirrer were switched on after the PTFE setup liner was connected. The parr reactor was allowed to run within the set time for a specific run.

8. At the end of the reaction, the heater was switched off and the reactor vessel was made to cool down to room temperature. The heater band was removed from the vessel, by sliding it down using its clamps and made to cool down. As the temperature dropped below 50°C, the gas release valve was opened to discharge any internal pressure built inside the reactor vessel during the reaction. After cooling, the slurry was filtered through a Whatman filter paper with a Buchner funnel. Washing was carried out for the recovered samples with 100 ml (5 times × 20mL) of deionised water. After washing, the lignin-rich component (retained on the filter paper) was dried using a convection oven at 55°C over night for 12 hours and stored at 55°C for the SEM and FTIR analysis. The liquid fraction (retained in the conical flask) was stored in centrifuge tubes in readiness for the BMP tests and also, for the sugar analyses using the HPLC.

9. Finally, the PTFE liner vessel was removed, and any solution remaining is decanted into a waste bottle and cleaned with deionized water. The vessel was further soaked in an acid bath for cleaning.

3.4.3 Experimental procedure for the BMP test after IL pretreatment

The procedure for the BMP test was similar to that reported in section 3.3.3.2 and the table for the substrate loading presented in Table 3-6. However, in this case also, the biodigester conditions of operation were obtained from the optimised parameters for both SCB or CS with SWW or DWW. Biodigesters A1 and A3 (Table 3-6) are the originally optimised conditions for SCB in both SWW and DWW, respectively while A2 and A4 are duplicates of the former. Likewise, B1 and B3 are the originally optimised conditions for CS in both SWW and DWW, respectively while B2 and B4 are duplicates of the former. Also, $C_{A1, A2}$, $C_{A3, A4}$, $C_{B1, B2}$ and $C_{B3, B4}$ in section 3.4 were made to represent the control setups for the eight (8) biodigesters whose contents were made of IL with water solution together with the substrates: WW, inoculum, and sludge. Table 3-6 shows the summary of the substrate mixtures for the biodigesters and the process conditions.

Table 3- 7. Summary of the substrate mixtures required and the operating conditions in terms of temperature and the OLR.

Biodigester #	Substrate mixture required	Temperature (°C)	OLR (gVS/100mL)
A1	SCB with SWW	25	0.5
A2	SCB with SWW	25	0.5
A3	SCB with DWW	55	1.0
A4	SCB with DWW	55	1.0
B1	CS with SWW	25	0.5
B2	CS with SWW	25	0.5
B3	CS with DWW	55	1.0
B4	CS with DWW	55	1.0
$C_{A1, A2}$	Control biodigester for A1 and A2	25	0.5
$C_{A3, A4}$	Control biodigester for A3 and A4	55	1.0
$C_{B1, B2}$	Control biodigester for B1 and B2	25	0.5
$C_{B3, B4}$	Control biodigester for B3 and B4	55	1.0

The experimental setup includes; 2L measuring cylinders, two circulating water baths to control the temperatures at both 25°C and 35°C, a trough to carry water for the inverted measuring cylinder, silicone tubes and 1L Schott bottles. The photograph of the experimental setup is shown in Figure 3-14.

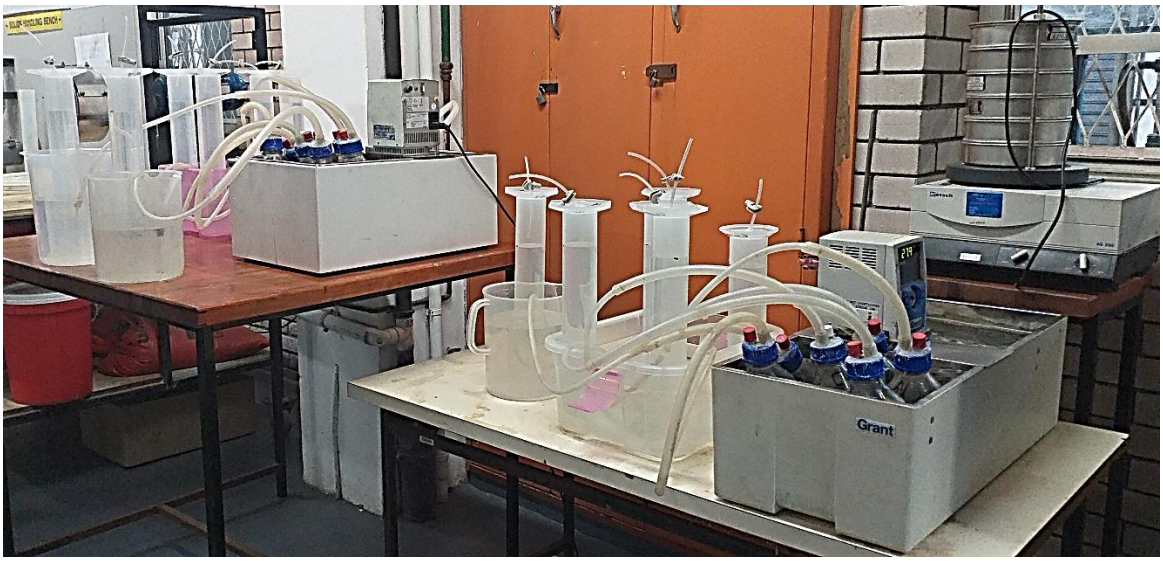

Figure 3- 13. Photograph of the BMP setup for biogas production after the IL pretreatment.

3.4.4 HPLC analysis

3.4.4.1 Preparation of the calibration curves

0.1g each of standard sucrose, fructose, xylose, mannose, arabinose, galactose, and glucose were measured using an analytical balance and dissolving in deionised water. It was then transferred into a 100 mL volumetric flask. The HPLC instrument was prepared for measurement using deionized water as the blank. Further, 5 µL of the standard solution is injected into the HPLC with the specifications in section 3.4.6.2 as the peaks for each sugar standard is plotted.

3.4.6.2. Analyses of sugars

The composition of the liquid phase obtained after IL pretreatment of SCB or CS was determined using the Shimadzu HPLC instrument (Figure 3-15) with the following specifications:

Mobile phase: 5 mM deionized water

Sample volume: 0.005 mL (5 µL); sample pH = approx. 5.4

Column temperature: 80 °C

Flowrate: 0.6 mL/min

Column type: Rezex column

Detector: Refractive index

The combined graph showing the plots of the sugar standards and the sugars present after IL pretreatment is depicted in Figure 5-52.

Figure 3- 14. Photographs of the Shimadzu HPLC instrument (Shimadzu Corporation, Kyoto, Japan).

3.5 Kinetic modelling

A range of kinetic models were modified and evaluated according to that developed by Xie *et al.* (2016b). Only the kinetic models below were considered since their input variables are within the scope of this work (equations 3.9 to 3.12). The optimum run from the set of experiments for the untreated and pretreated SCB and CS after the BMP tests were used for the kinetic model analysis. The cumulative data was then analysed using the solver add-in of the Microsoft® excel toolpak. The sum of square error (SSR) technique was used for the kinetic model curve fitting to calculate

the deviations of the predicted and measured values. Further, the SSR was minimized using the solver add-in whilst altering the other factors. This alteration continued until the measured and predicted values were fitted closely to each other via a generalized and reduced gradient for the curve fitting and optimization processes. Regression methods were adopted to obtain the regression values such as the correlation coefficient (R^2) and the graphs of the predicted versus the actual values as presented in chapter 5.6. The kinetic model equations are presented as equations (3.9) to (3.12).

First order

$$M(m) = P \times [1 - \exp(-kt)] \quad (3.9)$$

Chen & Hashimoto

$$M(m) = P \times \left(1 - \frac{K_{CH}}{HRT \times \mu_m + K_{CH} - 1}\right) \quad (3.10)$$

Modified Gompertz

$$M(m) = P \times \exp\left(-\exp\left[\frac{R_{max.e}}{B_o}[\lambda - t]\right] + 1\right) \quad (3.11)$$

Dual pooled first order

$$M(m) = P \times [1 - \alpha.\exp(-K_f t) - (1 - \alpha).\exp(-K_L t)] \quad (3.12)$$

Where

P is the highest biogas production (mL); C or λ denotes the lag phase of the process; μ_m is the microbial growth rate (h^{-1}); K_{CH} is the dimensionless constant of the Chen and Hashimoto model; SSR is the sum of squares errors; k represents the first-order rate constant (1/d); t is the digestion

time (d); Kft is the rate constant for speedily degradable substrate (d^{-1}); $K_L t$ is the rate constant for slowly degradable substrate (d^{-1}); α is the ratio of the rapidly degradable substrates to the total biodegradable substrates and K is equal to $R_{max}.e/B_o$ which represents the maximum specific substrate uptake rate per the highest biogas production.

CHAPTER 4

INSTRUMENTATION

4.1 Introduction

The chapter details the protocols employed for the operation of the instruments employed in this study for various characterisations and analyses. Schematic diagrams depicting the designs and operations are also presented.

4.2 High performance liquid chromatograph (HPLC)

The HPLC is a chromatographic instrument which is used for the separation of compounds to identify, quantify or purify the different components of a mixture. It consists of a mobile phase, a pump, an injector, a column, and a detector. With a little amount (about 0.05mL), the mixture to be separated (which is usually a liquid) is injected via the injector port with the help of an HPLC pump and made to pass through the mobile phase which permeates through a column at varying speed, interacting with the sorbent (stationary phase). The separation of the mixture of compounds do occur as they elude from the column, making the column the main component of the HPLC. Inside the HPLC columns are silica gel, an inert material which serves as the stationary phase due to its porosity and particle size which aids in the separation. The elution time, referred to as the retention time, denotes the time at which a specific analyte appears from the column, and this is specific for a particular component of a mixture. This is also dependent on the chemical nature of the mixture component, mobile phase composition and the type of column. Different types of columns employed are the normal phase columns, reverse phase columns, ion exchange columns

and the size exclusion columns. After the separation, the detector then detects and identifies the analytes in the sample mixture which is transmitted unto a data acquisition device such as a computer. A miscible combination of water and organic solvents which includes acetonitrile and methanol are usually employed as the mobile phase although water-free mobile phases can also be employed. HPLC has been applied in water purification units, pharmaceuticals, protein studies and the study of carbohydrates. Generally, a graph of retention time versus concentration is plotted for the standards and the concentration of the sample is determined using the equation of the calibrated graph. A schematic representation of the HPLC instrument is shown in Figure 4-1.

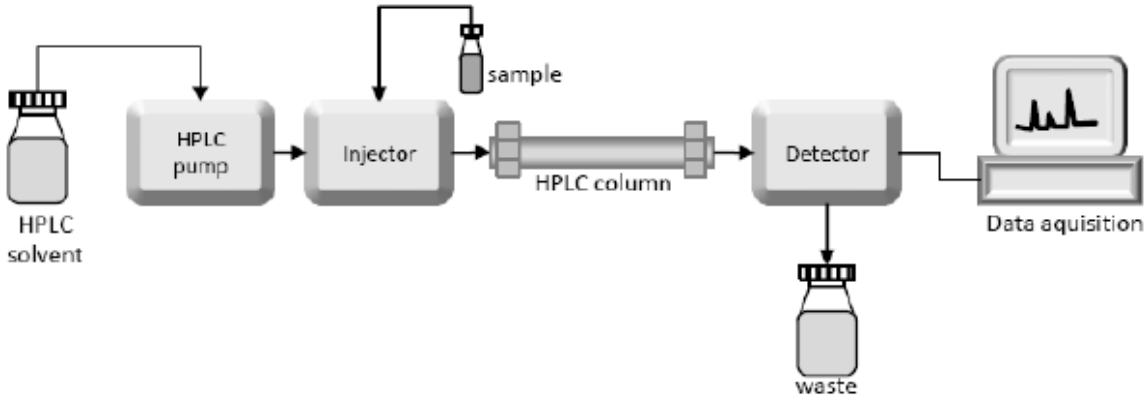

Figure 4- 1. Schematic diagram of the high-performance liquid chromatograph

4.3 Gas chromatograph (GC)

Gas chromatography (GC) is defined as an analytical method which is employed for the separation of chemical components of a sample mixture and further detected to show the presence, absence and the quantity present (Hilaire *et al.* 2017). GCs were developed as useful technique from the original works of James and Martin dated from the 1950s, to separate complicated combinations of volatile analytes. The chemical components are mostly gases or organic molecules which must be volatile and thermally stable to prevent degradation in the GC. GC is generally applied in the manufacturing companies, pharmaceuticals, research institutions and in the forensics. The sample

mixture is injected into the GC using an autosampler or a syringe through a septum. After, the GC uses a carrier gas which is employed as the mobile phase which transports the sample mixture through the GC (without reacting with the sample) into the column which contains the stationary phase as the separation occurs. Some of these gaseous mobile phase includes nitrogen (N_2), helium (He) and hydrogen (H_2). The detector is connected to the column which responds to the sample mixture eluting from the column to produce signal which is then recorded unto an acquisition software and unto a computer to generate chromatograms. The schematic diagram of the GC is shown in figure 4-2 which consist of an injection port, a column, a detector and the chromatographic peaks (chromatograms), displayed on a computer screen (Eiceman 1995). The magnitude of the signal is plotted against time (retention time) and a chromatogram is generated (De Llyod 1998). GC columns have smaller internal diameters which are longer than HPLC columns.

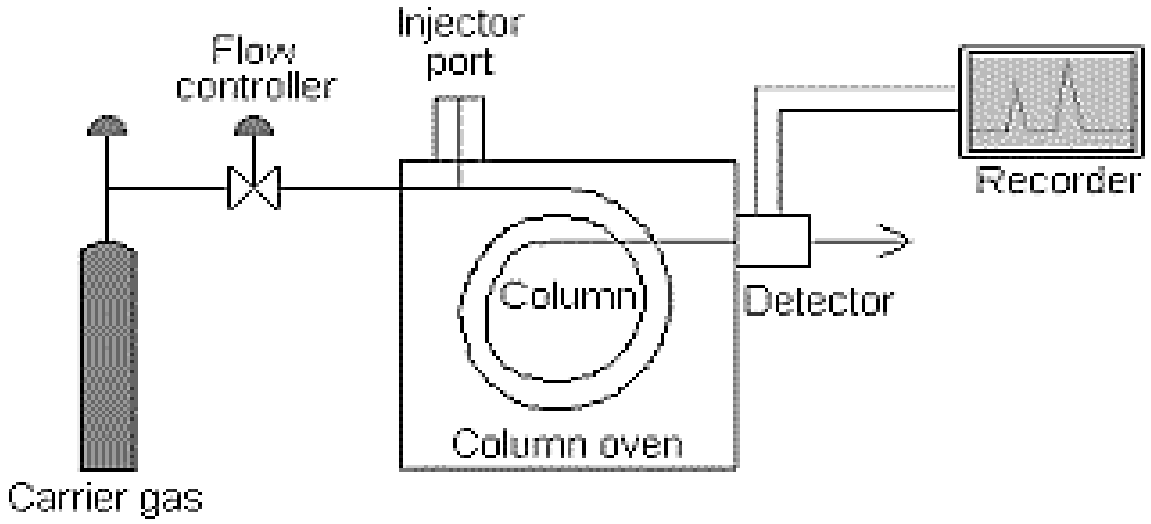

Figure 4- 2. Schematic diagram of the gas chromatograph.

4.4 Fourier transform infra-red (FTIR)

In IR spectroscopy, IR radiation is made to pass through a sample and absorbed by the sample with the remainder, transmitted. The resulting spectrum represents the molecular absorption and transmission to create a molecular fingerprint of the sample (Corro *et al.* 2013). FTIR is applied for the identification of unknown materials and the determination of the amount of components in a mixture with several advantages such as speed, sensitivity, mechanical simplicity and internally calibrated. The FTIR spectroscopy includes the bending, twisting, rotation, and vibrational motions of atoms. As the atom's interact with the IR radiations, fractions of the incident radiation are absorbed at specific wavelengths. The array of vibrations concurrently generates a multifaceted absorption spectrum, which is a sole characteristic of the presence of functional groups. This comprises of molecules under examination and the overall configuration of atoms present.

The IR spectra of the compounds appear at the absorption bands for a specific functional group with interactions to the surroundings of the atomic molecules. The spectrum, however, is an indication of the functional groups that are present in the molecule of interest. The functional group of an unknown molecule could be predicted from the assessment with a library of pure spectra permits in the identification (Willard *et al.* 1986; Tywabi 2015). Figure 4-3 represents the schematic representation of the FTIR spectrophotometer.

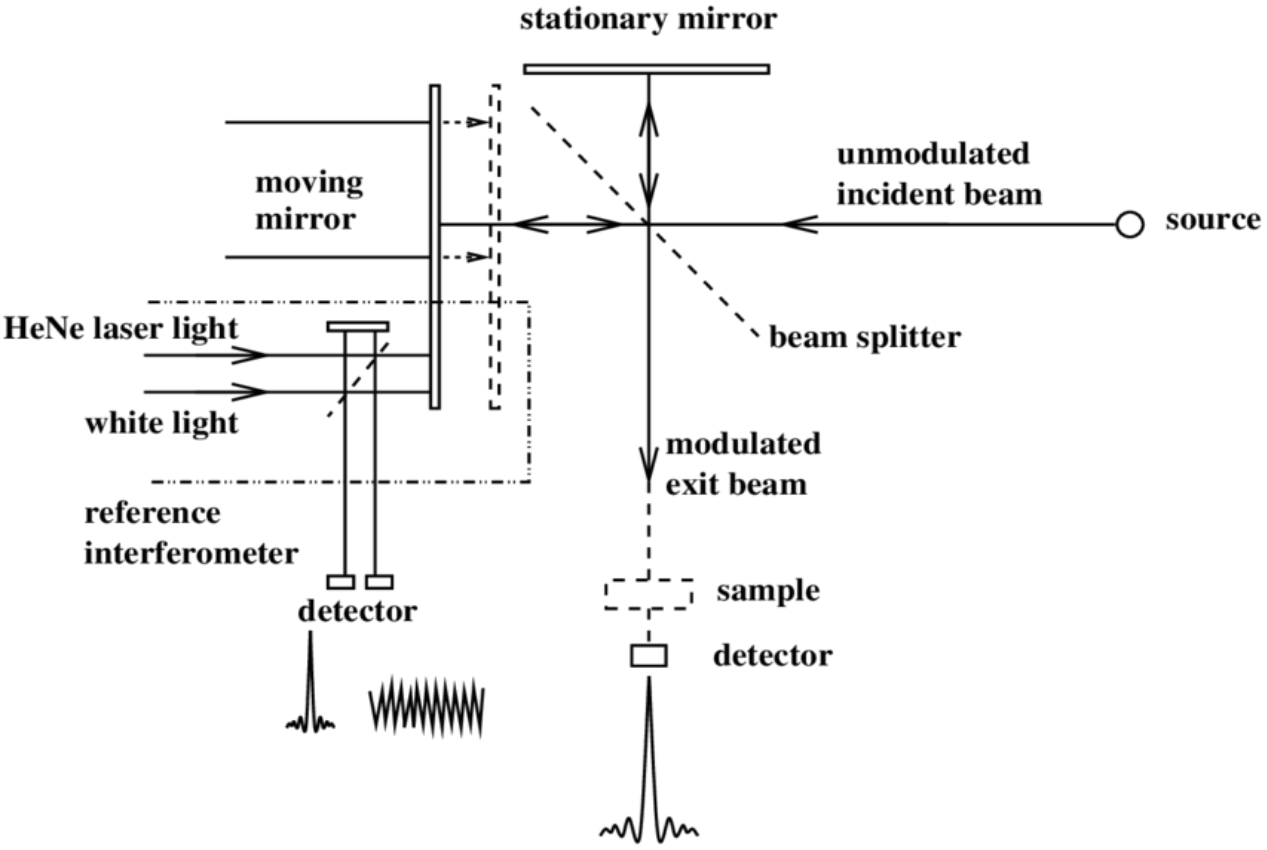

Figure 4- 3. A schematic diagram of a fourier transform infra-red spectrophotometer (Pérez León 2005).

4.5 Differential scanning calorimetry (DSC)

DSC is employed to determine a polymers's (a solution in a mixed, or in a solid phase) heat capacity, thermal transition, glass transition temperature and the melting point. For a material, a DSC gives indication of the enthalpy changes that do occur as a result of its changes in the physical and chemical properties with some advantages such as faster speed, high sensitivity and simple to use. It has been employed for use in many applications such as plastics and ploymers, food industries, pharmaceuticals, ceramic and glass industries and protein studies. The instrument is scanned at a rate of 10°C/min (mostly used) with few milligrams or less amount of the sample

required after calibration. Further, purge gases are used to control the sample environment to purge volatile from the system to prevent contamination. Nitrogen gas (N_2) is usually employed to provide an inert atmosphere and prevent the oxidation of the sample. Other gases include air, O_2 and helium. Sample is then fed into the DSC system and measured after running the standards. The heater is heated and signal is amplified unto a temperature recorder connected to a computer for recording. Indium has been the easiest standard used due to its stability and low melting point of 156.6°C. Figure 4-4 depicts the schematic diagram of a typical differential scanning calorimeter.

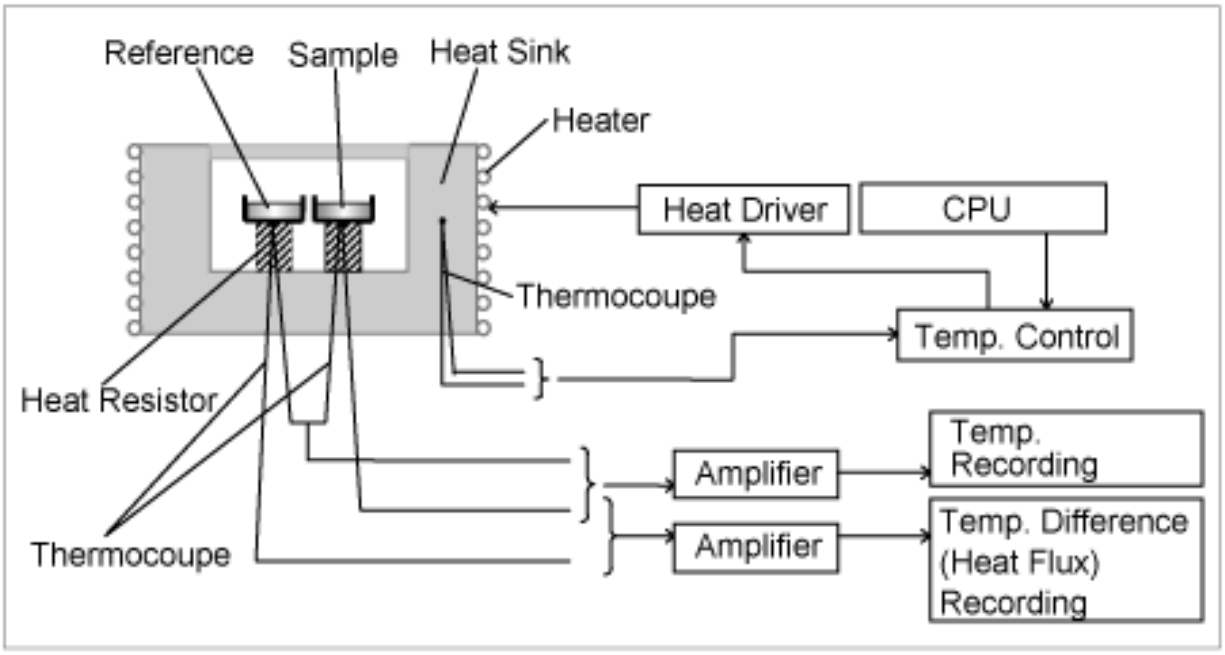

Figure 4- 4. Schematic diagram of a differential scanning calorimeter.

4.6 Thermogravimetric analysis (TGA)

TGA is an analytical technique that is employed to measure the variations in the mass of a sample over a range of temperatures under a controlled atmosphere and time. That is, as the sample is heated, its mass changes over temperature to obtain a material's thermal stability (Cheng *et al.* 2016). In this technique, the loss of mass in a sample is monitored if its thermal characteristics

involves the loss of a volatile component. The results provide a quantitative dimension of any weight changes associated with the observed transitions. The parameters are observed at a temperature of °25C to about 1100 °C. A reactive or inert atmosphere created for the derivatives of TG measurements usually enables the accomplishment of the weight-loss steps, thereby, causing an increase in the resolution of overlapping weight-loss occurrences (Willard *et al.* 1986; Mkhize *et al.* 2016). Sample weight is then plotted against temperature or time to show the material's thermal transition. The mechanisms of weight changes in a typical TGA instrument includes weight loss which consists of decomposition, evaporation, reduction and desorption and weight gain which consists of oxidation and absorption. Calibrations in the use of the TGA is affected by purge gas, flow rate, specimen pan type and heating rate. Its applications ranges from the the determination of filler contents in the resins of a polymeric material, the content of residual solvents, carbon black content and the the moisture content of organic and inorganic materials. Figure 4-5 shows the schematic diagram of a thermogravimetric analyser.

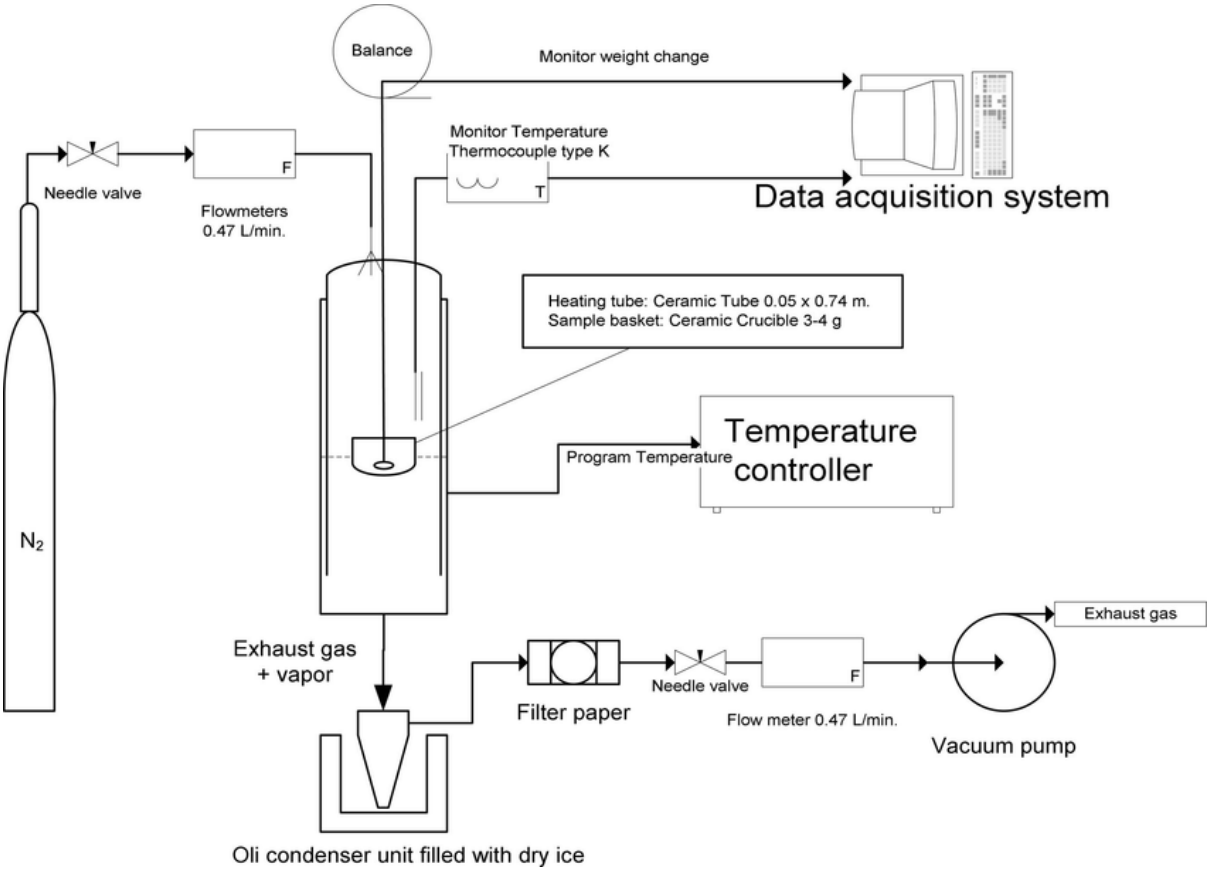

Figure 4- 5. Schematic diagram of a thermogravimetric analyser.

4.7 Scanning electron microscope (SEM)

SEM is classified as a multipurpose instrument used to observe the surface phenomenum for a material of interest. The visual images of a material with spatial resolution and high quality is achieved using the SEM. During its operation, the sample is exposed to a high-energy electron beam to give details on its morphology, composition, topography and the crystallography. The principle of the SEM is based on the use of an electron beam created by a suitable source, classically made of tungsten filament or in some cases, a field emission gun with an electron beam, which is accelerated by a high voltage. Further, this electron beam passes through a media of spaces with electromagnetic lenses to produce a thin beam of electrons, which scans the surface of

the specimen by means of scanning coils. Thereafter, the electrons are released from the specimen by the action of a scanning beam which is collected by a suitably positioned indicator. The beam scanning the surfaces of the specimen are precisely coordinated with a spot on the screen as the electron detector controls the intensity of the spot on the screen. Magnification is then calculated as the image formed by the ratio of the size of the screen with regards to the size of the area visualised on the specimen. Two major types of electronic images are formed which include; (a) the secondary electron image (SEI) which is used largely for image fracture surfaces, giving a higher resolution images and (b) the backscattered electron image (BEI) which is employed on a polished section. The brightness of the BEI is dependent on the atomic masses of the specimen or the average atomic masses for the compounds (Mkhize *et al.* 2016). Advantages of the SEM includes its good resolution, the provision of qualitative and elemental analysis when combined with the EDS and its traceable standards for magnification. A major drawback in the use of the SEM instrument is that, coating with gold or carbon before testing usually results in the formation of an artifacts (Golding *et al.* 2016). Figure 4-6 depicts the diagram of a scanning electron microscope.

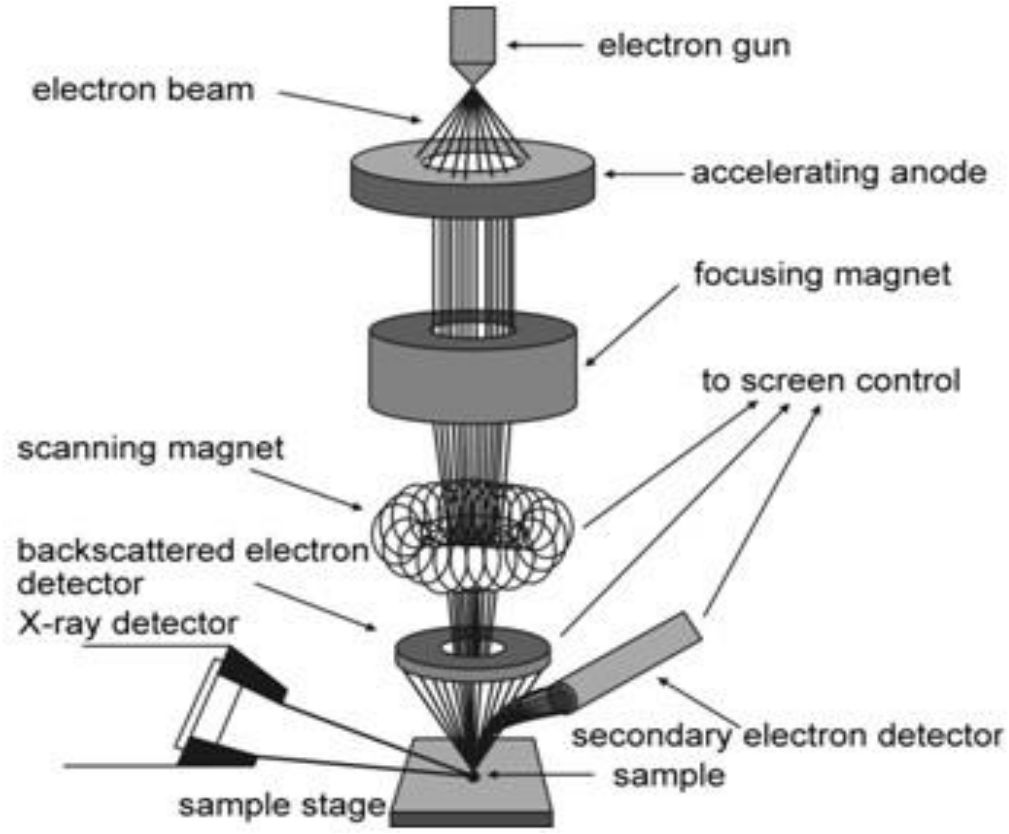

Figure 4- 6. Schematic diagram of the scanning electron microscope.

4.8 Karl Fischer titration

Water can be readily absorbed by laboratory reagents such as ionic liquids and other solvents from the atmosphere due to their hygroscopic nature during storage or experiments (Tywabi 2015). The moisture or water content in reagents or substances (solids or liquids) could be measured by the use of the Karl Fischer (KF) method of titration. The technique was first discovered in the 1930s by a *German chemist, Karl Fischer* hence the name. The KF titration is observed to be employed in an analytical chemistry that uses coulometric or volumetric titration to determine trace amounts of water in a sample. The coulometric titration is mostly suitable for samples with a low water contents (10µg to 100mg) whilst the volumetric titrationis is applied for samples with high water contents (0.1mg to 500mg). During the titration, iodine is added to the sample as the quantity of

iodine used is made to take-up the amount of water contained in the sample to be measured. With regards to the volumetric titration, a solution which contains an exactly known concentration of iodine is added to the sample as the quantity of iodine added is estimated from the volume of the iodine solution. Whereas in the case of the coulometric titration, the iodine is generated electronically as it is added to the sample by measuring the current required for the electrochemical production of the iodine. After, a brown iodine is observed to be reduced to a colorless iodide upon reaction with available water present in the sample under consideration. Applications of the Karl Fischer techniques have been extensively employed in the petrochemical industry for moisture identification in crude, fuels, oil, and lubricants. Other applications are in pharmaceutical industries and cosmetics factories. Chemical applications include the use in solvents, salts, organic matter, and metals and in food processing industries including liquids, formulae, and mixes. The schematics of the KF titrator are presented in Figure 4-7.

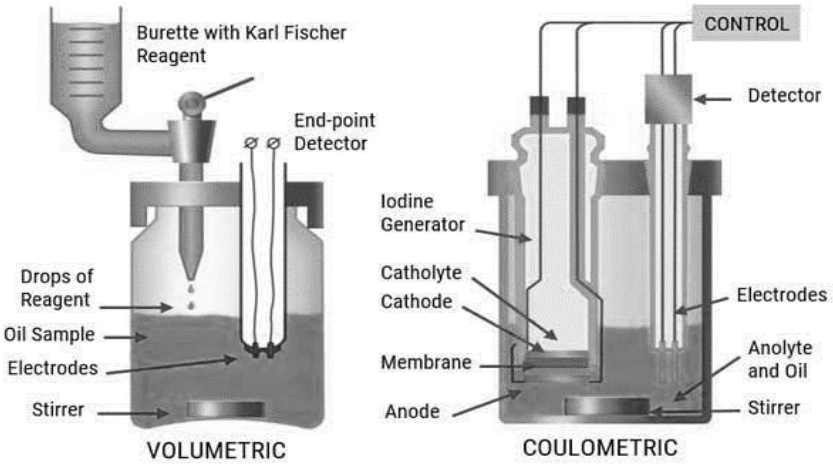

Figure 4- 7. A schematic diagram of a Karl Fischer titrator.

CHAPTER 5

RESULTS AND DISCUSSIONS

5.1 Introduction

The experimental results obtained from this present study is discussed in this chapter. **Section 5.1** introduces this chapter with a brief description of each sub-section and **section 5.2** details the data analysis for the characterisation techniques employed for each biomass. In **section 5.3**, the results of the BMP test for the untreated biomass is discussed. In this section, the effects of particle size for SCB and CS, preliminary experiments for WW selection based on the maximum yield and the interpretation of the process optimisation using response surface methodology is discussed. **Section 5.4** presents the interpretation of the BMP test for the treated biomass. In this section, the daily biogas production, biomethane potentials and the kinetic study after ionic liquid pretreatment are discussed. In **section 5.5**, the annual estimated energy derived from the biogas production rate in this study is presented. Finally in section 5.6, the data obtained from the BMP tests are fitted to existing AD kinetic models to predict the best fit based on the correlation coefficient, R^2.

5.2 Characterisation

5.2.1 Ultimate and proximate analysis for the SCB and CS

The ultimate analysis was carried out to determine elemental hydrogen (H), Carbon (C), Nitrogen (N), Phosphorous (P), Oxygen (O), Potassium (K), etc. for both the SCB and CS. The proximate analysis categorises the biomass in terms of its fixed solids, moisture content, total solids, volatile solids, and ash contents. The calculations of the proximate analysis proximate analysis are

presented in Appendix A2. The data supporting the proximate analysis of SCB and CS is presented in Tables A-1 and Table A-2 of CS. The ultimate and proximate analysis of the biomass plays a vital and important part of a process which gives the critical information needed for a rational design or better understanding of an entire process. It is paramount to understand that some of the carbon will be in the volatile matter with other fractions forming char. For example, the ash content is employed to identify if the biomass residue is nutrient-rich since higher ash contents give an indication of higher nutrient contents (Tawoma 2015). The moisture content was found to be greater in CS than in SCB indicating that much water is held up by the cells of CS than SCB (Table 5-1). It is, however, important to note that the reduction in weight is associated with the moisture content of the biomass under study which is considered important in processing units employing waste-to-energy technologies. Table 5-1 also presents the results of the proximate analysis for the SCB and CS.

Table 5- 1. Proximate analysis of feedstocks (% dry weight).

Parameters	**SCB**	**CS**
TS	94.1	93.0
VS	78.0	96.0
MC	5.9	7.0
FS	22.0	4.1
Ash	9.9	3.5

The estimation of the elemental composition of organic substances in biomass usually require knowledge of the mineral and non-mineral inorganic contents. Predominantly, carbon and oxygen were largely found in this study other than the other elementals as shown in Table 5-2.

Table 5- 2. Ultimate analysis of feedstocks (% dry weight).

Elementals	SCB (weight, %)	CS (weight, %)
C	27.0	27.0
O	72.0	72.3
Si	0.1	0.04
Fe	0.1	0.01

5.2.2 Proximate analysis for the WW streams

As presented in Appendix A3, the ultimate analysis which comprises of the total solids, volatile solids, total suspended solids, and volatile solids were reported. It was evidenced that all the WW streams are highly biodegradable since the VS/TS ratios are above 50% according to a study by Paritosh *et al.* (2018). The results of the analysis indicated that the increasing trend for the proximate analysis for the WW streams were found in the order; VSS < TSS < VS < TS. The average COD reported for the SWW, DWW, brewery WW and municipal WW were found to be 7,200 mg/L, 5,500 mg/L, 4,500 mg/L and 3,500 mg/L, respectively. It has been reported that WW with COD concentrations higher than 800 mg/L have been found to be suitable for AcoD processes (Enitan 2015), making these WW streams suitable for use in this study. Also, the pH of the WW streams and the sludge which is presented in the Appendix (Table A-8) were found in the range of 6.09 to 8.37, making these substrates suitable for use as co-substrates for AcoD.

5.2.3 SEM

The SEM was used to study the morphology of the feedstocks under this study for both the untreated and pretreated samples. The EDX spectra were collected using an Oxford X-Max 20mm^2

detector and Oxford INCA software, Oxford, UK. Magnification for the images taken are shown in Figure 5-1. Photographs of the SEM-EDX and SEM instrument employed in this study are presented in Figures A7 and A8, respectively. With regards to the images for the SEM analysis, it was observed that there were large fibre swellings or lumps on the surface of the CS (Figure 5-1a), agglomerating to some extent with fine layered structures shown for SCB (Figure 5-1b). The larger crystallites of different sizes on the CS were interwoven with each other, forming tightly bound nanoclusters, similar to a study by Sun *et al.* (2011), and this is commonly observed in most lignocellulosic biomasses. Also, these globular or lumpy structures have been reported to be associated with lignin condensation that were observed on the surface after pretreatment which is similar to previous study (Ejekwu 2019). SEM results for the untreated samples showed intact lamellar structure where hemicellulose and lignin wrapped around the cellulose in a hetero-matrix similar to that observed (Ejekwu 2019). Comparatively, the surface morphology of SCB was found to be finer/smoother and homogeneous when compared to CS which had heterogeneous layers. None of the images for the untreated biomasses showed any extent on the degree of porosity. In the case of the treated CS and SCB, it was found that the layers of the surfaces provided a non-uniform and porous structures with a thickness of 20 µm and 100 µm corresponding to magnifications of 2.5 kx and 500 x respectively as presented in Figure 5-1(c-f). This signified a better intermolecular bond formed with high porosity which enhanced the biodegradation process for higher biogas production. [EMIM][OAc] ionic liquid pretreated CS or SCB had a more irregular and corrugated surface with thinner fibres compared to the untreated forms. Many researchers have also reported that the structure of the biomass could become more porous, less crystalline, and susceptible to enzymatic attack after IL pretreatment (Mthembu 2016) as evidenced in this study. Nonetheless, irrespective of the type of biomass under study, the structure

becomes altered and favours enzymatic hydrolysis and microbial attack after ionic liquid pretreatment (Park *et al.* 2018). Both SCB and CS also showed distinct inner cavities which increases the surface area and thus the number of reactive sites. This was also confirmed by the measurements obtained from the FTIR spectra with lower absorbances and higher percentage transmitted (%T) observed after pretreatment as depicted in Figure 5-1a and Figure 5-1b. From the EDX (Thermo Fisher Nova NanoSEM, FEI, USA) values in Table A-9 and Table A10, higher amounts of oxygen and carbon could represent greater passitivity in the layer formation, similar to what Tetteh, Rathilal and Naidoo (2020) have reported. It is evidenced that some elements such as potassium (K), magnesium (Mg), copper (Cu), phosphorous (P), calcium (Ca), and iron (Fe) were found absent after the pretreatment process in comparison to that of the untreated feedstocks. This could be due to unstable or a faster degradation rate as the temperature increases. The SEM/EDS backed by the FTIR spectra analysis confirmed the extent of porosity and biomass breakdown efficiencies of a lignocellulosic structure after pretreatment (Ejekwu 2019).

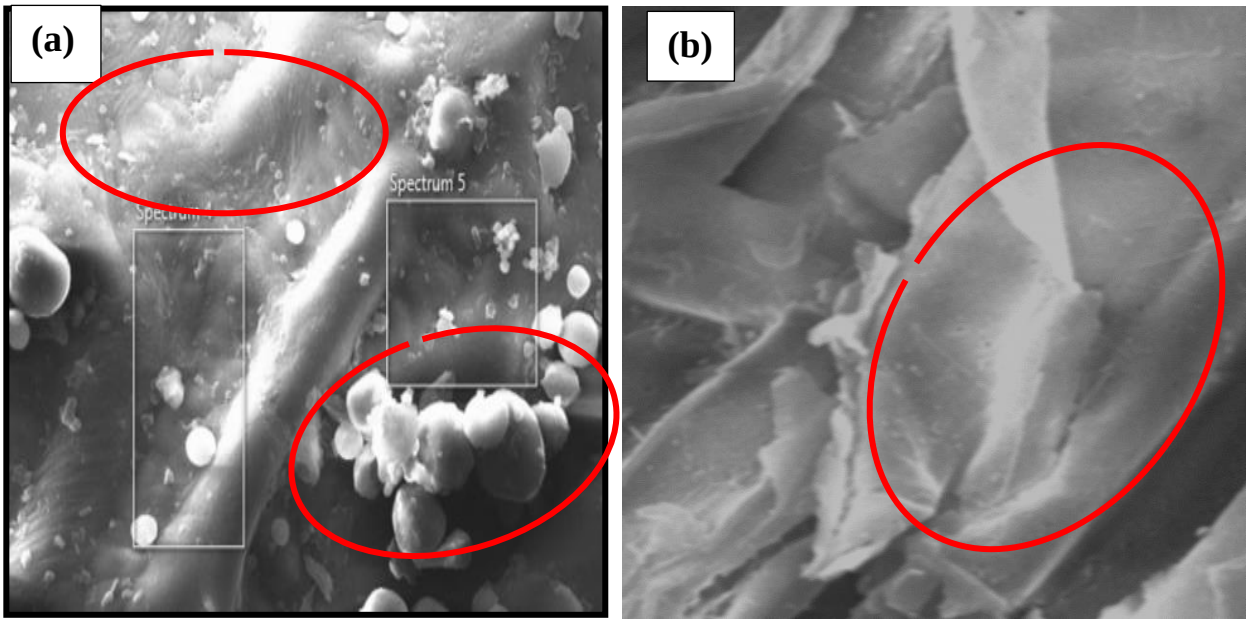

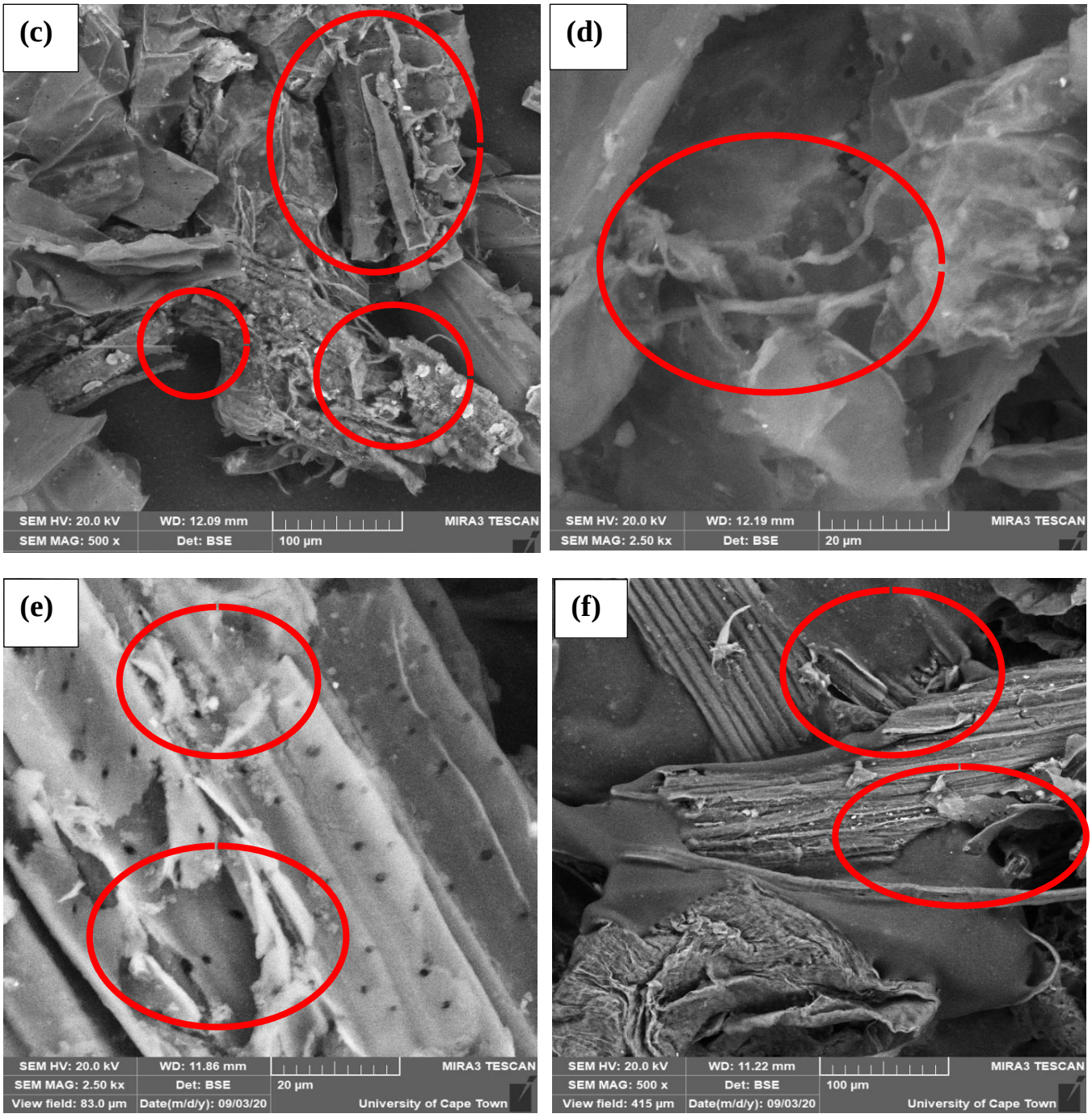

Figure 5- 1. SEM images of the (a) untreated CS, (b) untreated SCB, (c) IL pretreated mill-run SCB with magnification of 500 x, (d) IL pretreated mill-run SCB with magnification of 2.50 kx, (e) IL pretreated CS at a magnification of 2.50 kx and (f) IL pretreated eCS at a magnification of

silage at 500 x. Images (a), (b), (c), (d), (e) and (f) were scanned with the SEM (Tescan Mira3, Tescan, Czech Republic). Red oval/circles indicate extents of degradation of the feedstock after IL pretreatment.

5.2.4 TGA/DSC

In this study, the simultaneous differential scanning calorimeter and thermo-gravimetric analyser were employed to characterise the thermal stability (weight loss as a function of temperature) of the untreated SB or the CS. The TGA curves (Figure 5-2) show an exothermic peak at approximately 100 °C, which occurred due to moisture removal as the sample was heated. The curves exhibited the three phases of the degradation steps. The initial weight loss can be observed between 30°C and 100 °C in all scans, which could be attributed to the evaporation/dehydration of loosely bounded moisture on the surfaces of the samples due to crosslinking and condensation that takes place among the diverse functionalities and represented as the first step. During the decomposition step which was the second step (100 to 350°C), it was observed that most of the volatile products, for example, the loosely bound water, evaporated during the initial phases of heating. From the curves, the area under the main decomposition stage was very close (or similar) which gives an indication that similar amount of the biomass is decomposed as a function of temperature. The area underneath the derivative curve presents the amount of the substance decomposed in that temperature range. About 18 to 20 wt. % of either biomass was lost during the decomposition step. In the third step which occurred between 350°C and 800 °C, decomposed samples reported minimal loss of weight as the temperatures increased from 400°C to 800°C. The OriginPro Software by OriginLab® was used for plotting the TGA and DSC thermograms for both feedstocks as presented in Figures 5-2 and 5-3 respectively.

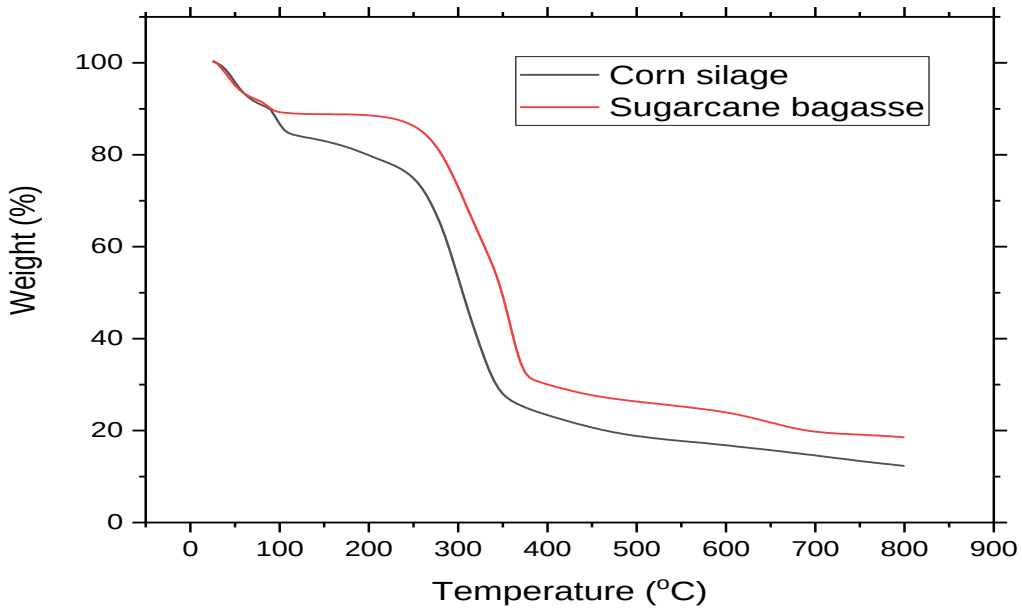

Figure 5- 2. Thermograms for the untreated SCB and corn silageCS.

For the DSC curves, the exothermic peaks that appeared at 350°C and 450 °C could be attributed to charring as reported in previous study (Mkhize *et al.* 2016). The trend in the rate of biomass degradation and decomposition observed in the curves from the TGA resulted in what is contained in the DSC as the rate of decomposition decreased with increasing temperature and time. The increase in temperature resulted in a decrease in the heat flow for both SCB and CS although it was more pronounced in SCB. The heat flow was observed to decrease drastically from 380°C to 800°C as presented in Figure 5-3. These could be due to the separation rate of the heat current which was found to be slower in the preliminary stages during the scan and became stabilised thereafter. Between 500°C to 600 ºC, both SCB or CS shifted into a negative phase suggesting a decomposition, crosslinking or oxidation. Also, this may be attributed to the heat flow of the sample which was lower than that of the reference as both peaks were observed to be in the negative direction.

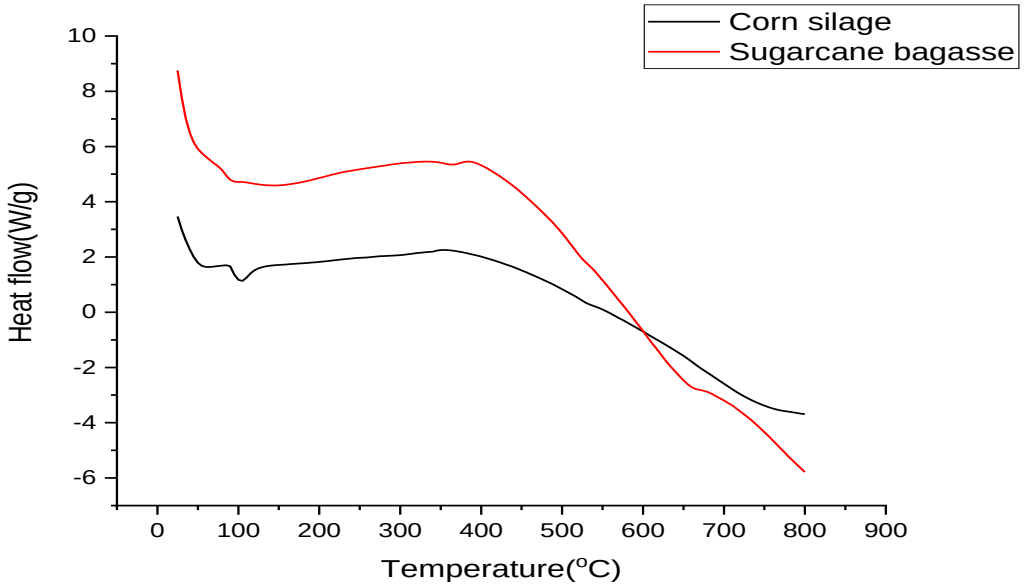

Figure 5- 3. Differential scanning plots of the untreated SCB and CS.

5.2.5 FTIR

The observation of the changes that occured with respect to the functional groups and the molecular conformation was carried out using the FTIR spectroscopy for both the treated and untreated feedstocks. These techniques have been used to recognise the occurrences of different functional groups present in a sample. In this regard, the changes in the chemical structure were done using the spectrum two FTIR spectrometer (Figure A-9) with the spectra recorded in the range of ν_{max} from 500 to 4000 cm^{-1}. The two major components of a lignocellulose biomass comprises of the holocellulose (hemicellulose and cellulose) and lignin which are known to generally consist of esters, alkenes, alcohols, ketones and aromatics with different oxygen containing functional groups. The percent transmittance, %T indicated the percentage of incidence light, which is transmitted, that is, the amount of light that successfully passed through the feedstock and observed on the other side. In this regard, the absorbances of each could be derived

from the % T by the relation, A = 2 - log(%T); where A is the absorbance and % T is the percentage transmitted. For this analysis, the spectra (Figure 5-4a and Figure 5-4b) showed an existence of several functional groups which represents the major components of lignocellulose as discussed above. The peaks observed for the wavelength of 3500 to 3300 cm^{-1} and 3000 to 2800 cm^{-1} represents an existence of stretching hydroxyl (O-H) and stretching alkane (C-C or C-H) group. In figure 5-5a, the stretching O-H peak was found to be sharper in the case of the untreated CS than the treated CS similar to a study by (Ejekwu 2019). This indicates that for the %T of 85% shown for the untreated at this peak, an absorbance of 0.071AU is obtained whilst in the case of the %T of 98% recorded for the treated feedstock, an absorbance of 0.009AU was obtained. This was different in the case of Figure 5-5b, where the stretching O-H peak was found to be sharper in the case of the treated SCB than the untreated CS. For example, a %T of 97% recorded and absorbance of 0.013AU for the untreated SCB whiles for %T of 94% recorded for the treated feedstock, an absorbance of 0.027AU. The corresponding peaks in 1745 cm^{-1} and 1644 cm^{-1} represent the stretching of C=O and C=C arising from esters and alkenes, respectively. Also, at the peaks of 1463 cm^{-1} and 1200 to 1100 cm^{-1} refer to the bending of an alkane (C-C) and the stretching of an alcohol (C-O-H). Further, broad bands appearing at 1096 cm^{-1} are as a result of a –C-O group, and the peak of 915 cm^{-1} corresponds to the –C-O-C group which is similar to that reported by Mkhize *et al.* (2016). Past studies have proposed that pretreatment could specifically help remove hemicellulose and lignin fractions for residual pre-treated material that is rich in cellulose. The band at 896 cm^{-1} is typical of a glycosidic bond β-(1 → 4) which corresponds to a C-H deformation in cellulose (Bezerra and Ragauskas 2016; Xie *et al.* 2016b). The region between 1200 and 1100 cm^{-1} indicates the presence of hollocellulose which displayed a maximum value of 1035 cm^{-1} due to the C-O stretching, and at 1164 cm^{-1}, the asymmetrical stretching of C-O-C. Bands observed at

2920 cm^{-1} and 2850 cm^{-1} corresponded to the C-H groups. The –COO group was linked to the peak at 1726 cm^{-1}. The band around 1515 cm^{-1} is due to C=C stretching of the aromatic ring that are present in lignin. The region to the right-hand side of the spectra (from about 800 to 400 cm^{1}) also contain a very complicated series of absorptions due to series of bending vibrations within the molecule under study and was considered to be the fingerprint region. Generally, it is observed that the amount of light absorbed by CS after the pretreatment was lower as compared to that absorbed for the untreated feedstock due to the fact that the lignocellulose structure is broken down and become relatively porous. This is evident in the SEM images (Figure 5-4) as the structure of the lignocellulosic components are exposed for microbial degradation. The FTIR spectra for the consecutive set of runs after ionic liquid pretreatment for both SCB and CS are presented in Figures C2-1 and C2-2, respectively. Table 5-3 gives a summary of the functional groups and their corresponding wavenumbers (frequencies).

Table 5- 3. Summary of the functional groups for lignocellulosic biomass.

Wavenumber (cm^{-1})	**Peak assignment**	**Compound**
3600-3000	O-H stretching	Acid, methanol
2860-2970	C-H stretching	Alkyl, aliphatic and aromatic
1700-1730; 1510-1560	C=O stretching	Ketone and carbonyl
1632	C=C stretching	Benzene stretching ring
1613;1450	C=C stretching	Aromatic skeletal mode
1470-1430	OCH_3	Methoxyl-O-CH_3 acid
1440-1400	OH bending	-
1402	C-H bending	-
1232	C-O-C stretching	Aryl-alkyl ether linkage
1215	C-O stretching	Phenol
1170; 1082	C-O-C stretching vibration	Pyranose ring skeletal
1108	O-H in plane deformation	C-OH
1060	Stretching -O, stretching vibration and C-O deformation	C-OH (ethanol)

The OriginPro Software by OriginLab® was used for plotting the FTIR graphs of the untreated and pretreated feedstocks which are presented as Figures (a) and (b).

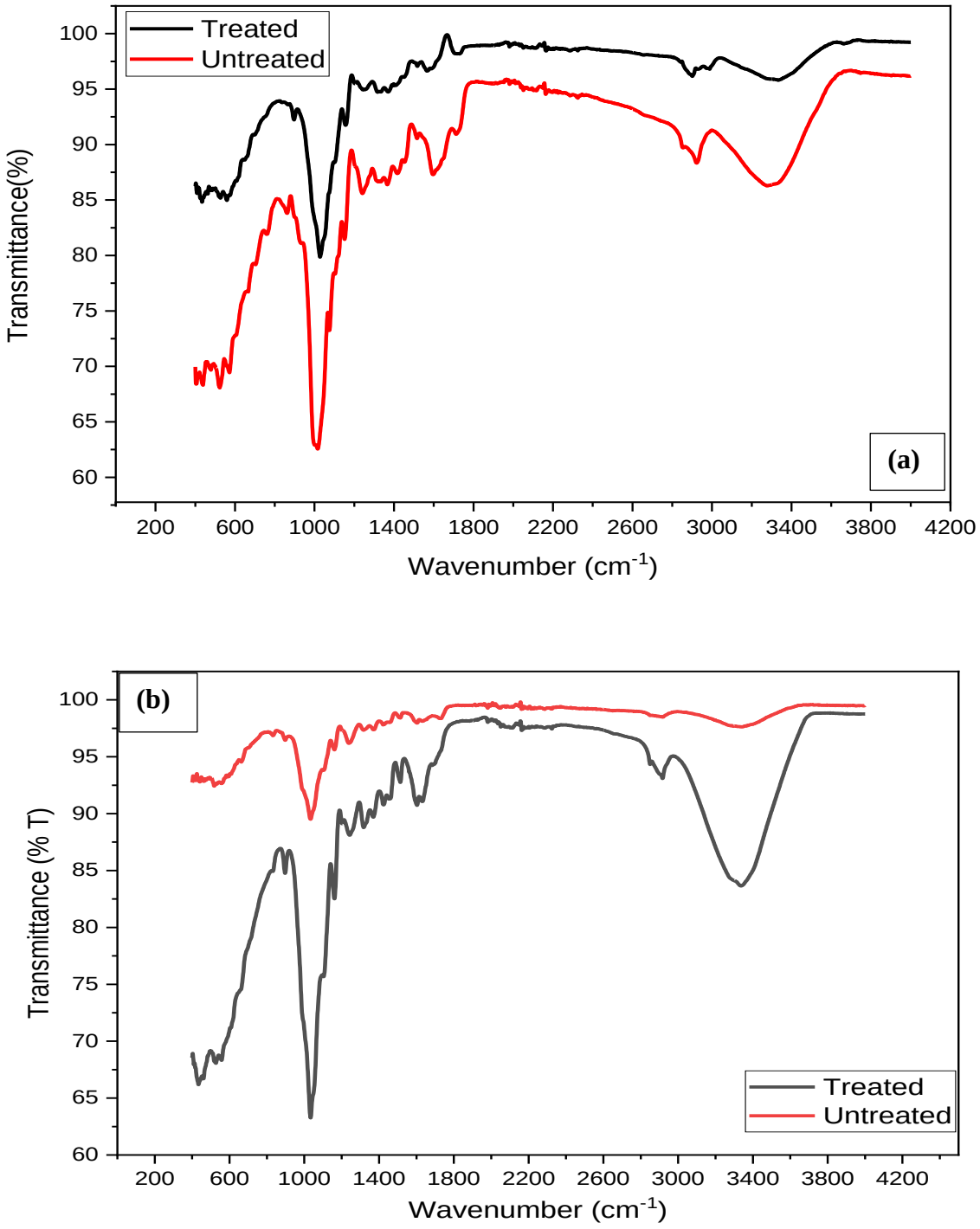

Figure 5- 4. (a) FTIR spectra for the untreated and pretreated CS; (b) FTIR spectra for the treated and pretreated SCB.

5.2.6 Compositional analyses: cellulose, hemicellulose and lignin The composition of cellulose, hemicellulose and lignin in lignocellulosic biomass have been reported in the range of 30 to 50%, 20 to 30% and 19 to 33%, respectively (Table 5-4) for SCB. For CS, the composition of cellulose, hemicellulose and lignin in lignocellulosic biomass have been reported in the range of 30 to 50%, 20 to 35% and 10 to 20%, respectively as presented in Table 5-5. Comparing these ranges to that of the cellulose, hemicellulose and lignin reported in this study (in asteriks) affirms the presence of cellulose which is the active site for energy storage for bioenergy production.

Table 5- 4. Summary of the chemical composition of raw SCB(% w/w, dry basis) from the literature.

Components (%)	**(Rainey 2009)**	**(da Silva *et al.* 2011)**	**(Rocha *et al.* 2011)**	**(Rabelo *et al.* 2011)**	**(Canilha *et al.* 2012)**	**(Chandel *et al.* 2012)**	**(Simo, Jong and Kapseu 2016)**	***This study**
Cellulose	47.0	38.8	45.5	38.4	45.0	39.53	43.6	46.1
Hemicellulose	27.0	26.0	27.0	23.2	25.8	25.63	17.2	22.8
Lignin	23.0	32.4	21.1	25.0	19.1	30.36	22.0	29.1

Table 5- 5. Summary of the chemical composition of untreated CS (%w/w, dry).

Components (%)	**(Hong *et al.* 2016)**	**(Prasad, Singh and Joshi 2007)**	***This study**
Cellulose	38	45	42
Hemicellulose	26	35	30
Lignin	19	15	16

Summary of objective one

The biodegradable fraction, VS was found greater in CS other than SCB which could contribute to an enhanced biogas potential in CS. Also, results of the SEM/EDS together with the FTIR spectra showed the extent of porosity and biomass breakdown efficiencies of a lignocellulosic structure after pretreatment. The thermal stability (TGA) of the biomass was observed at different degradation rates (3-phases) with greater crystallinity observed to be predominant in SCB than for CS which influenced the microbial accessibility. Comparatively, the cellulose, lignin and hemicellulose contents were found within the range as reported from previous studies.

5.3 BMP tests for the untreated biomass

5.3.1 Effect of particle size on biogas production

The stability and speed of an AD process is dependent on the size of the particles required for the input material under study. As described in section 3.3.1, the particle sizes of SCB and CS were varied at 2 mm, 1 mm, 0.6 mm and 0.4 mm. The results of the study showed that the maximum biogas production rate was found to be 125 mL/d using a particle size of 0.4 mm when both SCB and CS were anaerobically co-digested with WW. In another study, the maximum biogas production was found to be 16.96 mL/d for finely grounded biomass of particle size of 0.001 mm (Njoku *et al.* 2015). The lowest biogas production rate was reported for the largest particle size in that study at 6 mm which gives an indication that smaller particle sizes of the biomass favors the biogas production rate. Hence, better surface area of the biomass is achieved when the particle size of the biomass is smaller which aids in a better microbial accessibility and biodegradation. A significant change in pH of anaerobic biodigesters during AcoD have been found to cause system failure which affects the overall biogas production (Kougias *et al.* 2015). This mainly happens as

a result of organic acid (VFAs) accumulation which becomes greater than the CH_4 production rate as the pH is found to drop, inhibiting the methanogenic population (Shin *et al.* 2019). The reported pH before AcoD was in the range of 6.2 to 7.0 whilst that of the pH after AcoD was found in the range of 6.5 to 8.5 which affirms the optimum pH range of 6.0 to 8.5 reported in previous studies.

5.3.2 Preliminary experiments of wastewater selection for process optimisation

As described in section 3.3.2, it was important to ascertain which WW streams (2 out of the 4 selected in this study) produces better biogas potentials. In the discussion below, each of the WW stream is co-digested with SCB or CS to determine the biogas potential at 25°C, 35°C, and 55°C. Also, pH monitoring in anaerobic biodigesters have been found to be crucial for biogas production due to system fluctuations by VFA accumulations (Terboven, Ramm and Herrmann 2017) with an optimum range of 6.0 to 8.5 observed in previous studies. In this study, the pre-digestion pH ranges for the AcoD with the WW streams were reported as 6.4 to 6.7, 5.8 to 7.0, 6.0 to 6.7 and 5.9 to 7.0 for brewery WW, municipal WW, DWW, and SWW, respectively. Post pH ranges for the AcoD of the SCB and CS with the WW streams were reported as 7.5 to 8.2, 7.8 to 8.1, 7.1 to 8.1 and 6.9 to 8.0 for brewery WW, municipal WW, DWW, and SWW, respectively.

5.3.2.1 AcoD of selected feedstocks with brewery WW

The biogas production from SCB and CS with brewery WW was examined with reference to Table 3-1. In biodigester A (Figure 5-5), biogas production started on day 7 (longer lag phase) with 10mL produced with a slightly higher value (12 mL) observed on day 11 with a sharp decline on day 12 (5 mL) until it finally stopped on day 16 (5 mL). In biodigester B, biogas production started on day 3 and remained slightly constant (20 mL) over the period until day 7 where the highest biogas was generated (40 mL).

In Figure 5-5, the extent of production begun to fluctuate thereafter until day 18 where the biogas production ceased. In biodigester C, biogas production began on day 3 (5mL) and improved exponentially up to day 8 with 50 mL of biogas produced. The production of biogas declined slowly after day 8 as the volume was observed to be in the range of 10 to 40mL from day 9 to 21**.** In biodigester D, there was no lag phase as biogas production started on day 1 with 45mL produced from day 1 to 5. The highest volume of biogas (20 mL) was produced on day 5 as production stopped on day 10. Comparatively, the highest biogas production for all the biodigesters occurred on day 6 to day 8. This gives an indication that the microbes present in these biodigesters became extremely active within this period, making them produce more of the biogas required. Also, within those days, microbes are known to have acclimatized and have replicated, therefore, producing more biogas (Kougias and Angelidaki 2018). It was observed from this study that the biogas production rate (BPR) was 6.16, 21.2, 33.6 and 7.2 mL/gVS/d for biodigesters A, B, C and D respectively. Also, a higher volume of biogas corresponded to an increase in hydrolytic activity of the ferment and swift CO_2 production.

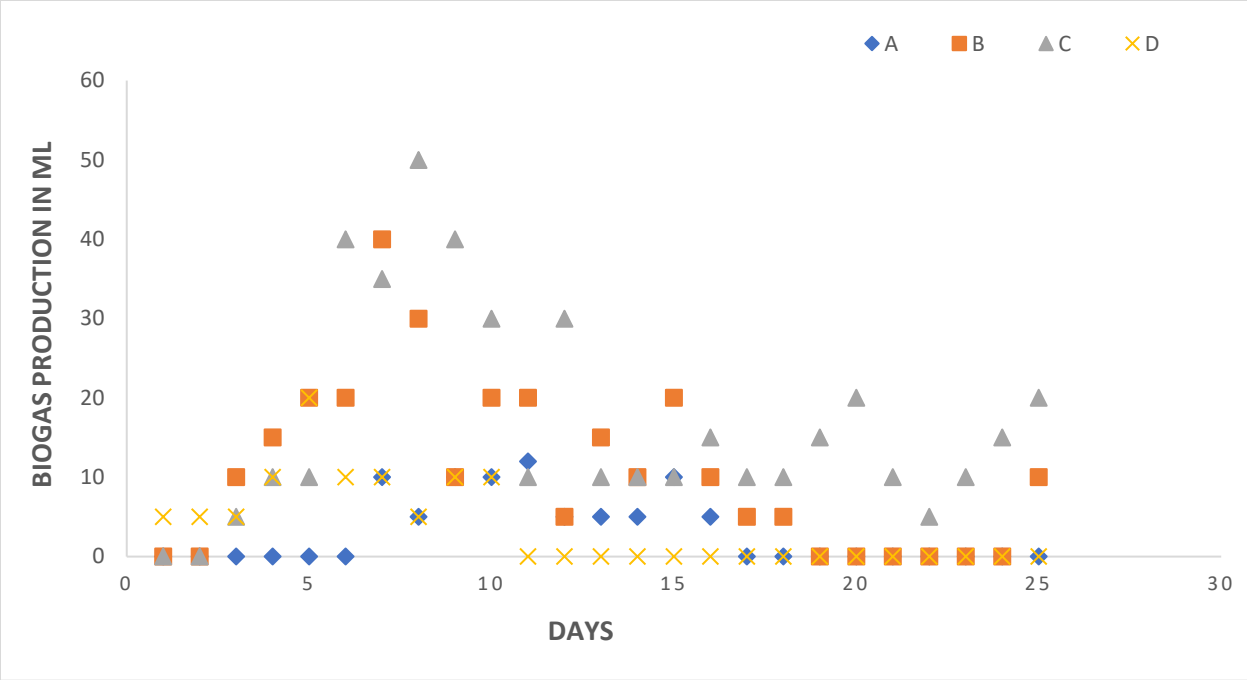

Figure 5- 5. Biogas production at 25°C.

In biodigester A, there was a lag phase of 6 days until biogas production began on day 7. The highest volume of biogas of 10 mL was observed which remained constant from day 9 to day 11 until a sharp decline on day 12 which remained constant with 5mL of biogas produced from day 12 to day 15 after which production stopped. Significantly, biogas production began within the first 24 hours of digestion (biodigester B) which was recorded as day 1 and increased steadily with the highest volume of 100 mL on day 5. A lower volume of biogas of 5 mL was recorded on days 12, 19 and 20 until biogas production stopped. In biodigester C, biogas production started on day 3 with the highest volume of 50 mL obtained on day 8. A total of 415 mL biogas was produced over the 25 days of digestion. In biodigester D, biogas production started on day 1 and increased to 5mL on day 2 and remained constant over the range of 10 to 20 mL until the digestion stopped on day 10. It could be confirmed that biogas production was found to be shortest for biodigester D as compared to biodigesters A, B and C (Figure 5-6). It was observed from this study that the

biogas production rates (BPR) were 4.8, 40.0, 33.2 and 8.0 mL/gVS/d for biodigesters A, B, C and D, respectively.

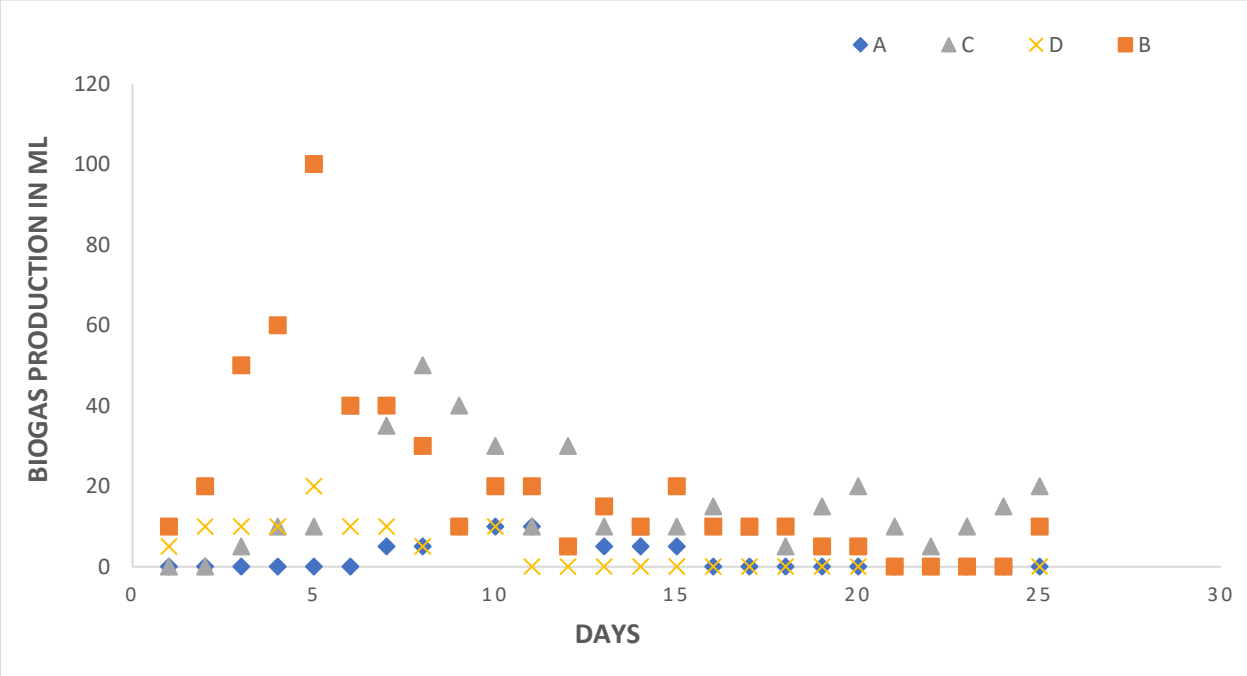

Figure 5- 6. Biogas production at 35°C.

Temperatures above 40°C have been reported to influence the biogas production (Terboven, Ramm and Herrmann 2017) in biodigesters as presented in Figure 5-7. For biodigester A, the production of biogas started on day 6 and stopped on day 15 which was attributed to microbial inactivity during the AcoD process (Wu *et al.* 2018). A higher volume of biogas of 15mL was observed on days 10 and 11 after which a total volume of 30mL biogas was recorded from days 12 to 15. For biodigester B, biogas production started on day 3 with the highest biogas of 101 mL produced on day 8. It was observed that production increased sharply from day 4 to day 11. For day 12, the biogas production declined by 60 mL from the previous day as production remained almost constant within the range of 10 to 30 mL from day 13 until the production stopped on day 25. The decreasing trends could be due to intermittent biodegradation pattern observed by the

microbial community (Wang *et al.* 2019). The complete and effectiveness of an organic matter breakdown into CH_4 under thermophilic temperatures was evidenced in this study which is in accordance to what Silvestre et al. (2014) reported. It could be deduced that the production of biogas is highly pronounced for biodigester B than biodigester C under thermophilic temperature. For biodigester C, biogas started on day 4 the with highest volume of biogas observed on days 5, 8 and 10 of 50 mL each. Whereas in biodigester D, a lag phase of one day was reported after which the biogas production commenced on day 2 and increased sharply on day 6 with 40 mL (highest) produced. This was higher than what was produced by biodigester A on the same day with a difference of 35 mL. Comparatively, the maximum volume of biogas was achieved from day 6 to day 10 in all the biodigesters controlled at 55°C. Biogas production rates (BPR) recorded were found to be 7.60, 74.08, 48.80 and 22.40 mL/gVS/d for biodigesters A, B, C and D, respectively.

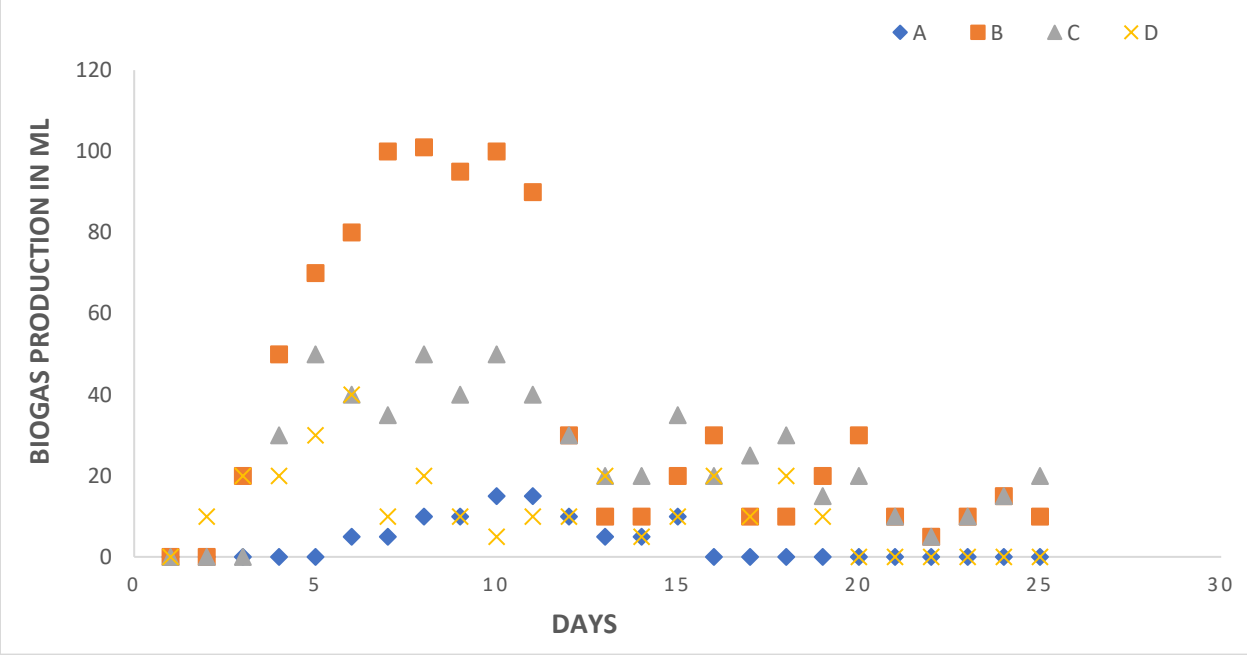

Figure 5- 7. Biogas production at 55°C.

5.3.2.2 AcoD of selected feedstocks with DWW

The biogas production from SCB and CS with DWW was examined with reference to Table 3-1. In Figure 5-8, the biogas production started on day 4 with 5 mL produced followed by a slight increase with the highest volume of biogas recorded on day 11 (12 mL) for biodigester A. Thereafter, the volume recorded was estimated to be in the range of 5-10mL after day 12 until day 18 when the biogas production ceased. For biodigester B, biogas production started on day 2 with 10mL produced, followed by a slight increase with highest volume of biogas recorded on day 7 (40 mL). Production declined slowly from day 8 to day 18 when digestion stopped. Biogas production began on day 2 (20 mL) for biodigester C as the volume kept increasing significantly in the range of 10 to 40 mL. The highest biogas volume of 50 mL was produced on day 8 as production declined slightly from day 9 until day 13. Biogas volume ranged from 10 to 20 mL from day 13 until day 25 when the digestion stopped. Comparatively, there was no lag phase for biodigester D as biogas production started on day 1 with 5 mL being produced. This increased slightly from day 4 to 5 with a sharp decrease from days 6 to 10. However, 20 mL of biogas was produced on day 11 after which 30 mL volume was recorded on day 12 to 14, and highest volume of 40 mL on day 15. A total of 35 mL of biogas was reported from day 16 to day 18 when the digestion process stopped. It was observed from this study that the biogas production rates (BPR) were 8.96, 22.8, 35.6 and 22.0 mL/gVS/d for biodigesters A, B, C and D, respectively.

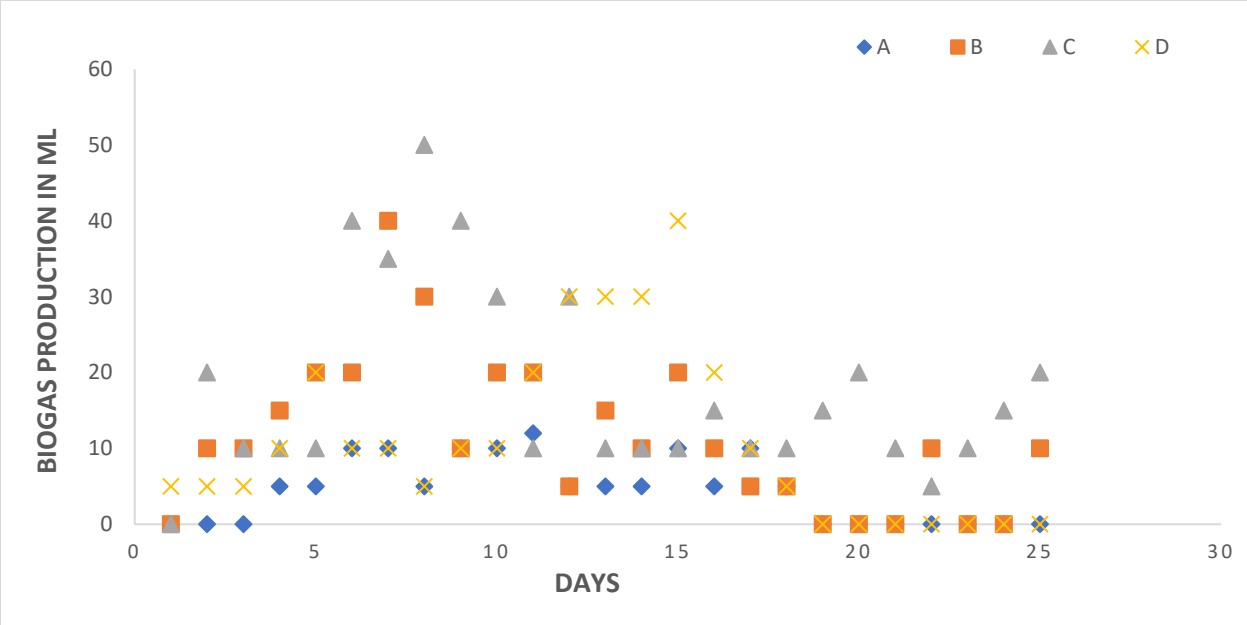

Figure 5- 8. Biogas production at 25°C.

In Figure 5-9, the biogas production started on day 3 with 10 mL produced and a total of 30 mL recorded from day 3 to day 5 as the highest volume of 15 mL was recorded on day 4 as production stopped on day 13 for biodigester A. There was no lag phase for biodigester B as biogas production started on day 1 with 5 mL recorded which increased significantly from day 2 to day 5. The highest volume of biogas was observed to be 90 mL which was recorded on day 5 and a slight decrease in volume within the range of 5 to 40 mL from day 6 to day 21 when the production ceased. For biodigester C (Figure 5-9), biogas production started on day 3 with 5 mL produced which increased slightly with the highest volume of 50 mL recorded on day 8. Thereafter, this decreased slightly from day 9 until the digestion process stopped on day 25. For biodigester D, biogas production started on day 2 (lag phase of 1 day) with 5 mL produced, after which there was a slight increase in the generation with the highest volume observed on day 5 (40 mL). Biogas production decreased

slightly from day 6 (30 mL) to day 17 (5 mL) when the generation ceased. The biogas production rates (BPR) were 6.56, 38.4, 31.2 and 14.8 mL/gVS/d for biodigesters A, B, C and D, respectively.

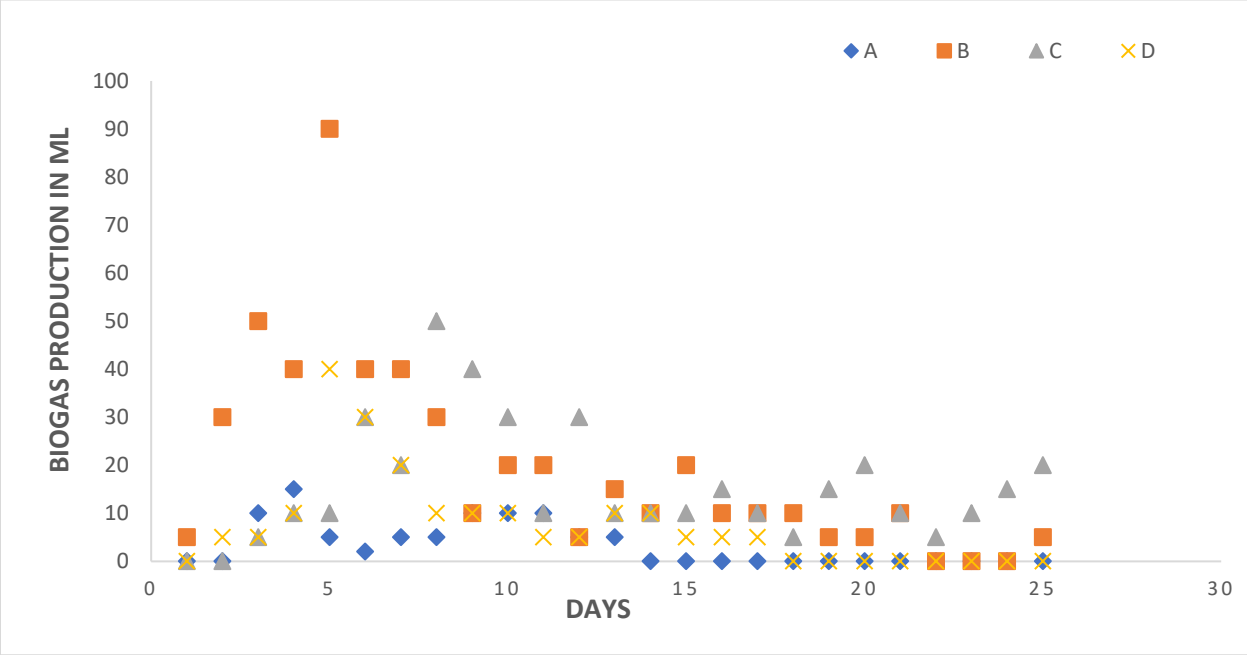

Figure 5- 9. Biogas production at 35°C.

For biodigester A, biogas production started on day 4 (5 mL) as the volume recorded ranged from 5 mL to 30 mL from day 4 to day 11 and 5 mL to 10 mL from day 12 to day 19 where the digestion process stopped as shown in Figure 5-10. The highest volume of biogas of 30 mL was recorded on day 11. Comparatively, the highest biogas with regards to the volume for the biodigesters increased in the order of 25°C < 35°C < 55°C, representing 12 mL, 15 mL and 30 mL, respectively. For biodigester B, 50 mL of biogas was produced on day 1 with a decrease to 10 mL on day 2 and a quick rise in production on day 3 to day 10 where the highest volume of 110 mL was reported. Increasing trends in volume for the highest production of biogas under each working temperature was recorded in the order as 25°C < 35°C < 55°C at 40 mL, 90 mL and 110 mL, respectively. It could be deduced that highest biogas volume was favorable over the period of day 4 to day 11.

In the case of biodigester C, 10 mL of biogas was reported on day 1 followed by an increase in its generation with highest volume of 60 mL recorded on day 12. Comparing the temperature differences, it could be deduced that maximum volume of biogas of 50 mL was recorded for both 25°C and 35°C with an approximately 17% increase at 55°C. For biodigester D, biogas production started on day 2 with 5 mL produced and an observed increasing trend from day 3 to day 6 with highest volume reported on day 4 (50 mL). Following was the decline in the volume recorded from day 7 to day 19 with amount of biogas found within the range of 10 mL to 20 mL until day 19 when the generation stopped. Amongst the working temperatures under this study for biodigester D, highest volume of biogas of 40 mL each were recorded at 25°C and 35°C while at 55°C, 50 mL was recorded. Biogas production rates (BPR) recorded were found to be 11.4, 92.4, 58.4 and 24.8 mL/gVS/d for biodigesters A, B, C and D, respectively.

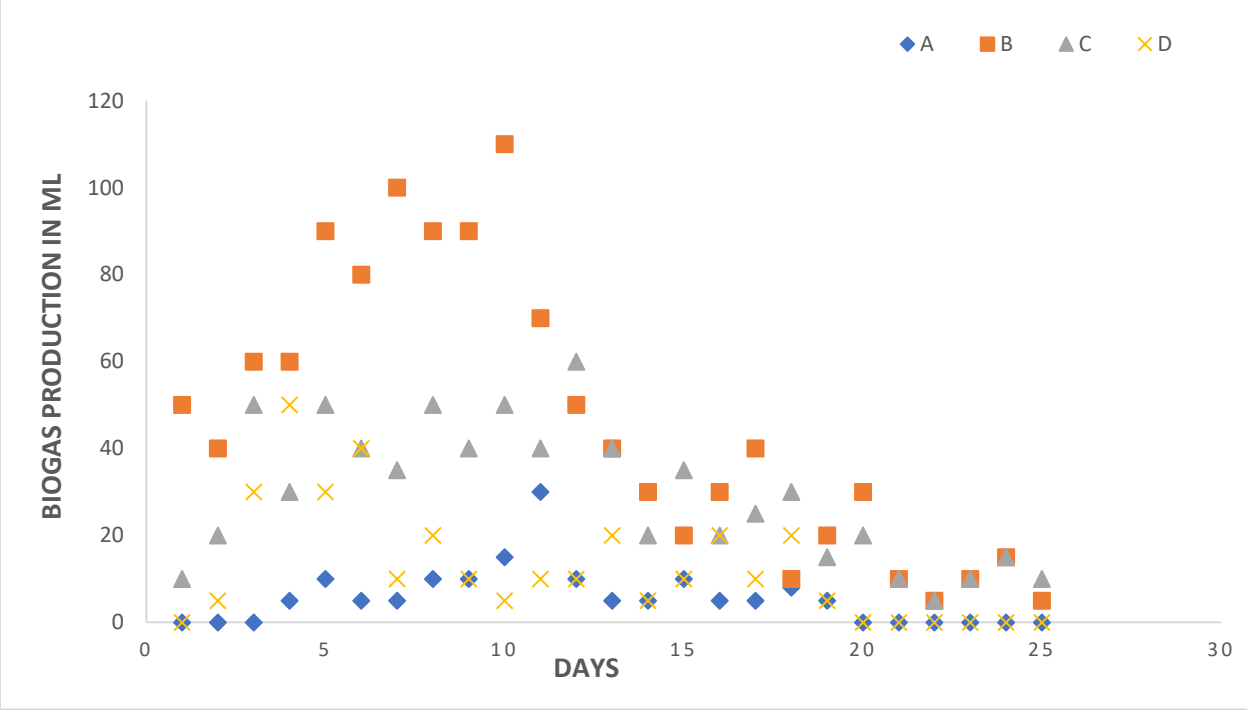

Figure 5- 10. Biogas production at 55°C.

5.3.2.3 AcoD of selected feedstocks with SWW

In Figure 5-11, the biogas production started on day 4 with 5 mL produced followed by a slight increase until day 9 when the production declined for biodigester A. The highest biogas volume of 50 mL was recorded on day 8 and overall production stopped on day 17. In biodigester B, biogas started by day 1 with 30 mL produced and the highest volume of 110 mL was observed on day 5. There was an observed increase in the production of biogas from the third day to the tenth day as production continued but this time, within the range of 10 mL to 60 mL until production ceased.

In biodigester C, biogas production began on day 1 (5 mL) with slight increases until day 7 where the highest volume (100 mL) was recorded. Comparatively, 75 mL of biogas was produced within the first 3 days for biodigester C as in the case of biodigester B, 170 mL of biogas was reported.

In biodigester D, a longer lag phase of 4 days was seen as production started on day 5 with 5 mL of biogas produced which increased sharply from day 6 to day 9 as highest volume (80 mL) was recorded on day 9. Production then dropped sharply which could be due to microbes becoming denatured over time and also, less biomass for microbes to feed on as the biomass becomes used-up on days 10 and 11 with volume of biogas found between the ranges of 5 mL to 3 mL from day 12 to day 25. It was observed from this study that the biogas production rates (BPR) were 17.6, 112, 66.4 and 37.2 mL/gVS/d for biodigesters A, B, C and D, respectively.

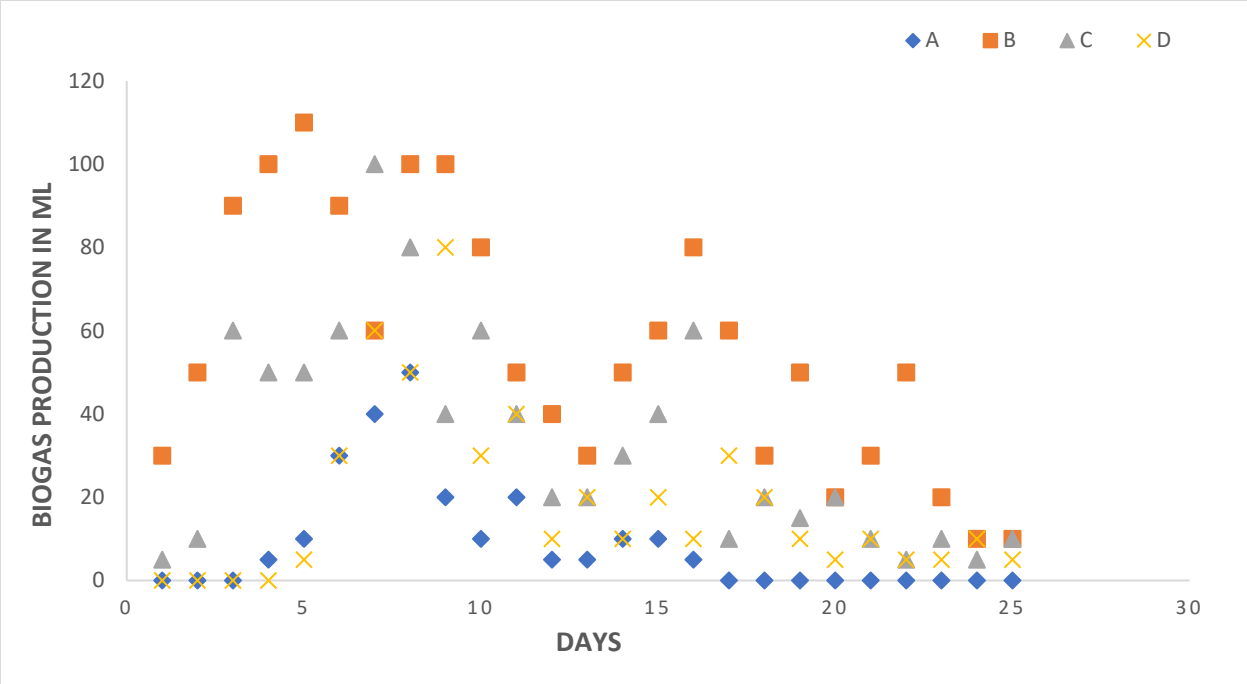

Figure 5- 11. Biogas production at 25°C.

In Figure 5-12, there was no lag phase as biogas production started by day 1 with 5 mL produced for biodigester A. The highest volume of 10 mL was observed on most of the days which includes; days 2, 3, 5, 6, 9, 10, 11 and 16. Comparatively, the total volume of biogas produced by biodigester A at 25°C and 35°C were reported to be 220 mL and 120 mL respectively. In biodigester B, biogas production started on day 1 with 10 mL produced after which there was a slight increase from day 2 (30 mL) with the highest reported on day 5 (80 mL). Interestingly, for biodigester B, day 5 recorded the highest volume of production of 110 mL and 80 mL at 25°C and 35°C, except at 55°C where the highest was observed to be 100 mL on day 10.

For biodigester C, biogas production started on day 3 with 5 mL produced which increased from day 6 to 8 where the highest volume of 50 mL was recorded. It could be deduced that twice the total volume was produced since at 35°C, a volume of 415 mL was recorded, and 830 mL at 25°C.

In the case of biodigester D, biogas production started on day 1 with 5 mL produced as there was a slight increase observed from day 2 with the highest volume (40 mL) recorded on day 14 with production ending on day 19. It was observed from this study that the biogas production rate (BPR) were 9.6, 38.8, 33.2 and 18.4 mL/gVS/d for biodigesters A, B, C and D, respectively.

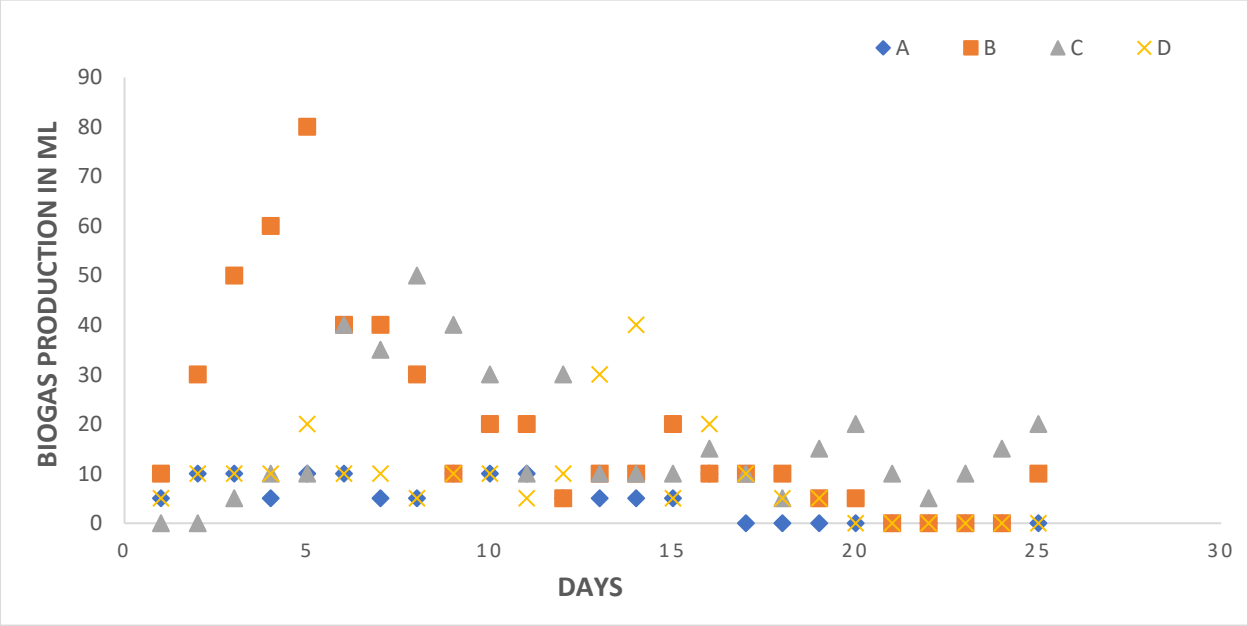

Figure 5- 12. Biogas production at 35°C.

For biodigester A in Figure 5-13, biogas production started by day 1 (10 mL) as the volume increased slightly from day 2 until production ceased on day 18. The highest volume of biogas of 30 mL was recorded on day 4. In the case of biodigester B, biogas production began on day 1 (30 mL) which increased slightly until the highest volume of 100 mL was produced on day 10. It could be observed that the total volume of biogas produced for biodigester B decreased from 25°C to 35°C and represented as 1400 mL and 485 mL respectively corresponding to 65% decrease in the overall biogas production. This gives an indication that considering biodigester B, the maximum biogas production was achieved at a lower temperature which could possibly be a suitable

surrounding for the available microbes. This further increased by 35% between 35°C and 55°C for the same biodigester. For biodigester C, 20 mL of biogas was produced on day 1 which increased slightly with highest volume recorded to be 115 mL on day 10 which declined significantly by day 11 by 74% to 30 mL. In the case of biodigester D, biogas production started on day 1 with 10 mL produced which then increased slightly in the range of 30 mL to 50 mL from day 2 to day 5. The highest biogas volume was observed on day 6 with 70 mL produced which decreased until digestion stopped on day 24 with 10 mL produced. Biogas production rates (BPR) recorded were found to be 17.2, 59.6, 65.5 and 44.0 mL/gVS/d for biodigesters A, B, C and D, respectively.

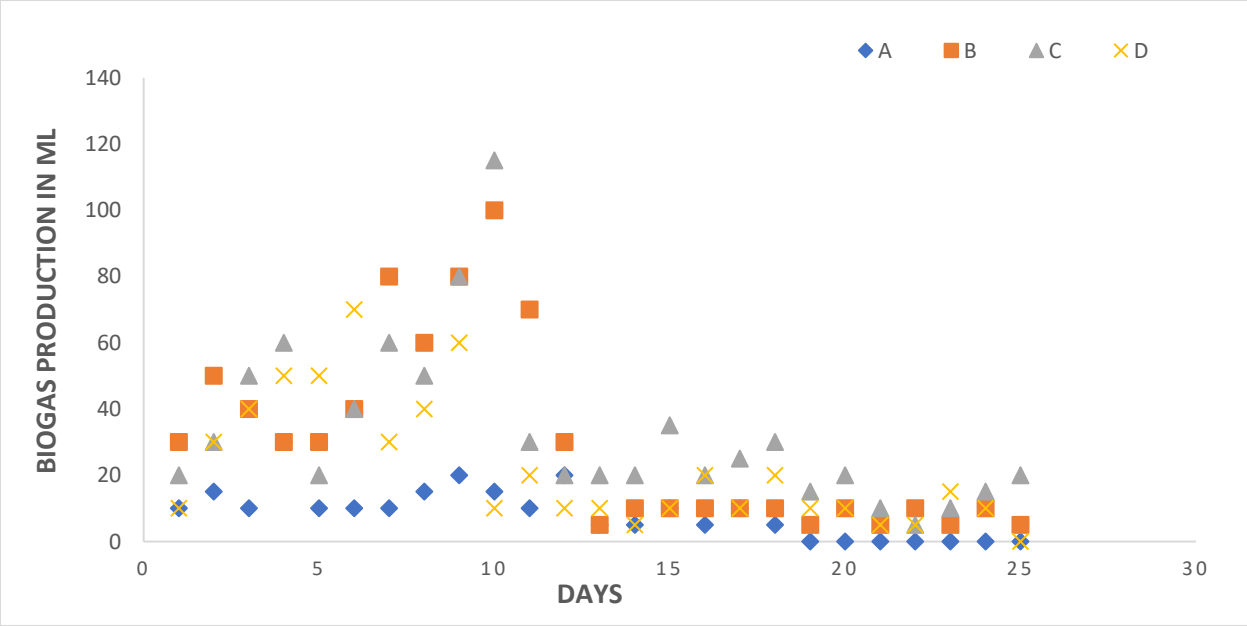

Figure 5- 13. Biogas production at 55°C.

5.3.2.4 AcoD of selected feedstocks with municipal WW

In biodigester A, biogas production started on day 5 with 5 mL produced followed by a slight increase with a total volume of 105 mL of total volume produced after the 25 days. The highest biogas volume of 20 mL was recorded on day 11 and the overall digestion process stopped on day

17. In biodigester B, biogas started by day 2 with 5 mL produced followed by slight increases in the volume generated with the highest volume of 40 mL observed on day 7. There was an observed increase reported on the biogas production rate from the 2nd to the 7th day as production continued, but this time, within the range of 10 mL to 40 mL until production was complete. In biodigester C, biogas production begun by day 3 (5 mL) with slight increases (day 3 to day 10) where the highest volume was obtained on day 8 with 50mL produced. A decreasing trend in the biogas production could be due to inadequate nutrients rich in carbohydrates which serve as essentials required by microorganisms for biodegradability (Tsapekos, Kougias and Angelidaki 2015).

Comparatively, no biogas was produced within the first 3 days for biodigesters A and D, 5 mL was produced for biodigester C and 15 mL by biodigester B. In biodigester D, the lag phase lasted until the third day as production started on day 4 with 10 mL of biogas produced which increased slightly within the range of 5 mL to 20 mL from day 4 to day 18 when the digestion process stopped. In all, 155 mL of biogas was produced by biodigester D, 50 mL higher than the total volume produced by biodigester A as shown in Figure 5-14. The biogas production rates (BPR) were 8.4, 20.8, 33.6 and 12.4 mL/gVS/d for biodigesters A, B, C and D, respectively.

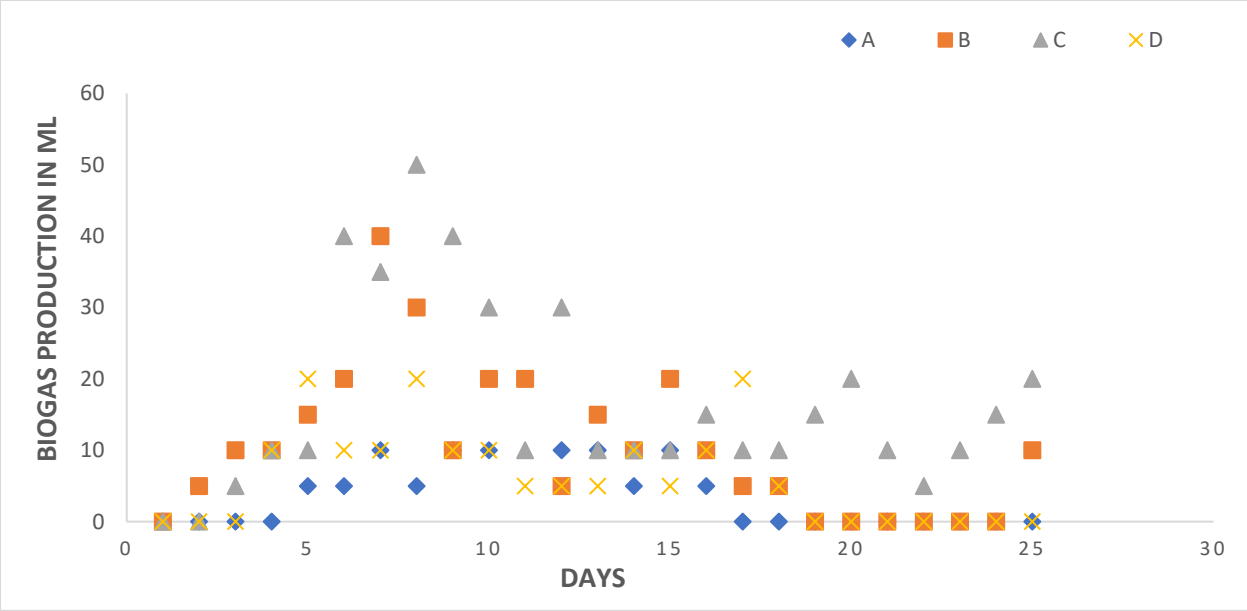

Figure 5- 14. Biogas production at 25°C.

In biodigester A, biogas production started on day 5 with 5 mL produced followed by a slight increase as highest volume of 10 mL was achieved on days 6, 9, 10 and 11 until the digestion process finally stopped on day 15 (Figure 5-15). In biodigester B, biogas production started on day 1 with 5 mL which increased significantly until day 11 (20 mL) where there was a sudden decrease on day 12 (5 mL) until day 20 (5 mL) with 60 mL observed to be the highest volume on day 5. In all, a total volume of 385 mL was recorded for biodigester B. In the case of biodigester C, biogas production begun by day 2 (5 mL) which increased slightly from day 4 to day 9 and remained constant over day 13 to day 15. A total of 395 mL of biogas was recorded which is estimated to be higher than that of biodigester B by 10 mL. In biodigester D, biogas started by day 2 with 5 mL which increased slightly from day 2 to day 6 as highest volume was recorded to be 30 mL. From day 7, the volume of biogas decreased slightly until the digestion process was over. The biogas production rates (BPR) were recorded to be 6.0, 30.8, 31.6 and 10.8mL/gVS/d for biodigesters A, B, C and D, respectively.

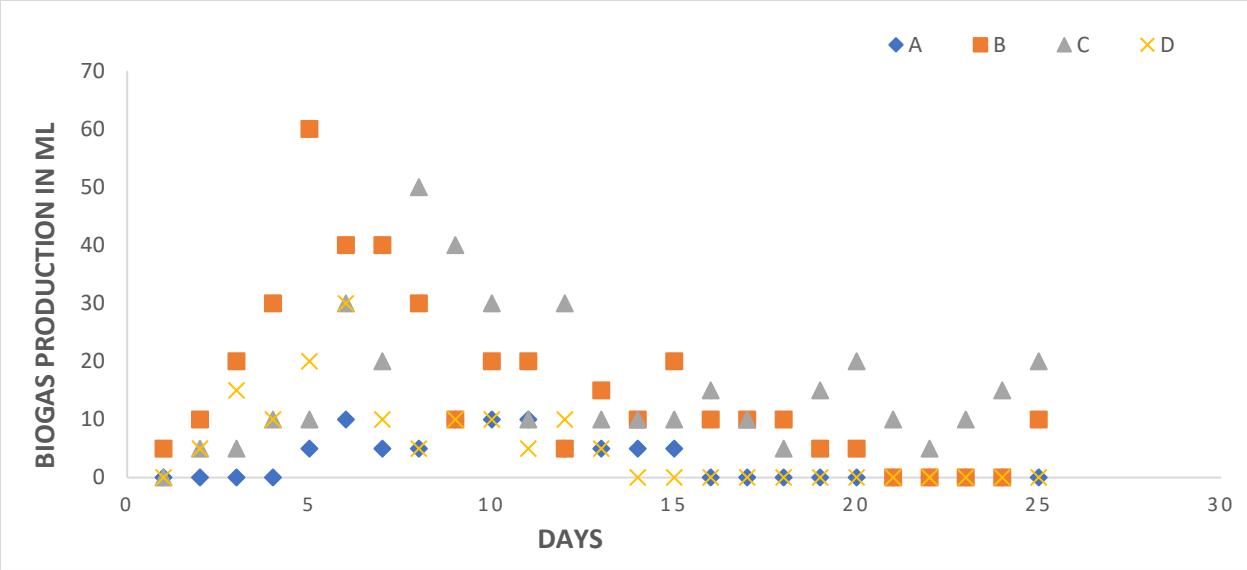

Figure 5- 15. Biogas production at 35°C.

For biodigester A, biogas production started on day 4 (5 mL) which increased slightly from the fourth day to the fifteenth day (Figure 5-16). The highest biogas was produced on day 11 at a volume of 15 mL. Total volume for biodigester A was maximised at 25°C (105 mL), followed by 55°C (95 mL) and finally 35°C (75 mL). For biodigester B, biogas production started from day 1 (5 mL) and increased slightly until day 9 (50 mL) and then declined slightly from day 16 (10 mL) to day 25 (5 mL). In the case of biodigester C, biogas production started on day 2 with 10 mL produced as the volume recorded was found to be in the range of 10 mL to 30 mL from day 2 to day 22 until digestion was complete. A total of 15 mL biogas was produced from day 23 to day 25 with a total volume of 345 mL over the 25 days. Biogas production rates (BPR) recorded were found to be 7.62, 38.0, 27.6 and 20.0 mL/gVS/d for biodigesters A, B, C and D, respectively.

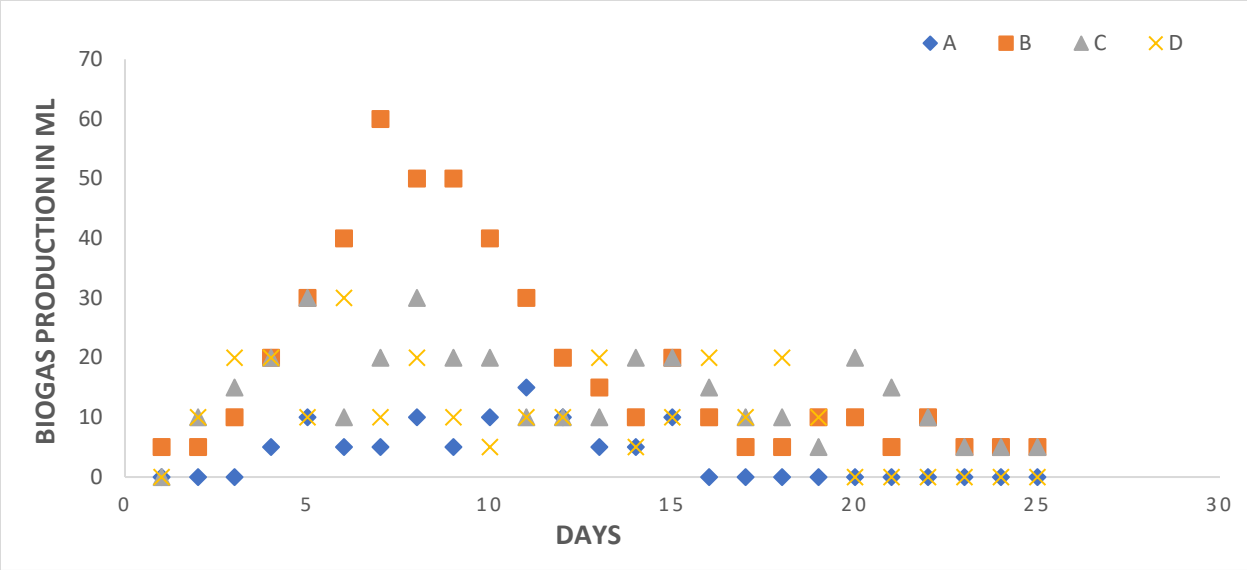

Figure 5- 16. Biogas production at 55°C.

In conclusion, it was deduced from the preliminary experiments that both SWW and DWW were the two best WW streams as as co-substrates for further process optimisation using the RSM.

5.3.3 Process optimisation using response surface methodology

The RSM based on the Box Behnken Design was employed for process optimisation in which the method is presented in section 3.3.3.1. To obtain the experimental design, two operating factors: temperature (25°C to 55°C) and OLR (0.5 gVS/100 mL to 1.5 gVS/100 mL) were varied and their interactive effects on biogas yield (m^3/kgVS) were analysed with 13 sets of experimental runs. The expectancy in the quantity of biogas produced is one of the important aspects in the design of anaerobic biodigesters. Substrate mixtures for model predictions from factors such as temperature and the OLR determines the potential biogas yield, which is a function of the input variables. The three levels; -1, 0 and +1 (Table 5.6 to Table 5.9) were estimated which corresponded to the minimum point, central point and maximum point for the factors considered. These minimum

points, central points and maximum points corresponded to 25°C, 35°C, and 55°C for the temperatures and 0.5gVS/100mL, 1.0gVS/100mL and 1.5gVS/100mL.

Table 5- 6. Coded matrix and responses for CS with DWW.

Runs	Factor A (coded)	Factor B (coded)	Response: Biogas yield (m^3/kgVS)		Residual
	Temperature (°C)	OLR (gVS/100 mL)	Actual	Predicted	
1	1	1	0.1871	0.2121	-0.0251
2	0	0	0.1673	0.1618	0.0056
3	1	0	0.0548	0.0485	0.0063
4	0	0	0.2025	0.1618	0.0407
5	1	-1	0.0447	0.0260	0.0187
6	0	1	0.4528	0.3806	0.0721
7	0	0	0.0447	0.1618	-0.1170
8	-1	0	0.2302	0.1578	0.0724
9	0	-1	0.1183	0.1117	0.0066
10	-1	-1	0.0548	0.0801	-0.0254
11	0	0	0.0548	0.1618	-0.1070
12	-1	1	0.3847	0.4318	-0.0471
13	0	0	0.2608	0.1618	0.0990

Table 5- 7. Coded matrix and response values for CS with SWW.

Runs	Factor A (coded)	Factor B (coded)	Response: Biogas yield (m^3/kgVS)		Residual
	Temperature (°C)	OLR (gVS/100 mL)	Actual	Predicted	
1	1	1	0.0920	0.5895	-0.4975
2	0	0	0.0140	0.0100	0.0040
3	1	0	0.0410	-0.4137	0.4547
4	0	0	0.0760	0.0100	0.0660
5	1	-1	0.0070	-0.0358	0.0428
6	0	1	0.1530	-0.5136	0.6666
7	0	0	0.0020	0.0100	-0.0080
8	-1	0	1.8600	2.4000	-0.5306
9	0	-1	0.4090	1.1500	-0.7424
10	-1	-1	5.0000	4.3000	0.6996
11	0	0	0.0310	0.0100	0.0210
12	-1	1	0.1760	0.3451	-0.1691
13	0	0	0.0030	0.0100	-0.0070

Table 5- 8. Coded matrix and response values for SCB with DWW.

Runs	Factor A (coded)	Factor B (coded)	Response: Biogas yield (m^3/KgVS)		Residual
	Temperature (°C)	OLR (gVS/mL)	Actual	Predicted	
1	1	1	0.0050	0.0131	-0.0081
2	0	0	0.0800	0.0367	0.0433
3	1	0	0.0210	0.0220	-0.0010
4	0	0	0.0030	0.0367	-0.0337
5	1	-1	0.0230	0.0264	-0.0034
6	0	1	0.1000	0.0865	0.0135
7	0	0	0.0700	0.0367	0.0333
8	-1	0	0.0110	0.0514	-0.0404
9	0	-1	0.0130	0.0118	0.0012
10	-1	-1	0.0200	-0.0029	0.0229
11	0	0	0.0040	0.0367	-0.0327
12	-1	1	0.1650	0.1600	0.0050
13	0	0	**	**	**

**denotes that no biogas was produced by the biodigester

Table 5- 9. Coded matrix and response values for SCB with SWW.

Runs	Factor A (coded)	Factor B (coded)	Response: Biogas yield (m^3/KgVS)		Residual
	Temperature (°C)	OLR (gVS/mL)	Actual	Predicted	
1	1	1	0.0650	0.0650	0.0000
2	0	0	0.0140	0.0494	-0.0354
3	1	0	0.0410	0.0410	0.0000
4	0	0	0.1390	0.0494	0.0896
5	1	-1	0.0070	0.0070	0.0000
6	0	1	0.0840	0.0840	0.0000
7	0	0	0.0020	0.0494	-0.0474
8	-1	0	1.8600	1.8700	0.0000
9	0	-1	0.4090	0.4090	0.0000
10	-1	-1	4.9700	4.9800	0.0000
11	0	0	0.0290	0.0494	-0.0204
12	-1	1	0.3230	0.3230	0.0000
13	0	0	0.0630	0.0494	0.0136

Another important factor to consider in the optimisation process using the RSM is the residual plots and the responses of the line of best fit for all the substrate mixtures which are presented in the Appendix (Figure B-9 to Figure B-12). The residual plots denote the difference between the inputted data values and the model's predicted values. In this study, the experimental data points were scattered randomly within the constant range of residuals along the graph for all the substrate mixtures. This shows the model is adequate, and there is no reason to suspect any violation of the independence or constant variance assumption in all the runs. The standardized residual plots indicate that the normal distribution of the points follows a straight line with only a few scattered. It was observed that few points were found to be scattered which are considered to be normally distributed. The normal probability plot, therefore, indicated good validity and significance for the approximation of the regression model which are presented also for all the substrate mixtures. Tables obtained from the model fitting equations such as the model fit summary and the sequential model sum of squares for the substrate mixtures are presented in the Appendix (Table B-22 to Table B-29).

5.3.3.1 SCB with DWW: ANOVA

In order to check the statistical accuracy and validity of the model, analysis of variance (ANOVA) was performed as presented in Table 5-10. The ANOVA assisted to ignore the factors that had no significant impact on the models, hence highlighted the relationship between the linear, quadratic, and interactional effects of the factors on the responses with the models found at 95% confidence level. The sum of the regression (sum of squares), Fisher variation ratio (F-values), probability (P-values), adequate precision (adeq precision) and the lack of fit (LOF) which are typical features of ANOVA values were all found within the limits used to define the significance of the model. These values show whether the model is statistically valid or not. This value is of immense statistical

significance, as it gives a clear indication of how good a dataset fits a model with the closer the R^2 value is to 1, the more meaningful the model. The R^2 values of 0.7287 was found to be close to 1, suggesting that the developed statistical model fitted well with the data obtained. The model f-value of 7.16 implies the model is significant. There is only a 1.18% chance that this f-value could occur due to noise since reported to be large. The p-values less than 0.0500 indicate model terms are significant and in this case, the sources: A, B, AB are significant model terms. The lack of fit f-value of 0.29 implies the lack of fit is not significant relative to the pure error and hence, there is 89.38% chances that this lack of fit f-value could occur due to noise as it was considered to be large. From Table 5-10, the predicted R^2 of 0.5059 is in reasonable agreement with the adjusted R^2 of 0.6270 with the difference less than 0.2. The values obtained for adequate precision (9.133) indicates an adequate signal can be used to navigate the design space since it was found to be greater than 4. The CV value of 71.97 indicates an adequate signal in which the model can be used to navigate the design space. However, based on the CV values reported, it could be deduced that models generated from SCB with SWW is more significant than that of SCB with DWW since the CV value of the former is greater than the latter.

Table 5- 10. ANOVA for the quadratic model fit: SCB with DWW.

Source	Sum of squares	Degree of freedom (df)	Mean square	F-value	p-value	
Model	0.0205	3	0.0068	7.16	0.0118	Significant
A-OLR	0.0051	1	0.0051	5.34	0.0496	
B-Temperature	0.0089	1	0.0089	9.28	0.0159	
AB	0.0080	1	0.0080	8.43	0.0198	
Residual	0.0076	8	0.0010	-	-	
Lack of fit	0.0025	5	0.0005	0.2869	0.8938	
Pure Error	0.0052	3	0.0017	-	-	
Cor Total	0.0281	11	-	-	-	
R^2 0.7287	Adj R^2 0.6270	CV % 71.97	Pred R^2 0.5059	Adeq Precision 9.1332	Mean 0.0429	SD 0.0309

CV = coefficient of variations; SD = standard deviation; Adj = Adjusted; R^2 = coefficient of correlation

5.3.3.2 SCB with DWW: Ramp plots

Figure 5-17 represents a ramp graph showing the optimum conditions for the operating parameters and the desirability obtained from the AcoD of CS with SWW. As inferred from the plot (Figure 5-17), to achieve maximum biogas yield of 0.160 m^3/kgVS, all operating parameters were at the maximum with a desirability of 96.9% biogas yield. This was observed to be translated into minimum OLR (0.500gVS/100mL) and lower temperature (55°C) to achieve the set goal of maximum biogas yield for the given range of factors. Table B20 (Appendix) reports the data for the other solutions.

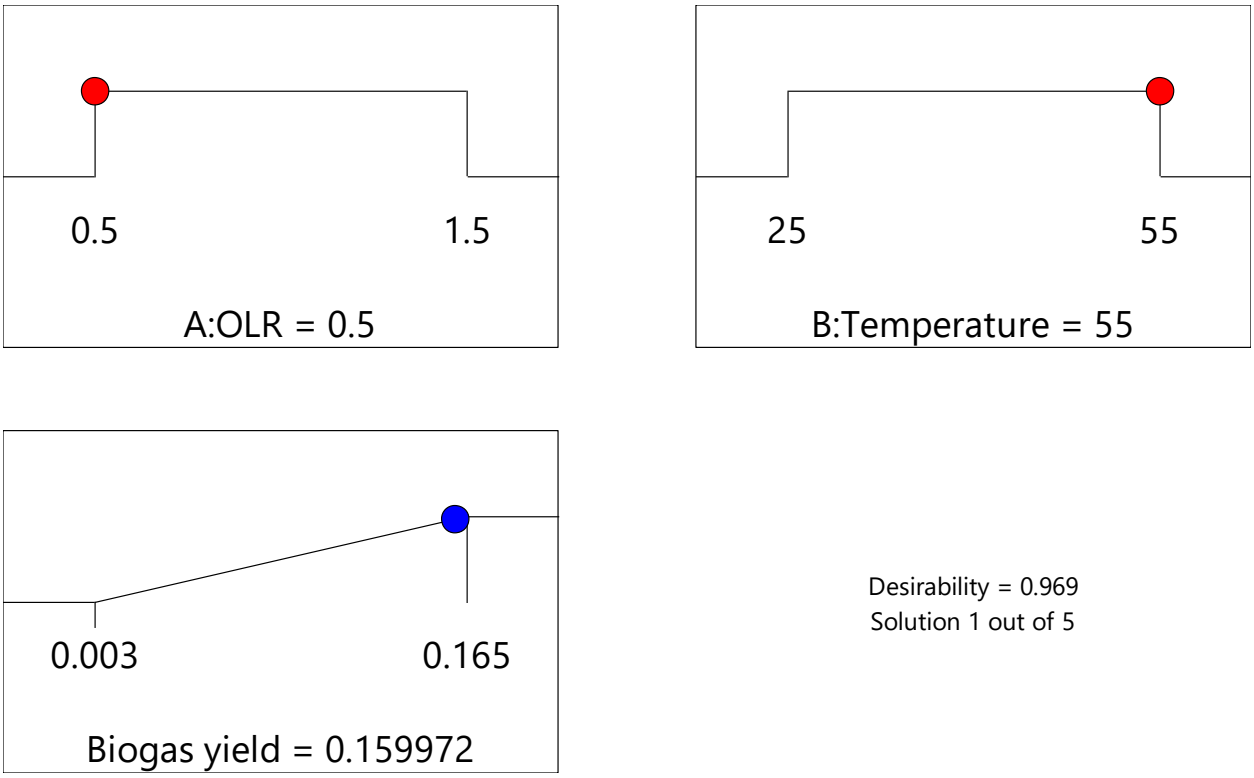

Figure 5- 17. Optimum operating conditions for SCB with DWW.

5.3.3.3 CS with DWW: ANOVA

The model f-value of 5.79 implies the model is significant. There is only a 1.98% chance that this F-value could occur due to noise since reported to be large. The lack of fit f-value of 2.26 implies the lack of fit is not significant relative to the pure error. Non-significant lack of fit is good as required for model to fit. A negative predicted R^2 implies that the overall mean may be a better predictor of the response than the current model. It was evident from the study that that the CV value (3.19%) given in the Table 5-11 is low enough to ensure significant models. The most significant parameter was temperature since the p value was 0.0041.

Table 5- 11. ANOVA for the quadratic model fit: CS with DWW.

Source	Sum of squares	Degree of freedom (df)	Mean square	F-value	*p*-value	
Model	0.0161	5	0.0032	5.79	0.0198	Significant
A-OLR	0.0024	1	0.0024	4.29	0.0772	
B-Temperature	0.0097	1	0.0097	17.51	0.0041	
AB	0.0013	1	0.0013	2.34	0.1696	
A^2	0.0010	1	0.0010	1.86	0.2147	
B^2	0.0010	1	0.0010	1.73	0.2297	
Residual	0.0039	7	0.0006	-	-	
Lack of fit	0.0024	3	0.0008	2.26	0.2236	
Pure Error	0.0014	4	0.0004	-	-	
Cor Total	0.0199	12	-	-	-	
R^2 0.8053	Adj R^2 0.6662	CV % 3.19	Predicted R^2 -0.62	Adequate Precision 7.7955	Mean 0.7382	SD 0.0235

5.3.3.4 CS with DWW: Ramp plot

In predicting the optimal parameters for the process parameters and their corresponding responses, a numerical optimisation was carried out. This displays the whole design space on the basis of the developed models to detect the optimum factor conditions for the given ranges with the goal of achieving maximum biogas yield. Figure 5-18 shows a ramp plot depicting the maximum biogas yield of 0.178 m^3/kgVS and a desirability of 87.6% biogas yield. The selection was based on the highest desirability as presented in Figure 5-18.

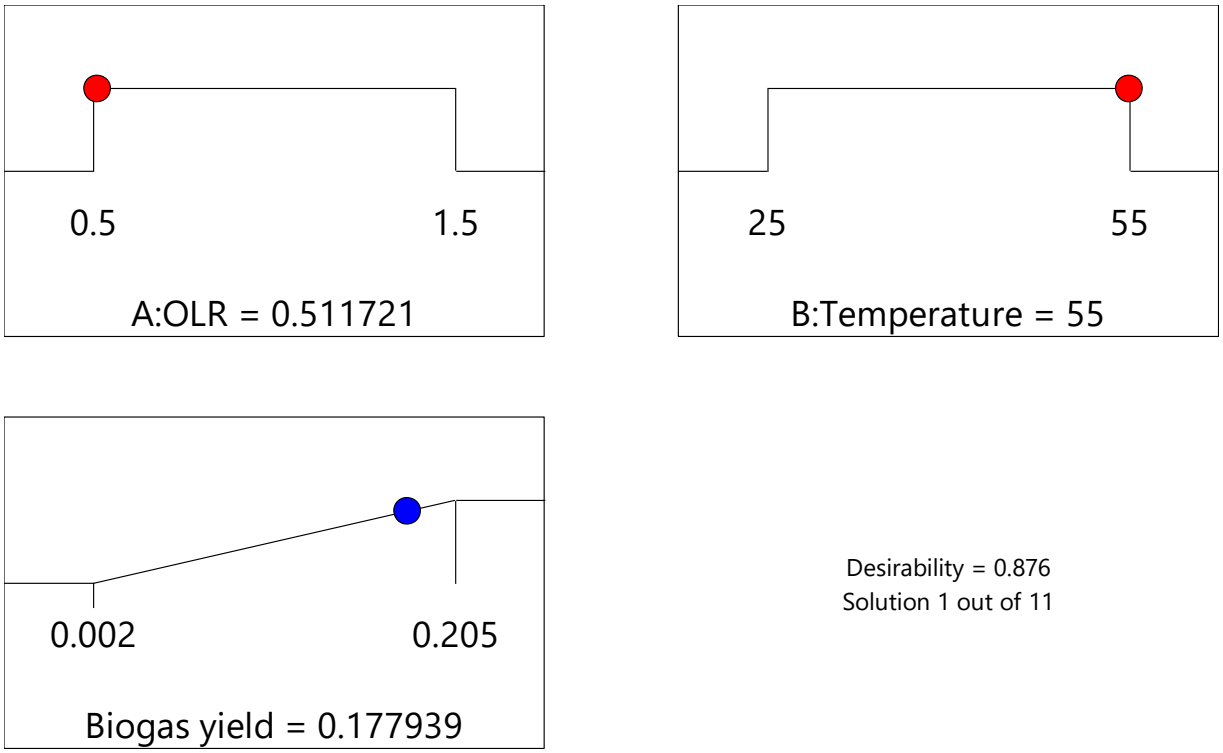

Figure 5- 18. Optimum operating conditions for CS with DWW.

5.3.3.5 CS with SWW: ANOVA

The model f-value of 13.46 and a p-value of 0.0018 implies the model is significant. There is only a 0.18% chance that this f-value could occur due to noise since the value is large. The p-values less than 0.0500 (95% confident level) indicate model terms are significant and in this case, the sources: A, B, AB, A^2 are significant model terms. The lack of fit f-value of 796.42 implies the lack of fit is significant. There is only a 0.01% chance that a lack of fit f-value this large could occur due to noise. The difference between the predicted R^2 and the adjusted R^2 is reported to be less than 0.2 as a greater value more than 0.2 is reported to indicate a large block effect or a possible problem with the model under study (Kweinor-Tetteh *et al.* 2018). From Table 5-12, the predicted R^2 of 0.0324 is not as close to the adjusted R^2 of 0.8385 as predicted and thus, could be due to the reason stated.

Table 5- 12. ANOVA for the quadratic model fit: CS with SWW.

Source	**Sum of squares**	**Degree of freedom (df)**	**Mean square**	**F-value**	***p*-value**	
Model	21.70	5	4.34	13.46	0.0018	Significant
A-OLR	6.17	1	6.17	19.14	0.0033	
B-Temperature	4.16	1	4.16	12.90	0.0088	
AB	5.44	1	5.44	16.88	0.0045	
A^2	2.66	1	2.66	8.24	0.0239	
B^2	0.9034	1	0.9034	2.80	0.1380	
Residual	2.26	7	0.3223	-	-	
Lack of fit	2.25	3	0.7508	796.42	<0.0001	
Pure Error	0.0038	4	0.0009	-	-	
Cor Total	23.95	12	-	-	-	
R^2 0.9058	Adj R^2 0.8385	CV % 93.79	Predicted R^2 0.0324	Adequate Precision 12.4814	Mean 0.6053	SD 0.5677

5.3.3.6 CS with SWW: Ramp plots

In predicting the optimal parameters for the process parameters and their corresponding responses, a numerical optimisation was done which displays the whole design space. Figure 5-19 shows a ramp plot depicting the maximum biogas yield of 4.30 m^3/kgVS and a desirability of 86.0% biogas yield.

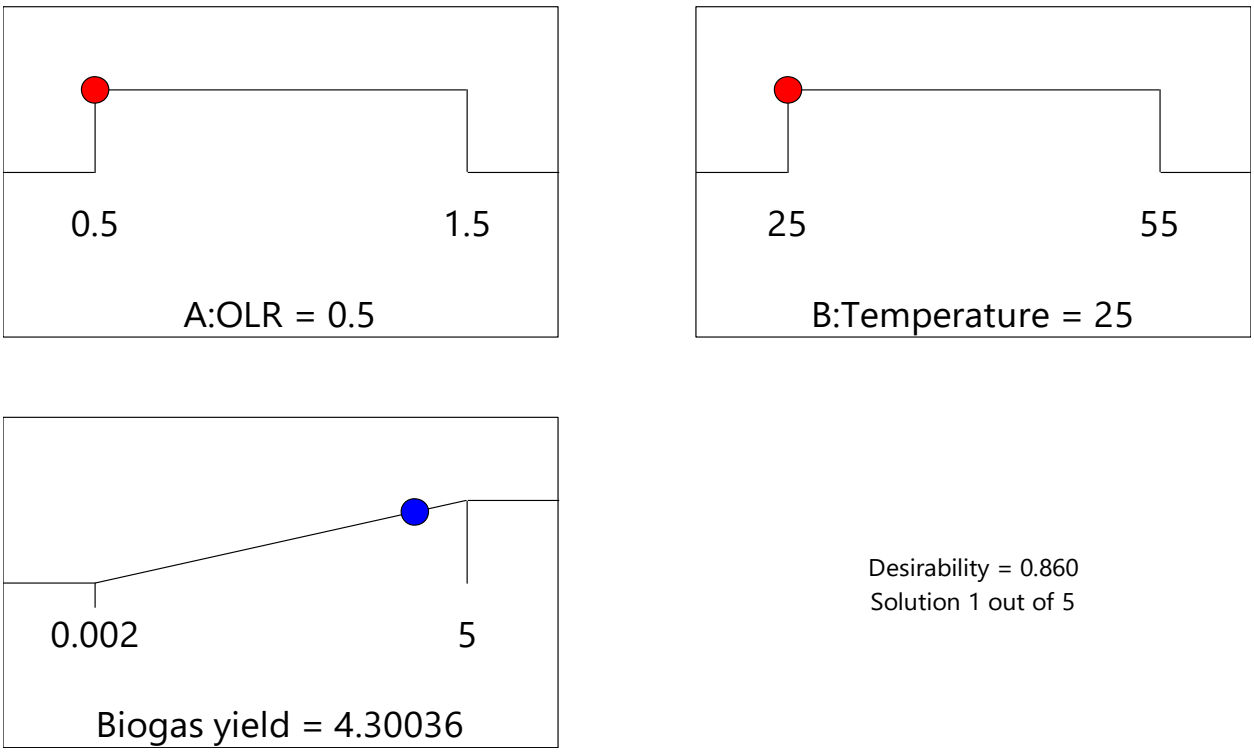

Figure 5- 19. Optimum operating conditions for CS with SWW.

5.3.3.7 SCB with SWW: ANOVA

The model f-value of 972.15 implies the model is significant. There is only a 0.01% chance that this f-value could occur due to noise since reported to be large. The p-values less than 0.0500 have been reported to indicate model terms that are significant and in this case, the sources: A, B, AB, A^2, B^2, A^2B, AB^2, A^2B^2 are significant model terms. The predicted R^2 was described as undefined since a leverage of 1.0000 was reported for the model fit. From Table 5-13, the values obtained for adequate precision (108.429) indicates an adequate signal can be used to navigate the design space. A CV value of 8.93% is low enough to ensure a significant model for SCB with SWW.

Table 5- 13. ANOVA for the quadratic model fit: SCB with SWW.

Source	**Sum of squares**	**Degree of freedom (df)**	**Mean square**	***F*-value**	***p*-value**	
Model	23.58	8	2.95	972.15	<0.0001	Significant
A-OLR	0.2640	1	0.2640	87.05	0.0007	
B-Temperature	0.0528	1	0.0528	17.42	0.0140	
AB	5.55	1	5.55	1828.98	<0.0001	
A^2	0.2591	1	0.2591	85.44	0.0008	
B^2	0.0836	1	0.0836	27.56	0.0063	
A^2B	1.30	1	1.30	427.48	<0.0001	
AB^2	0.7963	1	0.7963	262.62	<0.0001	
A^2B^2	0.1771	1	0.1771	58.40	0.0016	
Pure Error	0.0121	4	0.0030	-	-	
Cor Total	23.60	12	-	-	-	
R^2 0.9995	Adj R^2 0.9985	CV % 8.93	Pred R^2 **	Adeq Precision 108.4291	Mean 0.6166	SD 0.0551

CV = coefficient of variations; SD = standard deviation; Adj = Adjusted; R^2 = coefficient of correlation

5.3.3.8 SCB with SWW: Ramp plots

Figure 5-20 represents a ramp graph showing the optimum conditions for the operating parameters and the desirability obtained from the AcoD of SCB with SWW. As inferred from the plot (Figure 5-20), to achieve maximum biogas yield of 4.975 m^3/kgVS, all operating parameters were at the maximum with a desirability of 98.5% biogas yield. This was observed to be translated into minimum OLR (0.5gVS/100mL) and lower temperature (25°C) to achieve the set goal of maximum biogas yield for the given range of factors. Table B21 (Appendix) reports the data for the other solutions.

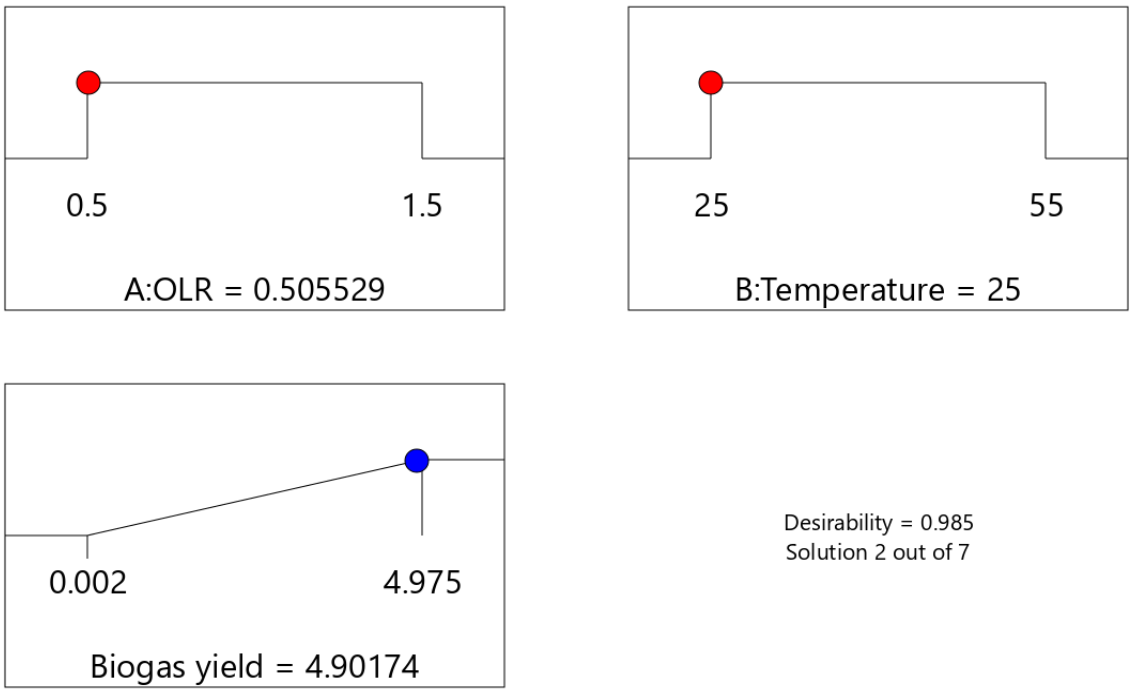

Figure 5- 20. Optimum operating conditions for SCB with SWW.

5.3.3.9 Daily biogas monitoring

The lag phase has been defined as the time taken by a biodigester to produce its first biogas (Malunga 2018). However, the rate of hydrolysis during the AD process has been reported to be influenced by the lag phase. That is, the longer the lag phase, the slower the rate of hydrolysis. In the same study, it was reported that at a lag phase of 1.65 days (longest), the biodigester reported the slowest hydrolysis reaction.

In Figure 5-21, R7 recorded the longest lag phase of 25 days which in this case was attributed to biodigester failure other than that defined by Malunga (2018) since it was found to be too long when compared to similar studies.

All the biodigesters were allowed to run for 24 hours after which readings were taken and reported as day 1 until the digestion was over. It was observed that each biodigester reported varying times

for the readings to be taken and was attributed to its lag phase period. The maximum biogas volume of 20,000 mL was produced by 30days with a maximum bioga production rate of 666.67 mL/day (Figure B-5) were achieved by biodigester R10. This gives an indication of a suitable medium for the microbial biodegradation and quality of biodigester performances owing to the reduced influences that arises from VFAs inhibition. Lina *et al.* (2018) reported in a similar study that biodigesters with maximum biogas production arises from process stability and good reactor performances. The shortest lag phase and fastest rate of hydrolysis corresponded to R10 since it reported the highest biogas production within the first day (less than 24 hours). The lowest volume of 15 mL and a higher rate of 0.5 mL/day were achieved by R7. Process parameters such as the OLR and the temperature have been reported to significantly influence the overall biogas production as the biodigesters that reported the maximum and the lowest biogas production (Janke *et al.* 2015).

The OLR and temperature for R10 were found to be 0.5 gVS/mL at 25 °C while that of R7 were at 1.0 gVS/mL and 35 °C, an indication that AcoD with the agricultural biomass is best achieved for substrates mixtures at lower temperatures. The maximum biogas volume was observed in C55 among the controls (substrate mixtures without addition of the agricultural biomass) considered, which was found to be 130 mL and 4.3 mL/day for the volume and the biogas production rate respectively. The lowest biogas volume was observed in C25 which indicated that biogas production without the agricultural biomass was favored at higher temperatures. Biogas production halted on days 5, 7, 12 and 26 for C35, C25, C55 and R7, respectively. Previous studies have indicated that the rate of biogas production is altered by factors such as the microbial activity inside the biodigester, the surface area or microorganisms to substrate ratio (Maile, Muzenda and Mbohwa 2016d). However, in this present study, lower biogas generation was related to the

increased VFA production, pH drops in biodigesters especially and the presence of NH_3 as inhibitors.

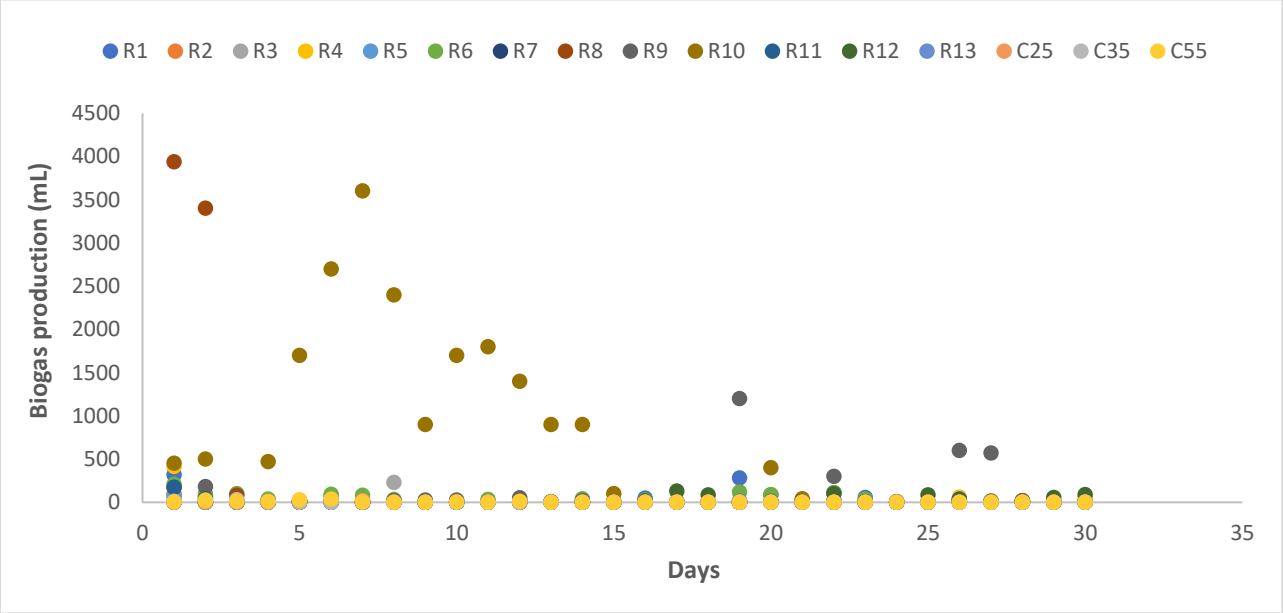

Figure 5- 21. Biogas production for CS with SWW.

In Figure 5-22, the first two days of the AcoD showed no generation of biogas in all the biodigesters which was predicted to be the overall lag phase. The shortest lag phase and fastest rate of hydrolysis corresponded to R8 with highest biogas volume recorded on day 3. For biodigester R10, the lowest volume of biogas and its corresponding maximum biogas production rate of 10 mL and 0.33 mL/day were reported. However, there was no biogas produced in C25 all throughout the process which could be attributed to system failure and instability of the biodigester. The maximum volume of biogas of 1640 mL and a maximum rate of 54.67 mL/day (Figure B-6) were achieved by R6 which corresponded to an OLR and temperature of 1.0gVS/mL and 55 °C, respectively. This is in contrast to what was reported previously in the AcoD of CS with SWW with maximum biogas production potential observed in R10 for this substrate mixture. On days 6, 8 and 22, higher volume for each 150 mL was produced by R6, thus accounting for

good performance and biodigester stability. In terms of the biodigesters employed for the control, the maximum biogas volume and production rate were reported for C35 at 300 mL and 3.0 mL/d respectively. No production was observed for C25 as reported earlier and thus, biogas production rate of 3.0 mL/d was reported for C55.

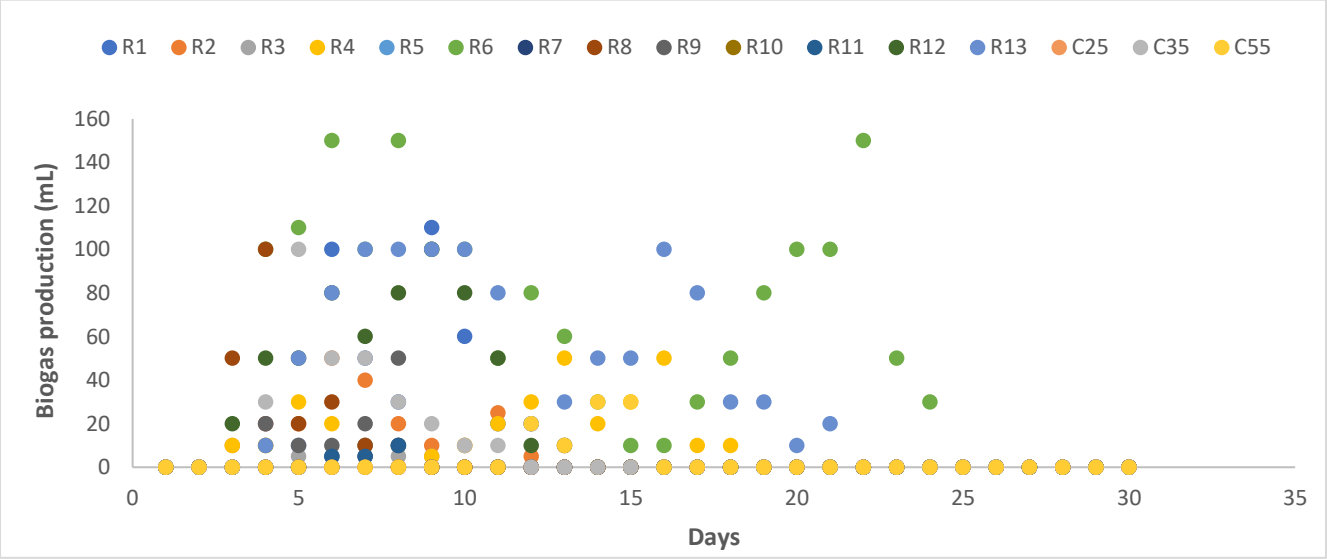

Figure 5- 22. Biogas production for CS with DWW.

In Figure 5-23, maximum biogas production of 19,900 mL and maximum biogas production rate of 663.33 mL/day (Figure B-7) were achieved by R10 at 0.5 gVS/mL at 25 °C. By far, AcoD of CS with SWW exceeded that of SCB with SWW by 0.5% for biodigester R10. This was found to be very close which gives an indication of the degradation potentials when SWW is used as a co-substrate other than DWW.

Studies in the past decades have attributed the potential of carbohydrate-rich substrates to be rich in their ability to produce higher biogas content as a result of the metabolic breakdown by anaerobic microbes (Weiland 2010). The shortest lag phase and fastest rate of hydrolysis corresponded to R8 with 3940 mL of biogas generated on the first day. Lowest biogas production

of 15 mL with maximum biogas production rate of 0.5 mL/day were achieved by R7. For the controls, maximum biogas potential and production rate were reported for C25 at 30 mL and 1.0 mL/d respectively. Both C35 and C55 recorded a biogas production rate of 0.7 mL/d.

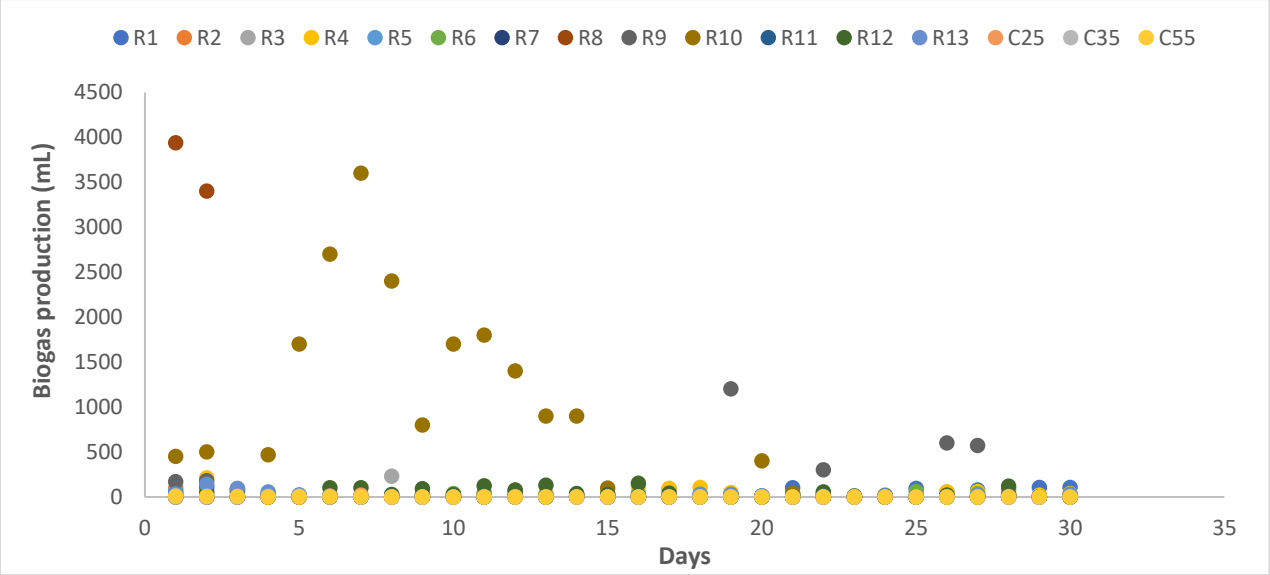

Figure 5- 23. Biogas production for SCB with SWW.

In Figure 5-24, it was found that most of the biodigesters; R4, R10, R13 and C25 started producing biogas after day 4. The shortest lag phase and fastest rate of hydrolysis corresponded to R12 and C55 with reported highest biogas production on day 4 by C55 (210 mL). No biogas was recorded for biodigester R13 for the entire digestion period. The maximum biogas volume of 800 mL and a maximum production rate of 26.7 mL/day (Figure B-8) were obtained for biodigester R6 which corresponded to an OLR and temperature of 1.0 gVS/mL and 55 °C, respectively.

In terms of the biodigesters employed for the control, the maximum biogas potential and production rate were reported for C55 at 660 mL and 22.0 mL/d, respectively. Following was C35 produced a maximum volume of biogas of 395 mL at a production rate of 13.7 mL/d, with the lowest volume reported for C25 at 30 mL and 1.0 mL/d, respectively.

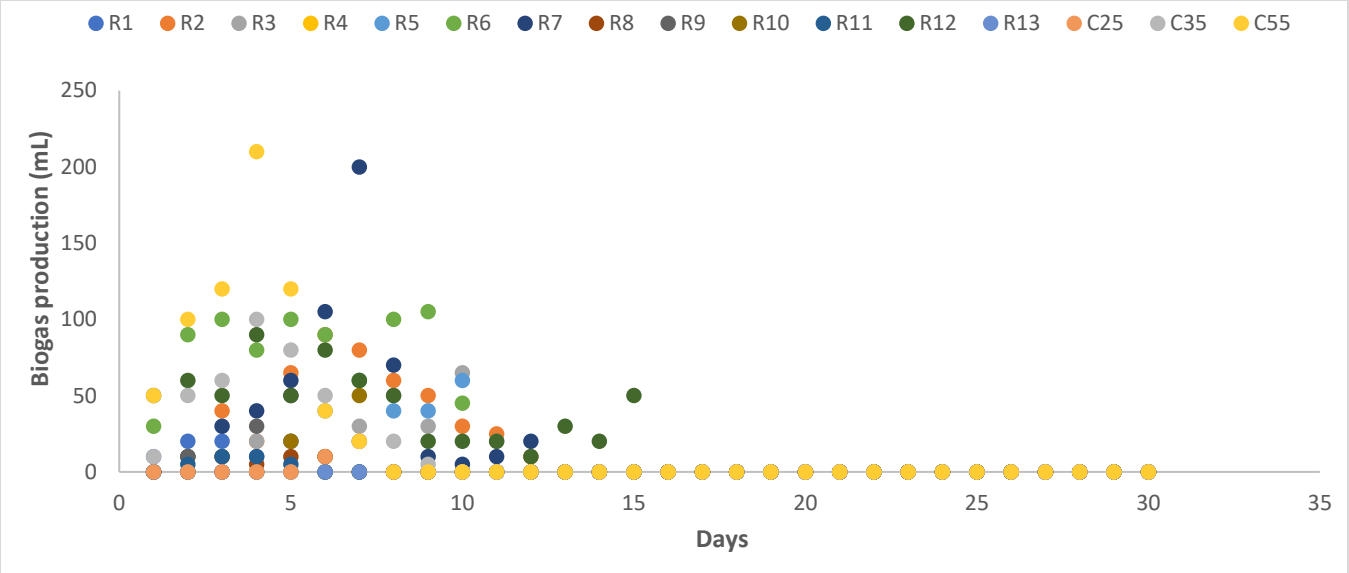

Figure 5- 24. Biogas production for SCB with DWW

5.3.3.10 pH

It is important to study the variations in the pH of anaerobic biodigesters since it adversely affect microbial growth which subsequently, leads to a decrease in biogas production (Maile, Muzenda and Mbohwa 2016d). The optimum pH range for the suitable AD process has been reported earlier to be in the range of 6.0 to 8.5 (Tsapekos *et al.* 2018) which was adopted in this study although some biodigesters recorded a pH below 6.0. In this study, the pH for each biodigester was recorded from the start (pre-digestion pH), that is, before the AD process and at the end (post-digestion pH) of the AD process since it was operated in batch mode. The pH for SCB and SWW is presented in Figure 5-25. A pH above 8.0 was observed for biodigesters containing single substrates such as sludge alone, wastewater alone or a combination of the sludge and the wastewater. Comparatively, this changed on the addition of biomass into the biodigester together with the sludge and sludge and wastewater streams as the pH was reported in the range of 5.8 to 8.2. This also gives an indication that AcoD with multiple feedstocks could be used for pH balancing in biodigesters. In

Figure 5-27, it was observed that the pH of the biodigesters from the beginning of the AD process was found to be higher than that of the post-digestion period.

The highest pre- and post- digestion pH of the biodigesters were reported for R5 (7.14) and R6 (6.37), respectively with a maximum biogas volume of 663.3 mL/d. The pH of a biodigester has been found to be a function of the concentration of VFAs generated, bicarbonate alkalinity within the system and the quantity of CO_2 produced (Nalinga and Legonda 2016). This stems from the fact that an improvement on the biogas production contributes to steady plant operation with regards to the range of pH.

Lower pH values were due to VFA accumulation during the AD process. However, all biodigesters recorded pre- and post-pH digestion were found to be within the optimum range 6.0 to 8.5 during the AcoD of SCB with SWW without any pH adjustment. This contrasts to what was reported in a study by Malunga (2018) with pH adjustments with synthetic feed to enhance a smooth AD process in biodigesters.

Similiar studies according to Maile, Muzenda and Mbohwa (2016e) investigated on the use of buffer systems for pH adjustment to achieve the optimum range for successful microbial biodegradation. In the AcoD of SCB with DWW, the highest pre- and post- digestion pH was reported in R6 (7.11) and R3(6.66), respectively. The lowest pH was recorded by R10 during post-digestion predominantly during the acidogenesis stage of the AD process which was found to have a direct influence on the overall biogas potential of 26.67 mL/d. A higher VFA production rate largely affects the rate of CH_4 produced, and this predominantly results in pH levels below the optimum range of 6.0 to 8.5 (Maragkaki *et al.* 2018). Methanogens become inhibited due to their

greater sensitivity in acidic environment which are sometimes corrected by decreasing CO_2 from the medium.

In Figure 5-26, the highest pre- and post- digestion pH was reported in R8 (6.79) and R2 (13.15) respectively. Both R2 and R8 had pH values above the maximum as 13.04 and 13.15, respectively which was evidenced in the biogas production. In R2, the total biogas production of 115 mL was recorded which corresponded to the significantly high post-pH readings. pH values recorded were found to adversely affect the production of CH_4 (Kougias and Angelidaki 2018).

It is reported that when the pH values surpasses the optimum, the AD process starts to decline and there is an abrupt reduction in the CH_4 production (Kougias and Angelidaki 2018). The post-pH of R8 was found to be exceedingly higher which resulted in the lower biogas production recorded on the first 3 days. This case was found to be different for the AcoD of CS with DWW (Figure 5-28) where both pre- and post-pH readings were within the optimum range (6.0 to 8.5) for complete AD process. It is important to note that error bars denote 95% confidence interval.

In conclusion, it was found that the pH reported in biodigesters during AD play an important role during biogas production with almost all the biodigesters reported pre- and post-pH values within the optimum with exceptions stated above. The optimum pH from previous study showed the range of 6.0 to 8.5 which was adopted in this present study. However, exceptions to this was biodigesters R2 and R8 which reported pH values of 13.04 and 13.15, respectively for CS with SWW.

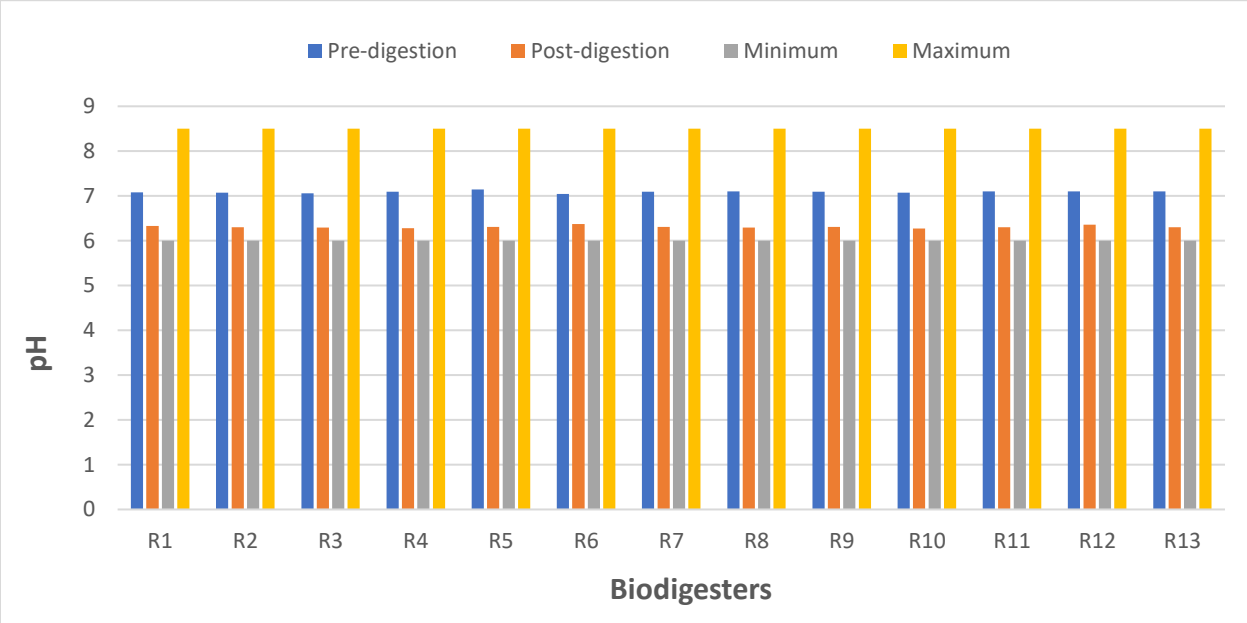

Figure 5- 25. Pre- and post-digestion pH: SCB and SWW

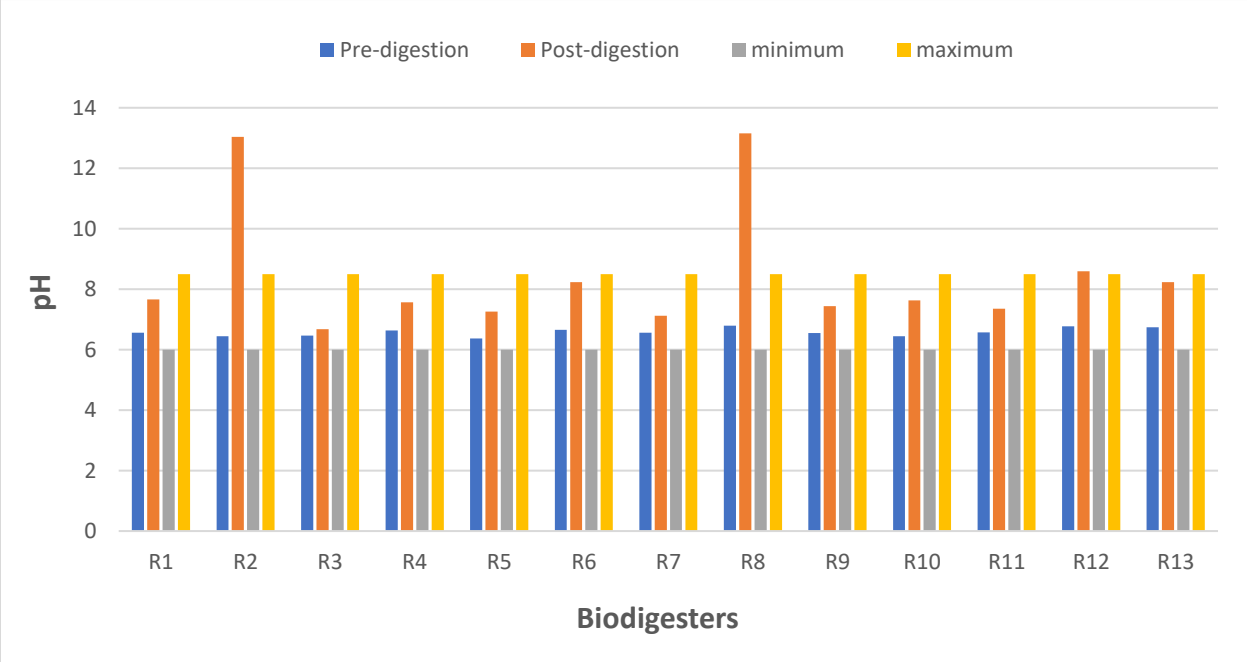

Figure 5- 26. Pre- and post-digestion pH: CS and SWW.

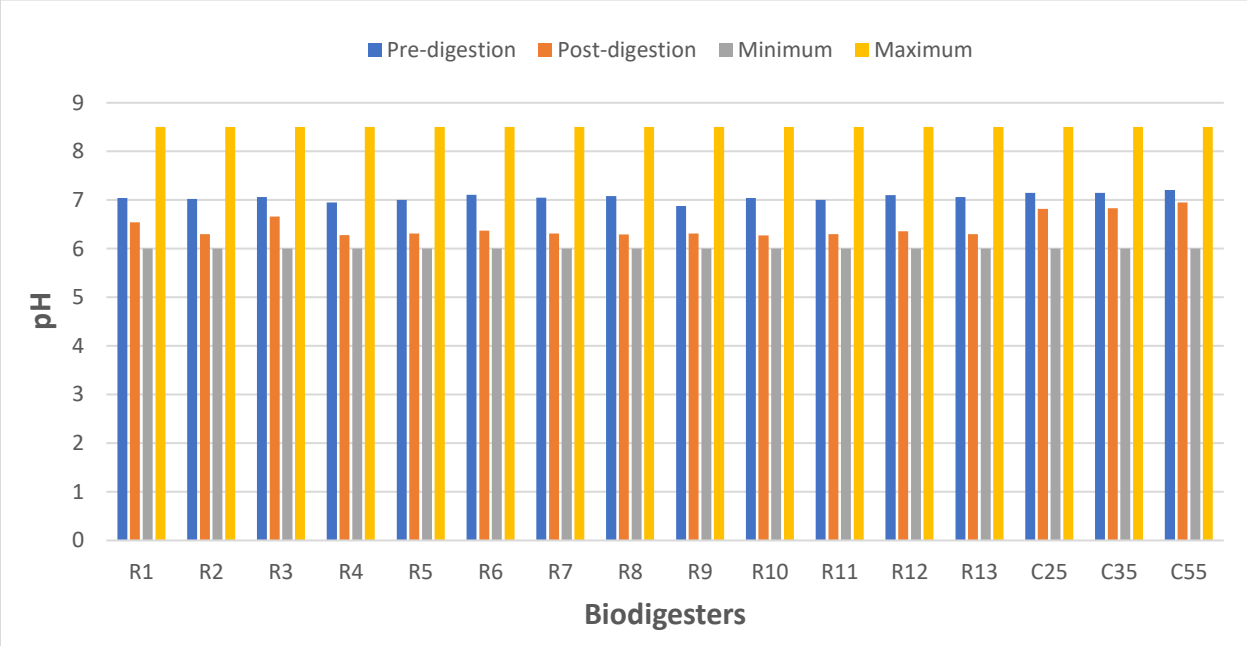

Figure 5- 27. Pre- and post-digestion pH: SCB and DWW.

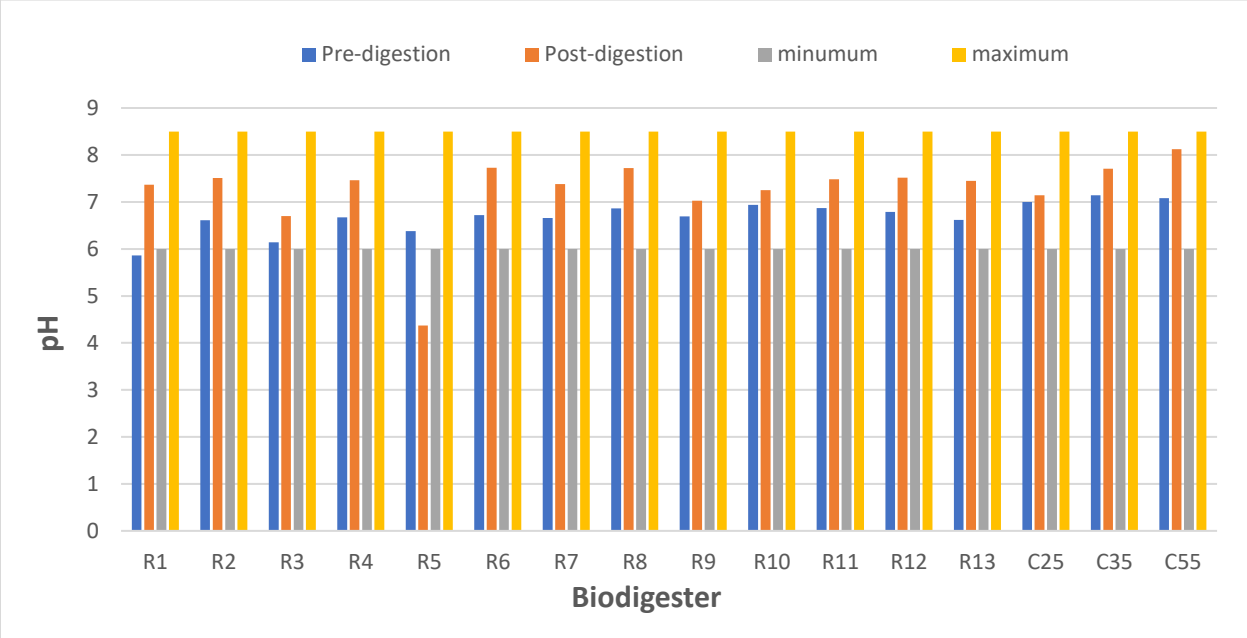

Figure 5- 28. Pre- and post-digestion pH: CS and DWW.

5.3.3.11 VS concentration and VS reduction

Many WWTPs employ the AD process to cause a reduction in the volume of biosolids before disposal and/or reuse. The significance of VS concentration, however, determines the organic matter undergoing biodegradation to produce biogas and it is reported that higher VS contents are directly influenced by the biogas generated for particular substrates under operation (Kuo and Dow 2017). The relationship between the biogas production and VS was found to support the argument that the desired substrates in anerobic biodigesters were more readily biodegradable like those in the municipal wastewater sludge. Influent (pre-digestion) and effluent (post-digestion) VS concentrations recorded were found to be in the range of 2,000 mg/L to 1,900 mg/L for all the substrates; and for CS with DWW (figure 5-32), SCB with DWW (figure 5-31) and CS with SWW (figure 5-30), except for SCB with SWW which was reported to be 8000 mg/L to 78,000 mg/L as presented in figure 5-29. It is be deduced that higher VS concentrations contributed to the lower biogas yield for the AcoD of SCB with SWW.

In relation to previous studies carried out in literature, the VS concentration was found to be higher and thus, a prediction of a possible reactor failure was predetermined but this did not occur in this study. The mathematical expression for the VS reduction is presented in the Appendix B2. In Figure 5-36, a maximum and minimum VS reduction rate of 52.6% (R6) and 18.5% (C35), respectively was observed for the AcoD of CS with DWW, which was far lower than that recorded in the AcoD of SCB with SWW.

The maximum VS reduction of 89.7% for biodigester R11 reported (ranging from 8,000 mg/L to 78,000 mg/L) did not show a direct influence on the total biogas produced (0.029 m^3/kgVS) as depicted in Figure 5-33 for SCB and SWW. A lower VS reduction of 18.2% was observed for biodigester C35 during the AcoD of CS with DWW (Figure 5-36) and also in SCB with DWW

(Figure 5-35). This similarity could be attributed to the use of common wastewater stream (dairy) in both separate runs. The higher VS reduction reported was 61.6 % and 52.6 % for R6 in the AcoD of CS with DWW and also in SCB with DWW.

In Figure 5-34, the maximum VS reduction rate of 75.0% was recorded in R9 (CS with SWW) and the minimum for R8, R2, R4 and R12 at 25.0%, with VS concentration ranging from 2,000 mg/L to 8,000,mg/L. It was observed in this study that when the biomasses were co-digested with SWW, a higher VS reduction was observed compared to that with DWW. This could be due to the presence of nutrient-rich carbohydrates and "free sugars" in the SWW stream for higher VS values, with the maximum VS reduction ranging from 70 to 90%, similar to that obtained in a study by Kuo and Dow (2017).

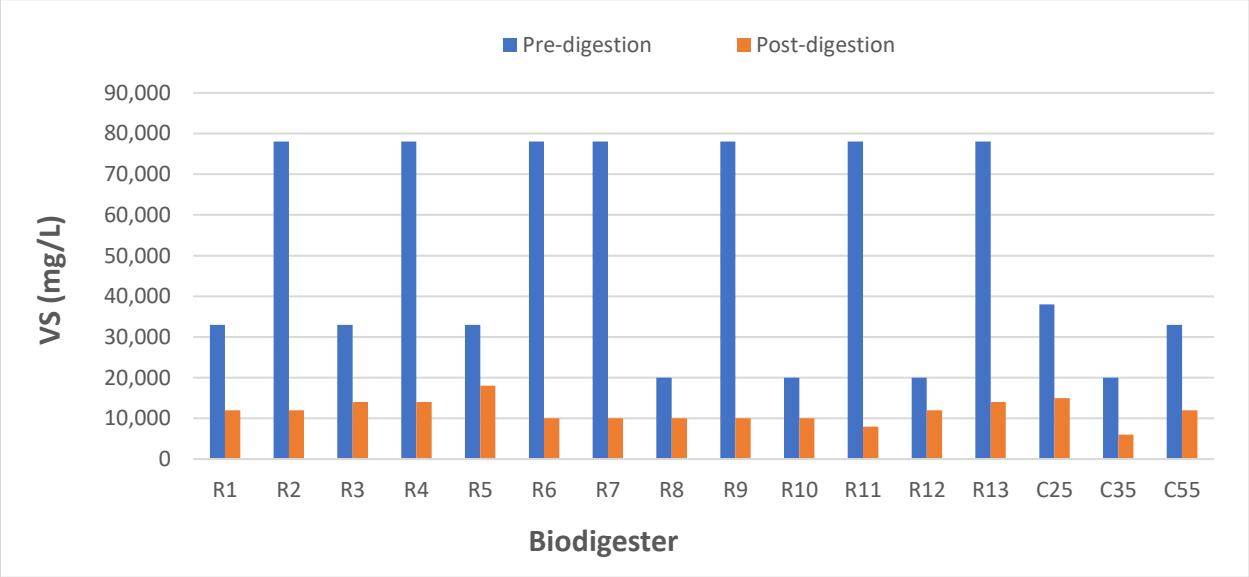

Figure 5- 29. Pre- and post-digestion of VS composition: SCB and SWW.

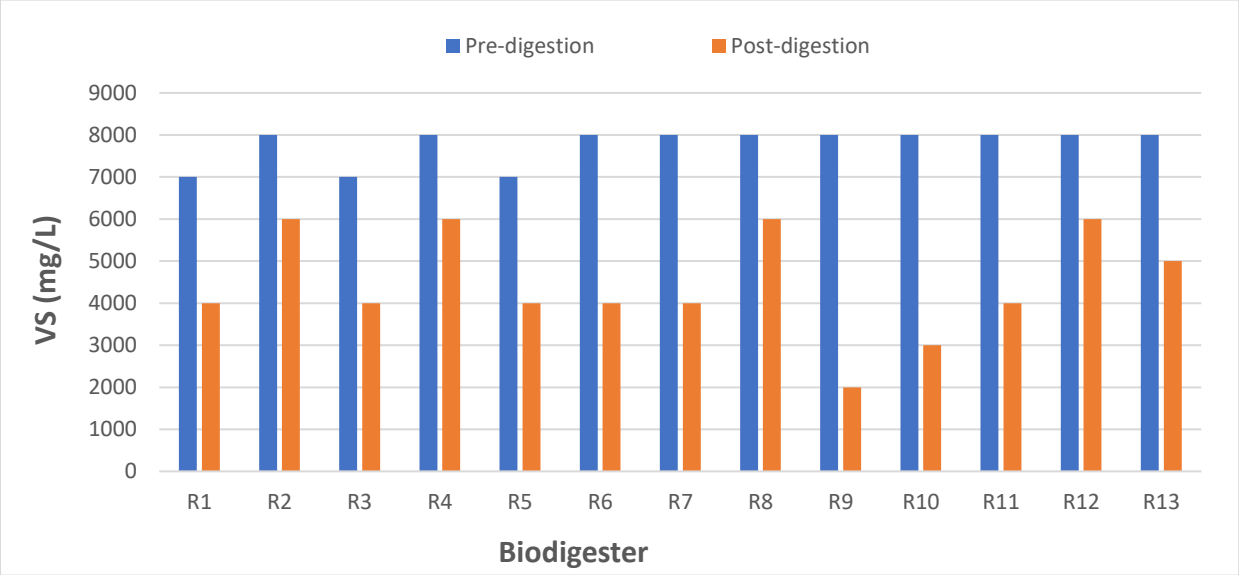

Figure 5- 30. Pre- and post-digestion of VS composition: CS and SWW.

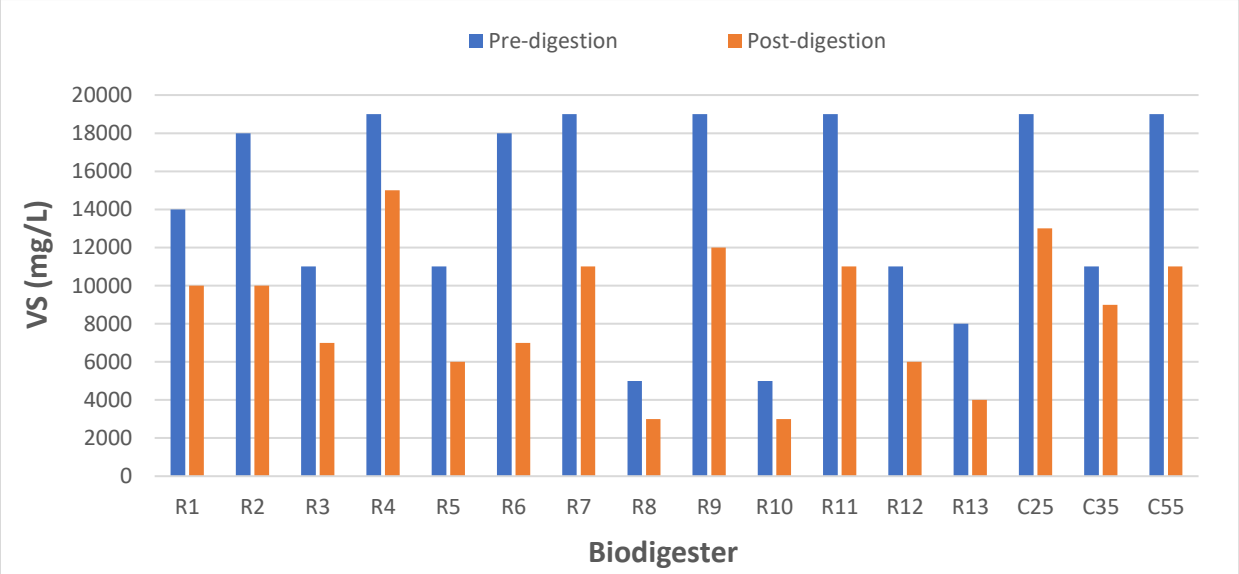

Figure 5- 31. Pre- and post-digestion of VS composition: SCB and DWW.

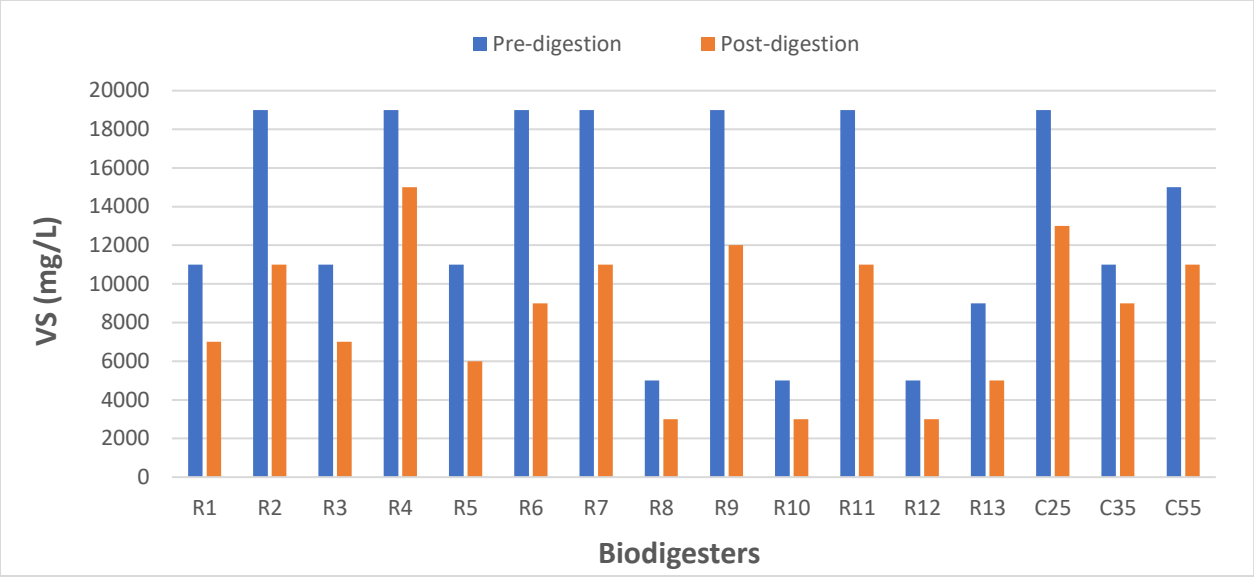

Figure 5- 32. Pre- and post-digestion of VS composition: CS and DWW.

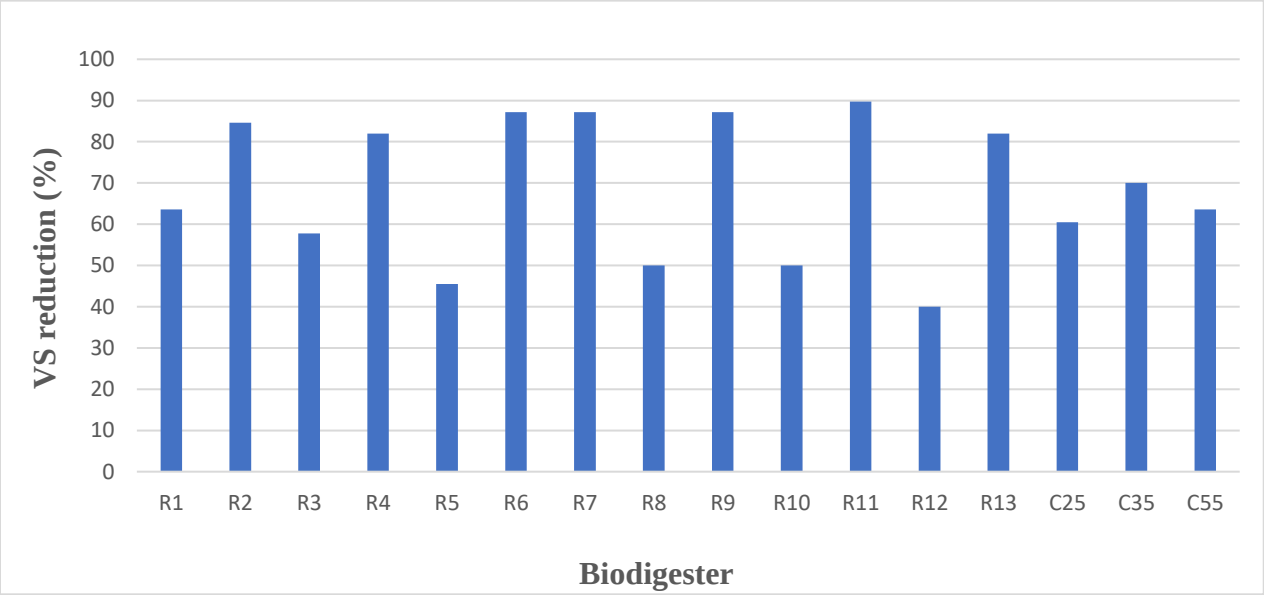

Figure 5- 33. VS reduction rate during pre- and post-digestion: SCB and SWW.

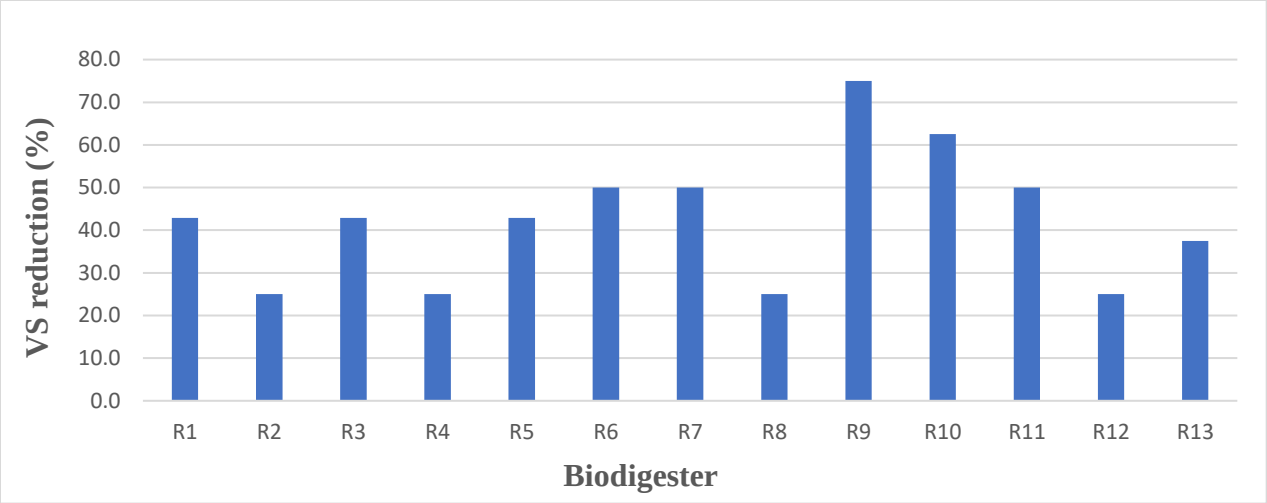

Figure 5- 34. VS reduction rate during pre- and post-digestion: CS and SWW.

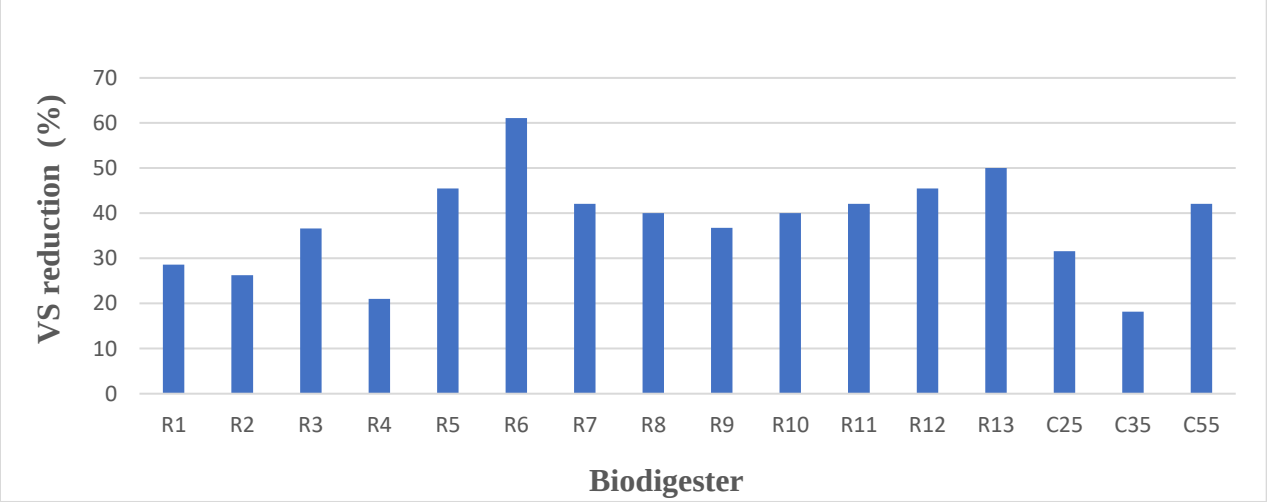

Figure 5- 35. VS reduction rate during the pre- and post-digestion: SCB and DWW.

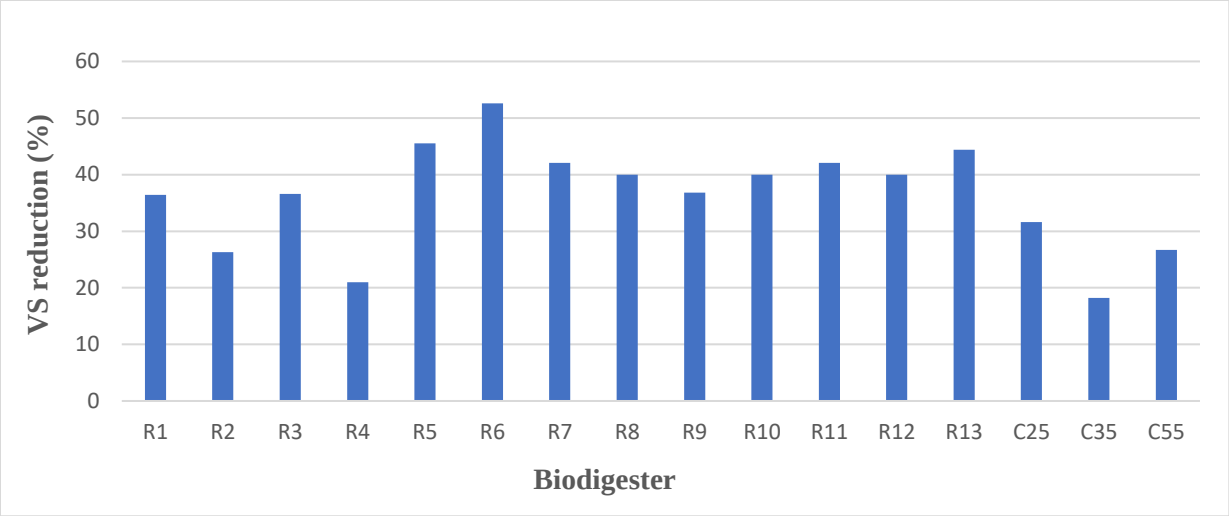

Figure 5- 36. VS reduction rate during the pre- and post-digestion: CS and DWW.

5.3.3.12 COD concentration and COD reduction

Under the operating conditions of temperature: 25°C, 35°C, 55°C and OLR in the range of 0.5 to 1.5gVS/100 mL, the influent (pre-digestion) and effluent (post-digestion) COD in all the biodigesters were found to be in range of 2,000 mg/L to 6,000mg/L (Figure 5-37 to 5-40). This is in relation to what has been reported by Zhang *et al.* (2017) where the COD values were reported in the range of 5,000 mg/L to 10,000 mg/L for a higher biodigester stability and performance.

In the same study, the biogas production was reported to be directly correlated to a decrease in COD of the substrate from the substrate, which means as COD is reduced the larger the amount of biogas produced. COD concentrations have been reported to be influenced by the HRT, as a maximum reduction in the COD was obtained at longer HRTs. Longer HRTs provides opportunities for anaerobic sludge and wastewater streams to contact longer so that the process of decomposition of organic matter becomes better and subsequently causing a reduction in the COD. Xie *et al.* (2016b) reported that a decrease in the concentration of the COD levels could result in

an increased HRT which was evidenced in this study for all the biodigesters. This is usually due to the gradual decomposition of organic material during microorganism's activity. The mathematical expression for the COD reduction is presented in the Appendix B2. Maximum COD reduction rate of 61.8% was observed for the AcoD of SCB with DWW (Figure 5-39), reporting higher biogas yield of 0.1 m^3/kg/VS.

This gives an indication that higher biogas production is achieved when the percentage COD reduction is higher. In Figure 5-42 and Figure 5-41, the maximum and minimum COD reduction was found to be 56.9% and 15.0% for biodigesters R6 and R5 respectively. Remarkably, this was slightly different in the case of Figure 5-41 where the maximum and minimum COD reduction was 44.4% (R10) and 12.9% (R7), respectively. Therefore, COD reduction could be employed as an alternative parameter to predict the biogas potential.

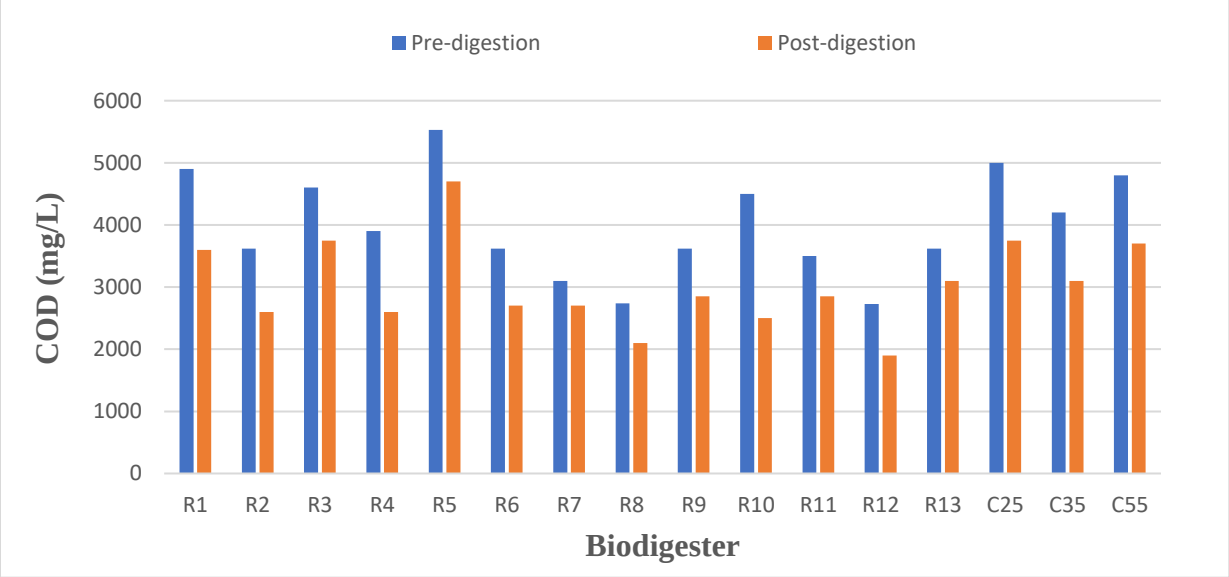

Figure 5- 37. Pre- and post-COD: SCB with SWW.

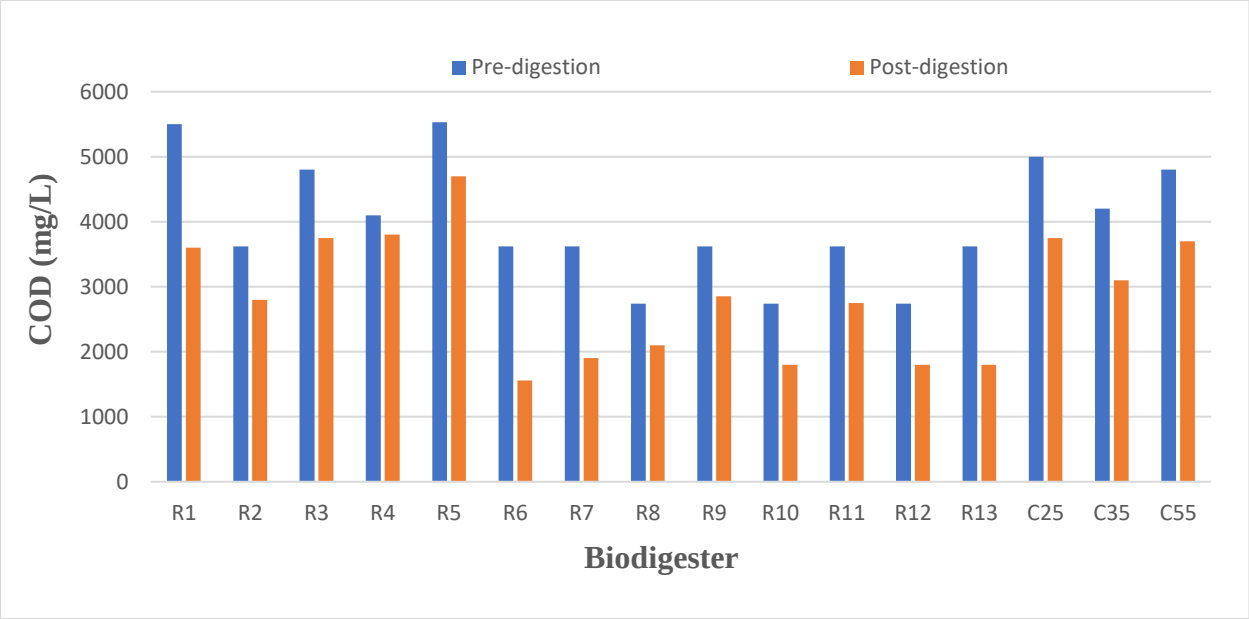

Figure 5- 38. Pre- and post-COD: CS with SWW.

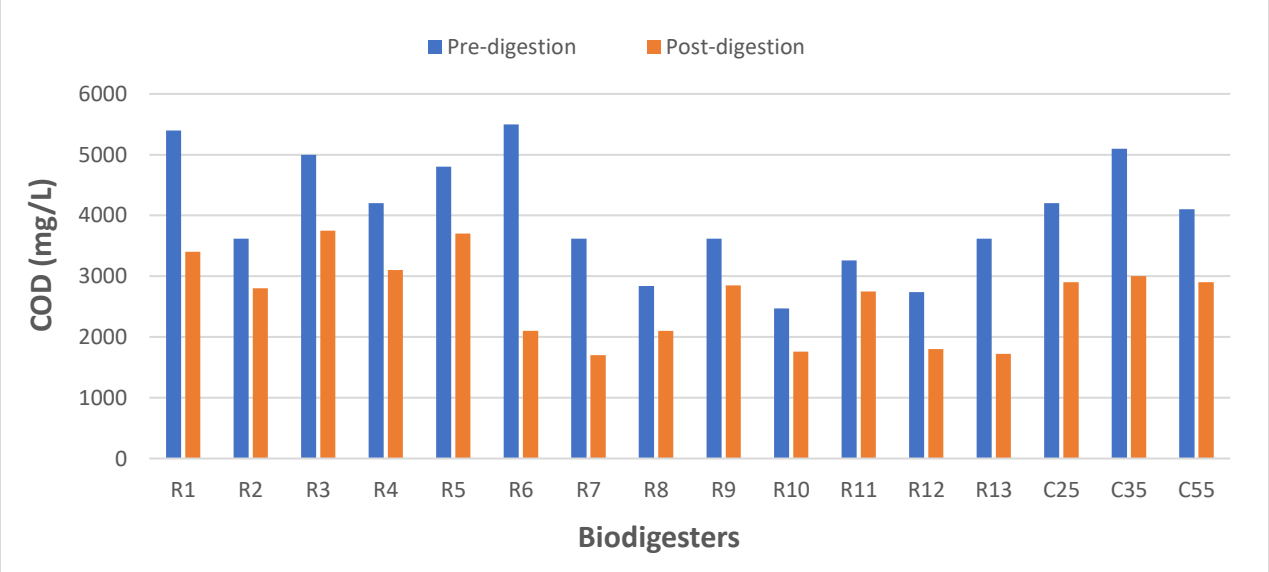

Figure 5- 39. Pre- and post-COD: SCB with DWW.

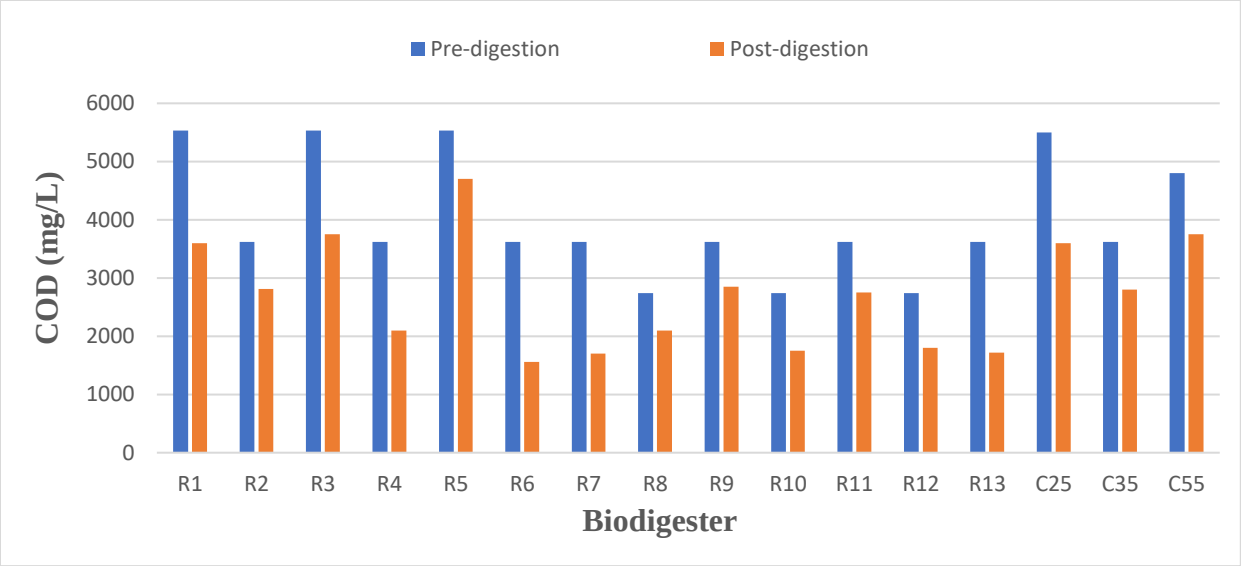

Figure 5- 40. Pre- and post-COD: CS with DWW.

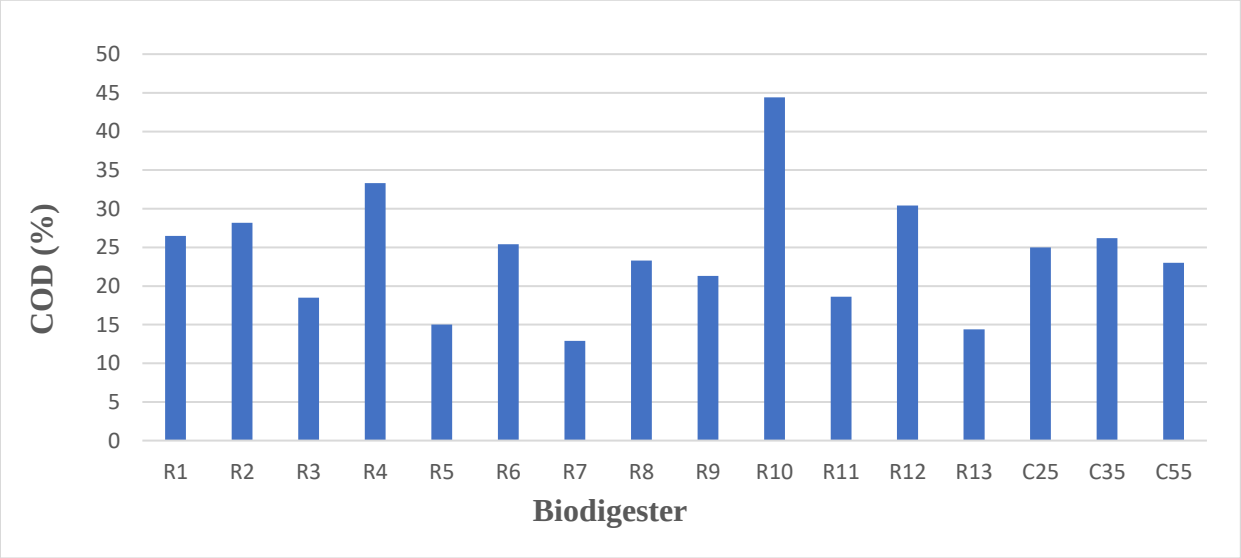

Figure 5- 41. COD reduction: SCB with SWW.

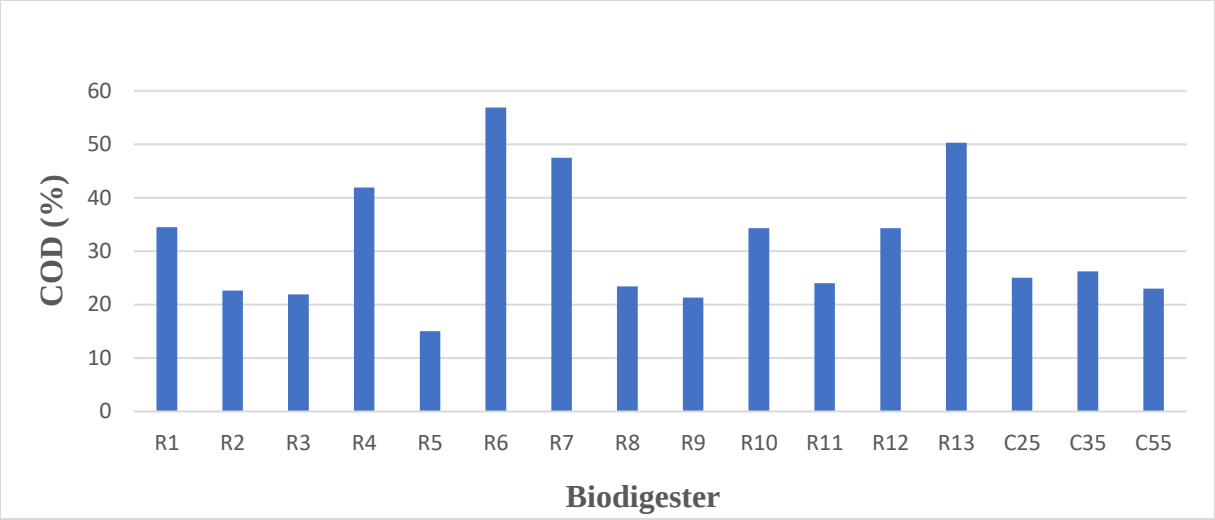

Figure 5- 42. COD reduction: CS with SWW.

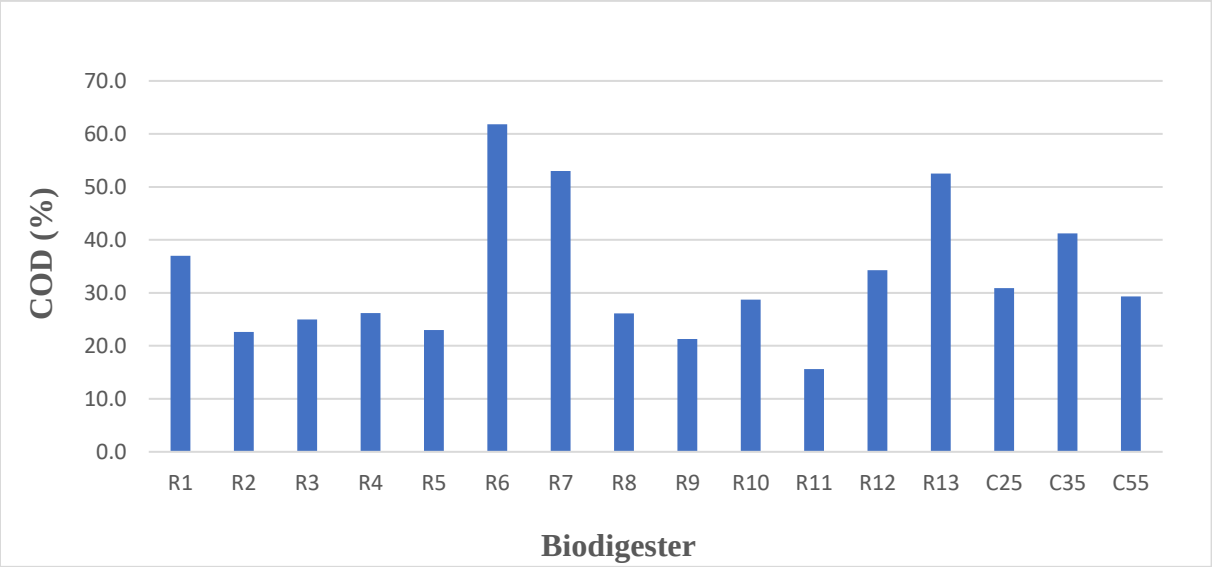

Figure 5- 43. COD reduction: SCB with DWW.

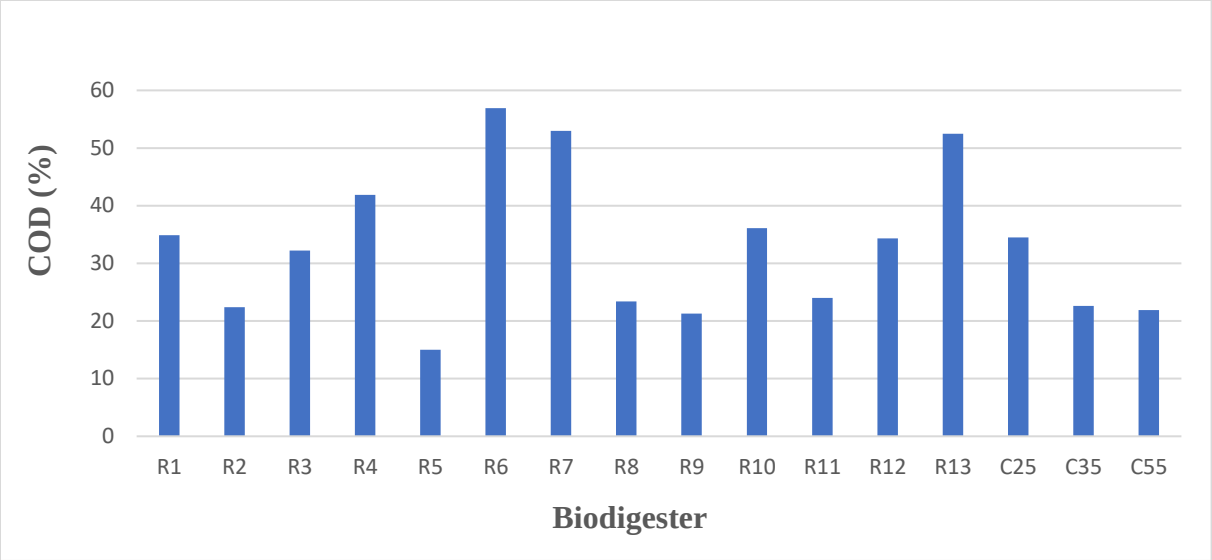

Figure 5- 44. COD reduction: CS with DWW.

5.3.3.13 Biogas composition: CH_4 and CO_2 contents for CS with DWW

In this section, the GC instrument was employed to measure the CH_4 and CO_2 contents for each biodigester according to method described to 3.3.3.2. The biogas composition was considered to be made up of only CH_4 and CO_2 in this present study. The highest CH_4 content of 79.11 % (54.67 mL/d) was observed for the AcoD of CS with DWW by R2 at an OLR of 1.0 gVS/100mL. The CO_2 content was found to be 20.88% with maximum biogas production observed in R6. This contrast to a study reported by Nalinga and Legonda (2016) where the highest biogas produced (16.96 mL/d) corresponded with the biodigester with maximum CH_4 content of 70% and production rate of 54.67 mL/d.

In Figure 5-45, the CH_4 content was found to be less than 10 % (7.96%) for R10 with higher CO_2 content of 92.06%. Studies have shown that if CH_4 is to be used for combined heat and power with biogas, then the equipment would have to be upgraded for safety reasons because of the flammability risk. Several methods have been employed for biogas upgrade such as amine

scrubbing and NaOH absorption. It was found that 82% of biodigesters recorded CH_4 contents greater than the amount of CO_2 produced, which is good prediction of their suitability for use in combined energy and power systems.

The CH_4 content differed between R5 and R10 by 6.48% with the amount of CO_2 found to be maximum in R10. The biogas composition for biodigesters R6, R7, R8, R9 and R13 was not presented in Figure 5-45 due to instrumental errors as GC recorded 100% CH_4 contents which was deduced not to be entirely realistic under this study.

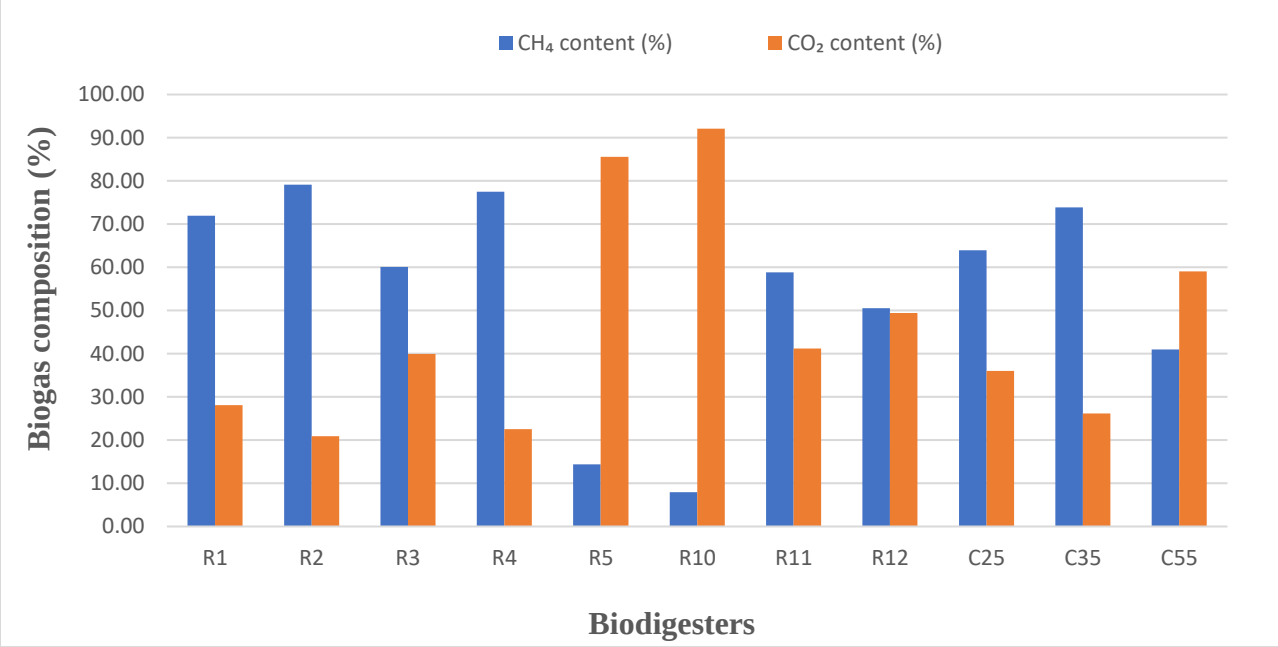

Figure 5- 45. Biogas composition after AcoD: CS and DWW

5.3.3.14 Biogas composition: CH_4 and CO_2 contents for CS with SWW

The highest CH_4 composition of 63.50%, a BPR of 666.7 mL/d and biogas yield of 5.0 m^3/kgVS was observed for the AcoD of CS with SWW by R10 at an OLR of 0.5 gVS/100 mL. The CO_2 composition was found to be 35.11% and CH_4 was 63.50% with maximum biogas production

observed in R10. It was found that 69% of biodigesters recorded CO_2 contents greater than the CH_4 as recorded in this study. The greater amount of CO_2 produced did not show a good prediction for the suitability of the AcoD of CS with SWW for use in domestic or industrial use. The highest biogas production rate of 666.7 mL/d was from the AcoD of CS with SWW amongst all the BMP test carried out in this study, but with the least CH_4 content. In Figure 5-46, R8 was reported to contain 71.10% of CO_2, making it suitable for biogas upgrading.

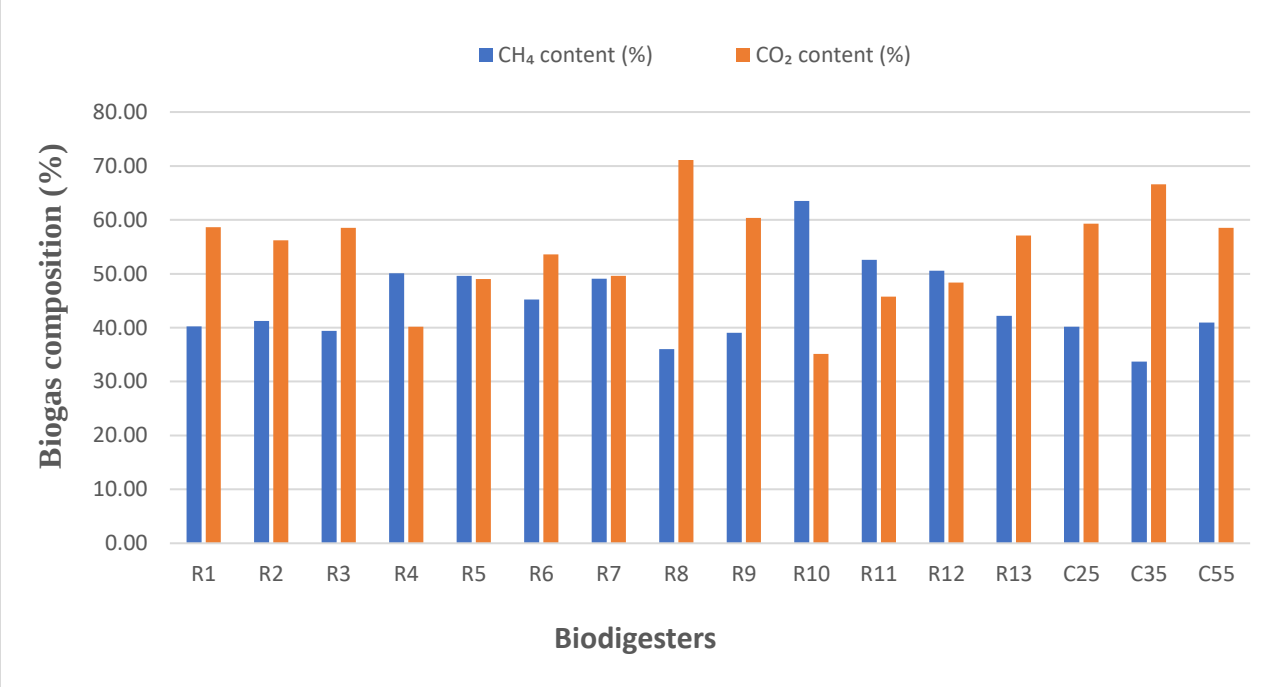

Figure 5- 46. Biogas composition after AcoD: CS and SWW

5.3.3.15 Biogas composition: CH_4 and CO_2 contents for SCB with SWW

Figure 5-47 shows the highest CH_4 content recorded was 79.56% (663.3 mL/d) as observed in the AcoD of SCB with SWW at an OLR of 0.5gVS/mL whiles the CO_2 content was found to be 20.77%. Following was R11 (77.56% CH_4 and 21% CO_2) with C55 (41.56% CH_4 and 55.26 CO_2) reporting the lowest biogas compositions. It was found that 81.25% of biodigesters recorded CH_4

contents greater than the CO_2 of 18.75% measured which was reported as 31%. Lowest CH_4 and highest CO_2 reported for C55 indicate the inflammability for industrial use and thus, biogas upgrading could be the way forward (Tsapekos, Kougias and Angelidaki 2015). Commonly used techniques developed for biogas upgrading in the past decades include; amine scrubbing and sodium hydroxide solutions for CO_2 absorption (Maile, Muzenda and Tesfagiorgis 2017; Kweinor-Tetteh *et al.* 2018). It was observed that 81% of biodigesters recorded CH_4 contents greater than the amount of CO_2 (19%) produced, a good prediction of the suitability for use in combined heat and power for use as an alternative means of energy.

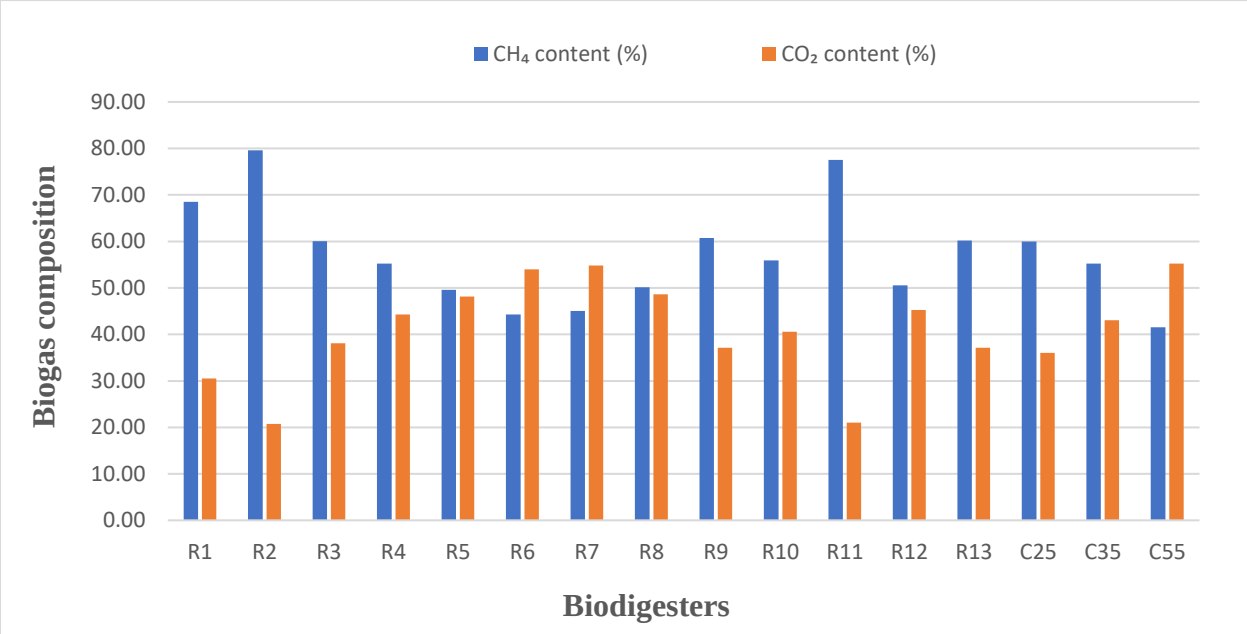

Figure 5- 47. Biogas composition after AcoD: SCB with SWW

5.3.3.16 Biogas composition: CH_4 and CO_2 contents for SCB with DWW

In Figure 5-48, the maximum CH_4 content of 68.54% (26.67 mL/d) was observed in the AcoD of SCB with SWW by R6 at an OLR of 1.0 gVS/mL. The CO_2 content was also found to be 29.61% with maximum biogas production observed in the same biodigester. It was found that 44% of

biodigesters recorded CH_4 contents greater than the CO_2 measured which was reported as 56%. The higher amount of CO_2 produced did not show a good prediction for the suitability of the AcoD of SCB with DWW for use in domestic or industrial use. In the case of R13, no biogas was produced all throughout the entire digestion process, and thus, no gas was collected which was attributed to failure of the biodigester. In all, the biogas yield was favored at lower OLR and higher temperatures for the AcoD of SCB with DWW.

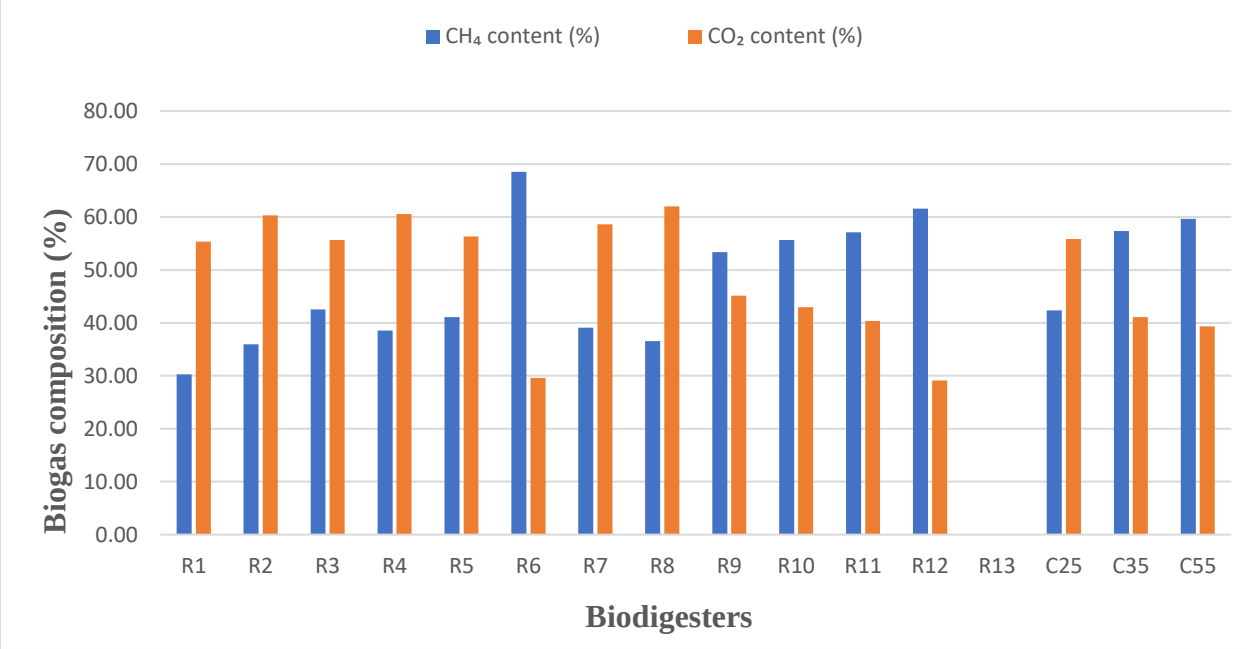

Figure 5- 48. Biogas composition after AcoD: SCB with DWW

Summary of objective two

The highest volume of biogas was reported for particle size of 0.4 mm for both SCB and CS which was used for the BMP test. The preliminary experiment showed that both SWW and DWW were selected as co-substrates for the AcoD process optimization amongst the four (4) WW streams based on the biogas potential. Using the untreated biomass, the maximum biogas potential was observed at 5.0 m^3/kgVS for CS with SWW. The highest CH4 composition was found to be 79% CH_4.

5.4 BMP tests after ionic liquid pretreatment

As described in section 3.3.3.2, BMP tests aids to ascertain the biogas potential for a given substrate mixture. Many studies have focused extensively on the glucose yield of lignocellulosic biomass after IL pretreatment without further determination of the biogas potential (Table 3-5 in section 3.4.1). This has resulted in little or no information about the amount of biogas that is produced after IL pretreatment of lignocellulosic biomass. In this section, the biogas potential after IL pretreatment of SCB and CS with [Emim][OAc] are reported. Also, another aim of this section was to determine if IL pretreatment of SCB and CS could improve the biogas potential in a BMP test as compared to that of the untreated biomass. Mkhize *et al.* (2016) reported the density and refractive index of [Emim][OAc] to be 1.079 gcm^{-3} and 1.499 n_D respectively. In the case of Wahlström and Suurnäkki (2015), it was found that the density and refractive index for [Emim][OAc] was 1.098 gcm^{-3} and 1.429 n_D respectively. Table 5-14 shows the physico-chemical properties of the [Emim][OAc] employed in this present study.

Table 5- 14. Chemical and physical properties of the [Emim][OAc].

Properties	Values
Molecular formula	$C_{10}H_{18}N_2O_2$
Density ($g.cm^{-3}$)	1.1038
Refractive index (n_D)	1.49867
Melting point (°C)	-45
Molar mass (g/mol)	170.21

Studies have shown that the amount of water content in an IL should be <1% as higher water content could significantly affect the physical properties and performance in the dissolution of cellulose of Ils and co-solvent (Tywabi 2015). Therefore, the dryness of IL is essential for optimum

dissolution of cellulose. In this study, a water content of 0.52% was observed for [Emim][OAc] which rendered it suitable for use. The experimental procedure for the IL pretreatment of the biomass with the WW streams for the BMP test is presented in section 3.4.3. The photograph for the analysis of the recovered and residuals are shown in Figure 5-49 with descriptions for each of (a) to (e).

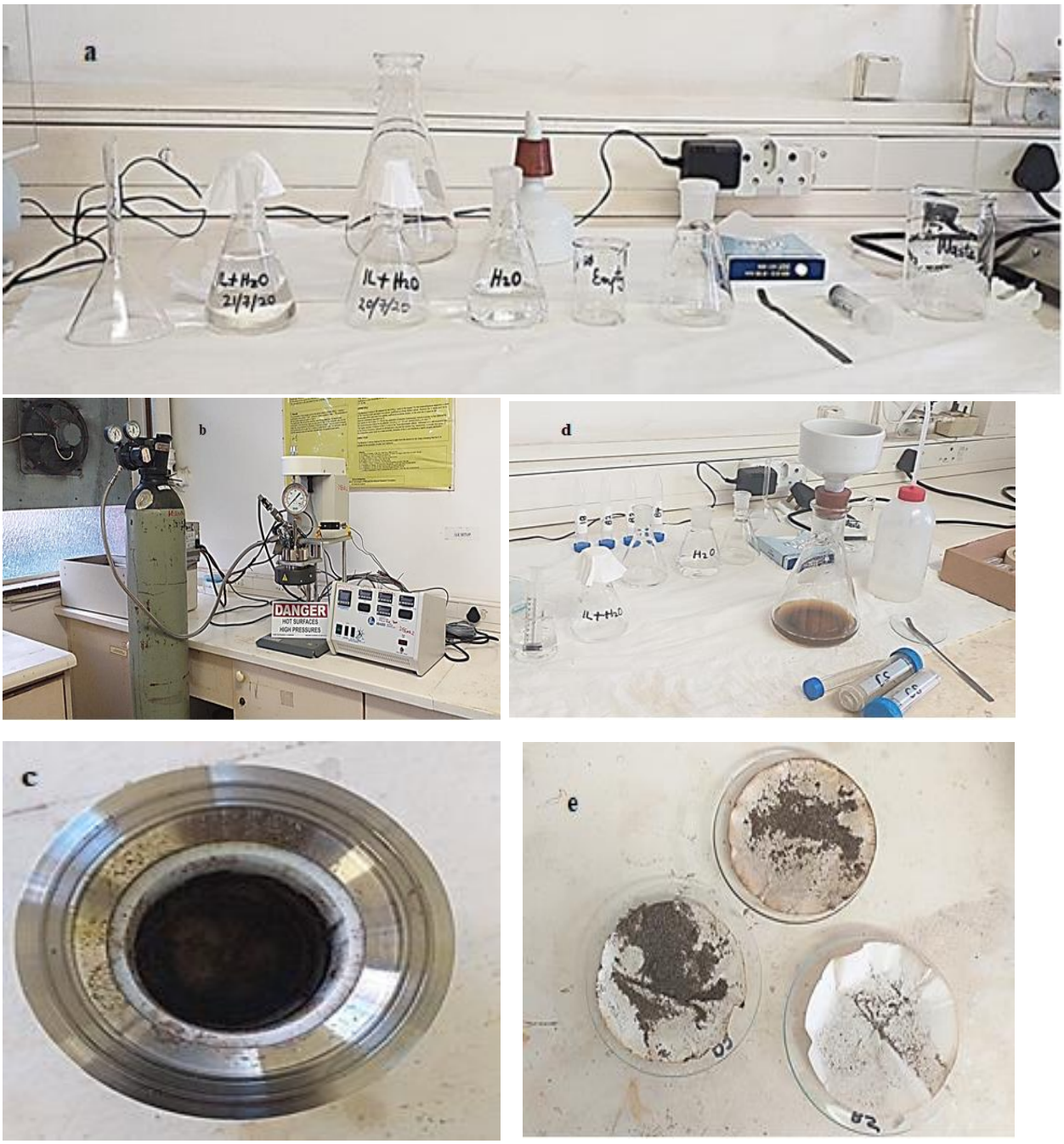

Figure 5- 49. Photographs of the (a) preparation of the IL with water solution and the biomass; (b) the 4560 Mini Benchtop Reactor (Parr Instrument Company, Moline IL 61265, Illinois, USA); (c) pulp recovery after pretreatment in the PTFE liner vessel; (d) washing and filtration of the mixture after pretreatment and (e) residue (solids retained on the filter paper during filtration) after oven drying at 55°C.

It is important to note that the quantity of WW, sludge and inoculum used for the BMP test of the untreated biomass is the same for that of the treated biomass. Table 5-15 shows the process parameters, operating conditions and pH readings for each biodigester for the treated biomass.

Table 5- 15. Process parameters, operating conditions and pH for the pretreated biomass.

Biodigester #	Mass of liquid fraction taken (g)	Temperature (°C)	OLR (gVS/100mL)	Pre-pH	Post-pH
A1	5.1	25	0.5	6.8	7.5
A2	5.1	25	0.5	6.8	7.6
A3	10.3	55	1.0	7.4	8.3
A4	10.3	55	1.0	7.7	8.2
B1	4.2	25	0.5	6.9	7.7
B2	4.2	25	0.5	6.8	7.7
B3	8.3	55	1.0	7.5	8.2
B4	8.3	55	1.0	7.5	8.4
$C_{A1, A2}$	5.089	25	0.5	6.9	8.3
$C_{A3, A4}$	10.278	55	1.0	7.4	8.1
$C_{B1, B2}$	4.172	25	0.5	6.9	7.6
$C_{B3, B4}$	8.245	55	1.0	7.4	7.7

5.4.1 Daily biogas production

Monitoring the daily biogas production is a crucial part of the BMP test as it gives a clue on the progress of the AcoD process and the biodigesters efficiencies (Tsapekos, Kougias and Angelidaki 2015). The experimental procedure and the operating conditions for the biogas production are presented in section 3.4.3. The shortest lag phase was observed for biodigesters B3 and $C_{B3,B4}$ as biogas production was recorded within the 24 hours from the start of the experiment, and the longest lag phase was observed for biodigesters B1 and B2 (descriptions given in Table 3-4) as biogas production started on day 5. The highest biogas production of 60 mL each was observed for days 5 and 6, corresponding to biodigesters B3 and B4, respectively. It is evidenced from Figure 5-50 that no biogas production was observed in all the biodigesters after day 18. Biogas production was observed to increase significantly for biodigester B4 from day 2 to day 6, after which there was a sharp decline. Also, the biogas production from the remaining biodigesters were found to increase slightly between day 2 and day 8, after which a significant drop in the biogas production was observed until the overall process, ceased. This could be due to the fact that the biomass became either partially or completely used-up by the microbes present, denatured or inactive due to saturation or perhaps, some of the products obtained during the AD process become harmful to the microbes causing the biomass breakdown (Liu and Kokare 2017). The highest BPR and biogas yield were reported for biodigester B4 (CS with DWW) at 1,031 mL/d and3.9 m^3/kgVS, respectively. Comparatively, the BPR recorded after IL pretreatment (1,031 mL/d) was found to be higher than that reported for the untreated biomass (666.7 mL/d), which could be attributed to enhanced biomass porosity after pretreatment of biomass during AD. This was followed by biodigester B3 at a BPR of 9.67 mL/d, indicating that the biogas production is influenced at higher temperatures and at higher OLRs. According to Lina *et al.* (2018) the operation of AcoD under

thermophilic conditions significantly override that of mesophilic and room temperatures, which is evidenced in this study. Considering the control biodigesters, $C_{B3,B4}$ recorded the maximum BPR of 3.50 mL/d, followed by $C_{A1,A2}$ at 1.33 which represents a 62% increase in production. Generally, biogas production was observed to be largely favored when CS is anaerobically co-digested with industrial WW. Without IL pretreatment, maximum biogas production was observed when CS was anaerobically co-digested with SWW at 25°C (20 litres). This was not the case of the biogas production after IL pretreatment as the maximum potential was observed when CS was anaerobically co-digested with DWW at 55°C (31 litres). The changes reported in terms of the WW streams could be due to over-saturation of carbohydrate-rich substrates arising from the SWW and that of the sugars released after the IL pretreatment. However, maximum production of biogas was reported for CS from IL pre-treated and untreated biomass.

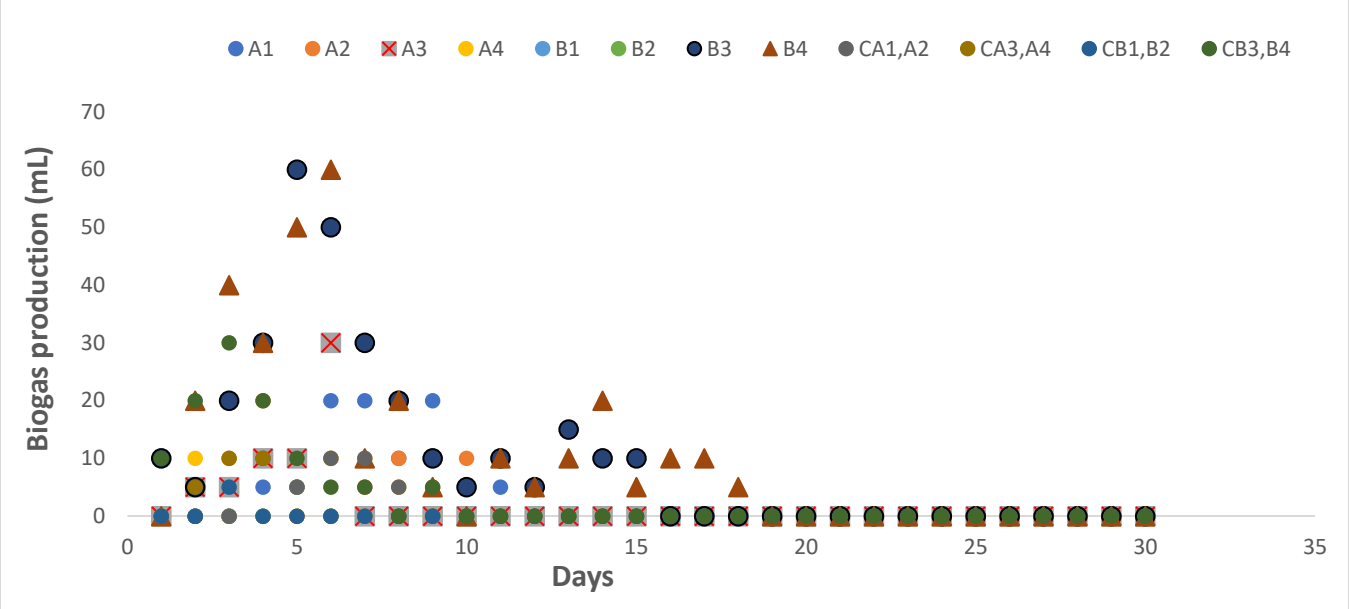

Figure 5- 50. Daily biogas production.

5.4.2 pH

As stated earlier, the optimum pH range was observed in a range of 6.0 to 8.5. The pre-digestion pH for all the biodigesters were observed in the range of 6.8 to 7.7 whilst the post-digestion was from 7.5 to 8.4. The highest pH value reported for the pre-digestion was observed for biodigester A4 (7.7) which comparatively, is greater than the highest pH value for SCB with DWW at a pH of 7.11. For the post-digestion pH, highest biogas volume was observed for biodigester B4 (8.4) which comparatively, is greater than the highest pH value for SCB with DWW at a pH of 7.7. Also, the lowest pre-digestion pH was reported for biodigesters A1 and A2 (6.8) which comparatively, is lower than that observed for SCB with SWW at 7.04. Biodigester B2 also reported a pre-digestion pH of 6.8 which was found to be higher than that observed at CS with SWW (pH of 6.3). The lowest pH value reported for the post-digestion was observed for biodigester A1 (7.5) which comparatively, is greater than that found in SCB with SWW at a pH of 6.2. Generally, the pH for biodigester A1 was found to be lower as compared to the other biodigesters and that, this did not significantly affect the bigas production in the overall process (Figure 5-51). Nonetheless, biodigester B4 which reported the highest post-digestion pH recorded the maximum volume of biogas as all the pH values for all the biodigesters were found within the optimum range.

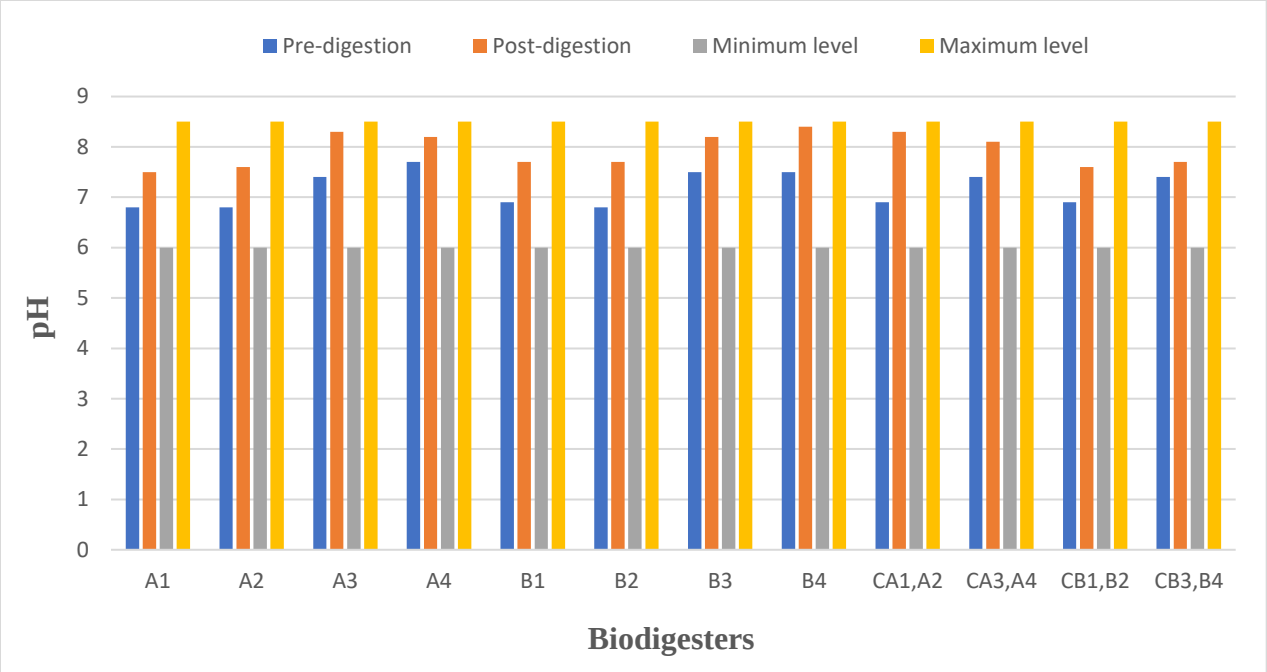

Figure 5- 51. Pre- and post-digestion pH.

5.4.3 Biomethane potential

As described in section 3.3.3.2, a 100 µL syringe was used to withdraw the biogas from each biodigester after the digestion time. In this present study, the highest CH_4 content was reported to be 86.55% for biodigester A1 as shown in Figure 5-52. Comparatively, the CH_4 content recorded after IL pretreatment was found to be 9% higher than the untreated biomass (79%). The next highest volume was recorded for biodigester B4 with 82.63% of CH_4 and 17.37%CO_2. It was evidenced that the CH_4 content for all the control biodigesters were found to be lower with higher CO_2 contents in the range of 80 to 90%. This higher CO_2 content in the control biodigesters could be due to the presence of IL which could possibly inhibit the generation of biogas making these biodigesters susceptible for biogas upgrading for use in electricity generation. Volumetrically, the AcoD of CS with WW has proven to be greater in which contrast to that of the AcoD of SCB with WW which produced greater CH_4 content.

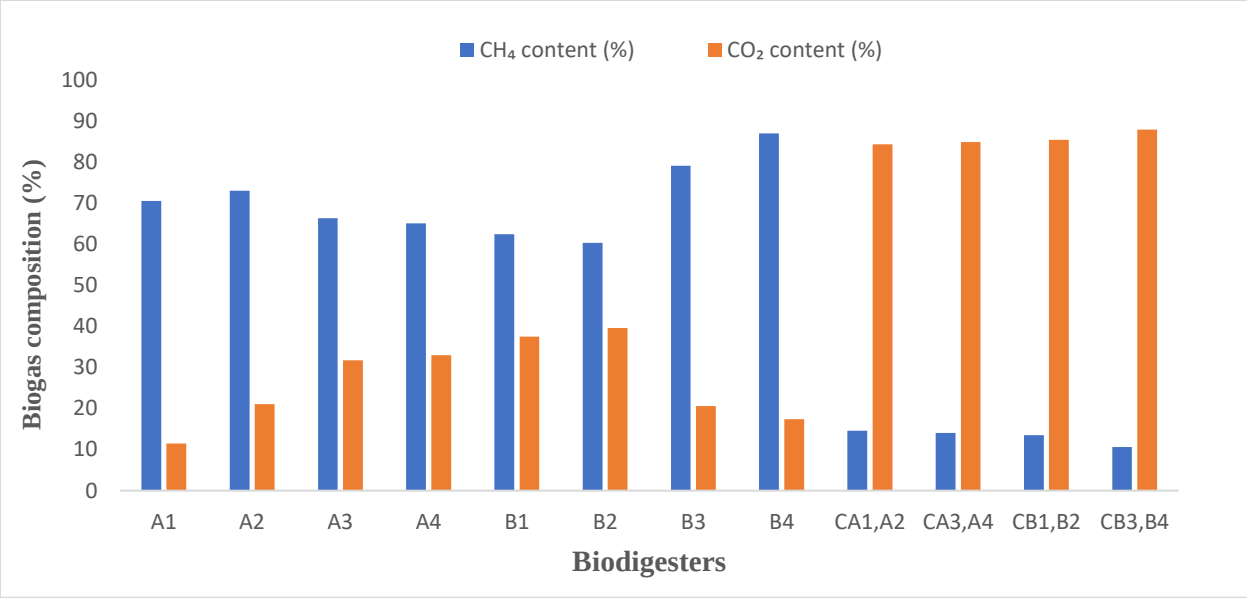

Figure 5- 52. Biogas composition after IL pretreatment.

5.4.4 Sugars released after IL pretreatment

The sugars present after IL pretreatment were analysed using the Shimadzu HPLC. Figure 5-53 shows the plot of the retention times (minutes) versus the different sugars present after the IL pretreatment. The calibration curves of the sugar standards were determined and the retention times (minutes) reported which were compared in relation with that of the sugars released after IL pretreatment. The removal of hemicellulose from SCB and CS was evidenced by the absence of xylose after IL pretreatment as shown in Figure 5-53. The letters, “A” and “B” in Figure 5-53 denotes the liquid fractions of SCB and CS after the IL pretreatment, respectively. The RT of the standards are denoted by the blue line which represents the retention times (min) of the sugar standards.

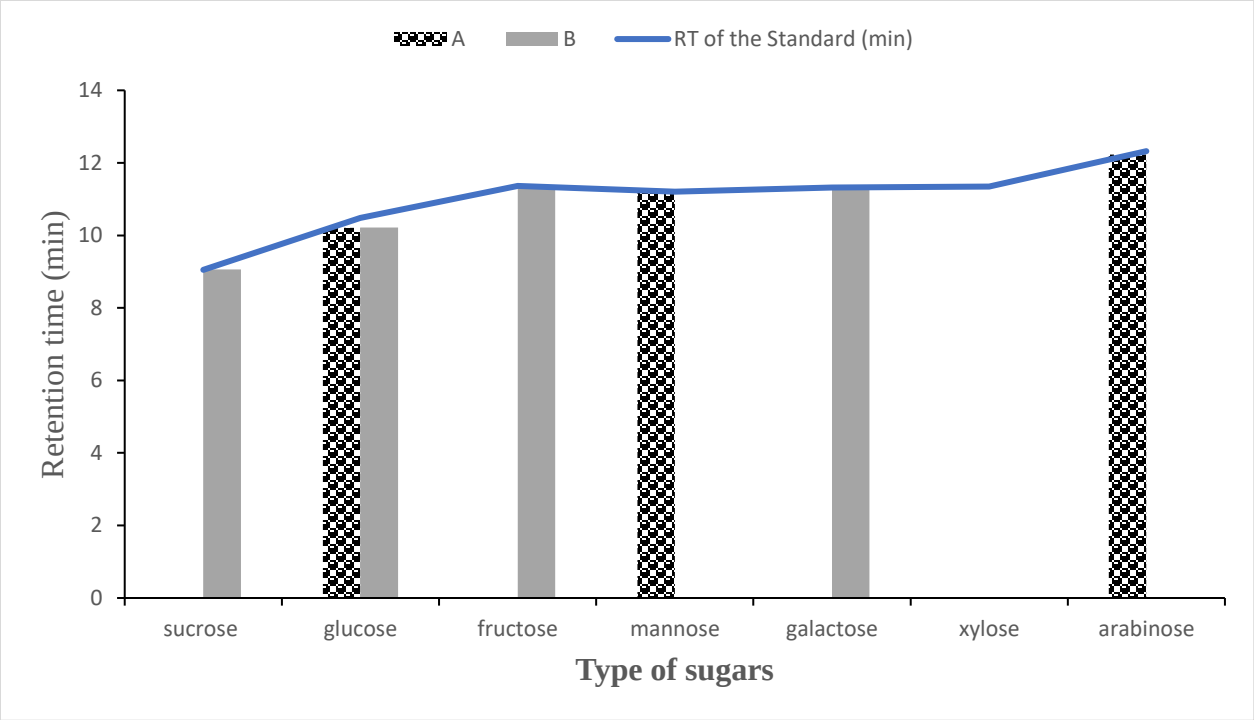

Figure 5- 53. Plot of the retention times (minutes) of sugars present after the IL pretreatment.

5.4.5 Biogas production and energy conversion

The amount of energy produced from biogas is considered a vital key to aid in supplementing a renewable form of energy for the country's electricity grid. In South Africa, the liquor industries (clear beer and wineries) have reported maximum biogas production of about 35×10^6 m^3/year with the least potential observed in pig farming of about 0.02×10^6 m^3/year (Primrose and Mugodo 2015). Total wastewater discharge from the sugar mill and DWW have been found to be approximately 1600×10^6 and 20.95×10^6 respectively, in the same study which are employed in this present study. It is estimated that an average of 86×10^6 m^3/year of biogas could be produced from some of these sectors in South Africa and other WW streams, which has the potential to be equivalent to 148 gigawatt hours (GWh) of electrical energy, twice the set 2030 target for biogas of 75 GWh. Biogas production of liquid waste (WW) was estimated from the COD readings taking

into consideration the optimum biogas potential. In this study, the optimum biogas potential for the untreated and pretreated were CS with SWW (R10) and CS with DWW (B4), respectively. In that case, the COD values selected for the estimation of the annual biogas production were R10 and B4 which are in bold and in asterisks (Appendix) in Table B-5 and Table B-10, respectively. It could be deduced that the overall energy output (GWh) for the pretreated was much lower than that of the untreated biomass because of the higher total wastewater discharge quantity of the latter than the former (Table 5-16). The table shows the summary of the process operations and energy outputs (GWh) for the pretreated and untreated biomass. The estimation of the energy outputs for both pretreated and untreated biomass are described as;

(a) Using the untreated feedstock, the highest biogas production was obtained from CS with SWW.

Total biogas production = 20,000 mL = 20 L = 0.02 m^3/L

$COD_{removed} = COD_{before\ AD} - COD_{after\ AD}$

= 2740 – 1800

= 0.94g/L

= 0.00094 kg/L

$$\text{Biogas yield} = \frac{\text{Total biogas production}}{COD_{removed}}$$

$$= \frac{0.02}{0.00094}$$

= 21.28 m^3/kg

The total wastewater discharge for the sugar mill is approximately, 1600 × 10^6L/yr.

Annual biogas production $\left(\frac{\mathrm{m}^3}{\mathrm{yr}}\right) = \mathrm{COD}_{\mathrm{removed}}\left(\frac{\mathrm{kg}}{\mathrm{L}}\right) \times$ Total WW discharge $\left(\frac{\mathrm{L}}{\mathrm{yr}}\right) \times$ biogas yield$\left(\frac{\mathrm{m}^3}{\mathrm{kg}}\right)$

$= 0.00094 \times 1600 \times 10^6 \times 21.27$

$= 32 \times 10^6\ \mathrm{m}^3/\mathrm{yr}$

However, if $86 \times 10^6 \mathrm{m}^3/\mathrm{yr} \sim 148\mathrm{GWh}$ of electrical energy, then $32 \times 10^6\ \mathrm{m}^3/\mathrm{yr} = 53.35$ GWh of electrical energy.

(b) Using the treated feedstock, the highest biogas production was obtained from CS with DWW.

Total biogas production = 31,000 mL = 31L = $0.031\mathrm{m}^3/\mathrm{L}$

$\mathrm{COD}_{\mathrm{removed}} = \mathrm{COD}_{\mathrm{before\ AD}} - \mathrm{COD}_{\mathrm{after\ AD}}$

$= 3620 - 1800$

$= 1.82\mathrm{g/L}$

$= 0.00182\ \mathrm{kg/L}$

Biogas yield $= \frac{\text{Total biogas production}}{\mathrm{COD}_{\mathrm{removed}}}$

$= \frac{0.031}{0.00182}$

$= 17.03\ \mathrm{m}^3/\mathrm{kg}$

The total wastewater discharge for the DWW is approximately, 20.95×10^6 L/yr.

Annual biogas production $\left(\frac{\mathrm{m}^3}{\mathrm{yr}}\right) = \mathrm{COD}_{\mathrm{removed}}\left(\frac{\mathrm{kg}}{\mathrm{L}}\right) \times$ Total WW discharge $\left(\frac{\mathrm{L}}{\mathrm{yr}}\right) \times$ biogas yield$\left(\frac{\mathrm{m}^3}{\mathrm{kg}}\right)$

$= 0.00182 \times 20.95 \times 10^6 \times 17.03$

$= 6.5 \times 10^5\ \mathrm{m}^3/\mathrm{yr}$

However, if 86×10^6 m^3/yr ~ 148GWh of electrical energy, then 6.5×10^5 m^3/yr = 1.12 GWh of electrical energy.

Table 5- 16. Summary of the energy output (GWh) from the optimal runs for the untreated and pretreated biomass.

Substrates	**Total biogas production (m^3/L)**	**$COD_{removed}$ (kg/L)**	**Total wastewater discharge (L/yr)**	**Annual biogas production (m^3/yr)**	**Energy output (GWh)**
Untreated: CS with SWW	0.020	0.00094	1600×10^6	32×10^6	53.35
Pretreated: CS with DWW	0.031	0.00182	20.95×10^6	6.5×10^5	1.12

Summary of objective three

In conclusion, [Emim][OAc] was found to be efficient for the IL pretreatment of SCB and CS for biogas production. The highest CH_4 content was found to be 87% for the AcoD of CS with DWW after IL pretreatment which was higher than that of the untreated biomass (79%). This 9% increase could be considered significant in terms of the purity of the biogas composition after IL pretreatment. Also, the removal of hemicellulose from SCB and CS was evidenced by the absence of xylose in the pulp after IL pretreatment. Also, the annual biogas production was found to be 32 $\times 10^6$ m^3/yr (53.35 GWh of electrical energy) for the untreated biomass and 6.5×10^5 m^3/yr (1.12 GWh of electrical energy) for the pretreated biomass.

5.6 Kinetic model study

The kinetic parameters needed for the use of steady-state models were found using a laboratory-scale batch biodigester with volume of 1,000 mL when industrial wastewater served as the co-substrate. Kinetic model equations, presented as equations 3.9 to 3.12 were employed to describe the cumulative production of biogas over digestion period of time. For example, the modified Gompertz has been found to describe the cumulative biogas production during AD or AcoD. The equation assumes that methanogen production rate of biogas in batch biodigesters correspond to its specific growth rate. Each biodigester during the BMP test was monitored for biogas production and the composition determined for the CH_4 and CO_2 at the end of the digestion period. To provide a common basis for comparing the different kinetic models, the cumulative biogas production data and reported lag phase (λ) from the experiments were fitted into each model, describing the cumulative biogas production. In batch assays, it is assumed that CH_4 production is a function of the bacterial growth. The kinetic and biodegradability parameters were assessed using a non-linear regression implemented via a solver function of the Microsoft Excel tool pack and the results for the estimated parameters. Parameter estimates were found to be an integral components for the model predictions and thus, reported in this section. The correlation coefficient, R^2 predicts the closeness of a set of data to the fitted regression line. However, the correctness of a particular model in describing the AD process was represented on the models ability in producing a higher R^2 value as it approaches 1 as reported by (Tetteh *et al.* 2020).

Also, it was found that the R^2 value of the linear plots attained information from the substrate mixture suggests the most suitable kinetic model describing the mechanism of biogas production. The input variables that gave the best fit: P, k, SSR, R^2, c, λ, K_{CH}, K_ft, K_Lt, μ_m and α are presented.

This section of the thesis, however, details the applicability of the kinetic models testing to predict the best fit.

5.6.1 CS and DWW for the untreated biomass

As observed from Table 5-17, the R^2 values are presented as 0.882, 0.992, 0.5054 and 0.888 for the first order, modified Gompertz, Chen and Hashimoto and dual pooled kinetic models, respectively.

Table 5- 17. Kinetic parameters from non-linear regression for the AcoD of CS and DWW for the untreated biomass

First order model		**Modified Gompertz**		**Chen & Hashimoto**		**Dual pooled first order**	
Parameter	Value	Parameter	Value	Parameter	Value	Parameter	Value
P	1233.0733	*P*	429.6629	*P*	346.7702	*P*	1285.6311
K	0.02655	K	0.51511	K_{CH}	0.93416	$K_f t$	0.026784
SSR	83935.674	C	6.70319	μ_m	0.57682	$K_L t$	0.012695
R^2	0.8823	SSR	4583.8208	SSR	287380.45	α	0.90008
		λ	1.0	R^2	0.5054	SSR	83953.48
		R^2	0.992			R^2	0.8818

The R^2 value of the Chen & Hashimoto model was oberved to be the least (0.5054) and was found inappropriate (weak regression). The results obtained authenticates what was reported by Xie *et al.* (2016a) that the first order, Gompertz model and the dual-pooled first order have been adapted in the simulation of biomethane production for AcoD processes. An R^2 value of 0.992 from the modified Gompertz model was found greatest and thus, shows a good fit and correlation to

experimental data to describe the biogas production. Figure 5-54 shows the closeness (fitness) of the modified Gompertz to the experimental data than the other three models tested. This suggested that the model fitted well with the given data. This could be attributed to the fact that the modified Gompertz considers the effect of any changes for an influent substrate concentration under prediction. Also, this shows that the modified Gompertz model could be used to successfully describe the overall anaerobic co-digestion of CS with DWW. This is in contrast to a study by Xie *et al.* (2016b) in whi ch the first order and Gompertz kinetic models were reported to be inappropriate for a similar study. The Contois and the Monod equations have also been used in the kinetic study of the AD of ice-cream wastewater (Hu, Thayanithy and Forster 2002). In that study, it was found that the former was more suitable than the later with an R^2 of 0.989. Results obtained, thus, indicated that the digestion could expand the reaction rate of the hydrolysis process and that the R^2 value is a good tool to predict model fitting. The sum of squares errors (SSR) was used as a statistical criteria to evaluate the deviation between the measured cumulative biogas production and the calculated cumulative biogas production over the experimental period (Lee *et al.* 2017). It presented the observed dependent variable and its mean and the dispersion of data points. The SSR was reported to be increased in the order of modified Gompertz (4583.8), first order (83935.7), dual pooled first order (83953.5) and the Chen and Hashimoto (287380.5). The SSR was found not to be influenced by the R^2 value and a lag phase, found to be unity for all the tested models. The maximum biogas production rate, *P* was obtained from the dual pooled (1285.6 mL) with the Chen and Hashimoto, being the least (346.8 mL) Following the dual pooled was the first order and the modified Gompertz models with *P* values of 1233.1 mL and 429.7 mL, respectively. Table 5-17 depicts the reported kinetic model parameters.

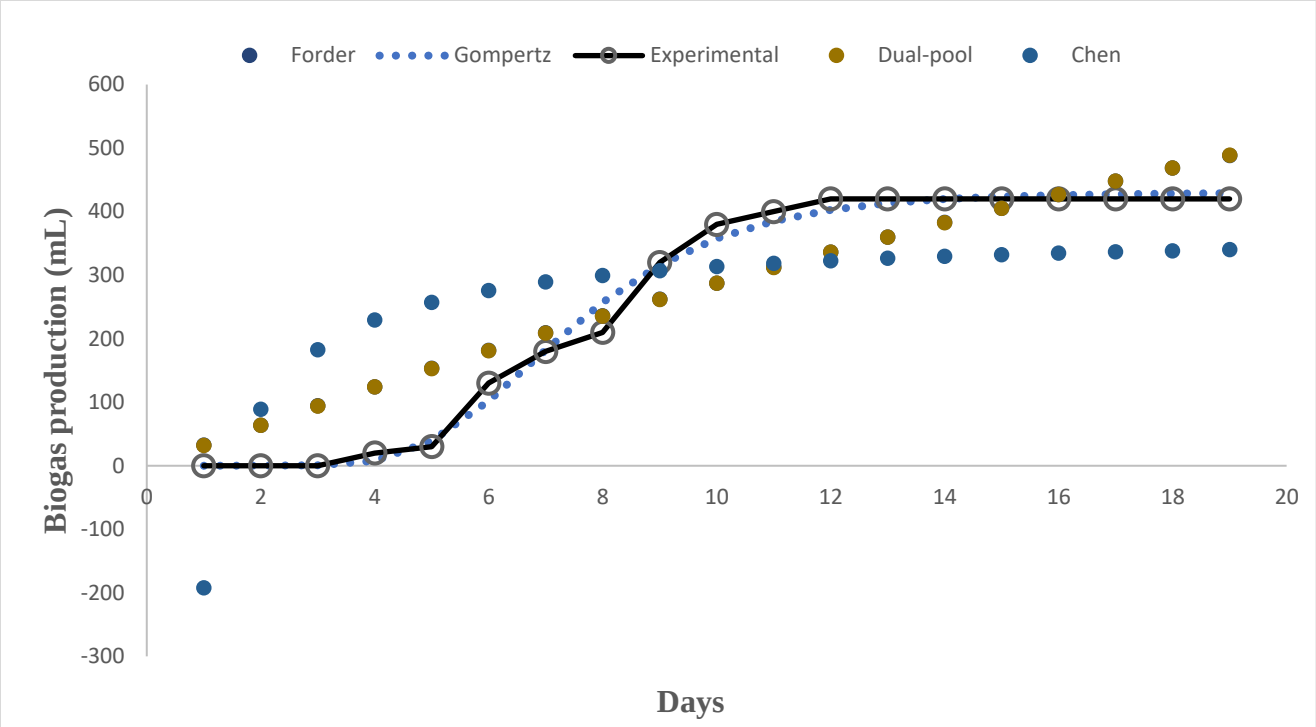

Figure 5- 54. Combined graphs of cumulative biogas yield versus digestion period (days).

In each model analysis, a straight-line plot was developed from the equation of a line: $y = mx + c$ and a linear regression analysis employed in establishing the 'best-fit' model. In this case, the modified Gompertz model was employed to establish the linear graph, relative to the experimental data. The plotting of biogas production (mL) versus days (d) yields a straight-line equation with a slope of 0.9946 and an intercept at 2.0698. The fitting equation between the cumulative biogas production and time is presented as $y = 0.9946x + 2.0698$ as shown in Figure 5-55.

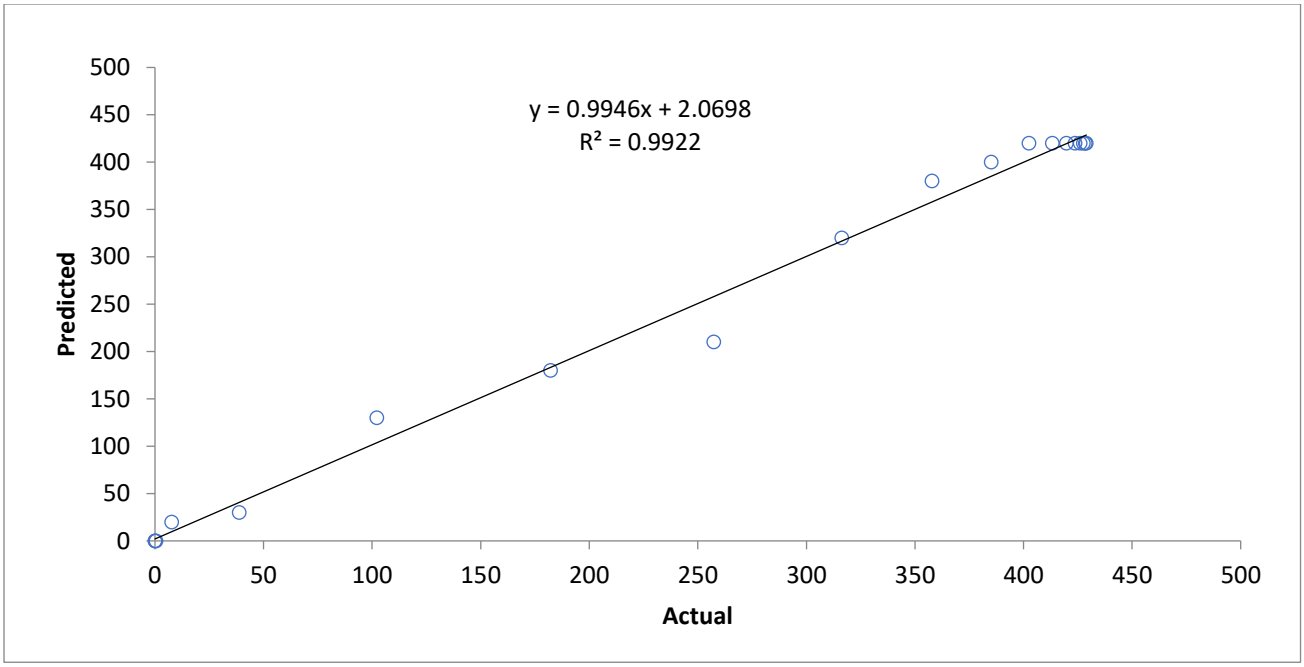

Figure 5- 55. Regression plots for the best fit model: modified Gompertz.

5.6.2 CS and SWW for the untreated biomass

From Table 5-18, the R^2 values were presented as 0.9213, 0.9974, 0.5874 and 0.9405 for the first order, modified Gompertz, Chen and Hashimoto and dual pooled kinetic models, respectively. The R^2 value of the Chen & Hashimoto model was oberved to be the least (0.5874) with weaker regression which is similar to what reported in the AcoD of CS with DWW (0.5054).

Table 5- 18. Kinetic parameters from non-linear regression for the AcoD of CS and SWW for the untreated biomass

First model		**Modified Gompertz**		**Chen & Hashimoto**		**Dual pooled first order**	
Parameter	Value	Parameter	Value	Parameter	Value	Parameter	Value
P	23679.2	*P*	20040.4	*P*	32236.04	*P*	2322.57
K	0.0838	K	0.3636	K_{CH}	1.417196	$K_f t$	0.04066
SSR	1504741	C	6.5034	μ_m	1.6117	$K_L t$	0.02923
R^2	0.9213	SSR	4092640	SSR	60965935	α	69.725
		λ	1.0	R^2	0.5874	SSR	130639
		R^2	0.9974			R^2	0.9405

The R^2 value of the dual-pooled model was not close to the first-order model as reported by (Xie *et al.* 2016b). The R^2 value of 0.997 for the modified Gompertz model was found greatest and thus, shows a good fit and correlation to experimental data to describe the biogas production. Figure 5-56 shows the closeness (fitness) of the modified Gompertz to the experimental data than the other three models tested. The modified Gompertz model in regard could be used to successfully describe the overall anaerobic co-digestion of CS with SWW. Results obtained, thus, indicated that the digestion could improve the reaction rate of the hydrolysis and that the R^2 value is a good tool to predict model fitting. The sum of squares errors (SSR) was used to evaluate the deviation according to study by Lee *et al.* (2017). The SSR was reported to be increased in the order of dual pooled (130639), first order (1504741), modified Gompertz (4092640) and the Chen and Hashimoto (60965935). In this run, the lag phase was also found to be unity for all the tested models. Also, the SSR was found not to be influenced by the R^2 value in this case with variations in the data obtained. The maximum biogas production rate, *P* was obtained from the Chen and

Hashimoto (32236.04 mL) with the modified Gompertz, being the least (20040.4). Following the Chen and Hashimoto was the first order and the dual pooled first order kinetic models with P values of 32236.04 mL and 2322.57 mL, respectively.

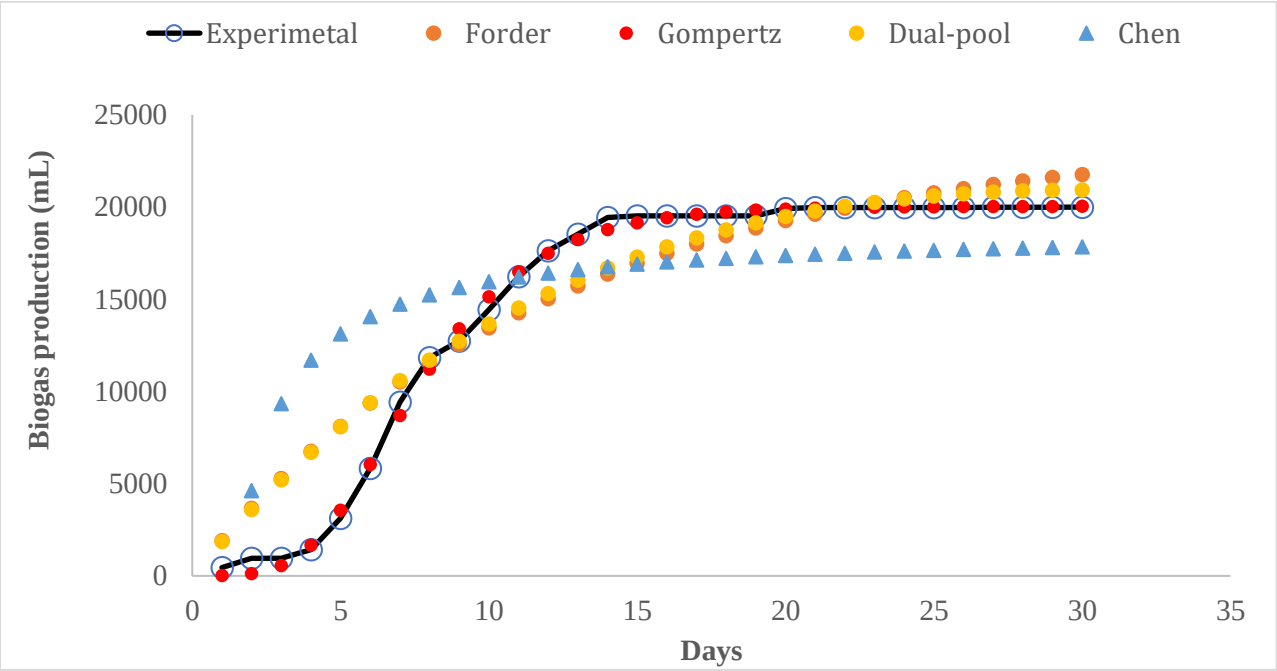

Figure 5- 56. Combined graphs of cumulative biogas yield versus digestion period (days).

A straight-line plot was developed for each model using the equation of a line: y = mx + c and a linear regression analysis was employed in the establishment of the 'best-fit' model. This was highlighted as a descriptive tool of the rate-limiting step for the biogas production. In this case, the modified Gompertz model was used for the establishment of the linear graph in relation to the experimental data. The plotting of biogas production (mL) versus days (d) yields a straight-line equation with a slope of 0.997 and a negative intercept of -196.68 as shown in Figure 5-57. The fitting equation between the cumulative biogas production and time is presented as y = 1.0103x – 196.68.

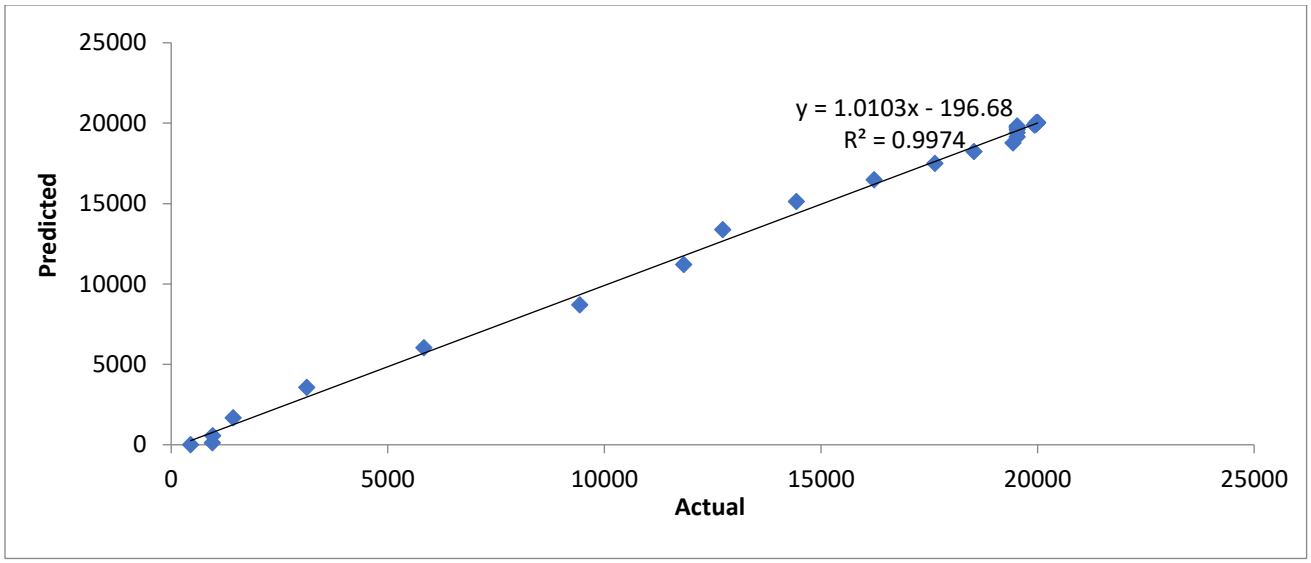

Figure 5- 57. Regression plots for the best fit model: modified Gompertz.

5.6.3 SCB and DWW for the untreated biomass

From Table 5-19, the R^2 values were presented as 0.946, 0.990, 0.769 and 0.9671 for the first order, modified Gompertz, Chen and Hashimoto and dual pooled kinetic models, respectively.

Table 5- 19. Kinetic parameters from non-linear regression for the AcoD of SCB and DWW for the untreated biomass

First model		**Modified Gompertz**		**Chen & Hashimoto**		**Dual pooled first order**	
Parameter	Value	Parameter	Value	Parameter	Value	Parameter	Value
P	841.9917	P	808.7961	P	645.4713	P	441.259
k	0.163545	K	0.39464	K_{CH}	0.735306	$K_f t$	0.1019
SSR	109260.2	C	3.93171	μ_m	0.45419	$K_L t$	0.03457
R^2	0.9461	SSR	14877.97	SSR	352657.3	A	3.66952
		λ	1.0	R^2	0.7698	SSR	76184.3
		R^2	0.9903			R^2	0.9671

The R^2 value of the Chen & Hashimoto model was oberved to be the least (0.7698) with weak regression which is similar to what reported in the AcoD of CS with DWW (0.5054) and the SCB with DWW. The R^2 (0.990) of the modified Gompertz model was found greatest and thus, shows a good fit and correlation to experimental data to describe the biogas production. The SSR was reported to be increased in the order of the modified Gompertz (14877.9), dual pooled first order (76184.3), the first order (109260.2) and the Chen and Hashimoto (352657.3). Although the R^2 value of the Chen and Hashimoto kinetic model was reported to be weaker in all the runs, this was contrary to what was reported in terms of the SSR value obtained. This gives an indication that, to some extent, the R^2 value is inversely proportional to the SSR value. Figure 5-58 shows the closeness (fitness) of the modified Gompertz to the experimental data than the other three models tested. A lag phase time of unity was reported in the AcoD of SCB with DWW. A shorter lag phase close to 0 has been reported in a study by Lebona *et al.* (2019) for the kinetic study of the AcoD of organic wastes. The maximum biogas production rate, *P* was obtained from the first order (841.9 mL) with the dual pooled first order (441.3 mL), being the least. Following the first order was the modified Gompertz and the Chen and Hashimoto with *P* values of 808.8 mL and 645.5 mL, respectively.

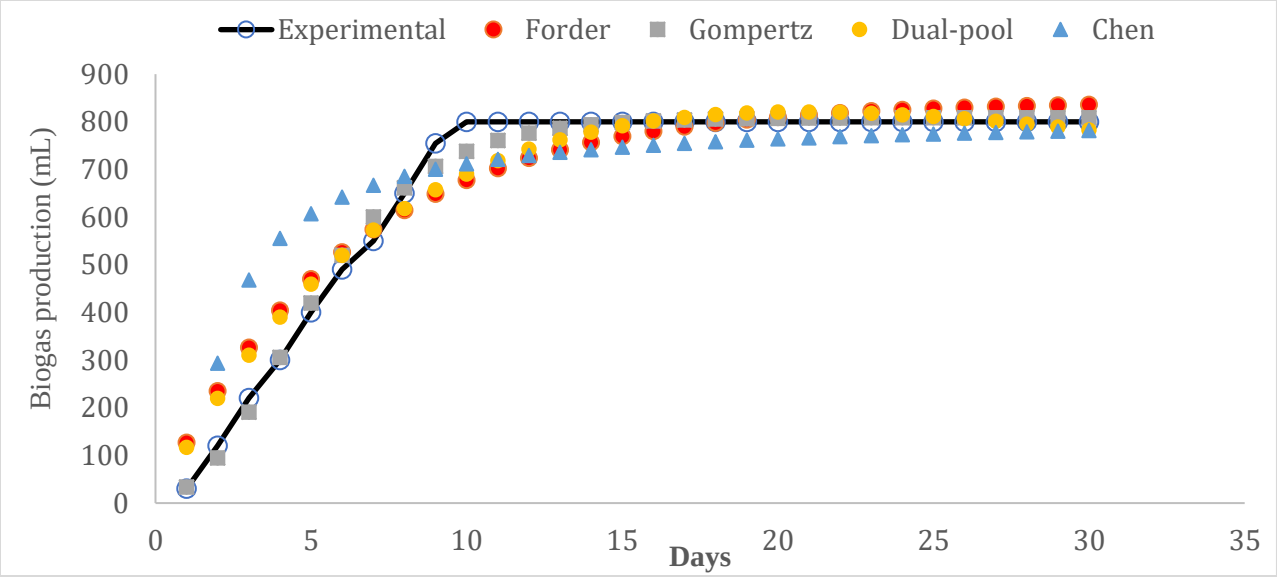

Figure 5- 58. Combined graphs of cumulative biogas yield versus digestion period (days).

The straight-line plot was developed for each model from the linear regression analysis for the establishment of the 'best-fit' model. Similar to earlier discussion, the modified Gompertz model was used for the establishment of the linear graph in relation to the experimental data. The plotting of biogas production (mL) versus days (d) yields a straight-line equation with a slope of 0.9981 and an intercept of 0.7261. The fitting equation between the cumulative biogas production and time is presented as $y = 0.9981x + 0.7261$.

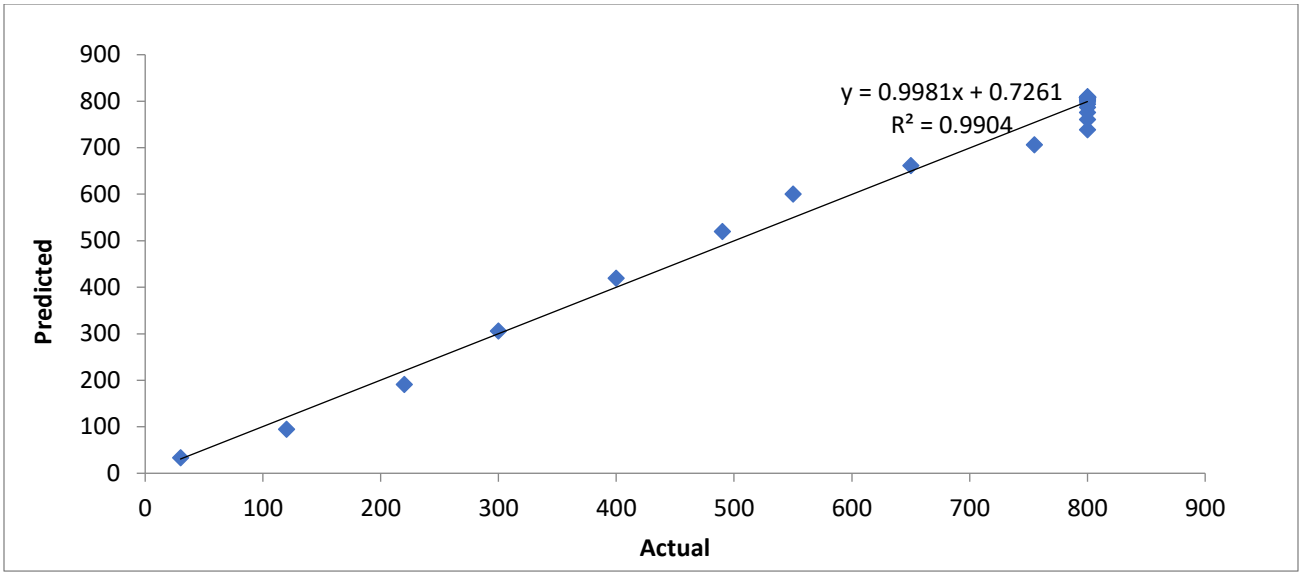

Figure 5- 59. Regression plots for the best fit model: modified Gompertz.

5.6.4 SCB and SWW for the untreated biomass

The R^2 values are presented as 0.922, 0.997, 0.588 and 0.938 for the first order, modified Gompertz, Chen and Hashimoto and dual pooled kinetic models, respectively.

Table 5- 20. Kinetic parameters from non-linear regression for the AcoD of SCB and SWW for the untreated biomass

First model		**Modified Gompertz**		**Chen & Hashimoto**		**Dual pooled first order**	
Parameter	**Value**	**Parameter**	**Value**	**Parameter**	**Value**	**Parameter**	**Value**
P	23551.4	*P*	19940.4	*P*	32080.2	*P*	4734.38
k	0.083952	K	0.3624	K_{CH}	1.41728	$K_f t$	0.04915
SSR	1.48E+08	C	6.49415	μ_m	1.6128	$K_L t$	0.02363
R^2	0.9217	SSR	4270057	SSR	6E+08	α	14.9017
		λ	1.0	R^2	0.5879	SSR	1.3E+08
		R^2	0.9973			R^2	0.9378

The R^2 value of the Chen & Hashimoto model was oberved to be the least (0.588) with weak regression which is similar to what reported in the AcoD of CS with DWW (0.5054) and SCB with DWW (0.7698). It was observed that the R^2 value of the dual-pooled first order (0.938) model was close to that of the first-order model (0.922) since the dual-pooled is presented as a derivation from first order with fractional consideration of two different substrates. It was reported that the R^2 (0.997) of the modified Gompertz model was found greatest and thus, shows a good fit and correlation to experimental data to describe the biogas production process. Figure 5-60 shows the closeness (fitness) of the modified Gompertz to the experimental data than the other three models tested. The modified Gompertz model in regard could be used to successfully describe the overall anaerobic co-digestion of SCB with SWW. Maximum SSR (6E + 08) and the *P* (32080) value was observed by the Chen and Hashimoto kinetic model which also corresponded to what have been reported earlier as shown to be influenced by a lower R^2 value of the substrate with maximum SSR value.

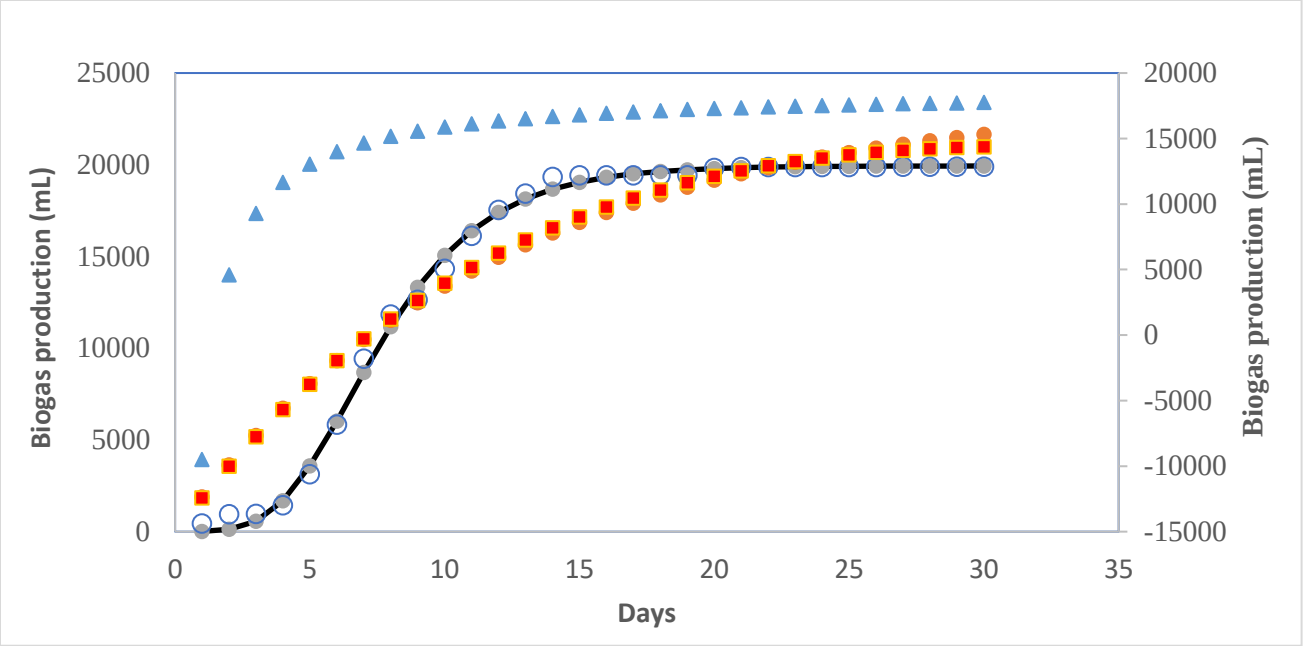

Figure 5- 60. Combined graphs of cumulative biogas yield versus digestion period (days).

The straight-line plot was developed for each model from the linear regression analysis for the establishment of the 'best-fit' model. The modified Gompertz model was used for the establishment of the linear graph in relation to the experimental data (Figure 5-61). The plotting of biogas production (mL) versus days (d) yields a straight-line equation with a slope of 1.0099 and a negative intercept of -189.23. The fitting equation between the cumulative biogas production and time is presented as y = 1.0099x – 189.23.

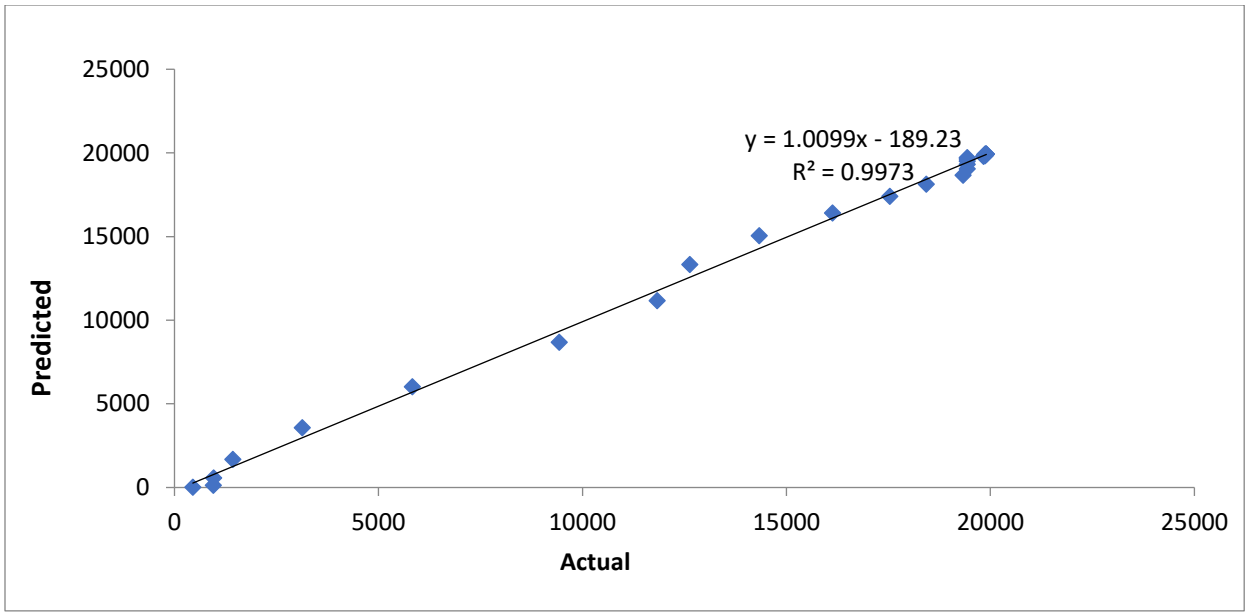

Figure 5- 61. Regression plots for the best fit model: modified Gompertz.

5.6.5 CS with DWW after pretreatment

To ascertain the best model fit after the BMP test with the pretreated biomass, it was observed that the input variables that gave the best fit were the P, k, SSR, R^2, c, λ, K_{CH}, $K_f t$, $K_L t$, μ_m and α values as presented in Table 5-21.

Table 5- 21. Kinetic parameters from non-linear regression for the AcoD of CS and DWW for the pretreated biomass

First order model		**Modified Gompertz**		**Chen & Hashimoto**		**Dual pooled first order**	
Parameter	Value	Parameter	Value	Parameter	Value	Parameter	Value
P	331.684	*P*	306.79	*P*	256.299	*P*	15.657
K	0.122	K	0.2993	K_{CH}	0.826	$K_f t$	0.0472
SSR	10890.27	C	4.4446	μ_m	0.509	$K_L t$	0.0381
R^2	0.968	SSR	5258.9	SSR	61401.7	α	246.694
		λ	1.0	R^2	0.752	SSR	8365.411
		R^2	0.979			R^2	0.975

The optimised substrate mixture (CS with DWW) after pretreated was selected to predict the best fit kinetic model. The R^2 values are presented as 0.968, 0.979, 0.752 and 0.975 for the first order, modified Gompertz, Chen and Hashimoto and dual pooled kinetic models, respectively. The R^2 value for the Chen & Hashimoto model was oberved to be the least (0.7521), similar to that reported for the untreated feedstocks which was found to be inappropriate (weaker regression). This slight difference could be attributed to the fact that the dual-pooled was predicted as a derivative from the first order with fractional reflection of two different substrates Xie *et al.* (2016a). The R^2 value for the modified Gompertz, 0.979 was found greatest and thus, shows a good fit and correlation to experimental data to describe the biogas production (Figure 5-62). To this effect, it could be concluded that the modified Gompertz model could be used to successfully define the overall anaerobic co-digestion of CS with DWW.

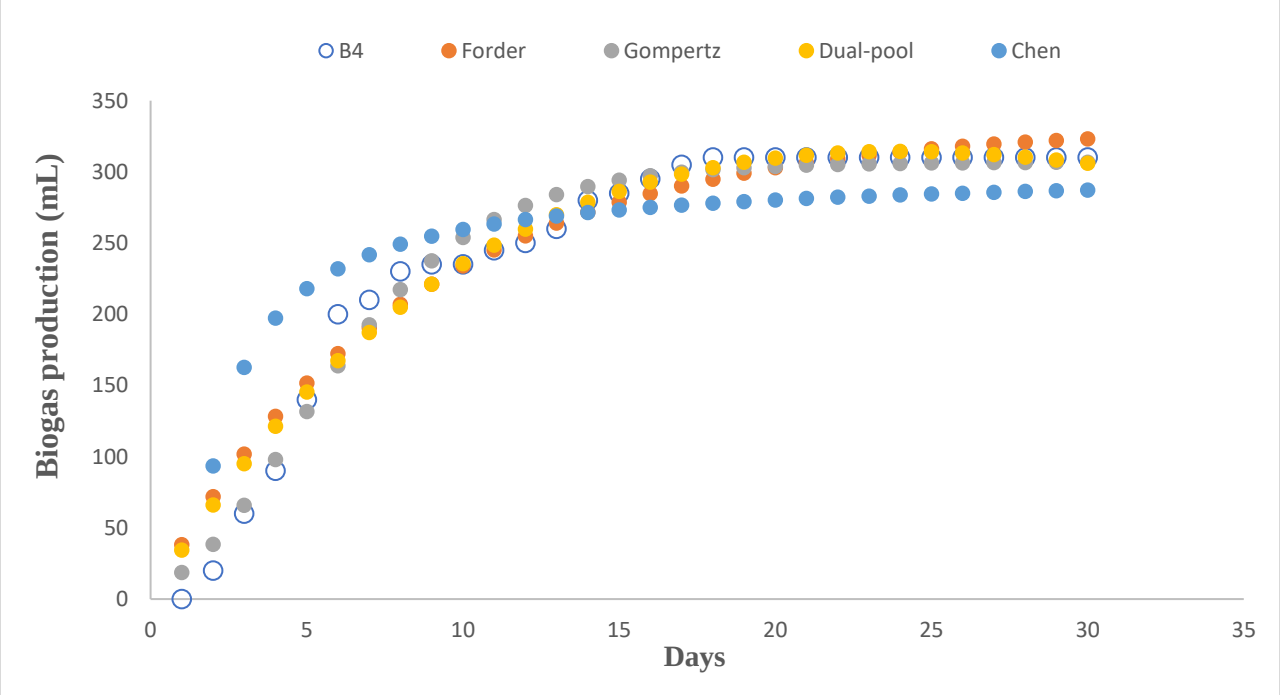

Figure 5- 62. Combined graphs of cumulative biogas yield versus digestion period (days).

Summary of objective four

In conclusion, the use of kinetic models can be used as pre-evaluation for the AcoD of a given substrate. The R^2 values of the modified Gompertz model for each of the substrate mixtures of the untreated as: 0.997 for CS with SWW, 0.997 for SCB with SWW, 0.992 for CS with DWW and 0.990 for SCB with DWW. The R^2 values for the pretreated was found to be 0.979. The R^2 for Chen and Hashimoto was observed to be the lowest with all substrates considered which could be due to its extensive applications in completely mixed continuous biodigesters rather than in batch mode. However, the modified Gompertz kinetic model was found the best fit amongst all the models tested for both the untreated and pretreated biomasses. The kinetic model outputs for each substrate mixtures of the biomasses with the WW streams are presented in Appendix D.

CHAPTER 6

CONCLUSIONS AND RECOMMENDATIONS

This chapter gives the significant findings achieved from this present study and points out various recommendations for further studies. The optimisation of the AcoD process parameters with the SCB or CS after characterisation was carried out using the OFAT method during the preliminary stage and the RSM approach. Further, ionic liquid pretreatment of the biomasses was carried out to ascertain their bioavailability for microbial degradation. Finally, data obtained from the optimisation study using the BMP for both untreated and pretreated biomasses were tested with kinetic models to predict the best fit based on the value of the R^2.

6.1 Conclusions

The findings below were drawn from this study based on the results obtained:

- Higher VS content (78% for SCB and 96% for CS) of the biomass was observed to influence the biogas potential which was evidenced by the thermal stability plots.
- Maximum biogas yield and CH_4 content for the untreated biomass were found to be 5.0 m^3/kgVS and 79% respectively for the AcoD of CS with SWW at an OLR of 0.5 gVS/100mL and temperature of 25°C.
- Biogas production after IL pretreatment showed that the maximum biogas yield and CH_4 contents were found to be 3.9 m^3/kgVS and 87% respectively at a temperature of 55°C and an OLR of 1.0gVS/100mL using 1-ethyl-3-methylimidazolium acetate. The IL pretreatment yielded lower biogas but of higher purity of CH_4 than the untreated biomass.

- Results of the study indicated that the modified Gompertz model (with maximum correlation coefficient, R^2 value of 0.9974 for CS with SWW) could be the preferred model for the study of AcoD for biogas production.
- Also, the maximum annual biogas production was found to be 32×10^6 m^3/yr (53.35 GWh of electrical energy) for the untreated biomass.
- Finally, the results of this study could assist decision-makers and the government to further implement the installation of biogas plants as an alternative source of energy in South Africa.

Therefore, employing anaerobic co-digestion to produce biogas from CS and SCB were found suitable and economically viable, serving as the alternative means of renewable energy source.

6.2 Recommendations

The following recommendations are proposed for future studies:

- This study focused on batch operation and produced suitable biogas yield; however, a pilot plant is recommended for large scale and continuous operation of AcoD with these selected feedstocks.
- Further analysis of the digestate contents from biodigesters after the AD process should be examined for its quality in terms of macro and micronutrients availability for agricultural purposes.
- Further process optimisation under AcoD operating conditions using CS or SCB with other WW streams as co-substrates which are readily available are warranted to predict the biogas yield.

- Varying different ionic liquids to determine their potential as lignocellulosic pretreatment chemicals for biogas production via anaerobic co-digestion.
- Further studies should focus on determining the different strains of microbes that are available for anaerobic co-digestion.

REFERENCES

Abbasi, T., Tauseef, S. and Abbasi, S. 2012. Anaerobic digestion for global warming control and energy generation—an overview. *Renewable and Sustainable Energy Reviews*, 16 (5): 3228-3242.

Achinas, S. and Euverink, G. J. W. 2016. Theoretical analysis of biogas potential prediction from agricultural waste. *Resource-Efficient Technologies*, 2 (3): 143-147.

Aditiya, H., Mahlia, T., Chong, W., Nur, H. and Sebayang, A. 2016. Second generation bioethanol production: A critical review. *Renewable and Sustainable Energy Reviews*, 66: 631-653.

Adl, M., Sheng, K. and Gharibi, A. 2012. Technical assessment of bioenergy recovery from cotton stalks through anaerobic digestion process and the effects of inexpensive pre-treatments. *Applied Energy*, 93: 251-260.

Aguiar, M. M., Ferreira, L. F. R. and Monteiro, R. T. R. 2010. Use of vinasse and sugarcane bagasse for the production of enzymes by lignocellulolytic fungi. *Brazilian archives of Biology and Technology*, 53 (5): 1245-1254.

Akhtar, J., Idris, A. and Lai, L. W. 2014. *Pretreatment of lignocellulosic biomass for organic acid production*. Penerbit UTM Press.Malaysia (Last accessed: 20/08/2018)

Al-Dahhan, M. H., Larachi, F., Dudukovic, M. P. and Laurent, A. 1997. High-pressure trickle-bed reactors: a review. *Industrial & Engineering Chemistry Research*, 36 (8): 3292-3314.

Alvira, P., Tomás-Pejó, E., Ballesteros, M. and Negro, M. 2010. Pretreatment technologies for an efficient bioethanol production process based on enzymatic hydrolysis: a review. *Bioresource Technology*, 101 (13): 4851-4861.

Amon, T., Amon, B., Kryvoruchko, V., Zollitsch, Mayer, K. and Gruber, L. 2007a. Biogas Production from maize and daily cattle manure-influence of biomass composition on the methane yield. *Agriculture Ecosystems and Environment*, 118: 173-182.

Amon, T., Amon, B., Kryvoruchko, V., Zollitsch, W., Mayer, K. and Gruber, L. 2007b. Biogas production from maize and dairy cattle manure—influence of biomass composition on the methane yield. *Agriculture, Ecosystems & Environment*, 118 (1-4): 173-182.

Anderson, E. M., Stone, M. L., Hülsey, M. J., Beckham, G. T. and Román-Leshkov, Y. 2018. Kinetic studies of lignin solvolysis and reduction by reductive catalytic fractionation decoupled in flow-through reactors. *ACS Sustainable Chemistry & Engineering*, 6 (6): 7951-7959.

Angelidaki, I. and Ahring, B. 1993. Thermophilic anaerobic digestion of livestock waste: the effect of ammonia. *Applied Microbiology and Biotechnology*, 38 (4): 560-564.

Angelidaki, I., Alves, M., Bolzonella, D., Borzacconi, L., Campos, J., Guwy, A., Kalyuzhnyi, S., Jenicek, P. and Van Lier, J. 2009. Defining the biomethane potential (BMP) of solid organic wastes and energy crops: a proposed protocol for batch assays. *Water Science and Technology*, 59 (5): 927-934.

APHA. 1998. *Standard Methods for the Examination of Water and Wastewater*. 20th Ed. American Public Health Association, American Water Works Association, Water Environment Federation, Washington D.C, United States of America. (Last accessed: 10/09/2018)

Appels, L., Baeyens, J., Degrève, J. and Dewil, R. 2008. Principles and potential of the anaerobic digestion of waste-activated sludge. *Progress in Energy and Combustion Science*, 34 (6): 755-781.

Arooj, M. F., Han, S.-K., Kim, S.-H., Kim, D.-H. and Shin, H.-S. 2008. Continuous biohydrogen production in a CSTR using starch as a substrate. *International Journal of Hydrogen Energy*, 33 (13): 3289-3294.

Babaee, A. and Shayegan, J. 2011. Effect of organic loading rates (OLR) on production of methane from anaerobic digestion of vegetables waste. In: Proceedings of *World Renewable Energy Congress*. Linköping University Electronic Press,Linköping, Sweden. Pp. 411-417.

Bahrani, S., Raeissi, S. and Sarshar, M. 2015. Experimental investigation of ionic liquid pretreatment of sugarcane bagasse with 1, 3-dimethylimadazolium dimethyl phosphate. *Bioresource Technology*, 185: 411-415.

Batstone, D. J., Keller, J., Angelidaki, I., Kalyuzhnyi, S., Pavlostathis, S., Rozzi, A., Sanders, W., Siegrist, H. and Vavilin, V. 2002. The IWA anaerobic digestion model no 1 (ADM1). *Water Science and Technology*, 45 (10): 65-73.

Behera, S., Arora, R., Nandhagopal, N. and Kumar, S. 2014. Importance of chemical pretreatment for bioconversion of lignocellulosic biomass. *Renewable and Sustainable Energy Reviews*, 36: 91-106.

Bezerra, T. L. and Ragauskas, A. J. 2016. A review of sugarcane bagasse for second-generation bioethanol and biopower production. *Biofuels, Bioproducts and Biorefining*, 10 (5): 634-647.

Biarnes, M. 2017. *Biomass to Biogas-Anaerobic Digestion*.(Last accessed: 09/08/2017).

Borowski, S., Domański, J. and Weatherley, L. 2014. Anaerobic co-digestion of swine and poultry manure with municipal sewage sludge. *Waste Management*, 34 (2): 513-521.

Bouallagui, H., Lahdheb, H., Romdan, E. B., Rachdi, B. and Hamdi, M. 2009. Improvement of fruit and vegetable waste anaerobic digestion performance and stability with co-substrates addition. *Journal of Environmental Management*, 90 (5): 1844-1849.

Bouallagui, H., Torrijos, M., Godon, J., Moletta, R., Cheikh, R. B., Touhami, Y., Delgenes, J. and Hamdi, M. 2004. Microbial monitoring by molecular tools of a two-phase anaerobic bioreactor treating fruit and vegetable wastes. *Biotechnology Letters*, 26 (10): 857-862.

Boubaker, F. and Ridha, B. C. 2008. Modelling of the mesophilic anaerobic co-digestion of olive mill wastewater with olive mill solid waste using anaerobic digestion model No. 1 (ADM1). *Bioresource Technology*, 99 (14): 6565-6577.

Brandon, S. K., Eiteman, M. A., Patel, K., Richbourg, M. M., Miller, D. J., Anderson, W. F. and Doran Peterson, J. 2008. Hydrolysis of Tifton 85 bermudagrass in a pressurized batch hot water reactor. *Journal of Chemical Technology and Biotechnology*, 83 (4): 505-512.

Browne, J. D. and Murphy, J. D. 2013. Assessment of the resource associated with biomethane from food waste. *Applied Energy*, 104: 170-177.

Cahyari, K., Syamsiah, S. and Prasetya, A. 2016. Performance of continuous stirred tank reactor (CSTR) on fermentative biohydrogen production from melon waste. In: Proceedings of *IOP Conference Series: Materials Science and Engineering*. IOP Publishing, 012013.

Callaghan, F., Wase, D., Thayanithy, K. and Forster, C. 2002a. Continuous co-digestion of cattle slurry with fruit and vegetable wastes and chicken manure. *Biomass and Bioenergy*, 1 (22): 71-77.

Callaghan, F., Wase, D., Thayanithy, K. and Forster, C. 2002b. Continuous co-digestion of cattle slurry with fruit and vegetable wastes and chicken manure. *Biomass and Bioenergy*, 22 (1): 71-77.

Campuzano, R. and González-Martínez, S. 2016. Characteristics of the organic fraction of municipal solid waste and methane production: A review. *Waste Management*, 54: 3-12.

Canilha, L., Chandel, A. K., Suzane dos Santos Milessi, T., Antunes, F. A. F., Luiz da Costa Freitas, W., das Graças Almeida Felipe, M. and da Silva, S. S. 2012. Bioconversion of sugarcane biomass into ethanol: an overview about composition, pretreatment methods, detoxification of hydrolysates, enzymatic saccharification, and ethanol fermentation. *BioMed Research International*, 2(5):1-11.

Chamane, Z. 2008. The effect of biomass acclimation on the co-digestion of toxic organic effluents in anaerobic digesters. Durban University of Technology, Durban, South Africa. Master of Technology in Engineering thesis.

Chandel, A. K., da Silva, S. S., Carvalho, W. and Singh, O. V. 2012. Sugarcane bagasse and leaves: foreseeable biomass of biofuel and bio-products. *Journal of Chemical Technology & Biotechnology*, 87 (1): 11-20.

Chandra, R., Takeuchi, H. and Hasegawa, T. 2012. Hydrothermal pretreatment of rice straw biomass: a potential and promising method for enhanced methane production. *Applied Energy*, 94: 129-140.

Chang, V. S., Kaar, W. E., Burr, B. and Holtzapple, M. T. 2001. Simultaneous saccharification and fermentation of lime-treated biomass. *Biotechnology Letters*, 23 (16): 1327-1333.

Chen, W.-H., Ye, S.-C. and Sheen, H.-K. 2012. Hydrolysis characteristics of sugarcane bagasse pretreated by dilute acid solution in a microwave irradiation environment. *Applied Energy*, 93: 237-244.

Chen, Y., Cheng, J. J. and Creamer, K. S. 2008. Inhibition of anaerobic digestion process: a review. *Bioresource Technology*, 99 (10): 4044-4064.

Cheng, J., Ding, L., Lin, R., Liu, M., Zhou, J. and Cen, K. 2016. Physicochemical characterization of typical municipal solid wastes for fermentative hydrogen and methane co-production. *Energy Conversion and Management*, 117: 297-304.

Chynoweth, D. P., Owens, J. M. and Legrand, R. 2001. Renewable methane from anaerobic digestion of biomass. *Renewable Energy*, 22 (1): 1-8.

Corro, G., Paniagua, L., Pal, U., Bañuelos, F. and Rosas, M. 2013. Generation of biogas from coffee-pulp and cow-dung co-digestion: Infrared studies of postcombustion emissions. *Energy Conversion and Management*, 74: 471-481.

Crawford, R. L. 1981. *Lignin biodegradation and transformation*. New York: John Wiley and Sons, New York, United States of America. (Last accessed: 10/03/2019)

da Costa Lopes, A. M., João, K. G., Morais, A. R. C., Bogel-Łukasik, E. and Bogel-Łukasik, R. 2013. Ionic liquids as a tool for lignocellulosic biomass fractionation. *Sustainable Chemical Processes*, 1 (1): 3.

Da Ros, C., Cavinato, C., Pavan, P. and Bolzonella, D. 2017. Mesophilic and thermophilic anaerobic co-digestion of winery wastewater sludge and wine lees: An integrated approach for sustainable wine production. *Journal of Environmental Management*, 203: 745-752.

da Silva, A. S. A., Lee, S.-H., Endo, T. and Bon, E. P. 2011. Major improvement in the rate and yield of enzymatic saccharification of sugarcane bagasse via pretreatment with the ionic liquid 1-ethyl-3-methylimidazolium acetate ([Emim][Ac]). *Bioresource Technology*, 102 (22): 10505-10509.

Daassi-Gnaba, H., Oussar, Y., Merlan, M., Ditchi, T., Géron, E. and Holé, S. 2017. Wood moisture content prediction using feature selection techniques and a kernel method. *Neurocomputing*, 237: 79-91.

Dar, H. G. and Tandon, S. M. 1987. Biogas Production from pretreated wheat straw, lantana residue, apple and peach leaf litter with cattle dung. *Biological Wastes*, 21: 75-83.

Dareioti, M. A. and Kornaros, M. 2014. Effect of hydraulic retention time (HRT) on the anaerobic co-digestion of agro-industrial wastes in a two-stage CSTR system. *Bioresource Technology*, 167: 407-415.

De Llyod, D. 1998. Gas Chromatography. The University of the West Indies. (Last accessed:01/09/2017).

Deepanraj, B., Sivasubramanian, V. and Jayaraj, S. 2014a. Biogas Generation through Anaerobic Digestion Process-An Overview. *Research Journal of Chemistry and Environment*, 18 (5): 80-93.

Deepanraj, B., Sivasubramanian, V. and Jayaraj, S. 2014b. Biogas Generation through Anaerobic Digestion Process-An Overview. *Research Journal of Chemistry and Environment*, 18 (5): 1-14.

Delfino, J. R., Pereira, T. C., Viegas, H. D. C., Marques, E. P., Ferreira, A. A. P., Zhang, L., Zhang, J. and Marques, A. L. B. 2018. A simple and fast method to determine water content in biodiesel by electrochemical impedance spectroscopy. *Talanta*, 179: 753-759.

Demirel, B. and Scherer, P. 2008. Production of methane from sugar beet silage without manure addition by a single-stage anaerobic digestion process. *Biomass and Bioenergy*, 32 (3): 203-209.

Dennehy, C., Lawlor, P. G., Gardiner, G. E., Jiang, Y., Cormican, P., McCabe, M. S. and Zhan, X. 2017. Process stability and microbial community composition in pig manure and food waste anaerobic co-digesters operated at low HRTs. *Frontiers of Environmental Science & Engineering*, 11 (3): 4.

Department of Agriculture. 2017. *South Africa's largest maize crop in history*. Available: brandsouthafrica.com/investments-immigration/south-africas-largest-maize-crop-history (Last accessed: 02/11/2019).

Department of Energy. 2015. *State of Renewable Energy in South Africa*. South Africa: Department of Energy.documents/state-renewable-energy-south-africa-5-oct-2015-0000?gclid=Cj0KCQiAyoeCBhCTARIsAOfpKxikQrifNcIt-ybbV7VUQJPx2MYU_xPbNhP97GTU9GKDLeFbPggVSb4aAitMEALw_wcB#. (Last accessed: 30/03/2019).

Derbal, K., Bencheikh-Lehocine, M., Cecchi, F., Meniai, A.-H. and Pavan, P. 2009. Application of the IWA ADM1 model to simulate anaerobic co-digestion of organic waste with waste activated sludge in mesophilic condition. *Bioresource Technology*, 100 (4): 1539-1543.

Deressa, L., Libsu, S., Chavan, R., Manaye, D. and Dabassa, A. 2015. Production of biogas from fruit and vegetable wastes mixed with different wastes. *Environment and Ecology Research*, 3 (3): 65-71.

Dhouib, A., Ellouz, M., Aloui, F. and Sayadi, S. 2006. Effect of bioaugmentation of activated sludge with white-rot fungi on olive mill wastewater detoxification. *Letters in Applied Microbiology*, 42 (4): 405-411.

Dieter, K., Brigitte, H., Hans-Peter, F. and Andreas, B. 2005. Angewandte Chemie International Edition. *Cellulose: Fascinating Biopolymer and Sustainable Raw Material*, 44 (22): 3358-5593.

Dragan, J. M., Zubov, A. and Sin, G. 2017. Methodology for Plantwide Design and Optimization of Wastewater Treatment Plants. In: *Computer Aided Chemical Engineering*. Pp. 859-864.

Dutta, A., Davies, C. and Ikumi, D. S. 2018. Performance of upflow anaerobic sludge blanket (UASB) reactor and other anaerobic reactor configurations for wastewater treatment: a comparative review and critical updates. *Journal of Water Supply: Research and Technology-Aqua*, 67 (8): 858-884.

Eiceman, G. A. 1995. *Instrumentation of Gas Chromatography* John Wiley & Sons Limited, Chichester, Hoboken, New Jersey, United States of America (Last accessed: 01/09/2017).

Ejekwu, O. 2019. Development of a Non-Derivatizing Solvent System for the Pretreatment of South African Corn Cob. University of the Witwatersrand, Johannesburg, South Africa. Master of Science thesis.

El-Sayed Zaher, U. 2005. Modelling and monitoring the anaerobic digestion process in view of optimisation and smooth operation of WWTP's. Ghent University, Belgium. Doctoral thesis.

Elbeshbishy, E., Nakhla, G. and Hafez, H. 2012. Biochemical methane potential (BMP) of food waste and primary sludge: influence of inoculum pre-incubation and inoculum source. *Bioresource Technology*, 110: 18-25.

Eliyan, C. 2007. Anaerobic digestion of municipal solid waste in thermophilic continuous operation. Asian School of Technology, Odisha, India. Master of Science thesis.

Enitan, A. M. 2015. Microbial community analysis of a UASB reactor and application of an evolutionary algorithm to enhance wastewater treatment and biogas production. Durban University of Technology, Durban, South Africa. Doctoral thesis.

Esposito, G., Frunzo, L., Giordano, A., Liotta, F., Panico, A. and Pirozzi, F. 2012. Anaerobic co-digestion of organic wastes. *Reviews in Environmental Science and Bio/Technology*, 11 (4): 325-341.

Estes, L., Bradley, B., Beukes, H., Hole, D., Lau, M., Oppenheimer, M., Schulze, R., Tadross, M. and Turner, W. 2013. Comparing mechanistic and empirical model projections of crop suitability and productivity: implications for ecological forecasting. *Global Ecology and Biogeography*, 22 (8): 1007-1018.

European Commission. 2011. *Renewable Energy-Targets by 2020, European Commission.*Available: ec.europa.eu/energy/en/topics/renewable-energy. (Last accessed: 20/09/2017).

Fagerström, A., Al Seadi, T., Rasi, S. and Briseid, T. 2018. The role of Anaerobic Digestion and Biogas in the Circular Economy. *IEA Bioenergy Task 37*, Paris, France.

Fan, S., Zhang, P., Li, F., Jin, S., Wang, S. and Zhou, S. 2016. A Review of Lignocellulose Change During Hydrothermal Pretreatment for Bioenergy Production. *Current Organic Chemistry*, 20: 1-11.

Favaro, L., Basaglia, M., Trento, A., Van Rensburg, E., García-Aparicio, M., Van Zyl, W. H. and Casella, S. 2013. Exploring grape marc as trove for new thermotolerant and inhibitor-tolerant Saccharomyces cerevisiae strains for second-generation bioethanol production. *Biotechnology for Biofuels*, 6 (1): 168.

Fernández-Cegrí, V., De la Rubia, M. Á., Raposo, F. and Borja, R. 2012. Effect of hydrothermal pretreatment of sunflower oil cake on biomethane potential focusing on fibre composition. *Bioresource Technology*, 123: 424-429.

Flörke, M. 2013. *Primary vs. Secondary: Types of Wastewater Treatment.* Yale University, Yale, United States of America. (Last assessed: 02/06/2018).

Foston, M. and Ragauskas, A. J. 2012. Biomass characterization: recent progress in understanding biomass recalcitrance. *Industrial Biotechnology*, 8 (4): 191-208.

Fu, D. and Mazza, G. 2011. Aqueous ionic liquid pretreatment of straw. *Bioresource Technology*, 102 (13): 7008-7011.

Gao, J., Chen, L., Yan, Z. and Wang, L. 2013. Effect of ionic liquid pretreatment on the composition, structure and biogas production of water hyacinth *(Eichhornia crassipes). Bioresource Technology*, 132: 361-364.

Geng, X. and Henderson, W. 2012. Pretreatment of corn stover by combining ionic liquid dissolution with alkali extraction. *Biotechnology and Bioengineering*, 109 (1): 84-91.

Gerardi, M. H. 2003. *The Microbiology of Anaerobic Digesters*. John Wiley & Sons. Hoboken, New Jersey, United States of America (Last accessed: 01/09/2017).

Ghasimi, D. S., Tao, Y., Kreuk, M., Zandvoort, M. H. and Lier, J. B. 2015. Microbial population dynamics during long-term sludge adaptation of thermophilic and mesophilic sequencing batch

digesters treating sewage fine sieved fraction at varying organic loading rates. *Biotechnology for Biofuels*, 8 (1): 171.

Gibson, L. J. 2013. The hierarchical structure and mechanics of plant materials. *Journal of the Royal Society Interface*, 9 (76): 2749-2766.

Gnanambal, V. S. and Swaminathan, K. 2015. Biogas production from renewable lignocellulosic biomass. *International Journal of Environment*, 4 (2): 341-347.

Golding, C. G., Lamboo, L. L., Beniac, D. R. and Booth, T. F. 2016. The scanning electron microscope in microbiology and diagnosis of infectious disease. *Scientific Reports*, 6: 26516.

Gomez, X., Cuetos, M., Cara, J., Morán, A. and Garcia, A. 2006. Anaerobic co-digestion of primary sludge and the fruit and vegetable fraction of the municipal solid wastes: conditions for mixing and evaluation of the organic loading rate. *Renewable Energy*, 31 (12): 2017-2024.

Gonzalez-Martinez, A., Sihvonen, M., Muñoz-Palazon, B., Rodriguez-Sanchez, A., Mikola, A. and Vahala, R. 2018. Microbial ecology of full-scale wastewater treatment systems in the Polar Arctic Circle: Archaea, Bacteria and Fungi. *Scientific Reports*, 8 (1): 2208.

Gu, Y., Chen, X., Liu, Z., Zhou, X. and Zhang, Y. 2014. Effect of inoculum sources on the anaerobic digestion of rice straw. *Bioresource Technology*, 158: 149-155.

Gueh, C. G. 2018. Comparison of lignin yield from sugarcane bagasse pellets using liquid hot water and ionic liquids pretreatment methods. Durban University of Technology, Durban, South Africa. Master of Applied Sciences thesis.

H.Hartmann and T.Böhm. 2016. Rapid moisture content determination of woodchips – results from comparative trials. In: Proceedings of *in Proceedings of the 1st World Conference on Biomass for Energy and Industry*,James & James Limited, Northampton, (Last accessed: 20/03/2019)

Haider, M. R., Yousaf, S., Malik, R. N. and Visvanathan, C. 2015. Effect of mixing ratio of food waste and rice husk co-digestion and substrate to inoculum ratio on biogas production. *Bioresource Technology*, 190: 451-457.

Hallenbeck, P. C. 2011. *Microbial Technologies in Advanced Biofuels Production*.Springer Science, New York, U.S.A. (Last accessed: 20/05/2019)

Hamelinck, C. N., Van Hooijdonk, G. and Faaij, A. P. 2005. Ethanol from lignocellulosic biomass: techno-economic performance in short-, middle-and long-term. *Biomass and Bioenergy*, 28 (4): 384-410.

Hamilton, D. W. 2009. *Anaerobic Digestion of Animal Manures: Understanding the Basic Processes*. Division of Agricultural Sciences and Natural Resources, Oklahoma State University, Oklahoma, United States of America. Master of Science thesis.

Hendriks, A. and Zeeman, G. 2009a. Pretreatments to enhance the digestibility of lignocellulosic biomass. *Bioresource Technology*, 100 (1): 10-18.

Hendriks, A. T. W. M. and Zeeman, G. 2009b. Pretreatments to enhance the digestibility of lignocellulosic biomass. *Bioresource Technololgy*, 100: 10-18.

Hilaire, F., Basset, E., Bayard, R., Gallardo, M., Thiebaut, D. and Vial, J. 2017. Comprehensive two-dimensional gas chromatography for biogas and biomethane analysis. *Journal of Chromatography A*, 1524: 222-232.

Hong, E., Kim, J., Rhie, S., Ha, S.-J., Kim, J. and Ryu, Y. 2016. Optimization of dilute sulfuric acid pretreatment of corn stover for enhanced xylose recovery and xylitol production. *Biotechnology and Bioprocess Engineering*, 21 (5): 612-619.

Hoyer, K., Galbe, M. and Zacchi, G. 2010. Effects of enzyme feeding strategy on ethanol yield in fed-batch simultaneous saccharification and fermentation of spruce at high dry matter. *Biotechnology for Biofuels*, 3 (1): 14.

Hu, F. and Ragauskas, A. 2012. Pretreatment and lignocellulosic chemistry. *Bioenergy Research*, 5 (4): 1043-1066.

Hu, W., Thayanithy, K. and Forster, C. 2002. A kinetic study of the anaerobic digestion of ice-cream wastewater. *Process Biochemistry*, 37 (9): 965-971.

Hutňan, M. 2016. Maize Silage as Substrate for Biogas Production, Advances in Silage Production and Utilization, Thiago da Silva and Edson Mauro Santos, IntechOpen, DOI: 10.5772/64378. Available from: https://www.intechopen.com/books/advances-in-silage-production-and-utilization/maize-silage-as-substrate-for-biogas-production.

Ibbett, R., Gaddipati, S., Hill, S. and Tucker, G. 2013. Structural reorganisation of cellulose fibrils in hydrothermally deconstructed lignocellulosic biomass and relationships with enzyme digestibility. *Biotechnology for Biofuels,* 6 (1): 33.

Ibrahim, M. H., Quaik, S. and Ismail, S. A. 2016. An Introduction to Anaerobic Digestion of Organic Wastes. In: *Prospects of Organic Waste Management and the Significance of Earthworms*, 2(5): 23-44.

James, C. 2015. Balestie & Balestie Ingenieros - Online Primer Website Series. New York, United States of America.(Last accessed: 15/05/2018)

Janke, L., Leite, A., Nikolausz, M., Schmidt, T., Liebetrau, J., Nelles, M. and Stinner, W. 2015. Biogas Production from Sugarcane Waste: Assessment on Kinetic Challenges for Process Designing. *International Journal of Molecular Sciences*, 16: 20685-20703.

Jarvis, Å., Nordberg, Å., Jarlsvik, T., Mathisen, B. and Svensson, B. 1997. Improvement of a grass-clover silage-fed biogas process by the addition of cobalt. *Biomass and Bioenergy*, 12 (6): 453-460.

Jayaweera, M. W., Dilhani, J. A., Kularatne, R. K. and Wijeyekoon, S. L. 2007. Biogas production from water hyacinth *(Eichhornia crassipes* (Mart.) Solms) grown under different nitrogen concentrations. *Journal of Environmental Science and Health Part A*, 42 (7): 925-932.

Jönsson, L. J. and Martín, C. 2016. Pretreatment of lignocellulose: formation of inhibitory by-products and strategies for minimizing their effects. *Bioresource Technology*, 199: 103-112.

Kainthola, J., Kalamdhada, A. S. and Goud, V. V. 2019. Optimization of methane production during anaerobic co-digestion of rice straw and hydrilla verticillata using response surface methodology. *Fuel*, 235: 92-99.

Kaparaju, P., Buendia, I., Ellegaard, L. and Angelidakia, I. 2008. Effects of mixing on methane production during thermophilic anaerobic digestion of manure: lab-scale and pilot-scale studies. *Bioresource Technology*, 99 (11): 4919-4928.

Karakashev, D., Batstone, D. J. and Angelidaki, I. 2005. Influence of environmental conditions on methanogenic compositions in anaerobic biogas reactors. *Applied and Environmental Microbiology*, 71 (1): 331-338.

Khalid, K., Arshad, M., Anjum, M., Mahmood, T. and Dawson, L. 2011. The anaerobic digestion of solid organic waste *Waste Management*, 31 (8): 1737-1744.

Khanal, S. K. 2008. *Anaerobic biotechnology for bioenergy production principles and applications*. Wiley-Blackwell, Singapore (Last accessed: 03/11/2019).

Khanal, S. K. 2011. *Anaerobic Biotechnology for Bioenergy Production: Principles and Applications*. John Wiley & Sons, Hoboken, New Jersey, United States of America. (Last accessed: 03/11/2019).

Koch, K., Helmreich, B. and Drewes, J. E. 2015. Co-digestion of food waste in municipal wastewater treatment plants: effect of different mixtures on methane yield and hydrolysis rate constant. *Applied Energy*, 137: 250-255.

Kong, F., Wang, A. and Ren, H.-Y. 2015. Optimized matching modes of bioelectrochemical module and anaerobic sludge in the integrated system for azo dye treatment. *Bioresource Technology*, 192: 486-493.

Koppram, R., Albers, E. and Olsson, L. 2012. Evolutionary engineering strategies to enhance tolerance of xylose utilizing recombinant yeast to inhibitors derived from spruce biomass. *Biotechnology for Biofuels*, 5 (1): 32.

Kosinkova, J., Ramirez, J. A., Nguyen, J., Ristovski, Z., Brown, R., Lin, C. S. and Rainey, T. J. 2015. Hydrothermal liquefaction of bagasse using ethanol and black liquor as solvents. *Biofuels, Bioproducts and Biorefining*, 9 (6): 630-638.

Kougias, P., Boe, K., Einarsdottir, E. and Angelidaki, I. 2015. Counteracting foaming caused by lipids or proteins in biogas reactors using rapeseed oil or oleic acid as antifoaming agents. *Water Research*, 79: 119-127.

Kougias, P. G. and Angelidaki, I. 2018. Biogas and its opportunities—A review. *Frontiers of Environmental Science & Engineering*, 12: 1-12.

Koupaie, E. H., Johnson, T. and Eskicioglu, C. 2017. Advanced anaerobic digestion of municipal sludge using a novel and energy-efficient radio frequency pretreatment system. *Water Research*, 118: 70-81.

Kovalovszki, A., Alvarado-Morales, M., Fotidis, I. A. and Angelidaki, I. 2017. A systematic methodology to extend the applicability of a bioconversion model for the simulation of various co-digestion scenarios. *Bioresource Technology*, 235: 157-166.

Kuo, J. and Dow, J. 2017. Biogas production from anaerobic digestion of food waste and relevant air quality implications. *Journal of the Air & Waste Management Association*, 67 (9): 1000-1011.

Kweinor-Tetteh, E., Amano, K. O., Asante-Sackey, D. and Armah, E. K. 2018. Response surface optimisation of biogas potential in co-digestion of miscanthus fuscus and cow dung *International Journal of Technology*, 5: 944-954.

Kwietniewska, E. and Tys, J. 2014. Process characteristics, inhibition factors and methane yields of anaerobic digestion process, with particular focus on microalgal biomass fermentation. *Renewable and Sustainable Energy Reviews*, 34: 491-500.

Labatut, R. A., Angenent, L. T. and Scott, N. R. 2014. Conventional mesophilic vs. thermophilic anaerobic digestion: a trade-off between performance and stability?.*Water Research*, 53: 249-258.

Laser, M., Schulman, D. and Allen, S. G. 2002. A comparison of liquid hot water and steam pretreatments of sugarcane bagasse for conversion to ethanol. *Bioresource Technology*

81: 33-44.

Lebona, E., Cailleta, H., Akinlabib, E., Madyirab, D. and Adelard, L. 2019. Kinetic study of anaerobic co-digestion, analysis and modelling. *Procedia Manufacturing*, 35: 321-326.

Lee, E., Cumberbatch, J., Wang, M. and Zhang, Q. 2017. Kinetic parameter estimation model for anaerobic co-digestion of waste activated sludge and microalgae. *Bioresource Technology*, 228: 9-17.

Li, D., Huang, X., Wang, Q., Yuan, Y., Yan, Z., Li, Z., Huang, Y. and Liu, X. 2016. Kinetics of methane production and hydrolysis in anaerobic digestion of corn stover. *Energy*, 102: 1-9.

Liew, L. N., Shi, J. and Li, Y. 2012. Methane production from solid-state anaerobic digestion of lignocellulosic biomass. *Biomass and Bioenergy*, 46: 125-132.

Lina, R., Cheng, J., Ding, L. and Murphy, J. D. 2018. Improved efficiency of anaerobic digestion through direct interspecies electron transfer at mesophilic and thermophilic temperature ranges. *Chemical Engineering Journal*, 350: 681-691.

Liu, C., Li, H., Zhang, Y. and Liu, C. 2016. Improve biogas production from low-organic-content sludge through high-solids anaerobic co-digestion with food waste. *Bioresource Technology*, 219: 252-260.

Liu, T., Sun, L., Müller, B. and Schnürer, A. 2017a. Importance of inoculum source and initial community structure for biogas production from agricultural substrates. *Bioresource Technology*, 245: 768-777.

Liu, X., Hiligsmann, S., Gourdon, R. and Bayard, R. 2017b. Anaerobic digestion of lignocellulosic biomasses pretreated with Ceriporiopsis subvermispora. *Journal of Environmental Management*, 193: 154-162.

Liu, X. and Kokare, C. 2017. Microbial enzymes of use in industry. In: *Biotechnology of microbial enzymes*. Academic Press, Santiniketan, West Bengal, India. (Last accessed: 15/03/2018).

Liyakathali, N. M. A. 2014. Ultrasonic Pretreatment of Energy Cane Bagasse for Biofuel Production.Louisiana State University and Agricultural and Mechanical College,Baton Rouge, Louisiana, United States of America. Master of Science thesis.

Madondo, N. I. 2017. optimization of anaerobic co-digestion of sewage sludge using biochemical substrtaes. Durban University of Technology, Durban, South Africa Master of Engineering thesis.

Mah, R. A. and Sussman, C. 1968. Microbiology of anaerobic sludge fermentation I. enumeration of the nonmethanogenic anaerobic bacteria. *Applied Microbiology*, 16 (2): 358-361.

Maile, I., Muzenda, E. and Mbohwa, C. 2016a. Biochemical methane potential of OFMSW for City of Johannesburg.7th International Conference on Biology, Environment and Chemistry. University of Johannesburg, Johannesburg, South Africa. Pp. 94-99.

Maile, I., Muzenda, E. and Mbohwa, C. 2016c. Biogas production from anaerobic digestion of fruit and vegetable waste from Johannesburg market.Proceedings of 2016 International Conference on Energy, University of Johannesburg, Johannesburg, South Africa. Pp. 1-5.

Maile, I., Muzenda, E. and Mbohwa, C. 2016d. Biogas production from anaerobic digestion of fruit and vegetable waste from Johannesburg market. *Internationa Conference on Biology, Environment and Chemistry*, 98: 100-104.

Maile, I. O., Muzenda, E. and Mbohwa, C. 2016e. BiochemicalMethane Potential of OFMSW for City of Johannesburg. Proceedings of 2016 International Conference on Energy, University of Johannesburg, Johannesburg, South Africa. Pp. 1-5.

Maile, O. I., Muzenda, E. and Tesfagiorgis, H. 2017. chemical absorption of carbon dioxide in biogas purification. Paper presented at the *Procedia Manufacturing*. 639-646. 18/10/2017).

Malunga, S. P. 2018. Production of biogas from sugarcane residues. Durban University of Technology, Durban, South Africa. Masters of Engineering thesis.

Mao, C., Feng, Y., Wang, X. and Ren, G. 2015a. Review on research achievements of biogas from anaerobic digestion. *Renewable and Sustainable Energy Reviews*, 45: 540-555.

Mao, D., Yu, S., Rysz, M., Luo, Y., Yang, F., Li, F., Hou, J., Mu, Q. and Alvarez, P. 2015b. Prevalence and proliferation of antibiotic resistance genes in two municipal wastewater treatment plants. *Water Research*, 85: 458-466.

Maragkaki, A., Vasileiadis, I., Fountoulakis, M., Kyriakou, A., Lasaridi, K. and Manios, T. 2018. Improving biogas production from anaerobic co-digestion of sewage sludge with a thermal dried mixture of food waste, cheese whey and olive mill wastewater. *Waste Management*, 71: 644-651.

Martin-Ryals, A. 2012. Evaluating the potential for improving anaerobic digestion of cellulosic waste via routine bioaugmentation and alkaline pretreatment.University of Illinois, Illinois, United States of America. Master of Science thesis.

Martone, P., Estevez, J., Lu, F., Ruel, K., Denny, M., Sommerville, C. and Ralph, J. 2009. Discovery of lignin in seaweed Reveals Convergent Evolution of Cell-wall Architecture. *Current Biology*, 19 (2): 169-175.

Mata-Alvarez, J., Dosta, J., Romero-Güiza, M., Fonoll, X., Peces, M. and Astals, S. 2014. A critical review on anaerobic co-digestion achievements between 2010 and 2013. *Renewable and Sustainable Energy Reviews*, 36 (C): 412-427.

Mata-Alvarez, J., Mace, S. and Llabres, P. 2000. Anaerobic digestion of organic solid wastes. An overview of research achievements and perspectives. *Bioresource Technology*, 74 (1): 3-16.

Mateescu, C. and Constantinescu, I. 2011. Comparative analysis of inoculum biomass for biogas potential in the anaerobic digestion. *The Scientific Bulletin*, 73 (3): 99-104.

McKendry, P. 2002. Energy production from biomass (part 1): overview of biomass. *Bioresource Technology*, 83 (1): 37-46.

Mkhize, T., Mthembu, L. D., Gupta, R., Kaur, A., Kuhad, R. C., Reddy, P. and Deenadayalu, N. 2016. Enzymatic saccharification of acid/alkali pre-treated, millrun, and depithed sugarcane bagasse. *BioResources*, 11 (3): 6267-6285.

Moeller, L., Goersch, K., Neuhaus, J., Zehnsdorf, A. and Mueller, R. A. 2012. Comparative review of foam formation in biogas plants and ruminant bloat. *Energy, Sustainability and Society*, 2 (1): 12.

Monnet, F. 2003a. An introduction to Anaerobic Digestion of Organic Wastes. *Bioresource Technology*, 2(1):1-48.

Mood, S. H., Golfeshan, A. H., Tabatabaei, M., Jouzani, G. S., Najafi, G. H., Gholami, M. and Ardjmand, M. 2013. Lignocellulosic biomass to bioethanol, a comprehensive review with a focus on pretreatment. *Renewable and Sustainable Energy Reviews*, 27: 77-93.

Moody, L., Burns, R., Wu-Haan, W. and Spajic, R. 2009. Use of biochemical methane potential (BMP) assays for predicting and enhancing anaerobic digester performance. In: Proceedings of *Proceedings of the 44th Croatian and the 4th International Symposium on Agriculture, Opatija, Croatia*, Pp. 6-15.

Mthembu, L. D. 2016. Production of levulinic acid from sugarcane bagasse. Durban University of Technology, Durban, South Africa. Master of Applied Science thesis.

Mustafa, A. M., Poulsen, T. G. and Sheng, K. 2016. Fungal pretreatment of rice straw with Pleurotus ostreatus and Trichoderma reesei to enhance methane production under solid-state anaerobic digestion. *Applied Energy*, 180: 661-671.

Nagao, N., Tajima, N., Kawai, M., Niwa, C., Kurosawa, N., Matsuyama, T., Yusoff, F. M. and Toda, T. 2012. Maximum organic loading rate for the single-stage wet anaerobic digestion of food waste. *Bioresource Technology*, 118: 210-218.

Nalinga, Y. and Legonda, I. 2016. The effect of particles size on biogas production. *International Journal of Innovative Research in Technology & Sciences*, 4 (2): 9-13.

Nayono, S. E. 2010. *Anaerobic digestion of organic solid waste for energy production*. KIT Scientific Publishing, Hannover, Germany (Last assessed: 5/10/2019).

Nazaroff, W. W. and Alvarez-Cohen, L. 2015. *Anaerobic Digestion of Wastewater Sludge*. John Wiley & Sons, Inc, Hoboken, New Jersey, United States of America.

Neshat, S. A., Mohammadi, M., Najafpour, G. D. and Lahijani, P. 2017. Anaerobic co-digestion of animal manures and lignocellulosic residues as a potent approach for sustainable biogas production. *Renewable and Sustainable Energy Reviews*, 79: 308-322.

Nges, I. A. 2012. Anaerobic digestion of crop and waste biomass: Impact of feedstock characteristics on process performance. Lund University, Lund, Sweden.

Nges, I. A. and Björnsson, L. 2012. High methane yields and stable operation during anaerobic digestion of nutrient-supplemented energy crop mixtures. *Biomass and Bioenergy*, 47: 62-70.

Nghiem, L. D., Nguyen, T. T., Manassa, P., Fitzgerald, S. K., Dawson, M. and Vierboom, S. 2014. Co-digestion of sewage sludge and crude glycerol for on-demand biogas production. *International Biodeterioration & Biodegradation*, 95: 160-166.

Nijaguna, B. T. 2012. *Biogas Technology*. New Age International Limited Publishers, New Delhi, India(Last assessed: 30/08/2018).

Nikolausz, M., Walter, R., Sträuber, H., Liebetrau, J., Schmidt, T., Kleinsteuber, S., Bratfisch, F., Günther, U. and Richnow, H. 2013. Evaluation of stable isotope fingerprinting techniques for the assessment of the predominant methanogenic pathways in anaerobic digesters. *Applied Microbiology and Biotechnology*, 97 (5): 2251-2262.

Njoku, P., Kinyua, R., Muthoni, P. and Nemoto, Y. 2015. Biogas Production Using Water Hyacinth (Eicchornia crassipes) for Electricity Generation in Kenya. *Energy and Power Engineering*, 7: 209-216.

O'Sullivan, C., Rounsefell, B., Grinham, A., Clarke, W. and Udy, J. 2010. Anaerobic digestion of harvested aquatic weeds: water hyacinth *(Eichhornia crassipes)*, cabomba (Cabomba Caroliniana) and salvinia (Salvinia molesta). *Ecological Engineering*, 36 (10): 1459-1468.

Olson, D. G., McBride, J. E., Shaw, A. J. and Lynd, L. R. 2012. Recent progress in consolidated bioprocessing. *Current Opinion in Biotechnology*, 23 (3): 396-405.

Pagés-Díaz, J., Pereda-Reyes, I., Taherzadeh, M. J., Sárvári-Horváth, I. and Lundin, M. 2014. Anaerobic co-digestion of solid slaughterhouse wastes with agro-residues: synergistic and antagonistic interactions determined in batch digestion assays. *Chemical Engineering Journal*, 245: 89-98.

Parawira, W. 2012. Enzyme research and applications in biotechnological intensification of biogas production. *Critical Reviews in Biotechnology*, 32 (2): 172-186.

Parawira, W., Kudita, I., Nyandoroh, M. G. and Zvauya, R. 2005. A study of industrial anaerobic treatment of opaque beer brewery wastewater in a tropical climate using a full-scale UASB reactor seeded with activated sludge. *Process Biochemistry*, 40 (0): 593-599.

Paritosh, K., Yadav, M., Mathur, S., Balan, V., Liao, W., Pareek, N. and Vivekanand, V. 2018. Organic fraction of municipal solid waste: overview of treatment methodologies to enhance anaerobic biodegradability. *Frontiers in Energy Research*, 6: 75.

Park, M.-R., Kim, H. S., Kim, S.-K. and Jeong, G.-T. 2018. Thermo-chemical conversion for production of levulinic and formic acids from glucosamine. *Fuel Processing Technology*, 172: 115-124.

Parra-Orobio, B. A., Donoso-Bravo, A., Ruiz-Sánchez, J. C., Valencia-Molina, K. J. and Torres-Lozada, P. 2018. Effect of inoculum on the anaerobic digestion of food waste accounting for the concentration of trace elements. *Waste Management*, 71: 342-349.

Parsamehr, M. 2012. Modeling and analysis of a UASB reactor. Luleå University of Technology, Luleå, Sweden. Master of Science Environmental Engineering.

Patel, V., Desai, M. and Madamwar, D. 1993. Thermochemical pretreatment of water hyacinth for improved biomethanation. *Applied Microbiology and Biotechnology*, 42 (1): 67-74.

Patil, J. H., AntonyRaj, M., Shankar, B., Shetty, M. K. and Kumar, B. P. 2014. Anaerobic co-digestion of water hyacinth and sheep waste. *Energy Procedia*, 52: 572-578.

Paul, S. and Dutta, A. 2018. Challenges and opportunities of lignocellulosic biomass for anaerobic digestion. *Resources, Conservation and Recycling*, 130: 164-174.

Prabhu, M. S. and Mutnuri, S. 2016. Anaerobic co-digestion of sewage sludge and food waste. *Waste Management & Research*, 34 (4): 307-315.

Prabhudessai, V. 2013. Anaerobic digestion of food waste in a horizontal plug flow reactor. Birla Institute of Technology and Science (BITS)-Pilani University, K K Birla Goa Campus, India. Master of Science thesis.

Prasad, S., Singh, A. and Joshi, H. 2007. Ethanol as an alternative fuel from agricultural, industrial and urban residues. *Resources, Conservation and Recycling*, 50 (1): 1-39.

Priadi, C., Wulandari, D., Rahmatika, I. and Moersidik, S. S. 2014. Biogas production in the anaerobic digestion of paper sludge. *APCBEE procedia*, 9: 65-69.

Primrose, M. and Mugodo, K. 2015. *Biogas production potential for South African sugar cane industry*.*South African Journal of Science*, 2:1-16.

Prutsch, W. 1991. Steam explosion-hydrothermolysis-organosolv-a comparison. In: Proceedings of *Steam Explosion Techniques: Fundamentals and Industrial Applications: Proceedings of the International Workshop on Steam Explosion Techniques: Fundamentals and Industrial Applications, Milan, Italy, 20-21 October 1988*.CRC Press, Pp. 59.

Qian, M., Li, R., Li, J., Wedwitschka, H., Nelles, M., Stinner, W. and Zhou, H. 2016. Industrial scale garage-type dry fermentation of municipal solid waste to biogas. *Bioresource Technology*, 217: 82-89.

Qiu, Z., Aita, G. M. and Walker, M. S. 2012. Effect of ionic liquid pretreatment on the chemical composition, structure and enzymatic hydrolysis of energy cane bagasse. *Bioresource Technology*, 44 (4): 1-11.

Rabelo, S., Carrere, H., Maciel Filho, R. and Costa, A. 2011. Production of bioethanol, methane and heat from sugarcane bagasse in a biorefinery concept. *Bioresource Technology*, 102 (17): 7887-7895.

Rainey, T. J. 2009. A study into the permeability and compressibility of Australian bagasse pulp.Queensland University of Technology,Brisbane, Queensland, Australia. Doctoral thesis.

Ramos, L. P. 2003. The chemistry involved in the steam treatment of lignocellulosic materials. *Química Nova*, 26 (6): 863-871.

Raposo, F., Fernández-Cegrí, V., De la Rubia, M., Borja, R., Béline, F., Cavinato, C., Demirer, G., Fernández, B., Fernández-Polanco, M. and Frigon, J. 2011. Biochemical methane potential

(BMP) of solid organic substrates: evaluation of anaerobic biodegradability using data from an international interlaboratory study. *Journal of Chemical Technology and Biotechnology*, 86 (8): 1088-1098.

Ratanatamskul, C., Wattanayommanaporn, O. and Yamamoto, K. 2015. An on-site prototype two-stage anaerobic digester for co-digestion of food waste and sewage sludge for biogas production from high-rise building. *International Biodeterioration & Biodegradation*, 102: 143-148.

Ravi, B. 2018. Investigating the use of anaerobic fungi to enhance the hydrolysis of lignocellulose in lab scale biodigesters. University of Guelph, Guelph, Ontario, Canada Master of Science thesis.

Reddy, P. 2015. A critical review of ionic liquids for the pretreatment of lignocellulosic biomass. *South African Journal of Science*, 111 (11/12): 1-9.

Ribeiro, F. R., Passos, F., Gurgel, L. V. A., Baêta, B. E. L. and de Aquino, S. F. 2017. Anaerobic digestion of hemicellulose hydrolysate produced after hydrothermal pretreatment of sugarcane bagasse in UASB reactor. *Science of the Total Environment*, 584: 1108-1113.

Rocha, D. G. J., Carlos, M., Barbosa, I. S., Souto, M. A. M., Macedo, H. B. and Moraes, A. C. D. 2011. Dilute mixed-acid pretreatment of sugarcane bagasse for ethanol production. *Biomass and Bioenergy*, 35 (1): 663-670.

Rodriguez-Chiang, L. M. and Dahl, O. P. 2014. Effect of inoculum to substrate ratio on the methane potential of microcrystalline cellulose production wastewater. *BioResources*, 10 (1): 898-911.

Rolfe, M. D., Rice, C. J., Lucchini, S., Pin, C., Thompson, A., Cameron, A. D., Alston, M., Stringer, M. F., Betts, R. P. and Baranyi, J. 2012. Lag phase is a distinct growth phase that prepares bacteria for exponential growth and involves transient metal accumulation. *Journal of Bacteriology*, 194 (3): 686-701.

Rubin, E. 2008. Genomics of cellulosic biofuels. *Nature*, 454:841–845.

Saady, N. M. C. and Massé, D. I. 2015. Impact of organic loading rate on psychrophilic anaerobic digestion of solid dairy manure. *Energies*, 8 (3): 1990-2007.

Sager, M. 2014. *Renewable Energy vision 2030-South Africa, WWF-S.A Report Summary*. South African Department of Environmental Affairs. (Last assessed: 31/03/2019)

Samuelsson, R., Burvall, J. and Jirjis, R. 2006. Comparison of different methods for the determination of moisture content in biomass. *Biomass and Bioenergy*, 30 (11): 929-934.

Saritha, M. and Arora, A. 2012. Biological pretreatment of lignocellulosic substrates for enhanced delignification and enzymatic digestibility. *Indian Journal of microbiology*, 52 (2): 122-130.

Schattauer, A., Abdoun, E., Weiland, P., Plöchl, M. and Heiermann, M. 2011. Abundance of trace elements in demonstration biogas plants. *Biosystems Engineering*, 108 (1): 57-65.

Scheller, H. V. and Ulvskov, P. 2010. Hemicelluloses. *Annual Review of Plant Biology*, 61: 263-289.

Scherer, P., Neumann, L., Demirel, B. and Schmidt, O. 2009. Long term fermentation studies about the nutritional requirements for biogasification of fodder beet silage as mono-substrate. *Biomass & Bioenergy*, 33 (5): 873-881.

Schnürer, A. and Jarvis, Å. 2009. *Microbiological Handbook for Biogas Plants*.Avfall Sverige, Svenskt Gastekniskt Center (SGC). Malmö, Sweden. (Last assessed: 20/06/2019).

Schnürer, A. and Nordberg, Å. 2008. Ammonia, a selective agent for methane production by syntrophic acetate oxidation at mesophilic temperature. *Water Science and Technology*, 57 (5): 735-740.

Shah, A. F., Mahmood, Q., Sha, M. M., Pervez, A. and Asad, A. S. 2014. Microbial ecology of anaerobic digesters: the key players of anaerobiosis. *The Scientific World Journal*, 2014

Shin, J., Jang, H. M., Shin, S. G. and Kim, Y. M. 2019. Thermophilic anaerobic digestion: Effect of start-up strategies on performance and microbial community. *Science of the Total Environment*, 687: 87-95.

Silvestre, G., Illa, J., Fernández, B. and Bonmatí, A. 2014. Thermophilic anaerobic co-digestion of sewage sludge with grease waste: effect of long chain fatty acids in the methane yield and its dewatering properties. *Applied Energy*, 117: 87-94.

Simo, W. S. F., Jong, N. E. and Kapseu, C. 2016. Improving Biogas Production of Sugarcane Bagasse by Hydrothermal Pretreatment. *Chemical and Biomolecular Engineering*, 1 (3): 21-25.

Sindhu, R., Binod, P., Pandey, A., Madhavan, A., Alphonsa, J. A., Vivek, N., Gnansounou, E., Castro, E. and Faraco, V. 2017. Water hyacinth a potential source for value addition: An overview. *Bioresource Technology,* 230: 152-162.

Singh, A., Kuila, A., Adak, S., Bishai, M. and Banerjee, R. 2012. Utilization of Vegetable Wastes for Bioenergy Generation. *Agricultural Research,* 1 (3): 213-222.

Sluiter, A., Hames, B., Ruiz, R., Scarlata, C., Sluiter, J., Templeton, D. and Crocker, D. 2008. Determination of structural carbohydrates and lignin in biomass. *Laboratory Analytical Procedure,* 1617: 1-16.

Smith, J., Van Rensburg, E. and Görgens, J. F. 2014. Simultaneously improving xylose fermentation and tolerance to lignocellulosic inhibitors through evolutionary engineering of recombinant Saccharomyces cerevisiae harbouring xylose isomerase. *BMC Biotechnology*, 14 (1): 41.

Söderström, J., Pilcher, L., Galbe, M. and Zacchi, G. 2002. Two-step steam pretreatment of softwood with SO2 impregnation for ethanol production. *Applied Biochemistry and Biotechnology*, 98 (1-9): 5.

Speece, R., Boonyakitsombut, S., Kim, M., Azbar, N. and Ursillo, P. 2006. Overview of Anaerobic Treatment: Thermophilic and Propionate Implications-Keynote Address—Association of Environmental Engineering and Science Professors—78th Annual Water Environment Federation Technical Exposition and Conference, Washington, DC, Oct. 29–Nov. 2, 2005. *Water Environment Research*, 78 (5): 460-473.

Sreekrishnan, T., Kohli, S. and Rana, V. 2004. Enhancement of biogas production from solid substrates using different techniques—a review. *Bioresource Technology*, 95 (1): 1-10.

Kirk-Othmer Encyclopedia of Chemical Technology. 2001. John Wiley & Sons.Hoboken, New Jersey, United States of America. (Last accessed: 02/12/2019).

Suhartini, S. 2014. The anaerobic digestion of sugar beet pulp. University of Southampton, Southampton,England. Master of Science thesis.

Suhartini, S., Heaven, S. and Banks, C. J. 2014. Comparison of mesophilic and thermophilic anaerobic digestion of sugar beet pulp: performance, dewaterability and foam control. *Bioresource Technology,* 152: 202-211.

Sun, J.-H., Dong, S.-Y., Feng, J.-L., Yin, X.-J. and Zhao, X.-C. 2011. Enhanced sunlight photocatalytic performance of Sn-doped ZnO for Methylene Blue degradation. *Journal of Molecular Catalysis A: Chemical*, 335 (1-2): 145-150.

Sun, N., Rahman, M., Qin, Y., Maxim, M. L., Rodríguez, H. and Rogers, R. D. 2009. Complete dissolution and partial delignification of wood in the ionic liquid 1-ethyl-3-methylimidazolium acetate. *Green Chemistry*, 11 (5): 646-655.

Talebnia, F., Karakashev, D. and Angelidaki, I. 2010. Production of bioethanol from wheat straw: an overview on pretreatment, hydrolysis and fermentation. *Bioresource Technology*, 101 (13): 4744-4753.

Tan, L., Qiu-Shi Cheng, Zhao-Yong Sun, Yue-Qin Tang and Kida, K. 2018. Effects of ammonium and/or sulfide on methane production from acetate or propionate using biochemical methane potential tests. *Journal of Bioscience and Bioengineering*, xx (xx): 1-8.

Tawoma, N. 2015. Valorisation of biowaste via production of biogas and Biofertilizer. MUniversity of Kwazulu-Natal, Durban, South Africa. Master of Science in Engineering thesis.

Teghammar, A. 2013. Biogas Production from Lignocelluloses: Pretreatment, Substrate Characterization, Co-Digestion and Economic Evaluation. Chalmers Tekniska Högskola, Göteborg, Sweden. Doctoral thesis.

Terboven, C., Ramm, P. and Herrmann, C. 2017. Demand-driven biogas production from sugar beet silage in a novel fixed bed disc reactor under mesophilic and thermophilic conditions. *Bioresource Technology*, 241: 582-592.

Tetteh, E., Rathilal, S. and Naidoo, D. 2020. photocatalytic degradation of oily waste and phenol from a local South Africa oil refinery wastewater using response methodology. *Scientific Reports*, 10 (1): 1-12.

Tetteh, E. K., Amano, K. O. A., Asante-Sackey, D. and Armah, E. K. 2017. Biochemical Methane Potential (BMP) of Miscanthus Fuscus for Anaerobic Digestion. *International Journal of Scientific and Research Publication*, 7 (12): 434-439.

Tetteh, E. T., Ezugbe, E. O., Rathilal, S. and Asante-Sackey, D. 2020. Removal of COD and SO42− from Oil Refinery Wastewater Using a Photo-Catalytic System-Comparing TiO2 and Zeolite Efficiencies. *Water*, 12 (214): 1-13.

Torgrip, R. J. and Fernández–Cano, V. 2017. Rapid X-ray based determination of moisture-, ash content and heating value of three biofuel assortments. *Biomass and Bioenergy*, 98: 161-171.

Trajano, H. L., Engle, N. L., Foston, M., Ragauskas, A. J., Tschaplinski, T. J. and Wyman, C. E. 2013. The fate of lignin during hydrothermal pretreatment. *Biotechnology for Biofuels*, 6 (1): 110.

Traversi, D., Villa, S., Acri, M., Pietrangeli, B., Degan, R. and Gilli, G. 2011. The role of different methanogen groups evaluated by Real-Time qPCR as high-efficiency bioindicators of wet anaerobic co-digestion of organic waste. *AMB Express*, 1 (1): 28.

Trnovec, W. and Britz, T. 1998. Influence of organic loading rate and hydraulic retention time on the efficiency of a UASB bioreactor treating a canning factory effluent. *Water SA*, 24 (2)

Tsapekos, P., Kougias, P., Treu, L., Campanaro, S. and Angelidaki, I. 2017. Process performance and comparative metagenomic analysis during co-digestion of manure and lignocellulosic biomass for biogas production. *Applied Energy*, 185: 126-135.

Tsapekos, P., Kougias, P. G. and Angelidaki, I. 2015. Anaerobic mono-and co-digestion of mechanically pretreated meadow grass for biogas production. *Energy & Fuels*, 29 (7): 4005-4010.

Tsapekos, P., Kougias, P. G., Kuthiala, S. and Angelidaki, I. 2018. Co-digestion and model simulations of source separated municipal organic waste with cattle manure under batch and continuously stirred tank reactors. *Energy Conversion and Management*, 159: 1-6.

Tywabi, Z. 2015. Processing of dissolving pulp in ionic liquids. Durban University of Technology, Durban, South Africa. Doctoral thesis.

Updegraff, D. M. 1969. Semimicro determination of cellulose in biological materials. *Analytical Biochemistry*, 32 (3): 420-424.

Van Lier, J., Van Der Zee, F., Frijters, C. and Ersahin, M. 2015. Celebrating 40 years anaerobic sludge bed reactors for industrial wastewater treatment. *Reviews in Environmental Science and BioTechnology*, 14 (4): 681-702.

Van Lier, J. B., Vashi, A., Van Der Lubbe, J. and Heffernan, B. 2010. Anaerobic sewage treatment using UASB reactors: Engineering and operational aspects. In: *Environmental Anaerobic Technology: Applications and New Developments*. World Scientific, 59-89.

Van Walsum, G. P., Allen, S. G., Spencer, M. J., Laser, M. S., Antal Jr, M. J. and Lynd, L. R. 1996. Conversion of lignocellulosics pretreated with liquid hot water to ethanol. In: Proceedings of *Seventeenth symposium on biotechnology for fuels and chemicals*.Springer, Pp. 157-170.

Vartak, D., Engler, C., Ricke, S. and McFarland, M. 1997. Organic loading rate and bioaugmentation effects in psychrophilic anaerobic digestion of dairy manure. *Paper-American Society of Agricultural Engineers*, (974051).

Verstraete, W., Van de Caveye, P. and Diamantis, V. 2009. Maximum use of resources present in domestic "used water". *Bioresource Technology*, 100 (23): 5537-5545.

Villamil, J. A., Mohedano, A. F., Rodríguez, J. J., Borja, R., la Rubia, D. and Angeles, M. 2018. Anaerobic co-digestion of the organic fraction of municipal solid waste and the liquid fraction from the hydrothermal carbonization of industrial sewage sludge under thermophilic conditions. *Frontiers in Sustainable Food Systems*, 2: 17.

Vlachopoulou, M. 2010a. The anaerobic digestion of food waste with and without sewage sludge: Achievements and the potential of the ADM1. London: Faculty of Natural Sciences, Centre for Environmental Policy, Imperial College London.

Vlachopoulou, M. 2010b. The anaerobic digestion of food waste with and without sewage sludge: Achievements and the potential of the ADM1. Imperial College London Press, London, United Kingdom. (Last assessed:10/03/2018).

Vorgelegt, V. 2017. Optimization of Anaerobic Digestion of Sugarcane Waste for Biogas Production in Brazil.University of Rostock, Rostock, Germany. Doctoral thesis.

Wahlström, R. and Suurnäkki, A. 2015. Enzymatic hydrolysis of lignocellulosic polysaccharides in the presence of ionic liquids. *Green Chemistry*, 17 (2): 694-714.

Wang, Q., Kuninobu, M., Kakimoto, K., Ogawa, H. I. and Kato, T. 1999. Upgrading of anaerobic digestion of waste activated sludge by ultrasonic pretreatment. *Bioresource Technology*, 68 (3): 309-313.

Wang, S., Ma, F., Ma, W., Wang, P., Zhao, G. and Lu, X. 2019. Influence of Temperature on Biogas Production Efficiency and Microbial Community in a Two-Phase Anaerobic Digestion System. *Water*, 11 (1): 133.

Wei, Y., Li, X., Yu, L., Zou, D. and Yuan, H. 2015. Mesophilic anaerobic co-digestion of cattle manure and corn stover with biological and chemical pretreatment. *Bioresource Technology*, 198: 431-436.

Weiland, P. 2010. Biogas production: current state and perspectives. *Applied Microbiology and Biotechnology*, 85 (4): 849-860.

Willard, H. H., Merritt, L. L., Dean, J. A. and Settle, F. A. 1986. Instrumental methods of analysis. 7th Ed. CBS Publishers, New Delhi, India. (Last assessed: 12/04/2019).

Wimalasena, T. T., Greetham, D., Marvin, M. E., Liti, G., Chandelia, Y., Hart, A., Louis, E. J., Phister, T. G., Tucker, G. A. and Smart, K. A. 2014. Phenotypic characterisation of Saccharomyces spp. yeast for tolerance to stresses encountered during fermentation of lignocellulosic residues to produce bioethanol. *Microbial Cell Factories*, 13 (1): 47.

Wu, W.-M., Hickey, R. F., Bhatnagar, L. and Zeikus, J. G. 2018. Fatty acid degradation as a tool to monitor anaerobic sludge activity and toxicity. In: Proceedings of *Proceedings of the 44th Industrial Waste Conference. Purdue University, United States of America.*. CRC Press, Pp. 13-21.

Wu, Y., Khadilkar, M. R., Al-Dahhan, M. H. and Duduković, M. P. 1996. Comparison of upflow and downflow two-phase flow packed-bed reactors with and without fines: experimental observations. *Industrial & Engineering Chemistry Research*, 35 (2): 397-405.

Wu, Y., Kovalovszki, A., Pan, J., Lin, C., Liu, H., Duan, N. and Angelidaki, I. 2019. Early warning indicators for mesophilic anaerobic digestion of corn stalk: a combined experimental and simulation approach. *Biotechnology for Biofuels*, 12 (1): 106.

Xiao, W. and Clarkson, W. W. 1997. Acid solubilisation of lignin and bioconversion of treated newsprint to methane. *Biodegradation*, 8: 61-66.

Xie, S., Faisal, I. H., Xinmin, Z., Wenshan, G., Hao, H. N., William, E. P. and Long, D. N. 2016a. Anaerobic co-digestion: A critical review of mathematical modelling for performance optimization. *Bioresource Technology*, 222: 498-512.

Xie, S., Hai, F. I., Zhan, X., Guo, W., Ngo, H. H., Price, W. E. and Nghiem, L. D. 2016b. Anaerobic co-digestion: a critical review of mathematical modelling for performance optimization. *Bioresource Technology*, 222: 498-512.

Xie, Y., Qin, H. and Yu, D. 2004. Nutrient limitation to the decomposition of water hyacinth *(Eichhornia crassipes). Hydrobiologia*, 529 (1-3): 105-112.

Xu, K., Lu, J., Gao, Y., Wu, Y. and Li, X. 2017. Determination of moisture content and moisture content profiles in wood during drying by low-field nuclear magnetic resonance. *Drying Technology*, 35 (15): 1909-1918.

Xu, S., Zhang, L., Huang, S., Zeeman, G., Rijnaarts, H. and Liu, Y. 2018. Improving the energy efficiency of a pilot-scale UASB-digester for low temperature domestic wastewater treatment. *Biochemical Engineering Journal*, 135: 71-78.

Yang, B. and Wyman, C. E. 2004. Effect of xylan and lignin removal by batch and flowthrough pretreatment on the enzymatic digestibility of corn stover cellulose. *Biotechnology and Bioengineering*, 86 (1): 88-98.

Yang, G. and Wang, J. 2017. Fermentative hydrogen production from sewage sludge. *Critical Reviews in Environmental Science and Technology*, 47 (14): 1219-1281.

Yashas Gowda, T., Sanjay, M., Subrahmanya Bhat, K., Madhu, P., Senthamaraikannan, P. and Yogesha, B. 2018. Polymer matrix-natural fiber composites: An overview. *Cogent Engineering*, 5 (1): 1446667.

Yoon, L. W., Ang, T. N., Ngoh, G. C. and Chua, A. S. M. 2012. Regression analysis on ionic liquid pre-treatment of sugarcane bagasse and assessment of structural changes. *Biomass and Bioenergy*, 36: 160-169.

Yoshida, H., Christensen, T. H. and Scheutz, C. 2013. Life cycle assessment of sewage sludge management: a review. *Waste Management & Research*, 31 (11): 1083-1101.

Young, B. 2012. Enhancement of the Mesophilic Anaerobic Co-Digestion of Municipal Sewage and Scum. University of Ottawa, Ottawa,Canada. Master of Applied Sciences in Environmental Engineering.

Yu, L., Wensel, P., Ma, J. and Chen, S. 2013. Mathematical modeling in anaerobic digestion (AD). *Journal of Bioremediation and Biodegradation*, 4 (2): 23-33.

Zainol, N. 2012. Kinetics of Biogas Production from Banana Stem Waste, Biogas. ISBN: 978-953-51-0204-5, InTechOpen.

Zhang, C., Wang, A., Jia, J., Zhao, L. and Song, W. 2017. Effect of parameters on anaerobic digestion EGSB reactor for producing biogas. *Procedia Engineering*, 205: 3749-3754.

Zhang, C., Xiao, G., Peng, L., Su, H. and Tan, T. 2013. The anaerobic co-digestion of food waste and cattle manure. *Bioresource Technology*, 129: 170-176.

Zhang, H., Wu, J., Gao, L., Yu, J., Yuan, X., Zhu, W., Wang, X. and Cui, Z. 2018. Aerobic deterioration of corn stalk silage and its effect on methane production and microbial community dynamics in anaerobic digestion. *Bioresource Technology*, 250: 828-837.

Zhang, L., Lee, Y.-W. and Jahng, D. 2011. Anaerobic co-digestion of food waste and piggery wastewater: focusing on the role of trace elements. *Bioresource Technology*, 102 (8): 5048-5059.

Zhang, R., El-Mashd, H., Hartman, K., Wang, F., Liu, G., Choate, C. and Gamble, P. 2007. Characterization of food waste as feedstock for anaerobic digestion. *Bioresource Technology*, 98: 929-935.

Zhang, Y., Zhang, Z., Suzuki, K. and Maekawa, T. 2003. Uptake and mass balance of trace metals for methane producing bacteria. *Biomass and Bioenergy*, 25 (4): 427-433.

Zhang, Z.-P., Show, K.-Y., Tay, J.-H., Liang, D. T., Lee, D.-J. and Jiang, W.-J. 2006. Effect of hydraulic retention time on biohydrogen production and anaerobic microbial community. *Process Biochemistry*, 41 (10): 2118-2123.

Zhen, G., Lu, X., Kato, H., Zhao, Y. and Li, Y.-Y. 2017. Overview of pretreatment strategies for enhancing sewage sludge disintegration and subsequent anaerobic digestion: Current advances, full-scale application and future perspectives. *Renewable and Sustainable Energy Reviews*, 69: 559-577.

Zheng, Y., Lin, H. M. and Tsao, G. T. 1998. Pretreatment for cellulose hydrolysis by carbon dioxide explosion. *Biotechnology Progress*, 14: 890-896.

Zheng, Y., Pan, Z. and Zhang, R. 2009. Overview of biomass pretreatment for cellulosic ethanol production. *International Journal of Agricultural and Biological Engineering*, 2 (3): 51-68.

Zhu, S. 2008. Perspective use of ionic liquids for the efficient utilization of lignocellulosic materials. *Journal of Chemical Technology and Biotechnology*, 83: 777-779.

Ziemiński, K., Romanowska, I. and Kowalska, M. 2012. Enzymatic pretreatment of lignocellulosic wastes to improve biogas production. *Waste Management*, 32 (6): 1131-1137.

APPENDIX A

A1: Proximate analysis for the SCB and CS

Table A- 1: Raw values for the proximate analysis of SCB.

Sample ID	M1 (g)	M6 (g)	M2(g)	M3 (g)	M4 (g)	M5 (g)	% TS	% MC	% VS	(%) FS	% Ash
A	43.33	2.00	45.33	45.21	47.25	44.55	94.16	5.84	76.14	23.85	12.68
B	44.25	2.00	46.25	46.13	46.33	43.70	94.23	5.77	79.85	20.14	9.93
C	44.25	2.00	46.25	46.13	46.33	43.71	94.22	5.76	79.85	20.14	9.93

Table A- 2: Raw values for the proximate analysis of CS.

Sample ID	M1 (g)	M2 (g)	M3 (g)	M4(g)	M5 (g)	M6 (g)	% TS	% MC	% VS	% FS	% Ash
A	43.20	46.20	46.01	46.01	43.32	3.00	93.7	6.3	95.7	4.2	3.5
B	41.96	44.96	44.74	44.74	42.07	3.00	92.7	7.3	96	4.0	3.5
C	44.21	47.21	46.99	46.99	44.32	3.00	92.7	7.3	96	4.0	3.5

Where M1 is the mass of the empty crucible, M2 is the mass of crucible + sample before oven drying, M3 is the mass of crucible + sample after oven drying, M4 is the mass of crucible + sample before furnace drying, M5 is the mass of crucible + sample after furnace drying and M6 is the mass of sample.

Table A- 3: Summary of results for the proximate analysis.

Parameters	SCB	CS
Moisture (g)	0.06	0.07
Moisture (%)	5.90	7.00
Total solids (g)	0.94	0.93
Total solids (%)	94.20	93.00
Average volatile solids based on TS (%)	78.00	96.00
VS/TS (g)	0.83	1.03
VS/TS (%)	82.80	103.20
Ash content (%)	9.90	3.50
Fixed solids (%)	22.00	4.10

A2: Calculations: Proximate analysis for the SCB and CS

A2.1 Total solids

$$\% \text{ Total solid} = \left[1 - \left(\frac{X1-X2}{X1}\right)\right] \times 100\ \%;$$

Therefore, % Total solid represents the total solid content of the sample expressed as a percentage; X1 is the weight of the sample as received and X2 is the weight of the sample after being dried for 4 hours minimum at 105 ^{o}C ± 2^{o}C.

For SCB,

$$A = \frac{(45.2140 - 43.3308)}{2.0000} \times 100\%$$

$$= 94.16\%$$

For CS,

$$A = \left(\frac{46.01 - 43.20}{46.20 - 43.20}\right) \times 100\%$$

$$= 93.7\%$$

A2.2 Moisture content

% Moisture content $= \left[\left(\frac{M1-M2}{M1}\right)\right] \times 100\ \%$

Therefore, M1 is the weight of the sample as received and M2 is the weight of the sample after being dried for 4 hours minimum at 105 ^{o}C ± 1^{o}C.

For SCB

A = (100 – 94.16) %

= 5.84%

For CS

A = (100 – 93.7) %

= 7.0%

A2.3 Fixed solids

% Fixed solids $= \left(\frac{\text{D - K}}{\text{A - K}}\right) \times 100\%;$

Where A is the weight of residue and the dish after ignition (g); K is the weight of the dish and D is the weight of dried residue and the dish (g)

For SCB,

$$\text{A} = \frac{(43.7800 - 43.3308)}{(45.2140 - 43.3308)} \times 100\%$$

$= 23.85\%$

For CS

$$\text{A} = \left(\frac{43.32 - 43.20}{46.01 - 43.20}\right) \times 100\%$$

= 4.2%

A2.4 Volatile solids

$$\% \text{ Volatile solids } = \left(\frac{X - Z}{X - Y}\right) \times 100\%;$$

Where Z is the weight of residue and the dish after ignition (g), Y is the weight of the dish and X is the weight of dried residue and dish (g).

For SCB,

$$A = \frac{(45.2140 - 43.7800)}{(45.2140 - 43.3308)} \times 100\%$$

$$= \frac{1.434}{1.8832} \times 100\%$$

$$= 76.14\%$$

For CS,

$$A = \left(\frac{46.01 - 3.32}{46.01 - 43.20}\right) \times 100\%$$

$$= 95.7\%$$

A2.5 Ash content

$$\% \text{ Ash content } = \left(\frac{S1 - S2}{S3 - S2}\right) \times 100\%;$$

Where S1 is the weight of crucible and weight of sample after 600ºC ashing (g), S3 is the weight of the crucible plus the weight of the sample before ashing (g) and S2 is the weight of dried residue plus the dish (g)

For SCB,

$$A = \frac{(44.5506 - 44.2526)}{(47.2527 - 44.2526)} \times 100\%$$

$$= 9.93\%$$

For CS,

$$A = \left(\frac{44.35 - 44.21}{48.21 - 44.21}\right) \times 100\%$$

= 3.5%

A3: Proximate analysis of wastewater streams: liquid fraction

A3.1 Sample calculation for TS

$$\text{TS (mg/L)} = \frac{(\text{B} - \text{A})\ g}{\text{SV (mL)} \times 1\text{g} \times 1\text{L}} \times 1{,}000\ \text{mL} \times 1{,}000\ \text{mg}$$

Where TS (mg/L) denotes the percentage of volatile solids, B is the average sample mass prior to being placed in the muffle furnace which is equal to (b1 + b2)/2, b1 and b2 are the masses of the sample prior to being placed in the muffle furnace in duplicate and A is the sample mass after removal from the muffle furnace.

Considering Brewery W1 in asteriks (Table A-4),

$$\text{TS (mg/L)} = \frac{(44.812 - 44.3262) \times 1{,}000 \times 1{,}000}{20 \times 1 \times 1}$$

= 7,750 mg/L

Table A- 4: Data obtained for the total solid (TS) measurement.

Sample	A (g)	b1	b2	B (g)	Sample volume (SV), mL	Total solid (mg/L)
*Brewery W1	44.3262	44.4804	44.4819	44.4812	20	7750.0
Brewery W2	40.2918	40.4466	40.4494	40.4480	20	7810.0
Dairy W1	42.0732	42.1686	42.1669	42.1678	20	4727.5
Dairy W2	44.9011	44.9924	44.9889	44.9907	20	4477.5
Municipal W1	42.6816	42.752	42.7533	42.7527	20	3552.5
Municipal W2	43.3233	43.4392	43.4307	43.4350	20	5582.5
Sugar W1	44.8999	44.9873	44.9892	44.9883	20	4417.5
Sugar W2	42.6803	42.7715	42.7736	42.7726	20	4612.5

*W1 and W2 denotes the duplication of the WW streams

A3.2 Sample calculation for VS

$$\text{VS (mg/L)} = \frac{(\text{B} - \text{A})\ g}{\text{SV (mL)} \times 1\text{g} \times 1\text{L}} \times 1{,}000\ \text{mL} \times 1{,}000\ \text{mg}$$

Where VS (mg/L) denotes the percentage of volatile solids, B is the average sample mass prior to being placed in the muffle furnace which is equal to (b1 + b2)/2, b1 and b2 are the masses of the sample prior to being placed in the muffle furnace in duplicate and A is the sample mass after removal from the muffle furnace.

Table A- 5:Data obtained for the volatile solid (VS) measurement.

Sample	A (g)	b1	b2	B (g)	Sample volume (mL)	Volatile solid(mg/L)
Brewery W1	44.4812	44.3788	44.3812	44.3800	20	5057.5
Brewery W2	40.4480	40.3467	40.3476	40.3472	20	5042.5
Dairy W1	42.1678	42.0864	42.0851	42.0858	20	4100.0
Dairy W2	44.9907	44.9140	44.9132	44.9136	20	3852.5
Municipal W1	42.7527	42.7008	42.7020	42.7014	20	2562.5
Municipal W2	43.4350	43.3467	43.3476	43.3472	20	4390.0
Sugar W1	44.9883	44.9198	44.9217	44.9208	20	3375.0
Sugar W2	42.7726	42.7038	42.7032	42.7035	20	3452.5

*W1 and W2 denotes the duplication of the WW streams

A3.3 Sample calculation for TSS

$$\text{TSS (mg/L)} = \frac{(\text{B} - \text{A})\ g}{\text{SV (mL)} \times 1\text{g} \times 1\text{L}} \times 1{,}000\ \text{mL} \times 1{,}000\ \text{mg}$$

Where TSS (mg/L) denotes the percentage of volatile solids, B is the average sample mass prior to being placed in the muffle furnace which is equal to (b1 + b2)/2, b1 and b2 are the masses of the sample prior to being placed in the muffle furnace in duplicate and A is the sample mass after removal from the muffle furnace.

Table A- 6: Data obtained for the total suspended solid (TSS) measurement.

Sample	A (g)	Filter weight (g)	b1	b2	B (g)	Sample volume (mL)	TSS (mg/L)
Dairy W1	42.6336	0.0965	42.748	42.7457	42.7469	20	837.5
Dairy W2	43.9806	0.0979	44.0929	44.092	44.0925	20	697.5
Municipal W1	43.3431	0.0969	43.4526	43.4461	43.4494	10	935.0
Municipal W2	44.2536	0.0967	44.3616	44.3593	44.3605	10	1015.0
Brewery W1	44.2465	0.0975	44.3567	44.3567	44.3567	20	635.0
Brewery W2	42.6336	0.0970	42.7439	42.7439	42.7439	20	665.0
Sugar W1	43.3271	0.0967	43.4352	43.4352	43.4352	20	570.0
Sugar W2	43.3270	0.0960	43.4452	43.4450	43.4350	20	564.0

*W1 and W2 denotes the duplication of the WW streams

A3.4 Sample calculation for VSS

$$\text{VSS (mg/L)} = \frac{(\text{B} - \text{A})\ g}{\text{SV (mL)} \times 1\text{g} \times 1\text{L}} \times 1{,}000\ \text{mL} \times 1{,}000\ \text{mg}$$

Where VSS (mg/L) denotes the percentage of volatile solids, B is the average sample mass prior to being placed in the muffle furnace which is equal to (b1 + b2)/2, b1 and b2 are the masses of the sample prior to being placed in the muffle furnace in duplicate and A is the sample mass after removal from the muffle furnace.

Table A- 7: Data obtained for the volatile suspended solid (VSS) measurement.

Sample	A (g)	b1	b2	B (g)	Sample volume (mL)	VSS (mg/L)
Dairy W1	42.7469	42.7284	42.7457	42.7371	20	490.0
Dairy W2	44.0925	44.0751	44.092	44.0836	20	445.0
Municipal S1	43.4494	43.4281	43.4233	43.4257	10	2365.0
Municipal S2	44.3605	44.3482	44.3435	44.3459	10	1460.0
Brewery W1	44.3567	44.3464	44.3464	44.3464	20	515.0
Brewery W2	42.7439	42.7334	42.7334	42.7334	20	525.0
Sugar W1	43.4352	43.4258	43.4258	43.4258	20	470.0
Sugar W2	43.4350	43.4255	43.4350	43.4250	20	467.0

*W1 and W2 denotes the duplication of the WW streams

Table A- 8: pH of wastewater streams prior to AcoD.

Substrates	1	2	Average pH
Sludge only	8.45	8.29	8.37
Sludge + SWW	8.00	8.02	8.01
Sludge + DWW	7.62	7.78	7.70
Sludge + BWW	7.54	7.38	7.46
Sludge + CS + SWW	6.13	6.04	6.09
Sludge +SCB + SWW	7.90	7.80	7.85
Sludge + SWW	8.09	8.04	8.07

A4: Ultimate analysis: SEM-EDX

A4.1 Preparation of the samples for SEM analysis

About 50 mL of the digestate and the activated sludge (post AD) were collected in centrifuge tubes, kept in a refrigerator and stored overnight. It was then transferred in a crucible and made to dry in a convection oven operating at 105°C for 2 hours prior to SEM analysis.

A4.2 EDX results of the untreated and pretreated SCB or CS

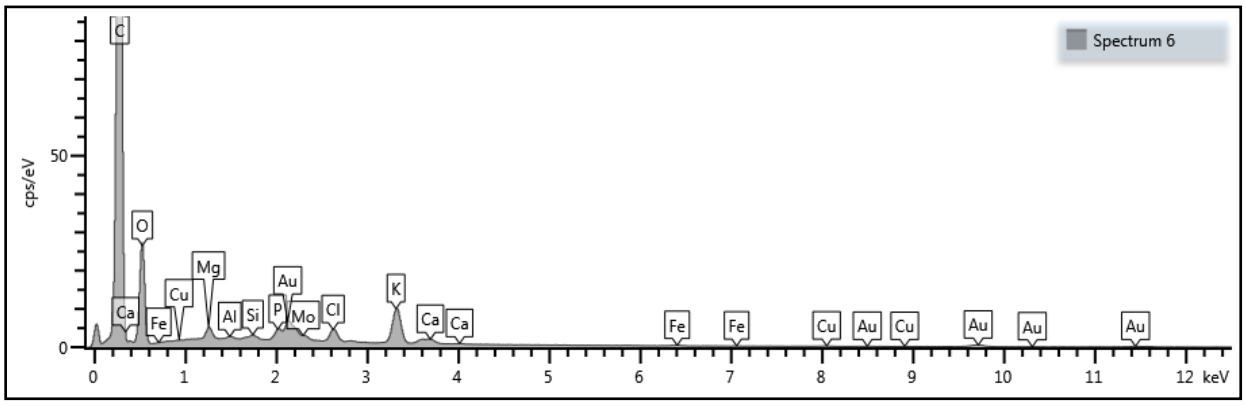

Figure A- 1: Photographs of the EDX for untreated CS.

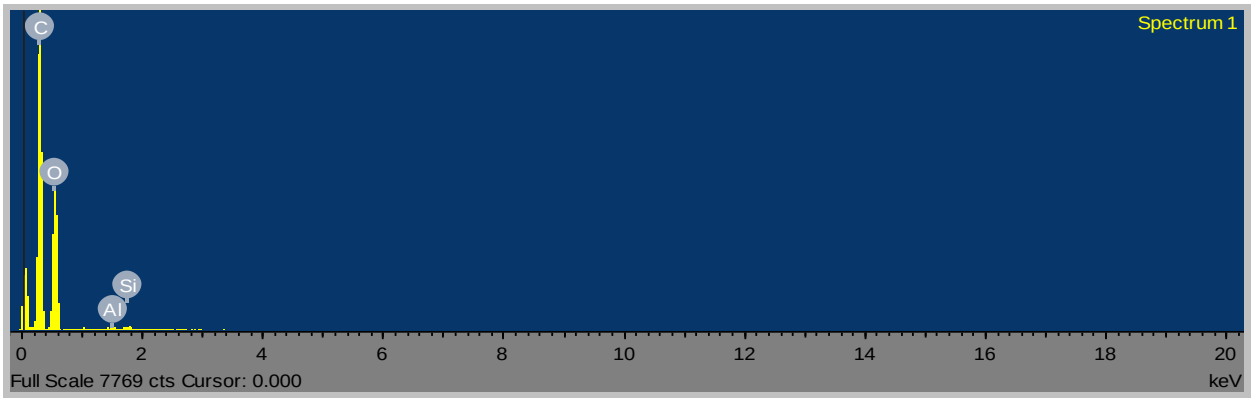

Figure A- 2: Photographs of the EDX after ionic liquid pretreatment of CS.

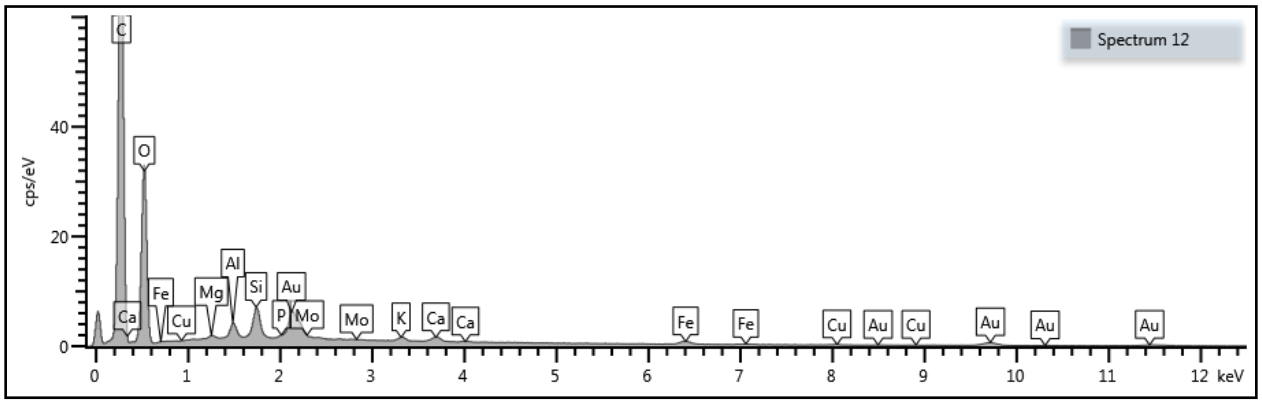

Figure A- 3: Photograph of the EDX of untreated SCB.

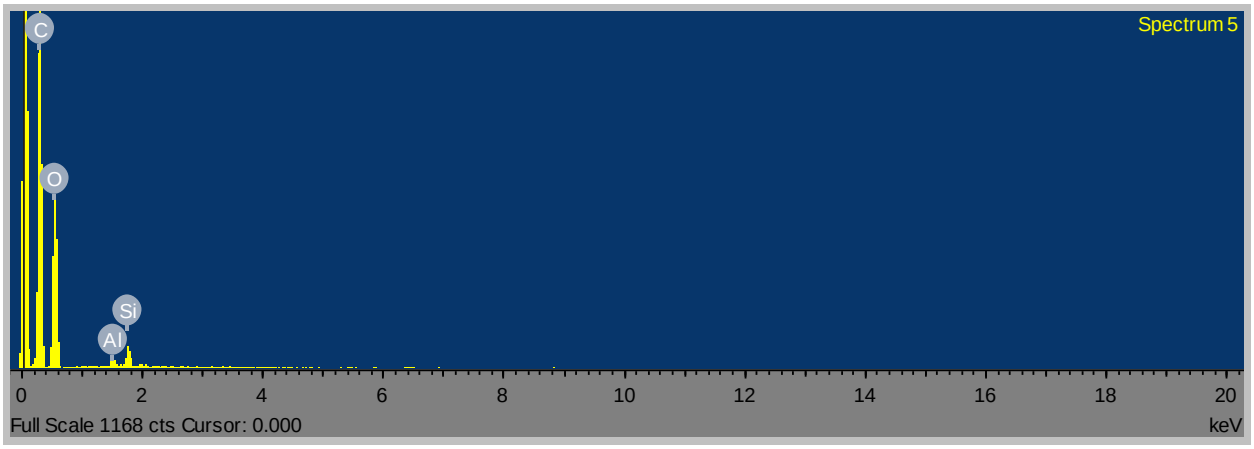

Figure A- 4: Photographs of the EDX after ionic liquid pretreatment of SCB.

Table A- 9: Elementals of the treated and untreated CS in weight (%).

Elements	Symbol	Weight (%), treated	Weight (%), untreated
Carbon	C	53.78	26.98
Oxygen	O	46.01	72.25
Magnesium	Mg	-	0.08
Aluminum	Al	0.11	0.02
Silicon	Si	0.10	0.05
Phosphorous	P	-	0.06
Sulphur	S	-	0.04
Chlorine	Cl	-	0.10
Potassium	K	-	0.33
Calcium	Ca	-	0.05
Iron	Fe	-	0.02
Copper	Cu	-	0.02
	Total	100.00	100.00

Table A- 10: Elementals of the treated and untreated SCB in weight (%).

Elements	Symbol	Weight (%), treated	Weight (%), untreated
Carbon	C	53.55	26.98
Oxygen	O	45.42	72.36
Magnesium	Mg	-	0.03
Aluminum	Al	0.26	0.11
Silicon	Si	0.77	0.21
Phosphorous	P	-	0.02
Potassium	K	-	0.04
Calcium	Ca	-	0.05
Iron	Fe	-	0.09
Copper	Cu	-	0.03
Molybdenum	Mo	-	0.07
	Total	100.0	100.00

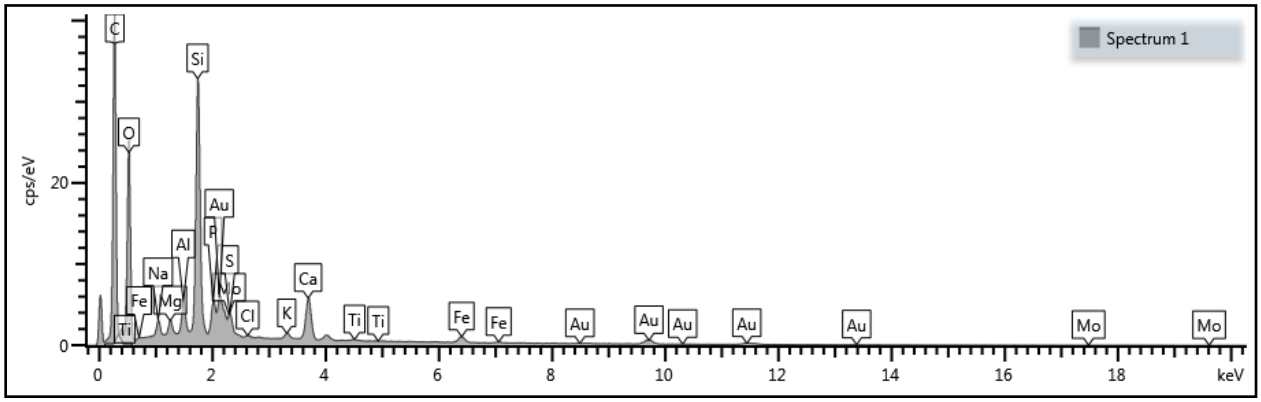

Figure A- 5: Photographs of the EDX report of sewage sludge.

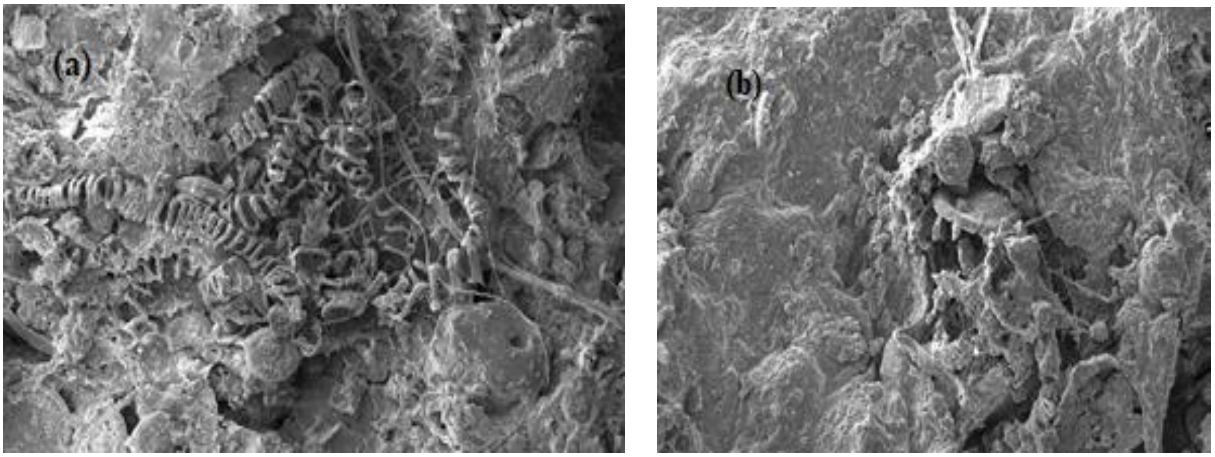

Figure A- 6: Microscopic image of the (a) optimised biodigester and (b) sewage sludge during AcoD of CS with SWW

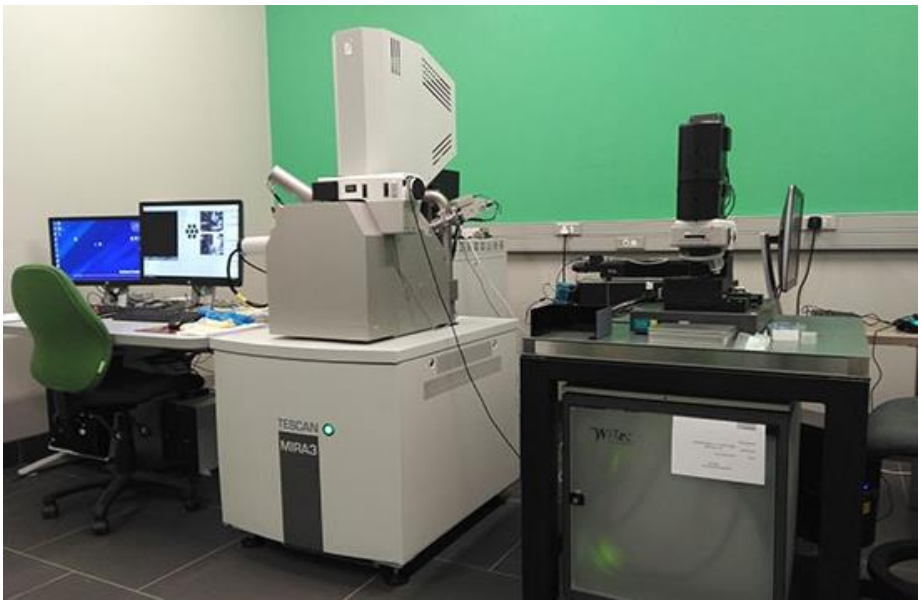

Figure A- 7: Photograph of the SEM (Tescan Mira3, Tescan, Czech Republic) and the EDX (Thermo Fisher Nova NanoSEM, FEI, USA).

Figure A- 8: The spectrum two Fourier transform infra-red spectrometer (Perkin Elmer, Waltham, USA).

Figure A- 9: Photograph of a Q600 simultaneous differential scanning calorimeter and thermo-gravimetric analyzer (DSC/TGA) (TA Instruments, Inc., France).

APPENDIX B

B1: Determination of the organic loading rate for the BMP test

In this study, the OLRs; 0.5, 1.0 and 1.5 gVS/100mL were selected based on the working range of systems under this working volume operating in batch mode.

Calculations

For CS at OLR of 0.5gVS/100 mL and %VS = 96% = 0.96 gVS

Total volume of biodigester = 1,000 mL

Biodigester working volume = 800 mL

Mass of corn silage for VS determination = 1 g

$0.5\text{gVS}/100\text{mL} \times 800\text{mL} = 0.5 \times 8$

$= 4\ \text{gVS}$

$1\text{g} = 0.96\text{gVS}$

$X = 4\ \text{gVS}$

$X = 4.2\ \text{g}$

Therefore, for 0.5 gVS/100mL, the mass of CS required is 4.2 g

For CS at OLR of 1.0gVS/100 mL and %VS = 96% = 0.96 gVS

Total volume of biodigester = 1,000 mL

Biodigester working volume = 800 mL

Mass of CS for VS determination = 1 g

$1.0\text{gVS}/100\text{mL} \times 800\text{mL} = 1.0 \times 8$

$= 8\ \text{gVS}$

$1\text{g} = 0.96\text{gVS}$

$X = 8\ \text{gVS}$

X = 8.3 g

Therefore, for 1.0gVS/100mL, the mass of CS required is 8.3 g

For at OLR of 1.5gVS/100 mL and %VS = 96% = 0.96 gVS

Total volume of biodigester = 1,000 mL

Biodigester working volume = 800 mL

Mass of CS for VS determination = 1 g

1.5gVS/100mL × 800 mL = 1.5 × 8

= 12 gVS

1g = 0.96gVS

X = 12.5 gVS

X = 12.5 g

Therefore, for 1.0gVS/100mL, the mass of corn silage required is 12.5g

For SCB at OLR of 0.5gVS/100 mL and %VS = 78% = 0.78 gVS

Total volume of biodigester = 1,000 mL

Biodigester working volume = 800 mL

Mass of CS for VS determination = 1 g

0.5gVS/100mL × 800 mL = 0.5 × 8

= 4 gVS

1g = 0.78 gVS

X = 4 gVS

X = 5.1 g

Therefore, for 1.0 gVS/100mL, the mass of CS required is 5.1 g

For SCB at OLR of 1.0gVS/100 mL and %VS = 78% = 0.78 gVS

Total volume of biodigester = 1,000 mL

Biodigester working volume = 800 mL

Mass of CS for VS determination = 1 g

1.0gVS/100mL × 800 mL = 1.0 × 8

= 8 gVS

1g = 0.78 gVS

X = 10.3 gVS

X = 10.3 g

Therefore, for 1.0 gVS/100mL, the mass of CS required is 10.3 g

For SCBe at OLR of 1.5gVS/100 mL and %VS = 78% = 0.78 gVS

Total volume of biodigester = 1,000 mL

Biodigester working volume = 800 mL

Mass of CS for VS determination = 1 g

1.5gVS/100mL × 800mL = 1.5 × 8

= 12 gVS

1g = 0.78 gVS

X = 15.4 gVS

X = 15.4 g

Therefore, for 1.5 gVS/100mL, the mass of cornCS required is 15.4 g

Table B- 1: Summary of the OLR and mass of SCB or CS added to each biodigester per the OLR.

Biomass	**%VS**	**0.5 gVS/100mL**	**1.0 gVS/100mL**	**1.5 gVS/100mL**
CS	96	4.2	8.3	12.5
SCB	78	5.1	10.3	15.4

B2: Sample calculations for the substrate mixtures during the BMP test

The calculations for the VS reduction (%) and COD reduction (%)

$$\text{VS reduction (\%)} = \frac{\text{Pre} - \text{digestion VS (mg/L)} - \text{Post} - \text{digestion VS (mg/L)}}{\text{Pre} - \text{digestion VS (mg/L)}} \times 100\%$$

$$\text{COD reduction (\%)} = \frac{\text{Pre} - \text{digestion COD (mg/L)} - \text{Post} - \text{digestion COD (mg/L)}}{\text{Pre} - \text{digestion COD (mg/L)}} \times 100\%$$

Table B- 2: Pre- and post- VS during AcoD for the untreated biomass.

Biodigester	Pre-digestion VS (mg/L)	Post-digestion VS (mg/L)	VS reduction (%)
R1	7000	4000	42.9
R2	8000	6000	25.0
R3	7000	4000	42.9
R4	8000	6000	25.0
R5	7000	4000	42.9
R6	8000	4000	50.0
R7	8000	4000	50.0
R8	8000	6000	25.0
R9	8000	2000	75.0
R10	8000	3000	62.5
R11	8000	4000	50.0
R12	8000	6000	25.0
R13	8000	5000	37.5

Table B- 3: Pre- and post- pH during AcoD for the untreated biomass.

Biodigester	Pre-digestion pH	Post-digestion pH	Minimum pH	Maximum pH
R1	6.56	7.66	6.0	8.5
R2	6.44	13.04	6.0	8.5
R3	6.47	6.68	6.0	8.5
R4	6.63	7.57	6.0	8.5
R5	6.37	7.26	6.0	8.5
R6	6.66	8.23	6.0	8.5
R7	6.56	7.12	6.0	8.5
R8	6.79	13.15	6.0	8.5
R9	6.55	7.44	6.0	8.5
R10	6.44	7.63	6.0	8.5
R11	6.57	7.35	6.0	8.5
R12	6.77	8.59	6.0	8.5
R13	6.74	8.23	6.0	8.5

Table B- 4: Biogas composition during AcoD for the untreated biomass.

Biodigester	CH_4 content (%)	CO_2 content (%)
R1	40.21	58.63
R2	41.26	56.23
R3	39.39	58.55
R4	50.10	40.20
R5	49.63	49.00
R6	45.22	53.60
R7	49.10	49.63
R8	36.02	71.10
R9	39.05	60.36
R10	63.50	35.11
R11	52.61	45.77
R12	50.56	48.36
R13	42.19	57.10
C25	40.20	59.28
C35	33.69	66.57
C55	40.95	58.50

Table B- 5: Pre- and post- COD during AcoD for the untreated biomass.

Biodigester	Pre-digestion COD (mg/L)	Post-digestion COD (mg/L)	COD reduction (%)
R1	5500	3600	34.5
R2	3620	2800	22.6
R3	4800	3750	21.9
R4	4100	3800	41.9
R5	5530	4700	15.0
R6	3620	1560	56.9
R7	3620	1900	47.5
R8	2740	2100	23.4
R9	3620	2850	21.3
***R10**	**2740**	**1800**	**34.3**
R11	3620	2750	24.0
R12	2740	1800	34.3
R13	3620	1800	50.3
C25	5000	3750	25.0
C35	4200	3100	26.2
C55	4800	3700	23.0

B3: AcoD of CS with DWW

Table B- 6: Pre- and post- pH during AcoD for the untreated biomass.

Biodigester	Pre-digestion pH	Post-digestion pH	Minimum pH	Maximum pH
R1	5.86	7.37	6.0	8.5
R2	6.61	7.51	6.0	8.5
R3	6.14	6.70	6.0	8.5
R4	6.67	7.46	6.0	8.5
R5	6.38	4.37	6.0	8.5
R6	6.72	7.73	6.0	8.5
R7	6.66	7.38	6.0	8.5
R8	6.86	7.72	6.0	8.5
R9	6.69	7.03	6.0	8.5
R10	6.94	7.25	6.0	8.5
R11	6.87	7.48	6.0	8.5
R12	6.79	7.52	6.0	8.5
R13	6.62	7.45	6.0	8.5
C25	7.00	7.14	6.0	8.5
C35	7.14	7.71	6.0	8.5
C55	7.08	8.12	6.0	8.5

Table B- 7: Pre- and post-VS during AcoD for the untreated biomass.

Biodigester	Pre-digestion VS (mg/L)	Post-digestion VS (mg/L)	VS reduction (%)
R1	11,000	7,000	36.4
R2	19,000	11,000	26.3
R3	11,000	7,000	36.6
R4	19,000	15,000	21.0
R5	11,000	6,000	45.5
R6	19,000	9,000	52.6
R7	19,000	11,000	42.1
R8	5,000	3,000	40.0
R9	19,000	12,000	36.8
R10	5,000	3,000	40.0
R11	19,000	11,000	42.1
R12	5,000	3,000	40.0
R13	9,000	5,000	44.4
C25	19,000	13,000	31.6
C35	11,000	9,000	18.2
C55	15,000	11,000	26.7

Table B- 8: Biogas composition during AcoD for the untreated biomass.

Runs	CH_4 content (%)	CO_2 content (%)
R1	71.91	28.08
R2	79.11	20.88
R3	60.06	39.93
R4	77.48	22.51
R5	14.41	85.58
R10	7.93	92.06
R11	58.83	41.17
R12	50.56	49.40
C25	63.96	36.04
C35	73.84	26.16
C55	40.95	59.04

Table B- 9: Pre- and post-COD during AcoD for the untreated biomass.

Biodigester	Pre-digestion COD (mg/L)	Post-digestion COD (mg/L)	COD reduction (%)
R1	5530	3600	34.9
R2	3620	2810	22.4
R3	5530	3750	32.2
R4	3620	2100	41.9
R5	5530	4700	15.0
R6	3620	1560	56.9
R7	3620	1700	53.0
R8	2740	2100	23.4
R9	3620	2850	21.3
R10	2740	1750	36.1
R11	3620	2750	24.0
R12	2740	1800	34.3
R13	3620	1720	52.5
C25	5500	3600	34.5
C35	3620	2800	22.6
C55	4800	3750	21.9

Table B- 10: Pre- and post- COD during AcoD for the pretreated biomass.

Biodigester	Pre-digestion COD (mg/L)	Pre-digestion COD (mg/L)	COD reduction (%)
A1	5530	4700	15.0
A2	5040	4100	18.6
A3	4600	3500	24.0
A4	4100	3050	25.6
B1	3850	2600	32.5
B2	4100	3500	14.6
B3	3620	2850	21.3
***B4**	**3620**	**1800**	**50.3**

B4: AcoD of SCB with DWW

Table B- 11: Pre- and post-pH during AcoD for the untreated biomass.

Biodigester	Pre-digestion pH	Post-digestion pH	Minimum pH	Maximum pH
R1	7.04	6.54	6.0	8.5
R2	7.02	6.30	6.0	8.5
R3	7.06	6.66	6.0	8.5
R4	6.95	6.28	6.0	8.5
R5	7.00	6.31	6.0	8.5
R6	7.11	6.37	6.0	8.5
R7	7.05	6.31	6.0	8.5
R8	7.08	6.29	6.0	8.5
R9	6.88	6.31	6.0	8.5
R10	7.04	6.27	6.0	8.5
R11	7.00	6.30	6.0	8.5
R12	7.10	6.36	6.0	8.5
R13	7.06	6.30	6.0	8.5
C25	7.15	6.82	6.0	8.5
C35	7.15	6.83	6.0	8.5
C55	7.21	6.95	6.0	8.5

Table B- 12: Pre- and post-VS during AcoD for the untreated biomass.

Biodigester	Pre-digestion VS (mg/L)	Post-digestion VS (mg/L)	VS reduction (%)
R1	14,000	10,000	28.6
R2	18,000	10,000	26.3
R3	11,000	7,000	36.6
R4	19,000	15,000	21.0
R5	11,000	6,000	45.5
R6	18,000	7,000	61.1
R7	19,000	11,000	42.1
R8	5,000	3,000	40.0
R9	19,000	12,000	36.8
R10	5,000	3,000	40.0
R11	19,000	11,000	42.1
R12	11,000	6,000	45.5
R13	8,000	4,000	50.0
C25	19,000	13,000	31.6
C35	11,000	9,000	18.2
C55	19000	11,000	42.1

Table B- 13: Biogas composition during AcoD for the untreated biomass.

Biodigester	CH_4 content (%)	CO_2 content (%)
R1	30.25	55.36
R2	35.96	60.32
R3	42.56	55.65
R4	38.56	60.56
R5	41.06	56.32
R6	68.54	29.61
R7	39.11	58.62
R8	36.54	62.00
R9	53.36	45.11
R10	55.65	42.96
R11	57.11	40.36
R12	61.55	29.11
R13	0.00	0.00
C25	42.36	55.86
C35	57.36	41.11
C55	59.65	39.36

Table B- 14: Pre- and post-COD during AcoD for the untreated biomass.

Biodigester	Pre-digestion COD (mg/L)	Pre-digestion COD (mg/L)
R1	5,400	3,400
R2	3,620	2,800
R3	5,000	3,750
R4	4,200	3,100
R5	4,800	3,700
R6	5500	2,100
R7	3,620	1,700
R8	2,840	2,100
R9	3,620	2,850
R10	2,470	1,760
R11	3,260	2,750
R12	2,740	1,800
R13	3,620	1,720
C25	4,200	2,900
C35	5,100	3,000
C55	4,100	2,900

B5: AcoD of SCB with SWW

Table B- 15: Pre- and post-pH during AcoD for the untreated biomass.

Biodigester	Pre-digestion pH	Post-digestion pH	Minimum pH	Maximum pH
R1	7.08	6.33	6.0	8.5
R2	7.07	6.30	6.0	8.5
R3	7.06	6.29	6.0	8.5
R4	7.09	6.28	6.0	8.5
R5	7.14	6.31	6.0	8.5
R6	7.04	6.37	6.0	8.5
R7	7.09	6.31	6.0	8.5
R8	7.10	6.29	6.0	8.5
R9	7.09	6.31	6.0	8.5
R10	7.07	6.27	6.0	8.5
R11	7.10	6.30	6.0	8.5
R12	7.10	6.36	6.0	8.5
R13	7.10	6.30	6.0	8.5

Table B- 16: Pre- and post-VS during AcoD for the untreated biomass.

Biodigester	Pre-digestion VS (mg/L)	Post-digestion VS (mg/L)	VS reduction (%)
R1	33,000	12,000	63.6
R2	78,000	12,000	84.6
R3	33,000	14,000	57.8
R4	78,000	14,000	82.0
R5	33,000	18,000	45.5
R6	78,000	10,000	87.2
R7	78,000	10,000	87.2
R8	20,000	10,000	50.0
R9	78,000	10,000	87.2
R10	20,000	10,000	50.0
R11	78,000	8,000	89.7
R12	20,000	12,000	40.0
R13	78,000	14,000	82.0
C25	38,000	15,000	60.5
C35	20,000	6,000	70.0
C55	33,000	12,000	63.6

Table B- 17: Biogas composition during AcoD for the untreated biomass.

Biodigester	CH_4 content (%)	CO_2 content (%)
R1	68.51	30.51
R2	79.56	20.77
R3	60.06	38.11
R4	55.20	44.26
R5	49.56	48.11
R6	44.25	54.01
R7	45.01	54.78
R8	50.16	48.63
R9	60.74	37.15
R10	55.89	40.55
R11	77.56	21.00
R12	50.56	45.26
R13	60.20	37.11
C25	60.00	36.04
C35	55.26	43.02
C55	41.56	55.26

Table B- 18: Pre- and post-COD during AcoD for the untreated biomass.

Biodigester	Pre-digestion COD (mg/L)	Post-digestion COD (mg/L)	COD reduction (%)
R1	4,900	3,600	26.5
R2	3,620	2,600	28.2
R3	4,600	3,750	18.5
R4	3,900	2,600	33.3
R5	5,530	4,700	15.0
R6	3,620	2,700	25.4
R7	3,100	2,700	12.9
R8	2,740	2,100	23.3
R9	3,620	2,850	21.3
R10	4,500	2,500	44.4
R11	3,500	2,850	18.6
R12	2,730	1,900	30.4
R13	3,620	3,100	14.4
C25	5,000	3,750	25.0
C35	4,200	3,100	26.2
C55	4,800	3,700	23.0

B6: Biogas potential calculations

B6.1 Biogas production rate (BPR)

For the untreated biomass, this is calculated in mL/gVS$_{added}$/d

Hence, CS with SWW will be

BPR = $\frac{20000}{4}/30$

= 167 mL/gVS$_{added}$/d

For the IL biomass, this is calculated in mL/gVS$_{added}$/d

Hence, CS with daily WW (B4) will be

BPR = $\frac{30{,}955}{8}/30$

= 1032 mL/d

B6.2 Specific biogas production rate (SBP)

For the untreated biomass, this is calculated in mL/d/gVS

Hence, CS with SWW will be

BPR = $\frac{20000}{30}/4$

= 167 mL/d/gVS

For the IL treated biomass, this is calculated in mL/gVS$_{added}$/d

Hence, CS with DWW (B4) will be

BPR = $\frac{30955}{30}/8$

= 129 mL/d/gVS

B6.3 Biogas yield (BY)

For the untreated biomass, this is calculated in m^3/kgVS or LCH4/gVS

Hence, CS with SWW will be

$$BPR = \frac{0.02}{0.004}$$

$$= 5.0\ m^3/KgVS$$

For the IL treated biomass, this is calculated in m^3/kgVS

Hence, For CS with DWW will be

$$BY = \frac{0.031}{0.008}$$

$$= 3.9\ m^3/KgVS$$

That is, 1.0 gVS/100mL OLR, mass in gVS = 8

B7: Plots of the biogas production yield

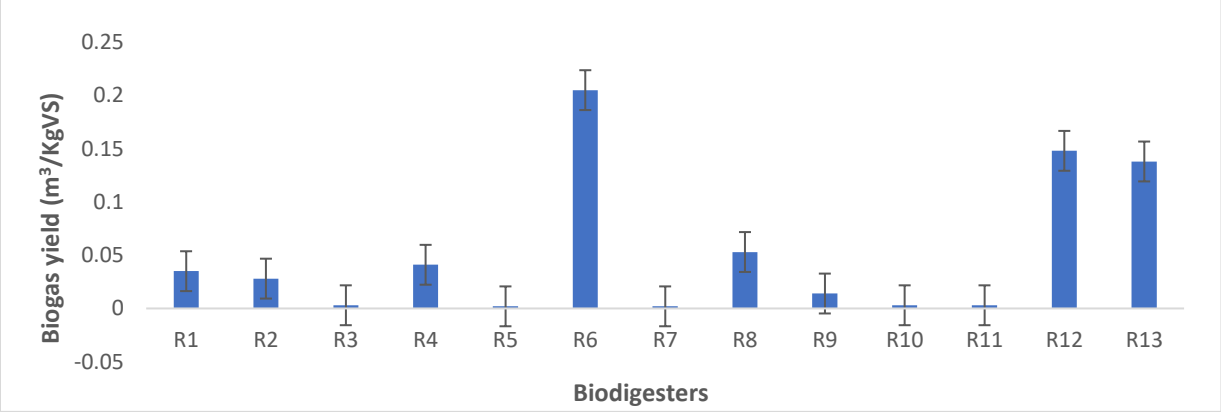

Figure B- 1: Biogas production yield of CS with DWW.

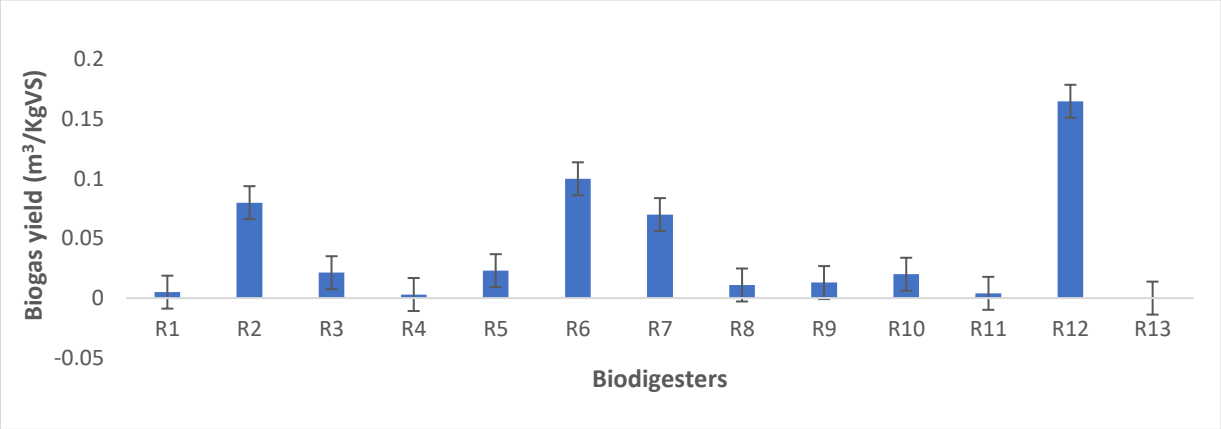

Figure B- 2: Biogas production yield of SCB with DWW.

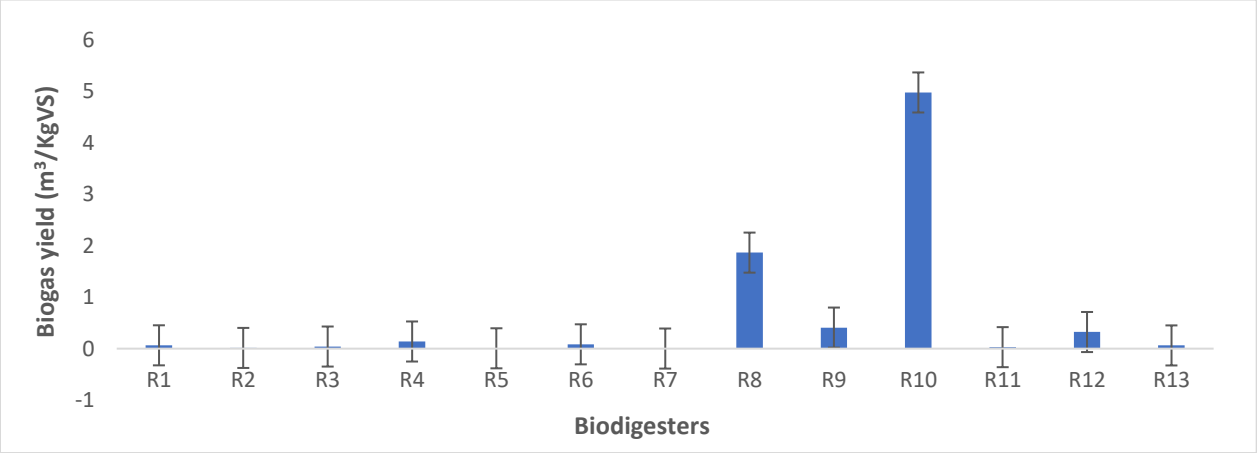

Figure B- 3: Biogas production yield of SCB with SWW.

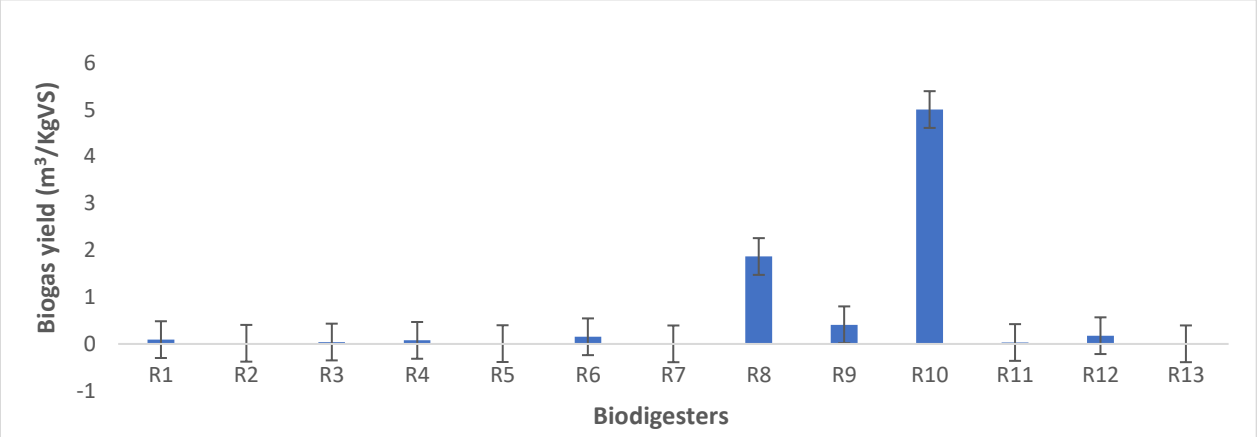

Figure B- 4: Biogas production yield of CSwith SWW.

B8: Plots of the biogas production rate

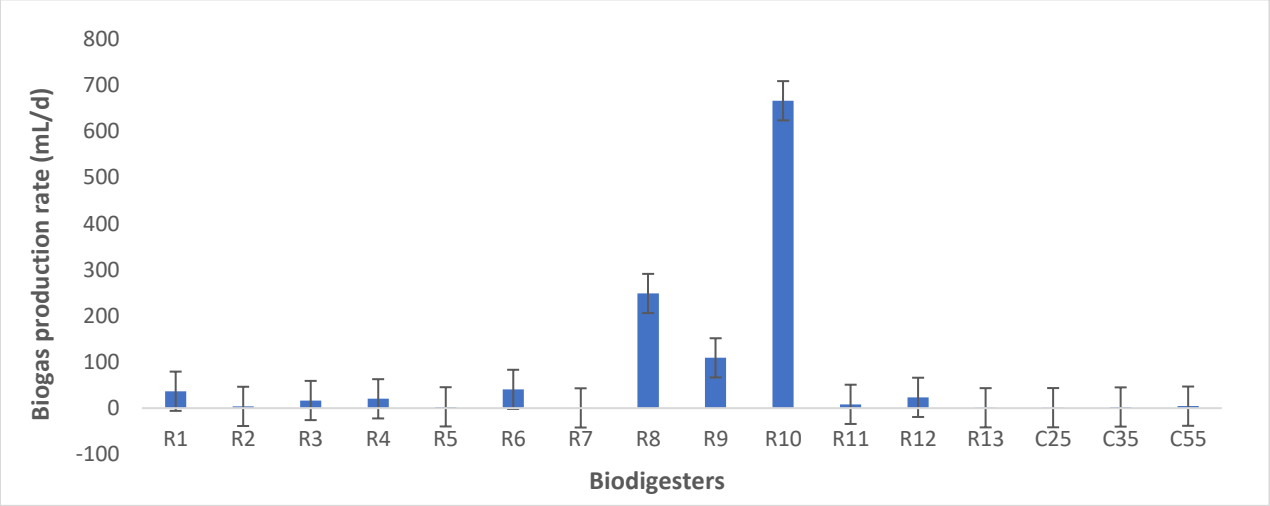

Figure B- 5: Biogas production rate of CS with SWW.

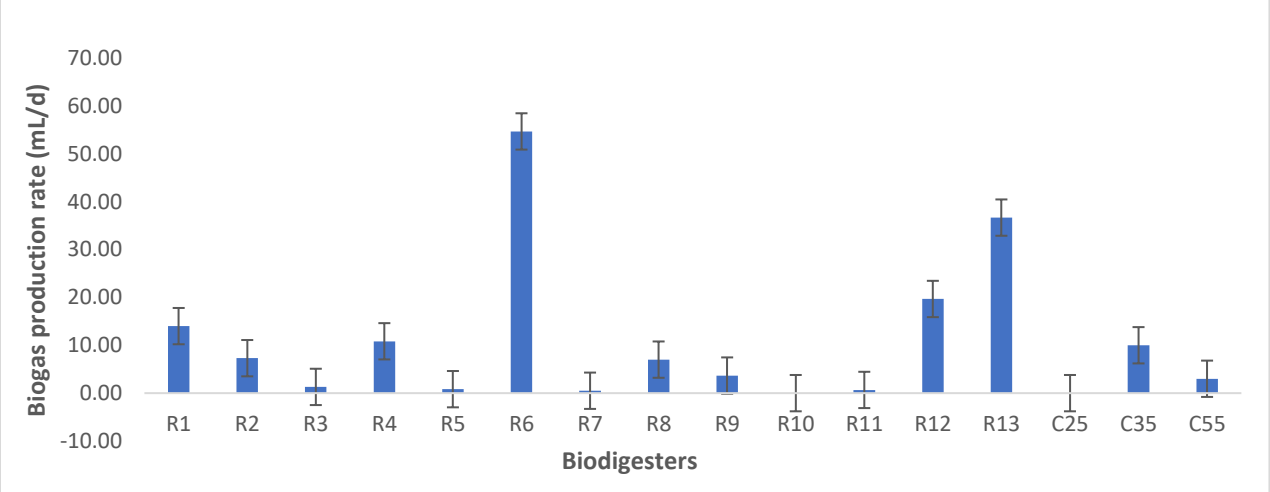

Figure B- 6: Biogas production rate of CS with DWW.

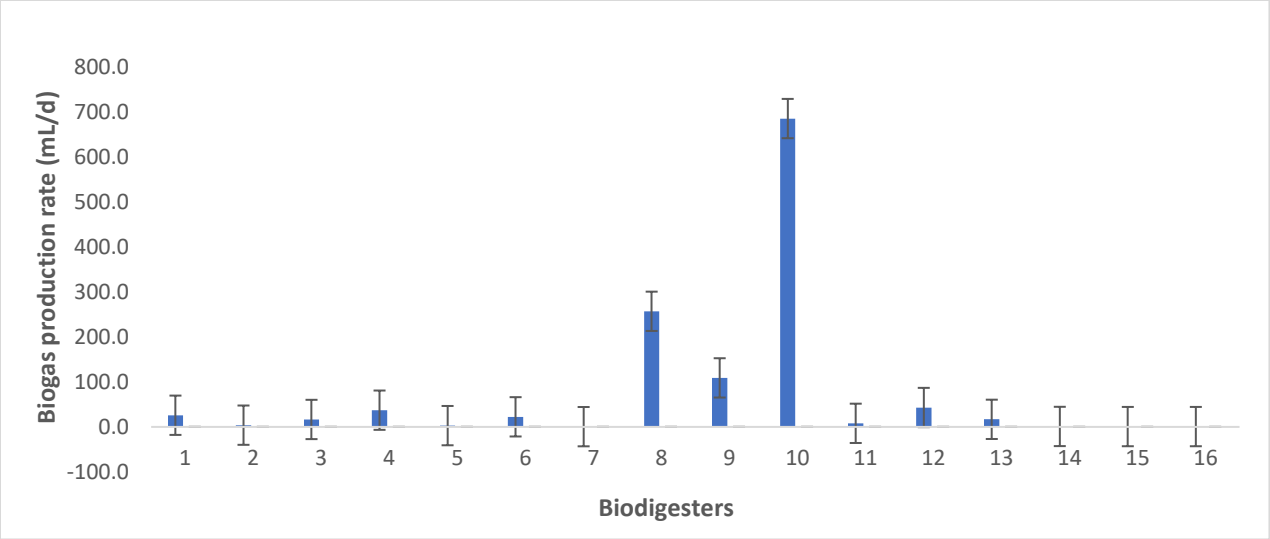

Figure B- 7: Biogas production rate of SCB with SWW.

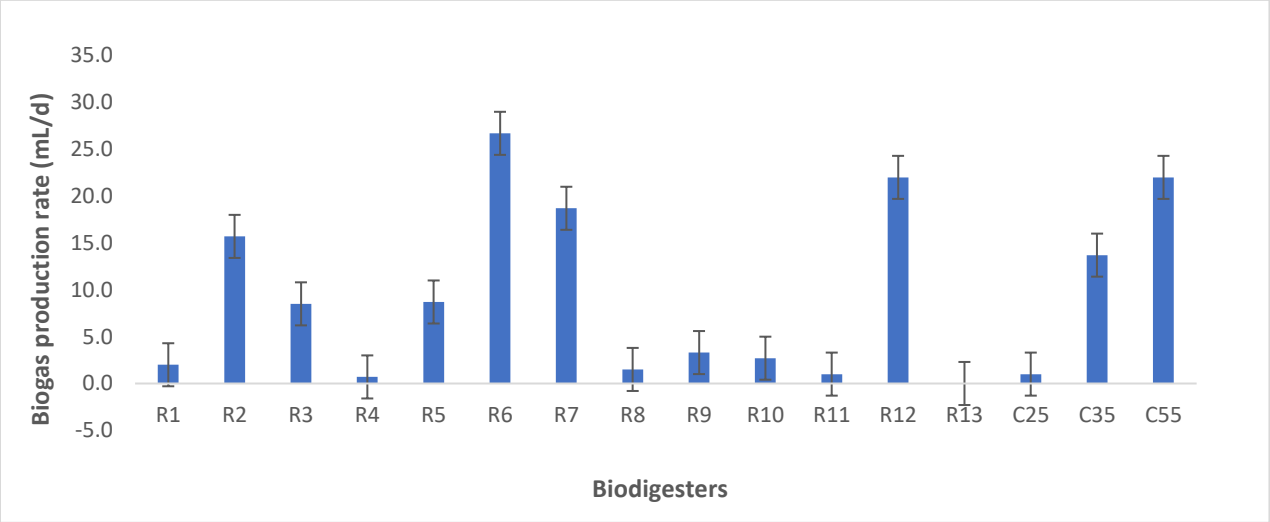

Figure B- 8: Biogas production rate of SCB with DWW.

B9: Data for the response surface plots and lines of best fit

Table B- 19: Distribution for the summary of fit: CS with DWW.

Source	Sequential p-value	Lack of Fit p-value	Adjusted R^2	Predicted R^2	
Linear	**0.0041**	**0.2076**	**0.6006**	**0.2806**	**Suggested**
2FI	0.1727	0.2374	0.6432	-0.0841	
Quadratic	0.3286	0.2236	0.6662	-0.6235	
Cubic	0.1871	0.2860	0.7610	-3.6897	Aliased

Table B- 20: Summary of the sequential model sum of squares for CS with DWW.

Source	Sum of Squares	df	Mean Square	F-value	p-value	
Mean vs Total	7.09	1	7.09			
Linear vs Mean	**0.0133**	**2**	**0.0067**	**10.02**	**0.0041**	**Suggested**
2FI vs Linear	0.0013	1	0.0013	2.19	0.1727	
Quadratic vs 2FI	0.0015	2	0.0007	1.31	0.3286	
Cubic vs Quadratic	0.0019	2	0.0009	2.39	0.1871	Aliased
Residual	0.0020	5	0.0004			
Total	7.10	13	0.5465			

Table B- 21: Distribution for the summary of fit: CS with SWW.

Source	Sequential p-value	Lack of Fit p-value	Adjusted R^2	Predicted R^2	
Linear	0.0501	< 0.0001	0.3406	-0.2775	
2FI	0.0329	< 0.0001	0.5701	-0.1522	
Quadratic	**0.0135**	**< 0.0001**	**0.8385**	**0.0324**	**Suggested**
Cubic	0.0010	0.0003	0.9857	0.0243	Aliased

Table B- 22: Summary of the sequential model sum of squares for CS with SWW.

Source	Sum of Squares	Df	Mean Square	F-value	p-value	
Mean vs Total	4.76	1	4.76			
Linear vs Mean	10.79	2	5.40	4.10	0.0501	
2FI vs Linear	5.44	1	5.44	6.34	0.0329	
Quadratic vs 2FI	**5.47**	**2**	**2.73**	**8.48**	**0.0135**	**Suggested**
Cubic vs Quadratic	2.11	2	1.06	36.92	0.0010	Aliased
Residual	0.1431	5	0.0286			
Total	28.72	13	2.21			

Table B- 23: Distribution for the summary of fit: SCB with DWW.

Source	Sequential p-value	Lack of Fit p-value	Adjusted R^2	Predicted R^2	
Linear	0.0719	0.5386	0.3190	-0.2998	
2FI	**0.0198**	**0.8938**	**0.6270**	**0.5059**	**Suggested**
Quadratic	0.7146	0.8119	0.5554	0.2023	
Cubic	0.6555	0.6780	0.4600	-1.5190	Aliased

Table B- 24: Summary of the sequential model sum of squares for SCB with DWW.

Source	Sum of Squares	df	Mean Square	F-value	p-value	
Mean vs Total	0.0221	1	0.0221			
Linear vs Mean	0.0125	2	0.0062	3.58	0.0719	
2FI vs Linear	**0.0080**	**1**	**0.0080**	**8.43**	**0.0198**	**Suggested**
Quadratic vs 2FI	0.0008	2	0.0004	0.3555	0.7146	
Cubic vs Quadratic	0.0013	2	0.0006	0.4702	0.6555	Aliased
Residual	0.0055	4	0.0014			
Total	0.0502	12	0.0042			

Table B- 25: Distribution for the summary of fit: SCB with SWW.

Source	Sequential p-value	Lack of Fit p-value	Adjusted R^2	Predicted R^2	
Linear	0.0424	< 0.0001	0.3622	-0.2291	
2FI	0.0383	< 0.0001	0.5715	-0.1868	
Quadratic	**0.0118**	**< 0.0001**	**0.8452**	**0.1047**	**Suggested**
Cubic	0.0024	0.0016	0.9808	-0.2593	Aliased

Table B- 26: Summary of the sequential model sum of squares for SCB with SWW.

Source	Sum of Squares	df	Mean Square	F-value	p-value	
Mean vs Total	4.94	1	4.94			
Linear vs Mean	11.06	2	5.53	4.41	0.0424	
2FI vs Linear	4.96	1	4.96	5.88	0.0383	
Quadratic vs 2FI	**5.45**	**2**	**2.73**	**8.96**	**0.0118**	**Suggested**
Cubic vs Quadratic	1.94	2	0.9705	25.65	0.0024	Aliased
Residual	0.1892	5	0.0378			
Total	28.54	13	2.20			

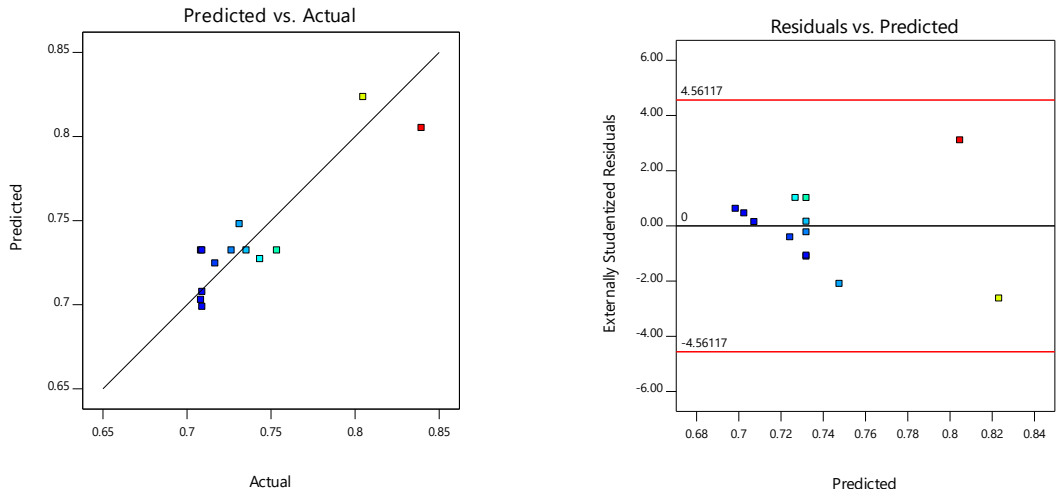

Figure B- 9: Figure B9: Plots of the (a) predicted versus actual and (b) residual versus predicted for CS with DWW.

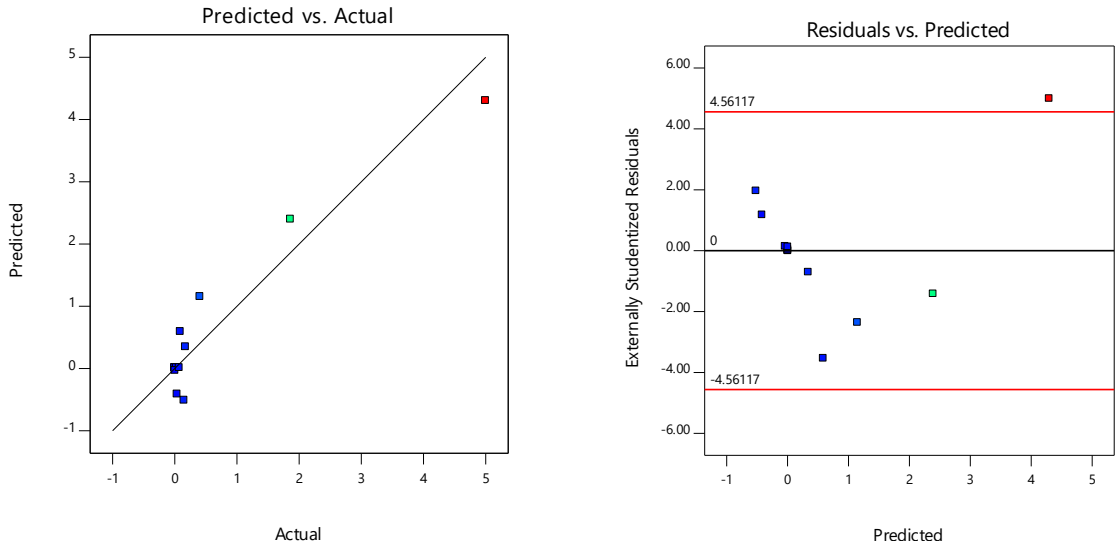

Figure B- 10: Figure B-10: Plots of the (a) predicted versus actual and (b) residual versus predicted for CS with SWW.

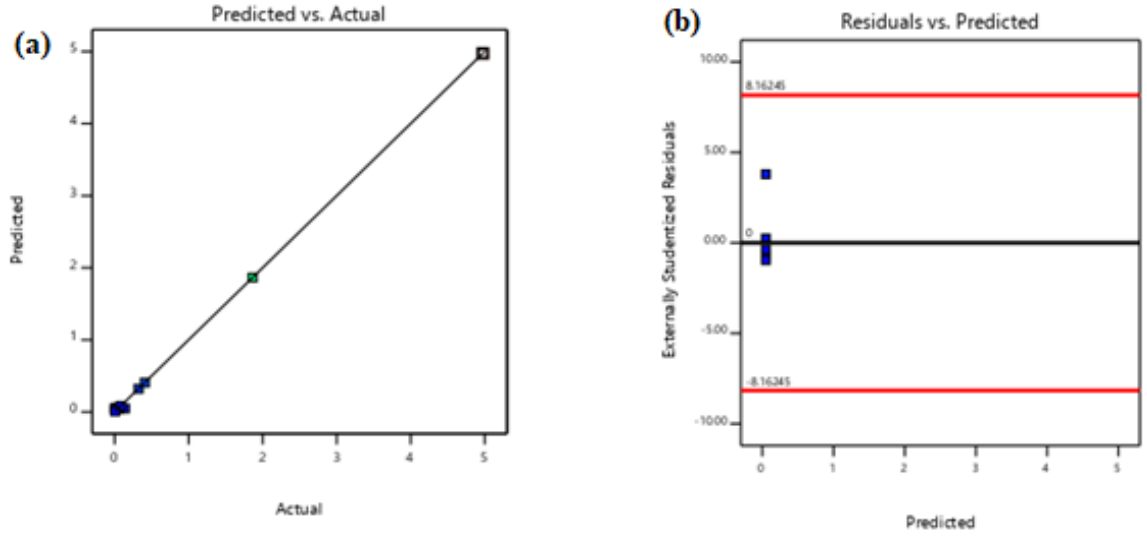

Figure B- 11: Figure B11: Plots of the predicted versus actual (a) and the residual versus predicted (b) for SCB with SWW.

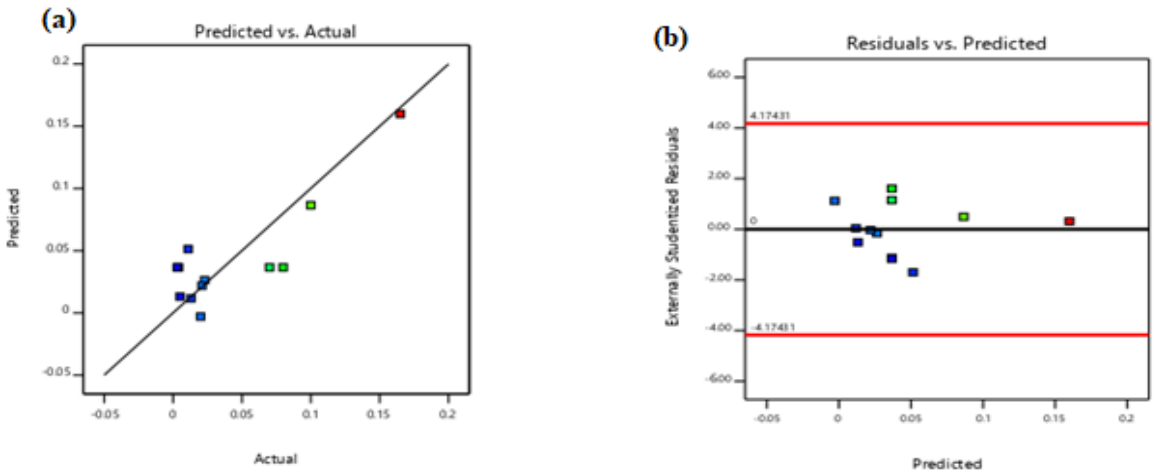

Figure B- 12: Figure B12: Plots of the predicted versus actual (a) and the residual versus predicted (b) for SCB with DWW.

B10: Gas chromatograph (GC)

B10-1 Calibration of the GC

The calibration curves were prepared via the injection specified volumes of high purity of CH_4, H_2 and CO_2.

B10-2 GC Analysis

Biogas composition was analyzed using a Shimadzu 2014 GC chromatograph (Figure B-9) which could detect H_2, CH_4 and CO_2 with respect to the following conditions:

Column: Packed poropak

Column flow: 20 mL/min

Carrier gas: Nitrogen (N_2)

Column temperature: 40 ºC

Detector type: Thermal conductivity detector (TCD)

Detector temperature: 250 ºC

Injection port temperature: 120 ºC

Nitrogen gas (N_2) was employed as the carrier gas under this study at a flow rate of 25.1 mL/min. The retention times of CH_4, H_2, and CO_2 were found to be approximately 1.5, 0.7 and 2.3 minutes, respectively. Samples of the biogas obtained were drawn from each biodigester by inserting the needle of a gas syringe (50 or 100 µL) through the rubber septum and withdrawing 40 to 50 µL from the headspace gas.

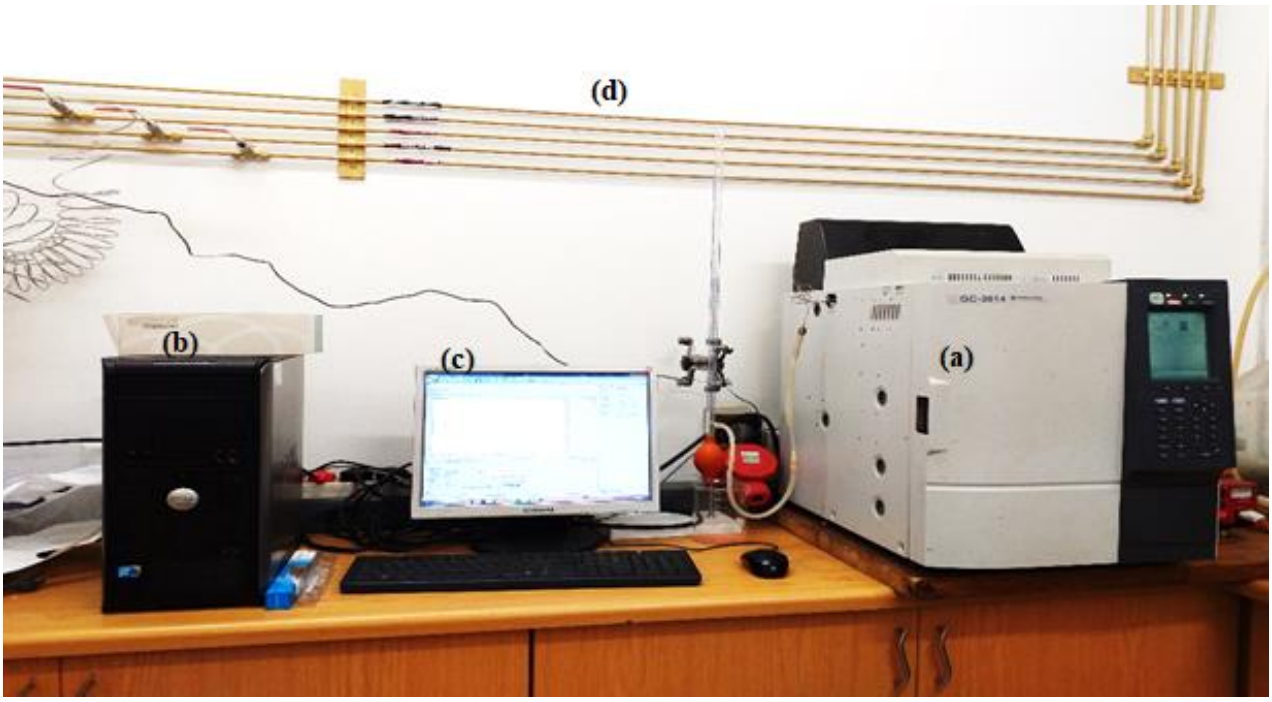

Figure B- 13: Photograph of the (a) Shimadzu 2014 GC chromatograph used in this study which is connected to a system unit (b) and a monitor (c) with carrier gas flow lines indicated as (d).

APPENDIX C

C1: Carbohydrates determination

Determination of cellulose in biomass

Materials needed

- Biomass
- Sodium chlorite ($NaClO_2$)
- Distilled water
- Electronic balance
- Autoclave @ 121 ± 3°C
- Filter paper
- Convection oven

The specifications for the autoclave in the determination of cellulose are as;

Name and source: Vertical Type Steam Sterilizer, D & E International corporation, Model: HL-34I, Taiwan.

Working temperature: 121-132°C

Voltage:220V

Current: 17A

Phase: 1P

Heater: 3.4kw

Serial number: S0609007

Determination of lignin

Materials needed

- 100 mL beaker
- 72% H_2SO_4
- Heating plate and magnetic stirrer @ 200 rpm
- Biomass (SCB, CS, etc.)
- Distilled water
- Filter paper
- Electronic balance
- Convection oven

Specification weighing balance (for lignin, cellulose, holocellulose)

Name: Radwag electronic balance (Made in Poland)

Model: AS220.R2

S/N: 460933

Max: 220g **Min:** 10mg

Supplier: LASEC SA (PTY) LTD South Africa

Determination of hollocellulose

Materials needed

- 500 mL flask
- 100 mL flask
- Heating plate and magnetic stirrer @ 200 rpm
- Biomass (SCB, CS, etc.)

- Distilled water
- sodium chlorite ($NaClO_2$)
- Glacial acetic acid
- Filter paper
- Electronic balance
- Convection oven
- Reflux setup
- Reaction chamber

C2: Pretreatment of biomass with ionic liquids

Table C- 1: Biomass loading during the BMP test after ionic liquid pretreatment.

Biodigesters	OLR	*M_f	*M_b	Temp (°C)	*Raw vol. (mL)	*Actual vol. (mL)	*Estimated vol. (mL)	Factor
A1	0.5	5.100	0.110	25	95	55	28,050	510
A2	0.5	5.100	0.110	25	80	40	20,400	510
A3	1.0	10.300	0.022	55	60	35	16,380	468
A4	1.0	10.300	0.022	55	45	20	21,060	468
B1	0.5	4.200	0.028	25	25	20	3,000	150
B2	0.5	4.200	0.028	25	15	10	1,500	150
B3	1.0	8.300	0.055	55	290	185	27,935	151
B4	1.0	8.300	0.055	55	310	205	30,955	151
$C_{A1,A2}$	0.5	5.089	0.110	25	40	-	-	-
$C_{A3,A4}$	1.0	10.278	0.022	55	25	-	-	-
$C_{B1,B2}$	0.5	4.172	0.028	25	5	-	-	-
$C_{B3,B4}$	1.0	8.242	0.055	55	105	-	-	-

*M_f = mass of filtrate added to biodigester

*M_b = mass of biomass in filtrate

*Raw vol. = biogas produced (in volume) during the digestion process without any deductions

*Actual vol. = volume of biogas produced after subtracting the raw vol. produced from the control biodigesters

*Estimated vol. = volume of biogas after multiplying the actual vol. by the factor

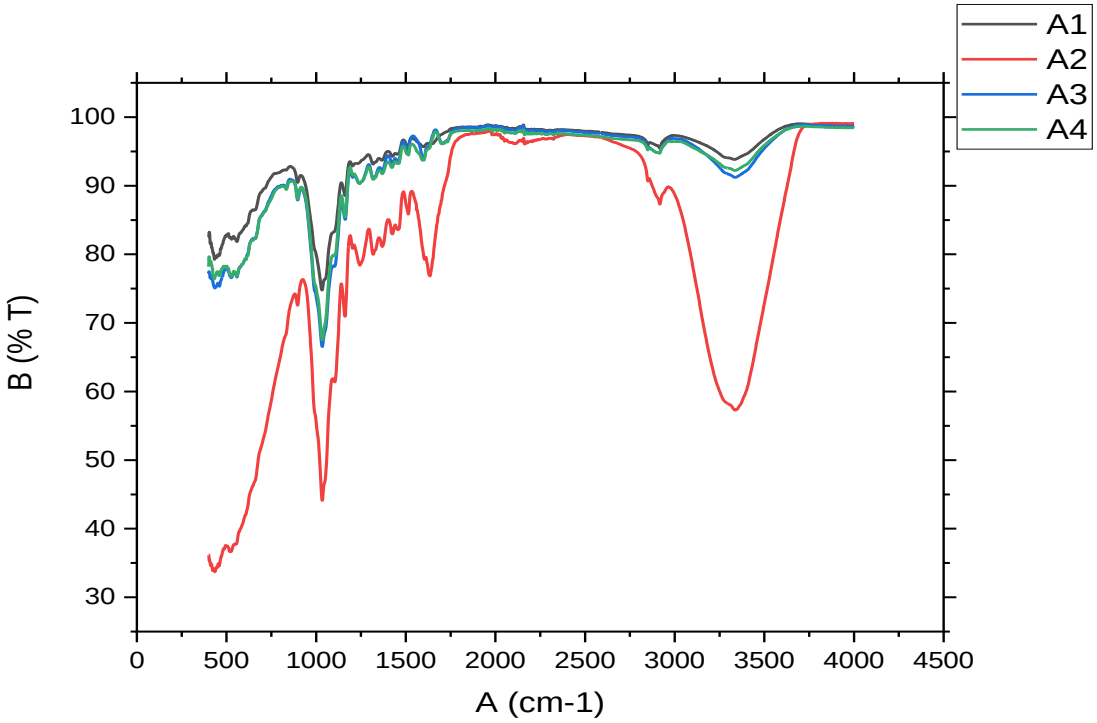

Figure C2- 1: FTIR spectra for the SCB represented as A1, A2, A3, A4 after IL pretreatment.

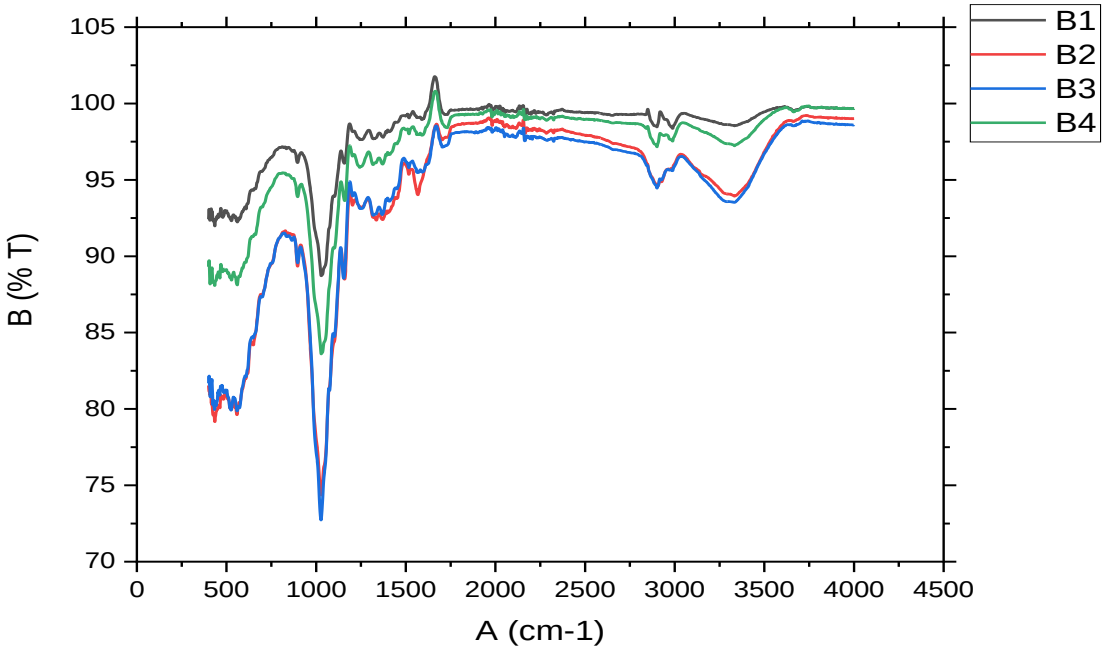

Figure C2- 2: FTIR spectra of the CS represented as B1, B2, B3, B4 after IL pretreatment.

APPENDIX D

D1: Kinetic modelling output: CS and DWW

Table D- 1: Summary of output and ANOVA.

Regression Statistics	
Multiple R	0.996069
R Square	0.992154
Adjusted R Square	0.991693
Standard Error	16.37602
Observations	19

Table D- 2: Summary of the regression analysis and the standard errors with lower and upper limits.

	df	SS	MS	F	Significance F
Regression	1	576514.7	576514.7	2149.779	2.43E-19
Residual	17	4558.958	268.174		
Total	18	581073.7			

	Coefficients	Standard Error	t Stat	P-value	Lower 95%	Upper 95%	Lower 95.0%	Upper 95.0%
Intercept	2.069803	6.797642	0.304488	0.764452	-12.272	16.41157	-12.272	16.41157
X Variable 1	0.994558	0.02145	46.36571	2.43E-19	0.949301	1.039814	0.949301	1.039814

Table D- 3: Summary of the residual outputs.

Observation	Predicted Y	Residuals	Standard Residuals
1	2.069806	-2.06981	-0.13006
2	2.075218	-2.07522	-0.1304
3	2.57683	-2.57683	-0.16192
4	9.705307	10.29469	0.64687
5	40.66169	-10.6617	-0.66993
6	103.6674	26.33262	1.654617
7	183.2187	-3.21875	-0.20225
8	257.9768	-47.9768	-3.01463
9	316.6449	3.355052	0.210816
10	357.9301	22.06992	1.386769
11	385.137	14.86297	0.933919
12	402.374	17.62605	1.107538
13	413.0397	6.960271	0.437351
14	419.5469	0.453079	0.028469
15	423.4836	-3.48358	-0.21889
16	425.8532	-5.85315	-0.36778
17	427.2752	-7.27517	-0.45714
18	428.127	-8.12699	-0.51066
19	428.6367	-8.63672	-0.54269

D2: Kinetic modelling output: CS and SWW

Table D- 4: Summary of output and ANOVA.

Regression Statistics	
Multiple R	0.998715131
R Square	0.997431913
Adjusted R Square	0.997340196
Standard Error	372.3715187
Observations	30

Table D- 5: Table D-5: Summary of the regression analysis and the standard errors with lower and upper limits.

	df	SS	MS	F	Significance F
Regression	1	1507941573	1507941573	10875.05852	8.12E-38
Residual	28	3882495.341	138660.5479		
Total	29	1511824069			

	Coefficients	Standard Error	t Stat	P-value	Lower 95%	Upper 95%	Lower 95.0%	Upper 95.0%
Intercept	-196.68194	160.5435157	-1.2251005	0.2307437	-526	132.17654	-525.540425	132.17654
X	1.0102548	0.009687576	104.283549	8.12E-38	0.99	1.0300989	0.99041072	1.0300989

Table D- 6: Summary of the residual outputs.

Observation	Predicted Gompertz	Residuals	Standard Residuals
1	257.93273	-245.6778169	-0.6714435
2	763.06014	-646.0915011	-1.7657839
3	773.16269	-211.9591321	-0.5792895
4	1247.9825	421.3125188	1.15145744
5	2965.4157	595.9130593	1.628645
6	5693.1037	337.5125046	0.92242995
7	9330.021	-633.0043518	-1.7300164
8	11754.633	-537.0185975	-1.467685
9	12663.862	724.65033	1.98048712
10	14381.295	759.1875263	2.07487812
11	16199.754	291.903891	0.79778049
12	17614.111	-112.8074468	-0.3083055
13	18523.34	-284.0164601	-0.7762239
14	19432.569	-661.9743819	-1.8091922
15	19533.595	-384.6117409	-1.0511533

16	19533.595	-117.1015016	-0.3200413
17	19533.595	71.04904731	0.19417879
18	19533.595	202.9095106	0.55455667
19	19533.595	295.0906174	0.80648989
20	19937.697	-44.68077544	-0.1221137
21	19978.107	-40.25055539	-0.1100058
22	19978.107	-9.021518782	-0.024656
23	19983.158	7.663972552	0.02094582
24	19983.158	22.78758791	0.06227904
25	19983.158	33.3070672	0.09102903
26	19983.158	40.62263427	0.11102266
27	19993.261	35.60686374	0.09731443
28	20003.363	29.04100159	0.07936977
29	20003.363	31.49979343	0.08608971
30	20008.415	28.15785437	0.07695611

D3: Kinetic modelling output: SCB and DWW

Table D- 7: Summary of output and ANOVA.

Regression Statistics	
Multiple R	0.995167
R Square	0.990356
Adjusted R Square	0.990012
Standard Error	23.03872
Observations	30

Table D- 8: Summary of the regression analysis and the standard errors with lower and upper limits.

	df	SS	MS	F	Significance F
Regression	1	1526251	1526251	2875.474	9.03E-30
Residual	28	14861.91	530.7825		
Total	29	1541113			

	Coefficients	Standard Error	t Stat	P-value	Lower 95%	Upper 95%	Lower 95.0%	Upper 95.0%
Intercept	0.726136	13.28707	0.05465	0.956806	-26.4912	27.94347	-26.4912	27.94347
x	0.998062	0.018612	53.62344	9.03E-30	0.959936	1.036188	0.959936	1.036188

Table D- 9: Summary of the residual outputs.

Observation	Predicted Gompertz	Residuals	Standard Residuals
1	30.668	2.958423	0.130684
2	120.4936	-25.6429	-1.13274
3	220.2998	-29.5125	-1.30367
4	300.1447	5.412185	0.239075
5	399.9509	19.74893	0.872379
6	489.7765	30.02475	1.326298
7	549.6602	50.74444	2.241559
8	649.4665	12.19585	0.538733
9	754.263	-47.8301	-2.11282
10	799.1758	-60.8744	-2.68904
11	799.1758	-38.5904	-1.70467
12	799.1758	-23.1945	-1.02458
13	799.1758	-12.6434	-0.5585
14	799.1758	-5.45197	-0.24083
15	799.1758	-0.56841	-0.02511
16	799.1758	2.739695	0.121022
17	799.1758	4.976836	0.219844
18	799.1758	6.488024	0.286599

19	799.1758	7.508054	0.331657
20	799.1758	8.196208	0.362055
21	799.1758	8.660304	0.382556
22	799.1758	8.97322	0.396378
23	799.1758	9.184172	0.405697
24	799.1758	9.326368	0.411978
25	799.1758	9.422212	0.416212
26	799.1758	9.48681	0.419065
27	799.1758	9.530348	0.420989
28	799.1758	9.55969	0.422285
29	799.1758	9.579465	0.423158
30	799.1758	9.592792	0.423747

D4: Kinetic modelling output: SCB and SWW

Table D- 10: Summary of output and ANOVA.

Regression Statistics	
Multiple R	0.998635
R Square	0.997271
Adjusted R Square	0.997174
Standard Error	381.5141
Observations	30

Table D- 11: Summary of the regression analysis and the standard errors with lower and upper limits.

	df	SS	MS	F	Significance F
Regression	1	1.49E+09	1.49E+09	10232.06	1.9E-37
Residual	28	4075484	145553		
Total	29	1.49E+09			

	Coefficients	Standard Error	t Stat	P-value	Lower 95%	Upper 95%	Lower 95.0%	Upper 95.0%
Intercept	-189.228	164.6128	-1.14953	0.26006	-526.422	147.9659	-526.422	147.9659
1	1.009875	0.009984	101.1536	1.9E-37	0.989425	1.030325	0.989425	1.030325

Observation	Predicted Gompertz	Residuals	Standard Residuals
1	265.2156	-252.058	-0.67237
2	770.1531	-648.238	-1.7292
3	780.2518	-206.125	-0.54984
4	1254.893	433.1528	1.155448
5	2971.68	604.137	1.611554
6	5698.343	330.9454	0.882807
7	9333.893	-660.628	-1.76225
8	11757.59	-586.569	-1.56469
9	12565.49	757.1652	2.019761
10	14282.28	778.0202	2.075393
11	16100.05	301.7158	0.804836
12	17513.88	-108.537	-0.28953
13	18422.77	-282.914	-0.75468
14	19331.65	-662.362	-1.76687
15	19432.64	-385.765	-1.02904
16	19432.64	-118.467	-0.31602
17	19432.64	69.78351	0.18615
18	19432.64	201.8885	0.538544
19	19432.64	294.3618	0.785219
20	19836.59	-44.9697	-0.11996
21	19876.99	-40.2651	-0.10741
22	19876.99	-8.815	-0.02351
23	19882.04	8.054385	0.021485
24	19882.04	23.32417	0.062218
25	19882.04	33.95891	0.090586
26	19882.04	41.36407	0.11034
27	19892.13	36.42095	0.097154
28	19902.23	29.91133	0.079789
29	19902.23	32.40975	0.086454
30	19907.28	29.09947	0.077624